Time Evolution of Primordial Magnetic Fields and Present Day Extragalactic Magnetism

Dissertation

zur Erlangung des Doktorgrades

des Department Physik

der Universität Hamburg

vorgelegt von

Andrey Saveliev

aus Moskau, Russland

Hamburg

2014

Gutachter der Dissertation:	Prof. Dr. Günter Sigl
	Prof. Dr. Robi Banerjee
Gutachter der Disputation:	Prof. Dr. Günter Sigl
	Prof. Dr. Wilfried Buchmüller
Datum der Disputation:	23. April 2014
Vorsitzender des Prüfungsausschusses:	Dr. Georg Steinbrück
Vorsitzende des Promotionsausschusses:	Prof. Dr. Daniela Pfannkuche
Dekan der Fakultät für Mathematik, Informatik und Naturwissenschaften:	Prof. Dr. Heinrich Graener

Zusammenfassung

Das Thema der vorliegenden Dissertation ist die zeitliche Entwicklung der Primordialen Magnetfelder, die im Frühen Universum entstanden sind. Unter der Annahme, dass dieses sogenannte Kosmologische Szenario der Magnetogenese zutrifft, wird im Folgenden gezeigt, dass sie die heutigen Extragalaktischen Magnetfelder erklären können. Dies ist insbesondere wichtig angesichts der jüngsten Beobachtungen von Gammastrahlung, die dazu verwendet werden, eine untere Grenze für die zugehörigen Magnetdfeldstärke herzuleiten, auch wenn ein alternativer Ansatz, welcher diese Beobachtungen stattdessen auf Wechselwirkungen mit dem Intergalaktischen Medium zurückführt, möglich ist und hier mithilfe von Monte Carlo Simulationen überprüft wird.

Um die oben genannte Entwicklung der Primordialen Magnetfelder zu beschreiben, wird ein Satz Master-Gleichungen für die spektralen magnetischen, kinetischen und helischen Komponenten des Systems hergeleitet und dann numerisch für das Frühe Universum gelöst. Diese semianalytische Methode erlaubt es, eine vollständige quantitative Untersuchung der zeitlichen Entwicklung der Leistungsspektren durchzuführen, insbesondere da die Rückreaktion des turbulenten Mediums auf die Magnetfelder berücksichtigt wird.

Durch Anwendung dieses Formalismus auf nichthelische Primordiale Magnetfelder, die auf einer charakteristischen Länge erzeugt wurden, wird im Folgenden gezeigt, dass ihr Spektrum auf großen Längenskalen L eine Flanke aufbaut, die sich wie $B \sim L^{-\frac{5}{2}}$ verhält und die Entwicklung der Kohärenz- (oder Integral-)Skala bestimmt. Außerdem wird nachgewiesen, dass die Behauptung einer Äquipartition zwischen der magnetischen und der kinetischen Energie wahr ist. Erweitert man diese Analyse auf helische Magnetfelder, so findet man, dass sich die zeitliche Entwicklung dramatisch ändert, was quantitativ bestätigt, dass eine Inverse Kaskade, d.h. ein effizienter Transport von Energie von kleinen zu großen Skalen, tatsächlich stattfindet, so wie es in früheren Arbeiten vorhergesagt wurde.

Abstract

The topic of the present thesis is the time evolution of Primordial Magnetic Fields which have been generated in the Early Universe. Assuming this so-called Cosmological Scenario of magnetogenesis to be true, it is shown in the following that this would account for the present day Extragalactic Magnetic Fields. This is particularly important in light of recent gamma ray observations which are used to derive a lower limit for the corresponding magnetic field strength, even though also an alternative approach, claiming instead that these observations are due to interactions with the Intergalactic Medium, is possible and will be tested here with Monte Carlo simulations.

In order to describe the aforementioned evolution of Primordial Magnetic Fields, a set of general Master Equations for the spectral magnetic, kinetic and helical components of the system are derived and then solved numerically for the Early Universe. This semi-analytical method allows it to perform a full quantitative study for the time development of the power spectra, in particular by fully taking into account the backreaction of the turbulent medium onto the magnetic fields.

Applying the formalism to non-helical Primordial Magnetic Fields created on some characteristic length measure, it will be shown that on large scales L their spectrum builds up a slope which behaves as $B \sim L^{-\frac{5}{2}}$ and governs the evolution of the coherence (or integral) scale. In addition, the claim of equipartition between the magnetic and the kinetic energy is found to be true. Extending the analysis to helical magnetic fields, it is observed that the time evolution changes dramatically, hence confirming quantitatively that an Inverse Cascade, i.e. an efficient transport of energy from small to large scales, as predicted in previous works, indeed does take place.

Science! true daughter of Old Time thou art!
Who alterest all things with thy peering eyes.
Why preyest thou thus upon the poet's heart,
Vulture, whose wings are dull realities?
How should he love thee? or how deem thee wise,
Who wouldst not leave him in his wandering
To seek for treasure in the jewelled skies,
Albeit he soared with an undaunted wing?
Hast thou not dragged Diana from her car?
And driven the Hamadryad from the wood
To seek a shelter in some happier star?
Hast thou not torn the Naiad from her flood,
The Elfin from the green grass, and from me
The summer dream beneath the tamarind tree?
— E. A. Poe, *Sonnet – To Science* (1829)

Contents

Introduction

> Geschrieben steht: "Im Anfang war das Wort!"
> Hier stock ich schon! Wer hilft mir weiter fort?
> Ich kann das Wort so hoch unmöglich schätzen,
> Ich muß es anders übersetzen, [...]
> Mir hilft der Geist! Auf einmal seh ich Rat
> Und schreibe getrost: Im Anfang war die Tat!
> — J. W. v. Goethe, *Faust. Eine Tragödie* (1808)

Magnetic fields are one of the most common and yet often least understood phenomena in physics. Starting from microscopic structures, they appear, in form of the Earth's magnetic field, in everyday life as well as on solar, galactic and even extragalactic scales.

Especially those on the latter, i.e. Extragalactic Magnetic Fields (EGMF), have been intensively studied in the past few years. This is due to their unique role in the understanding of the Universe as they connect various aspects of physics which, on first sight, might not seem to have much in common: Cosmology, as the EGMF are directly related to the creation and development of the Large Scale Structure (LSS) of the Universe; particle physics if primordial seed fields are created in the Early Universe and thus at the time when particles of a particular kind appeared for the first time; astroparticle physics since they dramatically influence the acceleration and propagation of charged particles; Magnetohydrodynamics, EGMF being an exceptional object to study aspects of the interaction between magnetic fields and matter under conditions which, due to, for example, the tremendous length scales involved, cannot be achieved in the laboratory to the same extent; and, finally, computational physics, as this large range of length scales of EGMF is a big challenge for present day and future computing systems such that it is necessary to develop more efficient numerical and analytical methods. In the present thesis these aspects will be discussed in detail in order to obtain a better understanding of this exciting topic.

The observed magnetic fields in astronomical structures of different sizes, ranging from stars up to galaxy clusters, are explained by an amplification of pre-existing weaker magnetic fields via flux conserving compression during gravitational collapse and by various types of dynamos. Both the dynamo and compression amplification mechanisms can act only if a non-zero magnetic "seed" field is present. This seed field for the amplification might be tiny, but it has to be generated by a different mechanism in the Early Universe. The uncertainty of the strength and of the origin of this initial seed field constitutes the long-standing problem of the origin of cosmic magnetic fields [1].

The various theories suggested to resolve this problem can be divided schematically into astrophysical and cosmological types. In Astrophysical Scenarios small seed magnetic fields are created during Structure Formation via some appropriate process (like, for example, the Biermann Battery) and then amplified by dynamo mechanisms. In Cosmological Scenarios strong seeds are generated in the Early Universe, most probably either during Inflation or a cosmological phase transition. Such initial fields are called Primordial Magnetic Fields which, if they turn out to have been indeed created,

would be a unique opportunity to study the Early Universe: In a similar way to the Cosmic Microwave Background (CMB) allowing to observe the state of the Universe at the Recombination epoch ($t \simeq 380\,000$ years after the Big Bang), Primordial Magnetic Fields would make it possible to draw conclusions about the physical phenomenon which caused their creation at times as early as $t \simeq 10^{-33}$ s.

The best possibility to determine the nature of the initial seed fields is to search for regions of the Universe where these fields might exist in their original form. Such regions are the voids of LSS where the Intergalactic Medium (IGM) and thus the residing primordial fields have been not distorted by plasma and magnetohydrodynamical (MHD) processes. Measurements of the EGMF might therefore provide an important clue on the origin of the seed fields. This idea is the prime motivation for the numerous efforts to detect the EGMF and to determine their parameters like the average magnetic field strength and the correlation length.

For a long period of time only upper limits on the average magnetic field strength of the EGMF existed. Recently several groups claimed to have derived *lower* limits on the strength and the filling factor of the EGMF [2, 3]. These authors used a method proposed in [4] which compares gamma ray data of distant blazars at different energies: At sufficiently high energies, photons emitted by such objects do not arrive at Earth directly, but react with the omnipresent Extragalactic Background Light (EBL) of which the most important components are the CMB and the Cosmic Infrared Background (CIB): High-energy photons scatter on the EBL and produce electron-positron pairs which, in turn, can upscatter low-energy EBL photons to high energies, thereby developing an electromagnetic cascade. If the high energy range of the photon spectrum for a given blazar is observed, the resulting cascade flux at lower energies can be calculated. Since the observed low energy flux is, for several sources, below the one expected from extrapolations under certain assumptions, it was concluded that the charged component of this cascade has been deflected out of the line of sight to the blazar by the EGMF. As a result, the secondary gamma ray flux would be spread over a wider solid angle which would explain that the observed intensity of the low energy gamma ray flux of such a beamed source is reduced. In addition, if a flare occurs, one would expect a time delayed echo due to the longer travelling time of reprocessed photons compared to the primary ones.

However, it has been claimed that this argumentation, based solely on the development of the electromagnetic cascade due to interactions with the EBL, might not be complete [5, 6]. In these publications it is suggested that interactions of electrons and positrons with the IGM, which consists mainly of ionized hydrogen and electrons, have to be considered as well, resulting, due to plasma instabilities, in an efficient energy transfer from the electron/positron pairs to the medium (therefore causing a heating-up of the IGM). By including the effects of these interactions in explicit Monte Carlo simulations the author of this thesis was able to quantify their influence in detail, confirming that they might be responsible for the suppression of the observed flux at GeV energies.

Assuming that the Cosmological Scenario of the origin of EGMF described above is true, magnetogenesis of the resulting Primordial Magnetic Fields takes place, for example, during either the Electroweak or the Quantumchromodynamical (QCD) Phase Transition, corresponding to the moments at which the temperature of the Universe, due to Expansion, decreased to the point at which the electroweak symmetry is broken or at which the free quarks form hadrons, respectively. In fact, even without pinning down a particular mechanism, generically it is very likely or even, as claimed recently, "unavoidable" [7] for strong magnetic fields to emerge in the Early Universe due to

a small scale dynamo amplification, thus providing an additional motivation for the discussion in this work.

It has been possible for the author to confirm, by deriving general Master Equations for their time evolution, that such fields indeed can account for present day EGMF by transporting magnetic energy from the small scales they were generated at to the large scales of today's voids between Galaxy Clusters. In addition, also the questions of the scaling behavior on large scales, the distribution of energy among the medium and the magnetic field and possible constraints on EGMF have been addressed. By including magnetic helicity, its impact, in particular the presence of the so-called Inverse Cascade, i.e. the efficient transport of magnetic energy from small to large scales, have been investigated, therefore quantitatively confirming former findings.

To obtain these results, a semi-analytic analysis has been performed by looking directly at the time development of the spectra of both the magnetic and the kinetic energy content of the turbulent medium by means of the aforementioned Master Equations. The main advantages of applying this method to the problem of Primordial Magnetic Fields are twofold: First, the interactions between the kinetic and magnetic energy components are fully taken into account in contrast to former similar approaches. In particular, in contrast to previous studies, the backreaction of the medium is considered, thus making the results more reliable from the physics point of view. Second, as the problem has been reduced to one dimension, a full analysis over the complete dynamic range, stretching over several orders of magnitude, is possible.

This work is structured as follows: In Chapter 1 the physical basics of the processes which occur when dealing with magnetic fields in the Early Universe are presented, namely Magnetohydrodynamics and Cosmology. Then, in Chapter 2, the current status of knowledge concerning Extragalactic Magnetic Fields is discussed, in particular focussing on the possibility to derive lower constraints on the magnetic field strength. In Chapter 3 the physics background, calculations and results for the time evolution of Primordial Magnetic Fields are presented, especially contrasting the differences between helical and non-helical scenarios. These considerations are based on the aforementioned Master Equations for which, due to their importance for this work, the full derivation and the discussion of their impact is presented. Finally, in Chapter 4, the conclusions of this thesis are drawn before giving an outlook on future prospects of the topic.

Parts of this work have been published in [8, 9] or submitted for publication to [10] peer reviewed journals.

Chapter 1

Magnetohydrodynamics and Cosmology

Some say the world will end in fire,
Some say in ice.
From what I've tasted of desire
I hold with those who favor fire.
But if it had to perish twice,
I think I know enough of hate
To say that for destruction ice
Is also great
And would suffice.
— R. Frost, *Fire and Ice* (1920)

In this chapter the two fields of study which are necessary in order to understand the physics of Primordial and Extragalactic Magnetic Fields are discussed: On the one hand, in Sec. 1.1, Magnetohydrodynamics, which describes the interaction of magnetic fields and fluids. On the other hand, in Sec. 1.2, Cosmology, which addresses the evolution of the Universe and thus has to be considered when looking at the time evolution of any phenomenon on large scales and over long periods of time.

1.1 Magnetohydrodynamics

Magnetohydrodynamics (MHD) describes the discipline of studying the interaction of magnetic fields and conductive fluids. Therefore, it combines the statistical approach to describe the physics of flows and electrodynamics which is governed by Maxwell's Equations. These two topics are connected by the Lorentz Force as the kinetic interaction onto the particles inside the fluid by magnetic and electric fields. Therefore, in the following first the fundamental equations describing Magnetohydrodynamics are presented (Sec. 1.1.1) before discussing magnetic helicity, a crucial quantity in MHD (Sec. 1.1.2), and concluding by possible approaches to address turbulence (Sec. 1.1.3).

1.1.1 Fundamental Equations

An important quantity in MHD is the current density $\mathbf{j}$ which is given by

$$\mathbf{j} = \mathbf{j}_{ext} + \sigma \left(\mathbf{E} + \mathbf{v} \times \mathbf{B} \right). \tag{1.1}$$

Here $\mathbf{j}_{ext}$ is some external current density, σ is the electric conductivity, $\mathbf{v}$ the (local) velocity of the fluid considered and $\mathbf{B}$ and $\mathbf{E}$ are the magnetic and electric fields, respectively. This is the general form of Ohm's Law.

Since magnetic and electric fields are involved, it is necessary to include the basic relations of electrodynamics, Maxwell's Equations:

$$\nabla \cdot \mathbf{E} = 4\pi\rho_{\mathrm{ch}}\,, \tag{1.2}$$

$$\nabla \cdot \mathbf{B} = 0\,, \tag{1.3}$$

$$\nabla \times \mathbf{E} = -\partial_t \mathbf{B}\,, \tag{1.4}$$

$$\nabla \times \mathbf{B} = 4\pi\mathbf{j} + \partial_t \mathbf{E}\,, \tag{1.5}$$

which are Gauss's Laws for the electric field (1.2), ρ_{ch} denoting the charge density, and for magnetism (1.3), Faraday's Law (1.4) and Ampère's Law (1.5). In the latter the displacement current is usually neglected in the following (unless stated otherwise) which is possible due to the so-called MHD approximation which states that typical flow velocities are much smaller than the speed of light.

The two equations from general hydrodynamics which will be used the most in the following are, on the one hand, the continuity equation for the mass density ρ,

$$\partial_t \rho + \nabla \cdot (\rho \mathbf{v}) = 0\,, \tag{1.6}$$

where $\mathbf{v}$ is the velocity of the plasma which is governed by the Navier-Stokes Equations, reading

$$\rho\left[\partial_t \mathbf{v} + (\mathbf{v}\cdot\nabla)\,\mathbf{v}\right] = -\nabla p + \mu\Delta\mathbf{v} + (\lambda+\mu)\nabla\left(\nabla\cdot\mathbf{v}\right) + \mathbf{F} \tag{1.7}$$

in the most general form. Here p is the pressure, λ and μ are Lamé's first and second parameter, respectively, which are related to the elasticity of the considered fluid (the latter also known as the shear modulus), and $\mathbf{F}$ is the density of the body forces.

Before considering the influence of magnetic field, i.e. before coming to MHD, an important quantity, the Reynolds Number $\mathcal{R}$, should be introduced. For this purpose (1.7) is treated in a simple case, i.e. an incompressible fluid ($\nabla\cdot\mathbf{v} = 0$) with homogeneous pressure ($\nabla p = 0$) and without external forces ($\mathbf{F} = 0$). This reduces (1.7) to

$$\rho\left[\partial_t \mathbf{v} + (\mathbf{v}\cdot\nabla)\,\mathbf{v}\right] = \mu\Delta\mathbf{v} \tag{1.8}$$

or

$$\partial_t \mathbf{v} = \frac{\mu}{\rho}\Delta\mathbf{v} - (\mathbf{v}\cdot\nabla)\,\mathbf{v}\,. \tag{1.9}$$

The two terms on the right side describe the two main processes governing the behavior of the system: On the one hand momentum convection (given by $-(\mathbf{v}\cdot\nabla)\,\mathbf{v}$), i.e. energy transport by particle flow, and on the other hand momentum diffusion (given by $\frac{\mu}{\rho}\Delta\mathbf{v}$ which describes a Heat Equation), i.e., in short, energy dissipation due to viscosity. The Reynolds Number $\mathcal{R}$ is given by the symbolic ratio between these two terms:

$$\mathcal{R} = \frac{|(\mathbf{v}\cdot\nabla)\,\mathbf{v}|}{|\frac{\mu}{\rho}\Delta\mathbf{v}|} \simeq \frac{v\frac{1}{L}v}{\frac{\mu}{\rho}\frac{1}{L^2}v} = \frac{\rho v L}{\mu} = \frac{vL}{\nu}\,, \tag{1.10}$$

where L is a typical length scale and v a typical velocity scale of the system, respectively, and $\nu = \frac{\mu}{\rho}$ is the so-called kinematic viscosity.

1.1.1.1 Time Evolution of the Magnetic Field Strength

With the equations presented above it is now possible to derive the differential equations which will be used in the following. Here, an incompressible (i.e. $\nabla\cdot\mathbf{v} = 0$) and turbulent

(i.e. $\mathcal{R} \gg 1$) setting is assumed. Solving (1.1) (without any external currents) for $\mathbf{E}$ gives

$$\mathbf{E} = \frac{\mathbf{j}}{\sigma} - \mathbf{v} \times \mathbf{B}. \tag{1.11}$$

Plugging this into (1.4) results in

$$\begin{aligned}\partial_t \mathbf{B} = -\nabla \times \mathbf{E} &\overset{(1.11)}{=} -\nabla \times \left(\frac{\mathbf{j}}{\sigma} - \mathbf{v} \times \mathbf{B} \right) = -\frac{1}{\sigma} \left(\nabla \times \mathbf{j} \right) + \nabla \times (\mathbf{v} \times \mathbf{B}) \\ &\overset{(1.5)}{=} -\frac{1}{\sigma} \nabla \times \left(\frac{1}{4\pi} \nabla \times \mathbf{B} \right) + \nabla \times (\mathbf{v} \times \mathbf{B}) = -\frac{1}{4\pi\sigma} \nabla \times (\nabla \times \mathbf{B}) + \nabla \times (\mathbf{v} \times \mathbf{B}) \\ &\overset{(A.7)}{=} -\frac{1}{4\pi\sigma} \left[\nabla \left(\nabla \cdot \mathbf{B} \right) - \Delta \mathbf{B} \right] + \nabla \times (\mathbf{v} \times \mathbf{B}) \, .\end{aligned} \tag{1.12}$$

This, using (1.3), can be transformed into the main differential equation for the time dependence of the magnetic field,

$$\partial_t \mathbf{B} = \frac{1}{4\pi\sigma} \Delta \mathbf{B} + \nabla \times (\mathbf{v} \times \mathbf{B}) \, . \tag{1.13}$$

The second part of the right hand side of this expression can be simplified by using (A.6) together with $\nabla \cdot \mathbf{v} = 0$ for an incompressible fluid and (1.3), giving

$$\partial_t \mathbf{B} = \frac{1}{4\pi\sigma} \Delta \mathbf{B} + (\mathbf{B} \cdot \nabla) \mathbf{v} - (\mathbf{v} \cdot \nabla) \mathbf{B} \, . \tag{1.14}$$

Now a better understanding of (1.13) is necessary. Following [11] here and later on, first the case where the first term of the right hand side of (1.13) is dominating is considered, i.e.

$$\partial_t \mathbf{B} \simeq \frac{1}{4\pi\sigma} \Delta \mathbf{B} \, . \tag{1.15}$$

This equation has the form of a Heat Equation and therefore describes a diffusion process, here the one for the magnetic field $\mathbf{B}$. To estimate the diffusion time τ_{diff} for a system of size L one can rewrite (1.15) as

$$\frac{B}{\tau_{\text{diff}}} \simeq \frac{1}{4\pi\sigma} \frac{B}{L^2} \tag{1.16}$$

and therefore

$$\tau_{\text{diff}} \simeq 4\pi\sigma L^2 \, . \tag{1.17}$$

To analyze the second term after the equality sign in (1.13) the assumption of a very large conductivity, i.e. $\sigma \to \infty$, is made, such that (1.13) reduces to

$$\partial_t \mathbf{B} = \nabla \times (\mathbf{v} \times \mathbf{B}) \, . \tag{1.18}$$

Assuming a loop S with the surface normal unit vector $\mathbf{S}$ is moving through the medium, there are two possible contributions to the change of the magnetic flux Φ through S,

$$\Phi = \int_S \mathbf{B} \cdot \mathrm{d}\mathbf{S} \, , \tag{1.19}$$

with time. On the one hand the magnetic field $\mathbf{B}$ may be time-dependent due to some external influences, such that it is

$$\frac{\mathrm{d}}{\mathrm{d}t} \Phi' = \int_S (\partial_t \mathbf{B}) \cdot \mathrm{d}\mathbf{S} \, , \tag{1.20}$$

and on the other hand the movement through the medium induces an electric field which is given by $\mathbf{E}_{\text{ind}} = \mathbf{v} \times \mathbf{B}$. Therefore one can write

$$\frac{\mathrm{d}}{\mathrm{d}t}\mathbf{B} \overset{(1.4)}{=} -\nabla \times \mathbf{E}_{\text{ind}} = -\nabla \times (\mathbf{v} \times \mathbf{B}) \tag{1.21}$$

and thus

$$\frac{\mathrm{d}}{\mathrm{d}t}\Phi'' = \int_S \frac{\mathrm{d}}{\mathrm{d}t}\mathbf{B} \cdot \mathrm{d}\mathbf{S} = -\int_S \nabla \times (\mathbf{v} \times \mathbf{B}) \cdot \mathrm{d}\mathbf{S}\,. \tag{1.22}$$

So, on the total one obtains

$$\begin{aligned} \frac{\mathrm{d}}{\mathrm{d}t}\Phi = \frac{\mathrm{d}}{\mathrm{d}t}\Phi' + \frac{\mathrm{d}}{\mathrm{d}t}\Phi'' &= \int_S (\partial_t \mathbf{B}) \cdot \mathrm{d}\mathbf{S} - \int_S \nabla \times (\mathbf{v} \times \mathbf{B}) \cdot \mathrm{d}\mathbf{S} \\ &= \int_S \{(\partial_t \mathbf{B}) - \nabla \times (\mathbf{v} \times \mathbf{B})\} \cdot \mathrm{d}\mathbf{S} \overset{(1.18)}{=} 0\,, \end{aligned} \tag{1.23}$$

i.e. the magnetic flux through S is constant. This effect, caused by the second term on the right hand side of (1.13), is called magnetic flux freezing.

Finally, to have a measure to compare the influence of the two terms of (1.13), the Magnetic Reynolds Number $\mathcal{R}_{\text{m}}$, its magnitude giving the relative importance of magnetic flux freezing to the diffusion of the magnetic field, shall be introduced, which is given by the symbolic ratio

$$\mathcal{R}_{\text{m}} = \frac{|\nabla \times (\mathbf{v} \times \mathbf{B})\,|}{|\frac{1}{4\pi\sigma}\Delta\mathbf{B}|} \simeq \frac{\frac{1}{L}vB}{\frac{1}{4\pi\sigma}\frac{1}{L^2}B} = 4\pi\sigma v L\,, \tag{1.24}$$

where, again, L is a typical length scale and v a typical velocity scale of the system, respectively.

1.1.1.2 Time Evolution of the Kinetic Field Strength

Using the Lorentz force density $\mathbf{F}_{\text{L}}$ explicitly,

$$\mathbf{F}_{\text{L}} = \mathbf{j} \times \mathbf{B}, \tag{1.25}$$

the final form of the Navier-Stokes Equations with the assumptions stated above reads

$$\rho\left[\partial_t \mathbf{v} + (\mathbf{v} \cdot \nabla)\,\mathbf{v}\right] = -\nabla p + \mathbf{j} \times \mathbf{B} + \mathbf{F}\,. \tag{1.26}$$

Now it is possible to rewrite (1.26) by plugging in (1.5). Neglecting the ∇p term due to the assumed homogeneity and dividing by ρ gives the main differential equation for the time dependence of the velocity $\mathbf{v}$:

$$\partial_t \mathbf{v} = -(\mathbf{v} \cdot \nabla)\,\mathbf{v} + \frac{1}{4\pi\rho}(\nabla \times \mathbf{B}) \times \mathbf{B} + \mathbf{f}\,. \tag{1.27}$$

Here again the second part on the right hand side can be simplified by using (A.4), such that the new expression for (1.27) now reads

$$\partial_t \mathbf{v} = -(\mathbf{v} \cdot \nabla)\,\mathbf{v} + \frac{1}{4\pi\rho}\left[(\mathbf{B} \cdot \nabla)\mathbf{B} - \frac{1}{2}\nabla(\mathbf{B} \cdot \mathbf{B})\right] + \mathbf{f} \tag{1.28}$$

Defining the (local) Alfvén speed by equaling the magnetic and the kinetic energy densities u_B and u_{K}, i.e. from (1.55), which will be derived later on,

$$\frac{1}{2}\rho\mathbf{v}_{\text{A}}^2 = \frac{1}{8\pi}\mathbf{B}^2\,, \tag{1.29}$$

meaning

$$\mathbf{v}_\mathrm{A} = \frac{1}{(4\pi\rho)^{\frac{1}{2}}}\mathbf{B}\,, \tag{1.30}$$

(1.27) may be reformulated as

$$\partial_t \mathbf{v} = -\left(\mathbf{v}\cdot\nabla\right)\mathbf{v} + \left(\nabla\times\mathbf{v}_\mathrm{A}\right)\times\mathbf{v}_\mathrm{A} + \mathbf{f}\,. \tag{1.31}$$

1.1.1.3 Kinetic Vorticity and Helicity

Another important quantity in MHD is the vorticity $\boldsymbol{\zeta}$ which is defined by

$$\boldsymbol{\zeta} \equiv \nabla\times\mathbf{v}\,. \tag{1.32}$$

In order to derive its time evolution, one has to look at (1.26), rewritten as

$$\partial_t \mathbf{v} = -\left(\mathbf{v}\cdot\nabla\right)\mathbf{v} - \frac{\nabla p}{\rho} + \frac{\mathbf{j}\times\mathbf{B}}{\rho} + \mathbf{f}\,. \tag{1.33}$$

Applying the curl operator to this equation gives

$$\begin{aligned}\partial_t\boldsymbol{\zeta} &= -\nabla\times\left[\left(\mathbf{v}\cdot\nabla\right)\mathbf{v}\right] - \nabla\times\left(\frac{\nabla p}{\rho}\right) + \nabla\times\left(\frac{\mathbf{j}\times\mathbf{B}}{\rho}+\mathbf{f}\right)\\ &\overset{(A.4),(A.3)}{=} -\nabla\times\left[\frac{1}{2}\nabla\left(\mathbf{v}\cdot\mathbf{v}\right) - \mathbf{v}\times\boldsymbol{\zeta}\right] - \left[\frac{1}{\rho}\nabla\times\left(\nabla p\right) + \nabla p\times\nabla\left(\frac{1}{\rho}\right)\right]\\ &\quad + \nabla\times\left(\frac{\mathbf{j}\times\mathbf{B}}{\rho}+\mathbf{f}\right) \overset{(A.8)}{=} \nabla\times\left(\mathbf{v}\times\boldsymbol{\zeta}\right) + \frac{\nabla\rho\times\nabla p}{\rho^2} + \nabla\times\left(\frac{\mathbf{j}\times\mathbf{B}}{\rho}+\mathbf{f}\right)\,.\end{aligned} \tag{1.34}$$

As will be shown in Sec. 2.1, vorticity is a major component in most of the scenarios to produce magnetic fields in the Early Universe.

Furthermore, using vorticity, in fluid mechanics the (kinetic) helicity $\mathfrak{H}_\mathrm{K}$ is defined as

$$\mathfrak{H}_\mathrm{K} = \int\left(\nabla\times\mathbf{v}\right)\cdot\mathbf{v}\,\mathrm{d}^3r = \int\boldsymbol{\zeta}\cdot\mathbf{v}\,\mathrm{d}^3r\,, \tag{1.35}$$

while the average helicity density is given by

$$h_\mathrm{K} = \frac{\mathfrak{H}_\mathrm{K}}{V} = \frac{1}{V}\int\left(\nabla\times\mathbf{v}\right)\cdot\mathbf{v}\,\mathrm{d}^3r = \frac{1}{V}\int\boldsymbol{\zeta}\cdot\mathbf{v}\,\mathrm{d}^3r\,. \tag{1.36}$$

1.1.1.4 Electromagnetic Potentials

There is a way to formulate Maxwell's Equations in a more elegant way, namely by using the electromagnetic potentials,

$$\mathbf{E} = -\nabla\phi - \partial_t\mathbf{A}\,, \tag{1.37}$$

$$\mathbf{B} = \nabla\times\mathbf{A}\,, \tag{1.38}$$

where ϕ is the scalar and $\mathbf{A}$ the (magnetic) vector potential, respectively. The latter can be introduced from the idea that since, according to (1.3), it is $\nabla\cdot\mathbf{B} = 0$, using (A.9), there has to be some vector field for which (1.38) is true such that $\mathbf{A}$ is exactly the magnetic vector potential introduced above. However, one has to keep in mind that this definition for $\mathbf{A}$ is not unique as it is possible to change it by an arbitrary scalar function ψ in the form

$$\mathbf{A}' = \mathbf{A} + \nabla\psi \tag{1.39}$$

without changing the magnetic field itself since it is

$$\mathbf{B}' = \nabla \times \mathbf{A}' = \nabla \times (\mathbf{A} + \nabla\psi) = \nabla \times \mathbf{A} + \nabla \times (\nabla\psi) \overset{(A.8)}{=} \nabla \times \mathbf{A} = \mathbf{B}\,. \tag{1.40}$$

Therefore, by choosing a specific function ψ one fixes the so-called gauge of the magnetic vector potential $\mathbf{A}$. The most widely used gauge fixings are, on the one hand, the Lorentz Gauge, given by

$$\nabla \cdot \mathbf{A} = -\frac{\partial\phi}{\partial t}\,, \tag{1.41}$$

and, on the other hand, the Coulomb Gauge (also called Radiation or Transversal Gauge), fulfilling the condition

$$\nabla \cdot \mathbf{A} = 0\,. \tag{1.42}$$

Throughout this work, unless noted otherwise, Coulomb Gauge is used. For further reading see [12, 13].

As it will be needed later on, it is important to investigate the evolution of the magnetic vector potential with time. To derive it, one has to look at the third line of (1.12),

$$\partial_t \mathbf{B} = -\frac{1}{4\pi\sigma}\nabla \times (\nabla \times \mathbf{B}) + \nabla \times (\mathbf{v} \times \mathbf{B}) = \nabla \times \left[-\frac{1}{4\pi\sigma}(\nabla \times \mathbf{B}) + \mathbf{v} \times \mathbf{B}\right]\,, \tag{1.43}$$

from which, as it is $\mathbf{B} = \nabla \times \mathbf{A}$, one can directly deduce

$$\partial_t \mathbf{A} = -\frac{1}{4\pi\sigma}(\nabla \times \mathbf{B}) + \mathbf{v} \times \mathbf{B}\,. \tag{1.44}$$

A final remark, important for the calculations carried out in the following, has to be made. Applying the Fourier Transform to (1.38) and using (A.23) results in

$$\hat{\mathbf{B}} = i\mathbf{k} \times \hat{\mathbf{A}}\,. \tag{1.45}$$

With Coulomb Gauge, given by (1.42), this can be transformed into

$$\hat{\mathbf{A}} = i\frac{\mathbf{k}}{k^2} \times \hat{\mathbf{B}}\,, \tag{1.46}$$

which gives the direct relation between the Fourier Transforms of the magnetic field and the magnetic vector potential. In $\mathbf{r}$-space this relation has a more complex form which is given by the Biot-Savart Law, reading [12]

$$\mathbf{A}(\mathbf{r}) = \frac{1}{4\pi}\int_V \left(\frac{\mathbf{r}' - \mathbf{r}}{|\mathbf{r}' - \mathbf{r}|^3} \times \mathbf{B}(\mathbf{r}')\right) \mathrm{d}^3 r' \tag{1.47}$$

1.1.1.5 Magnetic Moment

Finally, for the sake of completeness, the magnetic moment $\boldsymbol{\mu}$ should be introduced. It is defined by [12]

$$\boldsymbol{\mu} = \frac{1}{2}\int \mathbf{r} \times \mathbf{j}(\mathbf{r})\,\mathrm{d}^3\mathrm{r} \tag{1.48}$$

and is a useful quantity in electrodynamics as, once calculated, it can be used to compute the magnetic vector potential for a magnetic dipole by

$$\mathbf{A}(\mathbf{r}) = \frac{\boldsymbol{\mu} \times \mathbf{r}}{r^3} \tag{1.49}$$

and the magnetic field by

$$\mathbf{B}(\mathbf{r}) = 3\frac{(\boldsymbol{\mu}\cdot\mathbf{r})\,\mathbf{r}}{r^5} - \frac{\boldsymbol{\mu}}{r^3}\,. \tag{1.50}$$

Therefore the magnetic moment can be regarded as a measure for the strength of a magnetic dipole, which is often a good approximation for a localized current distribution.

1.1.1.6 Energy Considerations

In order to derive the expressions for the energy content of the MHD system it is once again necessary to take a look at the continuity equation (1.6) as well as at the Euler Equations (1.26). Multiplying the former by $\frac{1}{2}\mathbf{v}^2$ and the latter by $\mathbf{v}$ and then adding both gives

$$\frac{1}{2}\mathbf{v}^2\partial_t\rho + \frac{1}{2}\mathbf{v}^2\nabla\cdot(\rho\mathbf{v}) + \rho\mathbf{v}\cdot\partial_t\mathbf{v} + \rho\mathbf{v}\cdot[(\mathbf{v}\cdot\nabla)\,\mathbf{v}] = \mathbf{v}\cdot(\mathbf{j}\times\mathbf{B}) + \mathbf{v}\cdot\mathbf{F}\,. \tag{1.51}$$

The left hand side can be rewritten as

$$\begin{aligned}
&\frac{1}{2}\mathbf{v}^2\partial_t\rho + \frac{1}{2}\mathbf{v}^2\nabla\cdot(\rho\mathbf{v}) + \rho\mathbf{v}\cdot\partial_t\mathbf{v} + \rho\mathbf{v}\cdot[(\mathbf{v}\cdot\nabla)\,\mathbf{v}]\\
&= \left[\frac{1}{2}\mathbf{v}^2\partial_t\rho + \rho\mathbf{v}\cdot\partial_t\mathbf{v}\right] + \left\{\frac{1}{2}\mathbf{v}^2\nabla\cdot(\rho\mathbf{v}) + \rho\mathbf{v}\cdot[(\mathbf{v}\cdot\nabla)\,\mathbf{v}]\right\}\\
&= \partial_t\left(\frac{1}{2}\rho\mathbf{v}^2\right) + \left\{\frac{1}{2}\mathbf{v}^2\nabla\cdot(\rho\mathbf{v}) + \rho\mathbf{v}\cdot[(\mathbf{v}\cdot\nabla)\,\mathbf{v}]\right\}\\
&\overset{(A.4)}{=} \partial_t\left(\frac{1}{2}\rho\mathbf{v}^2\right) + \left\{\frac{1}{2}\mathbf{v}^2\nabla\cdot(\rho\mathbf{v}) + \rho\mathbf{v}\cdot\left[\frac{1}{2}\nabla(\mathbf{v}\cdot\mathbf{v}) - \mathbf{v}\times(\nabla\times\mathbf{v})\right]\right\}\\
&\overset{(A.2)}{=} \partial_t\left(\frac{1}{2}\rho\mathbf{v}^2\right) + \nabla\cdot\left(\frac{1}{2}\mathbf{v}^2\rho\mathbf{v}\right)\,.
\end{aligned} \tag{1.52}$$

On the other hand the first term of the right hand side reads

$$\begin{aligned}
\mathbf{v}\cdot(\mathbf{j}\times\mathbf{B}) = -\mathbf{j}\cdot(\mathbf{v}\times\mathbf{B}) &\overset{(1.11)}{=} -\mathbf{j}\cdot\left(\frac{\mathbf{j}}{\sigma} - \mathbf{E}\right) = \mathbf{j}\cdot\mathbf{E} - \frac{\mathbf{j}^2}{\sigma}\\
&\overset{(1.5)}{=} \frac{1}{4\pi}\left[(\nabla\times\mathbf{B})\cdot\mathbf{E} - (\partial_t\mathbf{E})\cdot\mathbf{E}\right] - \frac{\mathbf{j}^2}{\sigma}\\
&\overset{(A.5)}{=} \frac{1}{4\pi}\left[\mathbf{B}\cdot(\nabla\times\mathbf{E}) - \nabla\cdot(\mathbf{E}\times\mathbf{B}) - (\partial_t\mathbf{E})\cdot\mathbf{E}\right] - \frac{\mathbf{j}^2}{\sigma}\\
&\overset{(1.4)}{=} -\frac{1}{4\pi}\left[\mathbf{B}\cdot\partial_t\mathbf{B} + \nabla\cdot(\mathbf{E}\times\mathbf{B}) + \mathbf{E}\cdot\partial_t\mathbf{E}\right] - \frac{\mathbf{j}^2}{\sigma}\\
&= -\frac{1}{8\pi}\partial_t\left(\mathbf{B}^2 + \mathbf{E}^2\right) - \frac{1}{4\pi}\nabla\cdot(\mathbf{E}\times\mathbf{B}) - \frac{\mathbf{j}^2}{\sigma}\,.
\end{aligned} \tag{1.53}$$

Plugging (1.52) and (1.53) into (1.51), after some minor rearrangements, gives

$$\partial_t\left(\frac{1}{2}\rho\mathbf{v}^2 + \frac{1}{8\pi}\mathbf{B}^2 + \frac{1}{8\pi}\mathbf{E}^2\right) + \nabla\cdot\left(\frac{1}{2}\rho\mathbf{v}^2\mathbf{v} + \frac{1}{4\pi}\mathbf{E}\times\mathbf{B}\right) = -\frac{\mathbf{j}^2}{\sigma} + \mathbf{F}\cdot\mathbf{v}\,, \tag{1.54}$$

respectively, which is the continuity equation for energy. Inside the time derivative there are the expression for the (local) kinetic, magnetic and kinetic energy densities, given by

$$u_\mathrm{K} = \frac{1}{2}\rho\mathbf{v}^2,\; u_B = \frac{1}{8\pi}\mathbf{B}^2,\; u_E = \frac{1}{8\pi}\mathbf{E}^2\,, \tag{1.55}$$

while inside the divergence there are the kinetic energy flux $\frac{1}{2}\rho\mathbf{v}^2\mathbf{v}$ and the electromagnetic energy flux given by the so-called Poynting Vector

$$\mathbf{S} = \frac{1}{4\pi}\mathbf{E}\times\mathbf{B}\,. \tag{1.56}$$

Furthermore, the right hand side of (1.54) gives the energy loss terms, on the one hand the resistive decay, given by $-\mathbf{j}^2/\sigma$, which happens due to finite resistivity, and on the other hand other energy dissipation mechanisms represented by $\mathbf{F}\cdot\mathbf{v}$. Finally, the total energies corresponding to the first two parts of (1.55) (while the energy content of the electric field is omitted in the following due to the considerations discussed above) are given by

$$E_\mathrm{K} = \frac{1}{2}\int \rho\mathbf{v}^2\,\mathrm{d}^3r,\; E_B = \frac{1}{8\pi}\int \mathbf{B}^2\,\mathrm{d}^3r\,. \tag{1.57}$$

Considering the energy content of the fields, a further interesting quantity is the spectral energy density. In order to derive an expression for it, one can rewrite u_B and u_K from (1.55) as averaged energy densities ϵ_B and ϵ_K:

$$\epsilon_B = \frac{1}{V}\int u_B\,\mathrm{d}^3r = \frac{1}{8\pi V}\int \mathbf{B}^2\,\mathrm{d}^3r\,, \tag{1.58}$$

$$\epsilon_\mathrm{K} = \frac{1}{V}\int u_K\,\mathrm{d}^3r = \frac{1}{2V}\int \rho\mathbf{v}^2\,\mathrm{d}^3r\,, \tag{1.59}$$

where V is the total volume of the system.

Using Parseval's Theorem, (A.32), for a constant mass density ρ, these two expressions can be presented in terms of the wavevector $\mathbf{k}$ as

$$\epsilon_B = \tfrac{1}{8\pi V}\textstyle\int \mathbf{B}^2(\mathbf{r})\,\mathrm{d}^3r = \tfrac{1}{8\pi}\int \left|\hat{\mathbf{B}}(\mathbf{k})\right|^2\,\mathrm{d}^3k \equiv \rho\int M_k\,\mathrm{d}k\,, \tag{1.60}$$

$$\epsilon_K = \tfrac{\rho}{2V}\textstyle\int \mathbf{v}^2(\mathbf{r})\,\mathrm{d}^3r = \tfrac{\rho}{2}\int |\hat{\mathbf{v}}(\mathbf{k})|^2\,\mathrm{d}^3k \equiv \rho\int U_k\,\mathrm{d}k\,, \tag{1.61}$$

where for both in the last step a reduction from three to one dimension of the integration have been performed, thus defining the magnetic spectral energy M_k and the kinetic spectral energy U_k. Expressing $\mathbf{k}$ and the corresponding integral, for example, in spherical coordinates (k,ϕ,θ), this would mean

$$M_k = \tfrac{1}{8\pi\rho}\iint \left|\hat{\mathbf{B}}(\mathbf{k})\right|^2 k^2\sin\theta\,\mathrm{d}\phi\mathrm{d}\theta\,, \tag{1.62}$$

$$U_k = \tfrac{1}{2}\iint |\hat{\mathbf{v}}(\mathbf{k})|^2\,k^2\sin\theta\,\mathrm{d}\phi\mathrm{d}\theta\,. \tag{1.63}$$

A further simplification may be found by assuming that the integrands are functions only of the magnitude $k\equiv|\mathbf{k}|$ of the wave vector $\mathbf{k}$. Then the integrals of (1.62) and (1.63) may be evaluated, giving

$$M_k = \tfrac{k^2}{2\rho}|\hat{\mathbf{B}}(k)|^2\,, \tag{1.64}$$

$$U_k = 2\pi k^2|\hat{\mathbf{v}}(k)|^2\,. \tag{1.65}$$

1.1.2 Magnetic Helicity

The Magnetic helicity $\mathfrak{H}$ is defined by

$$\mathfrak{H} = \int_V \mathbf{A}\cdot\mathbf{B}\,\mathrm{d}^3r\,. \tag{1.66}$$

In the original definition of magnetic helicity the boundary of the integration volume V has to be chosen in a way such that no magnetic field lines are crossing the boundary [14], i.e. for the normal component B_n of the magnetic field at the boundary ∂V it is

$$B_\mathrm{n}(\partial V) = 0\,. \tag{1.67}$$

This is also a condition which is assumed to be true throughout this work as then V denotes the volume of the Universe for which the magnetic field can be assumed to vanish at the boundary. However, in general there are also possibilities to drop the restriction (1.67) and investigate the more general case [15].

It should be noted that (1.66) is a consistent definition of a quantity which, in contrast to $\mathbf{A}$ (as shown in Sec. 1.1.1.4), is a well-defined observable since choosing a certain gauge for $\mathbf{A}$ does not change the value of helicity. To see this one has to use

$$\begin{aligned}\mathfrak{H}' &= \int_V \mathbf{A}'\cdot\mathbf{B}\,\mathrm{d}^3r = \int_V (\mathbf{A}+\nabla\chi)\cdot\mathbf{B}\,\mathrm{d}^3r \\ &= \int_V (\mathbf{A}\cdot\mathbf{B} + (\nabla\chi)\cdot\mathbf{B})\,\mathrm{d}^3r = \mathfrak{H} + \int_V (\nabla\chi)\cdot\mathbf{B}\,\mathrm{d}^3r\end{aligned} \tag{1.68}$$

where for the second term of the last equation can write

$$\begin{aligned}\int_V (\nabla\chi)\cdot\mathbf{B}\,\mathrm{d}^3r &\overset{(A.2)}{=} \int_V [\nabla\cdot(\chi\mathbf{B}) - \chi\,(\nabla\cdot\mathbf{B})]\,\mathrm{d}^3r \\ &\overset{(1.3)}{=} \int_V \nabla\cdot(\chi\mathbf{B})\,\mathrm{d}^3r \overset{(A.10)}{=} \oint_{\partial V}\chi\mathbf{B}\cdot\mathrm{d}\mathbf{S}\,,\end{aligned} \tag{1.69}$$

which, however, vanishes due to (1.67) and therefore (1.68) gives $\mathfrak{H}' = \mathfrak{H}$.

Finally, in a similar way as it has been done for the energy content in Sec. 1.1.1.6, it is important to extract the spectral values of helicity. To do so, first the average magnetic helicity density for the total volume V of the system is written down as

$$h_B = \frac{\mathfrak{H}}{V} = \frac{1}{V}\int \mathbf{A}(\mathbf{r})\cdot\mathbf{B}(\mathbf{r})\,\mathrm{d}^3r\,, \tag{1.70}$$

which then, using $\nabla\cdot\mathbf{A} = 0$, i.e. Coulomb Gauge, can be expressed as

$$\begin{aligned}h_B &= \frac{1}{V}\int \mathbf{A}\cdot(\nabla\times\mathbf{A})\,\mathrm{d}^3r = \frac{1}{V}\int \mathbf{A}\cdot\mathbf{B}\,\mathrm{d}^3r \\ &\overset{(1.46),(A.32)}{=} i\int\left(\frac{\mathbf{k}}{k^2}\times\hat{\mathbf{B}}(\mathbf{k})\right)\cdot\hat{\mathbf{B}}(\mathbf{k})^*\,\mathrm{d}^3k \equiv \rho\int\mathcal{H}_k\,\mathrm{d}k\end{aligned} \tag{1.71}$$

for $\rho = \text{const}$, hereby defining the spectral magnetic helicity density $\mathcal{H}_k$. In spherical coordinates it reads

$$\mathcal{H}_k = \frac{i}{\rho}\iint\left(\frac{\mathbf{k}}{k^2}\times\hat{\mathbf{B}}(\mathbf{k})\right)\cdot\hat{\mathbf{B}}(\mathbf{k})^* k^2\sin\theta\,\mathrm{d}\phi\mathrm{d}\theta\,, \tag{1.72}$$

which, assuming, in addition, that the integrand does only depend on the magnitude k of the wavevector $\mathbf{k}$, i.e. $\hat{\mathbf{B}}(\mathbf{k}) = \hat{\mathbf{B}}(k)$, reduces to

$$\mathcal{H}_k = \frac{4\pi i}{\rho}\left(\mathbf{k}\times\hat{\mathbf{B}}(\mathbf{k})\right)\cdot\hat{\mathbf{B}}(\mathbf{k})^*\,. \tag{1.73}$$

As a side remark it should be noted that in a similar way also a spectral kinetic helicity density may be derived, given by

$$\mathcal{H}_k^\mathrm{K} = \frac{4\pi i k^2}{\rho}\,(\mathbf{k}\times\hat{\mathbf{v}}(\mathbf{k}))\cdot\hat{\mathbf{v}}(\mathbf{k})^*\,. \tag{1.74}$$

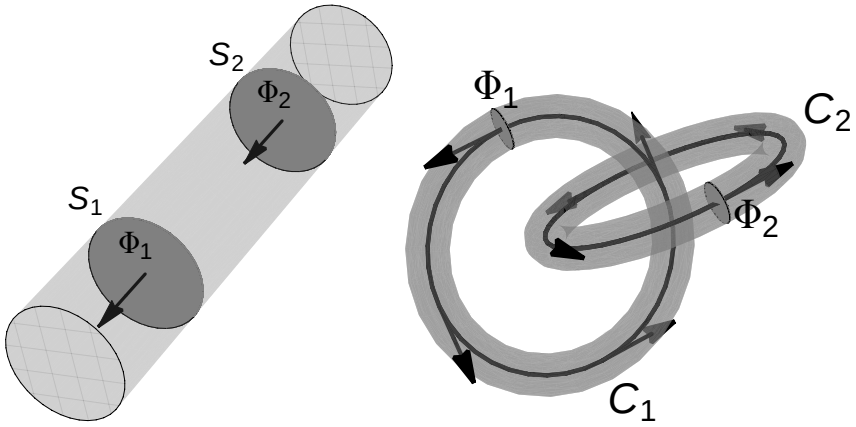

Figure 1.1: *Left panel*: Sketch of a magnetic flux tube with the arrows showing the direction of the magnetic field. For two arbitrary cross sections (S_1 and S_2) the corresponding magnetic fluxes, Φ_1 and Φ_2 turn out to be equal, i.e. $\Phi_1 = \Phi_2$. *Right panel*: Two interconnected flux tubes characterized by the loops C_1 and C_2, having the magnetic flux Φ_1 and Φ_2, respectively, measured at the sketched arbitrary cross sections. The arrows show the direction of the corresponding magnetic fields inside the flux tubes while outside the magnetic field vanishes.

1.1.2.1 Magnetic Helicity and the Topology of the Magnetic Field

The defining equation of helicity, (1.66), contains $\mathbf{A}$, the magnetic vector potential, and $\mathbf{B} = \nabla \times \mathbf{A}$, its curl. Since the latter is a measure of rotation in a given point of space, the scalar product of these two gives a quantitative description of how much $\mathbf{A}$ follows a helical or corkscrew-like topology, therefore also making a statement on the structure of the corresponding magnetic field.

In fact, an even stronger statement can be made by using the concept of magnetic flux tubes as shown in the left panel of Fig. 1.1. A flux tube is defined as a cylinder-like structure for which the magnetic field is tangential everywhere at its lateral surface. This, however, means that the magnetic flux Φ_{lat} through this lateral surface is zero which is also true for the magnetic flux Φ_{tot} of any cut-out of the tube between two arbitrary cross sections (and therefore also for the complete tube) due to the non-existence of magnetic monopoles. Therefore, for two cross-sections S_1 and S_2 with the corresponding magnetic fluxes, as depicted in the left panel of Fig. 1.1, Φ_1 and Φ_2 it is

$$\Phi_{\text{tot}} = \Phi_1 - \Phi_2 + \Phi_{\text{lat}} = \Phi_1 - \Phi_2 + 0 = 0 \tag{1.75}$$

where Φ_1 and Φ_2 have different signs due to the different orientation of the normal vectors of S_1 and S_2 in relation to the magnetic field lines. Thus (1.75) gives $\Phi_1 = \Phi_2$, meaning that the magnetic flux through a given cross section is constant throughout the tube and can be used as the quantity characterizing it.

As has been pointed out by [16], a magnetic field can be regarded, to some extent, as being consisted of an infinite number of such flux tubes, each carrying an infinitesimal amount of flux. This describes the concept of field lines. Therefore some elementary topological considerations may be performed for two flux tubes which then turn out to be applicable to field lines and therefore to magnetic fields in general [17].

Following [17], the situation shown in the right panel of Fig. 1.1 is considered, where one has two interconnected flux tubes labeled 1 and 2, with the magnetic fluxes Φ_1 and Φ_2, respectively, while the magnetic field outside the tubes is zero. The helicity for one

of the flux tubes ($i = 1, 2$) may be calculated as

$$\begin{aligned}\mathfrak{H}_i &\overset{(1.66)}{=} \int_{V_i} \mathbf{A}\cdot\mathbf{B}\,\mathrm{d}^3r = \oint_{C_i} \mathbf{A}\cdot(\Phi_i \mathrm{d}\mathbf{r}) = \Phi_i \oint_{C_i} \mathbf{A}\cdot\mathrm{d}\mathbf{r} \\ &\overset{(A.11)}{=} \Phi_i \int_{C_i} (\nabla\times\mathbf{A})\cdot\mathrm{d}\mathbf{S} \overset{(1.38)}{=} \Phi_i \int_{C_i} \mathbf{B}\cdot\mathrm{d}\mathbf{S}\,,\end{aligned} \tag{1.76}$$

where the integral $\oint_{C_i} ... \mathrm{d}\mathbf{r}$ is to be understood as the line integral along the loop C_i, whereas $\int_{C_i} ... \mathrm{d}\mathbf{S}$ is the surface integral over the surface for which this loop is the border. The integral in the final step of (1.76) gives the flux which passes through the circuit C_i. Since the field outside the tubes is zero, the only flux is given by the one of the interlinked tube, also depending on how many times and in which direction (with respect to the magnetic field lines) they traverse each other, which corresponds exactly to the linkage number of the system. For the situation in the right panel of Fig. 1.1 one would therefore get

$$\int_{C_1} \mathbf{B}\cdot\mathrm{d}\mathbf{S} = \Phi_2\,,\ \int_{C_2} \mathbf{B}\cdot\mathrm{d}\mathbf{S} = \Phi_1\,, \tag{1.77}$$

such that, from (1.70), it is $\mathfrak{H}_1 = \mathfrak{H}_2 = \Phi_1\Phi_2$ and hence the total magnetic helicity is $\mathfrak{H} = \mathfrak{H}_1 + \mathfrak{H}_2 = 2\Phi_1\Phi_2$. This is a remarkable result as the total helicity does not depend on the actual form of the (closed) flux tubes, but only on the corresponding fluxes and the linkage. More generally, for N flux tubes the helicity is given by

$$\mathfrak{H} = \sum_{i=1}^{N}\sum_{j=1}^{N} \mathfrak{L}_{ij}\Phi_i\Phi_j\,, \tag{1.78}$$

where $\mathfrak{L}_{ij}$ is the Linking Number between the closed curves C_i and C_j, given by Gauss' Linking Integral [16]

$$\mathfrak{L}_{ij} = \frac{1}{4\pi}\oint_{C_i}\oint_{C_j} \frac{\mathbf{r}_i - \mathbf{r}_j}{|\mathbf{r}_i - \mathbf{r}_j|}\cdot(\mathrm{d}\mathbf{r}_i\times\mathrm{d}\mathbf{r}_j)\,. \tag{1.79}$$

Plugging this into the general summand of (1.78) gives

$$\begin{aligned}\mathfrak{L}_{ij}\Phi_i\Phi_j &= \frac{1}{4\pi}\oint_{C_i}\oint_{C_j} \frac{\mathbf{r}_i - \mathbf{r}_j}{|\mathbf{r}_i - \mathbf{r}_j|}\cdot(\Phi_i\mathrm{d}\mathbf{r}_i\times\Phi_j\mathrm{d}\mathbf{r}_j) \\ &= \frac{1}{4\pi}\int_{V_i}\int_{V_j} \frac{\mathbf{r}_i - \mathbf{r}_j}{|\mathbf{r}_i - \mathbf{r}_j|}\cdot\big(\mathbf{B}(\mathbf{r}_i)\mathrm{d}^3r_i\times\mathbf{B}(\mathbf{r}_j)\mathrm{d}^3r_j\big) \\ &= \frac{1}{4\pi}\int_{V_i}\int_{V_j} \frac{\mathbf{r}_i - \mathbf{r}_j}{|\mathbf{r}_i - \mathbf{r}_j|}\cdot\big(\mathbf{B}(\mathbf{r}_i)\times\mathbf{B}(\mathbf{r}_j)\,\mathrm{d}^3r_i\mathrm{d}^3r_j\big) \\ &\overset{(1.47)}{=} \int_{V_j}\mathbf{B}(\mathbf{r}_j)\cdot\mathbf{A}(\mathbf{r}_j)\,\mathrm{d}^3r_j = -\int_{V_i}\mathbf{B}(\mathbf{r}_i)\cdot\mathbf{A}(\mathbf{r}_i)\,\mathrm{d}^3r_i\,,\end{aligned} \tag{1.80}$$

giving exactly the formula for the partial helicities as in (1.66). Hence, taking the infinitesimal limit of (1.78), i.e. going from the flux tube picture to actual field lines, one indeed sees the general direct connection between the Linking Number (and therefore the topology) of a magnetic field and its helicity.

1.1.2.2 Conservation of Magnetic Helicity

In addition to the mentioned above properties of magnetic helicity which make it a consistent quantity, there are two more which make it physically relevant and of which

both have been proven by [18] for the first time. The first of the two is the conservation law for magnetic helicity which will be presented in the following. Starting with the time derivative of (1.66) it is

$$\frac{\mathrm{d}\mathfrak{H}}{\mathrm{d}t} = \int_V \frac{\partial}{\partial t}\left(\mathbf{A}\cdot\mathbf{B}\right)\mathrm{d}^3r = \int_V \frac{\partial \mathbf{A}}{\partial t}\cdot\mathbf{B}\,\mathrm{d}^3r + \int_V \mathbf{A}\cdot\frac{\partial \mathbf{B}}{\partial t}\,\mathrm{d}^3r\,, \tag{1.81}$$

which, using (1.12) and (1.44), can be transformed into

$$\begin{aligned}
\frac{\mathrm{d}\mathfrak{H}}{\mathrm{d}t} &= \int_V \left[-\frac{\nabla\times\mathbf{B}}{4\pi\sigma} + \mathbf{v}\times\mathbf{B}\right]\cdot\mathbf{B}\,\mathrm{d}^3r + \int_V \mathbf{A}\cdot\left[-\frac{\nabla\times(\nabla\times\mathbf{B})}{4\pi\sigma} + \nabla\times(\mathbf{v}\times\mathbf{B})\right]\mathrm{d}^3r \\
&\overset{(A.7),(1.3)}{=} \int_V \mathbf{A}\cdot\left[\nabla\times(\mathbf{v}\times\mathbf{B})\right]\mathrm{d}^3r - \frac{1}{4\pi\sigma}\int_V\left[(\nabla\times\mathbf{B})\cdot\mathbf{B} - \mathbf{A}\cdot\Delta\mathbf{B}\right]\mathrm{d}^3r \\
&\overset{(A.5),(1.38)}{=} \int_V \nabla\cdot\left[(\mathbf{v}\times\mathbf{B})\times\mathbf{A}\right]\mathrm{d}^3r - \frac{1}{4\pi\sigma}\int_V\left[(\nabla\times\mathbf{B})\cdot\mathbf{B} - \mathbf{A}\cdot\Delta\mathbf{B}\right]\mathrm{d}^3r \\
&\overset{(A.10)}{=} \oint_{\partial V}\left[(\mathbf{v}\times\mathbf{B})\times\mathbf{A}\right]\cdot\mathrm{d}\mathbf{S} - \frac{1}{4\pi\sigma}\int_V\left[(\nabla\times\mathbf{B})\cdot\mathbf{B} - \mathbf{A}\cdot\Delta\mathbf{B}\right]\mathrm{d}^3r\,,
\end{aligned} \tag{1.82}$$

where $(\mathbf{v}\times\mathbf{B})\cdot\mathbf{B} = 0$ has been used. The first term in (1.82) vanishes due to (1.67), while the second one is zero if one assumes $\sigma\to\infty$. Under these conditions therefore it is

$$\frac{\mathrm{d}\mathfrak{H}}{\mathrm{d}t} = 0\,, \tag{1.83}$$

i.e. magnetic helicity is conserved, which is also known as First Woltjer Theorem.

1.1.2.3 Magnetic Helicity and Plasma Relaxation

The second of the two properties of helicity mentioned above, also known as Second Woltjer Theorem, deals with the energy content of the magnetic field. If its minimum shall be found, one has to use variational calculus on the second part of (1.57), minding, however, (1.83) by including the Lagrange Multiplier λ which, together with (1.66), gives

$$\delta E_B - \frac{\lambda}{8\pi}\delta\mathfrak{H} = \frac{1}{8\pi}\int_V 2\mathbf{B}\cdot\delta\mathbf{B}\,\mathrm{d}^3r - \frac{\lambda}{8\pi}\int_V\left(\delta\mathbf{A}\cdot\mathbf{B} + \mathbf{A}\cdot\delta\mathbf{B}\right)\mathrm{d}^3r = 0\,. \tag{1.84}$$

Now it is

$$\begin{aligned}
&\int_V \mathbf{A}\cdot\delta\mathbf{B}\,\mathrm{d}^3r = \int_V \mathbf{A}\cdot(\nabla\times\delta\mathbf{A})\,\mathrm{d}^3r \overset{(A.5)}{=} \int_V\left[\nabla\cdot(\delta\mathbf{A}\times\mathbf{A}) + \delta\mathbf{A}\cdot(\nabla\times\mathbf{A})\right]\mathrm{d}^3r \\
&= \int_V\left[\nabla\cdot(\delta\mathbf{A}\times\mathbf{A}) + \delta\mathbf{A}\cdot\mathbf{B}\right]\mathrm{d}^3r = \int_V \delta\mathbf{A}\cdot\mathbf{B}\,\mathrm{d}^3r\,,
\end{aligned} \tag{1.85}$$

where for the last step Gauss' Theorem, (A.10), and the fact that the variation vanishes on the surface have been used. Plugging this into (1.84) gives

$$\frac{1}{8\pi}\int_V\left[2\mathbf{B}\cdot\delta\mathbf{B} - 2\lambda\mathbf{A}\cdot\delta\mathbf{B}\right]\mathrm{d}^3x = 0 \tag{1.86}$$

and therefore (1.84) is satisfied if

$$\mathbf{B} = \lambda\mathbf{A} \tag{1.87}$$

or, after applying the curl operator on both sides,

$$\nabla \times \mathbf{B} = \lambda \mathbf{B}\,. \tag{1.88}$$

The physical meaning of this expression has been first recognized by [19]. For a plasma with high conductivity one can take the magnetic helicity to be constant according to (1.83) which determines the value of λ in (1.87). Under this assumption magnetic energy approaches its minimum while the corresponding magnetic field, according to (1.88), becomes force-free – a phenomenon known as plasma relaxation. Following that, even if the conductivity is finite (but still very large), resistive decay affects magnetic energy more efficient than it affects magnetic helicity. The result is that even then helicity is still almost constant while the energy is acquiring its minimal value. This is in particular important for astrophysical applications.

1.1.2.4 Maximal Helicity

There is another interesting connection between the total magnetic energy and helicity of a system. It can be seen by rewriting (1.60) as

$$\epsilon_B = \frac{1}{8\pi}\int |\hat{\mathbf{B}}(\mathbf{k})|^2\,\mathrm{d}^3k \overset{(1.45)}{=} \frac{1}{8\pi}\int |i\mathbf{k}\times\hat{\mathbf{A}}(\mathbf{k})|^2\,\mathrm{d}^3k = \frac{1}{8\pi}\int |\mathbf{k}\times\hat{\mathbf{A}}(\mathbf{k})|^2\,\mathrm{d}^3k\,. \tag{1.89}$$

Here it is now possible to decompose $\hat{\mathbf{A}}$ in the form [20]

$$\hat{\mathbf{A}}(\mathbf{k}) = a^+_{\mathbf{k}} h^+_{\mathbf{k}} + a^-_{\mathbf{k}} h^-_{\mathbf{k}} + a^{\mathrm{l}}_{\mathbf{k}} h^{\mathrm{l}}_{\mathbf{k}} \tag{1.90}$$

where $h^\pm_{\mathbf{k}}$ are the eigenfunctions of the curl operator, i.e.

$$i\mathbf{k}\times h^\pm_{\mathbf{k}} = \pm k h^\pm_{\mathbf{k}}\,, \tag{1.91}$$

given by

$$h^\pm_{\mathbf{k}} = \frac{1}{\sqrt{2}}\frac{\mathbf{k}\times(\mathbf{k}\times\mathbf{e}) \mp ik\,(\mathbf{k}\times\mathbf{e})}{k^2\left(1-\frac{(\mathbf{k}\cdot\mathbf{e})^2}{k^2}\right)^{\frac{1}{2}}} \tag{1.92}$$

for an arbitrary unit vector $\mathbf{e} \nparallel \mathbf{k}$, and $a^{\mathrm{l}}_{\mathbf{k}} h^{\mathrm{l}}_{\mathbf{k}}$ is the longitudinal part which, however, vanishes for Coulomb Gauge. The actual form of the $h^\pm_{\mathbf{k}}$, given by (1.92), is not important for the following calculations, but rather the fact that they satisfy (1.91) and the following relations (which can be shown by plugging in):

$$h^+_{\mathbf{k}}\cdot h^{+*}_{\mathbf{k}} = h^-_{\mathbf{k}}\cdot h^{-*}_{\mathbf{k}} = 1\,,\; h^+_{\mathbf{k}}\cdot h^{-*}_{\mathbf{k}} = h^-_{\mathbf{k}}\cdot h^{+*}_{\mathbf{k}} = 0\,. \tag{1.93}$$

Finally, $a^+_{\mathbf{k}}$, $a^-_{\mathbf{k}}$ and $a^{\mathrm{l}}_{\mathbf{k}}$ are some complex coefficients which depend on $\mathbf{k}$ (and on the time t). Using (1.60) together with (1.89), one can now write down an expression for M_k in terms of the decomposition of $\hat{\mathbf{A}}$:

$$\begin{aligned} M_k &= \frac{k^2}{2\rho}\left|\mathbf{k}\times\hat{\mathbf{A}}(\mathbf{k})\right|^2 \overset{(1.90)}{=} \frac{k^2}{2\rho}\left|\mathbf{k}\times\left(a^+_{\mathbf{k}}h^+_{\mathbf{k}} + a^-_{\mathbf{k}}h^-_{\mathbf{k}}\right)\right|^2 \\ &\overset{(1.91)}{=} \frac{k^2}{2\rho}\left|k\left(a^+_{\mathbf{k}}h^+_{\mathbf{k}} - a^-_{\mathbf{k}}h^-_{\mathbf{k}}\right)\right|^2 \overset{(1.93)}{=} \frac{k^4}{2\rho}\left(\left|a^+_{\mathbf{k}}\right|^2 + \left|a^-_{\mathbf{k}}\right|^2\right)\,. \end{aligned} \tag{1.94}$$

In the same manner (1.71) becomes

$$\begin{aligned} h_B &= \int \hat{\mathbf{A}}(\mathbf{k}) \cdot \hat{\mathbf{B}}(\mathbf{k})^* \mathrm{d}^3k \overset{(1.45)}{=} \int \hat{\mathbf{A}}(\mathbf{k}) \cdot \left(i\mathbf{k} \times \hat{\mathbf{A}}(\mathbf{k}) \right)^* \mathrm{d}^3k \\ &\overset{(1.90)}{=} \int \left[a_{\mathbf{k}}^+ h_{\mathbf{k}}^+ + a_{\mathbf{k}}^- h_{\mathbf{k}}^- \right] \cdot \left[i\mathbf{k} \times \left(a_{\mathbf{k}}^+ h_{\mathbf{k}}^+ + a_{\mathbf{k}}^- h_{\mathbf{k}}^- \right) \right]^* \mathrm{d}^3k \\ &\overset{(1.91)}{=} \int \left[a_{\mathbf{k}}^+ h_{\mathbf{k}}^+ + a_{\mathbf{k}}^- h_{\mathbf{k}}^- \right] \cdot \left[a_{\mathbf{k}}^+ k h_{\mathbf{k}}^+ - a_{\mathbf{k}}^- k h_{\mathbf{k}}^- \right]^* \mathrm{d}^3k \\ &= \int k \left(\left| a_{\mathbf{k}}^+ \right|^2 \left| h_{\mathbf{k}}^+ \right|^2 - \left| a_{\mathbf{k}}^- \right|^2 \left| h_{\mathbf{k}}^- \right|^2 \right) \mathrm{d}^3k \overset{(1.93)}{=} \int k \left(\left| a_{\mathbf{k}}^+ \right|^2 - \left| a_{\mathbf{k}}^- \right|^2 \right) \mathrm{d}^3k \end{aligned} \tag{1.95}$$

and therefore, from (1.71),

$$\mathcal{H}_k = \frac{4\pi k^2}{\rho} \left[\hat{\mathbf{A}}(\mathbf{k}) \cdot \left(i\mathbf{k} \times \hat{\mathbf{A}}(\mathbf{k}) \right)^* \right] = \frac{4\pi k^3}{\rho} \left(\left| a_{\mathbf{k}}^+ \right|^2 - \left| a_{\mathbf{k}}^- \right|^2 \right) . \tag{1.96}$$

Since, furthermore, it is $-\left|a_{\mathbf{k}}^+\right|^2 \leq \left|a_{\mathbf{k}}^+\right|^2$ and $-\left|a_{\mathbf{k}}^-\right|^2 \leq \left|a_{\mathbf{k}}^-\right|^2$, such that

$$\left|a_{\mathbf{k}}^-\right|^2 - \left|a_{\mathbf{k}}^+\right|^2 \leq \left|a_{\mathbf{k}}^-\right|^2 + \left|a_{\mathbf{k}}^+\right|^2 , \; \left|a_{\mathbf{k}}^+\right|^2 - \left|a_{\mathbf{k}}^-\right|^2 \leq \left|a_{\mathbf{k}}^+\right|^2 + \left|a_{\mathbf{k}}^-\right|^2 , \tag{1.97}$$

one can write

$$\left| \left|a_{\mathbf{k}}^-\right|^2 - \left|a_{\mathbf{k}}^+\right|^2 \right| = \max \left(\left|a_{\mathbf{k}}^-\right|^2 - \left|a_{\mathbf{k}}^+\right|^2 , \left|a_{\mathbf{k}}^+\right|^2 - \left|a_{\mathbf{k}}^-\right|^2 \right) \leq \left|a_{\mathbf{k}}^+\right|^2 + \left|a_{\mathbf{k}}^-\right|^2 \tag{1.98}$$

which, according to (1.94) and (1.96), means

$$\left| \frac{\rho}{4\pi k^3} \mathcal{H}_k \right| \leq \frac{2\rho}{k^4} M_k \tag{1.99}$$

or

$$|\mathcal{H}_k| \leq \frac{8\pi}{k} M_k \, , \tag{1.100}$$

such that for a given wavenumber the spectral helicity density has a maximum value determined by the spectral magnetic energy density. This is also known as the realizability condition and is a crucial result as it sets limits to the possible initial conditions for helicity. For a maximally helical field it is therefore

$$\mathcal{H}_k = \pm \frac{8\pi}{k} M_k \, . \tag{1.101}$$

1.1.3 Statistical Treatment of Turbulence

In most MHD scenarios in astrophysics one has to deal with turbulence. Although numerous efforts have been made to find a decent understanding, to the present day its nature remains a mystery. Even giving a clear definition for turbulence is difficult. The usual procedure is to give a number of (magneto)hydrodynamic properties which every turbulent motion does possess. A possible, but debatable and not exhausting list of these properties is [21–23]: *Randomness* (or *irregularity*) which describes the fact that turbulent flows are chaotic and unpredictable in detail both in space and time, such that statistic methods as described in this section are needed; a *large Reynolds Number* since for values of $\mathcal{R}$ above some critical value the system is sensitive to even small perturbations which then produces turbulence; *cascading*, a phenomenon describing the fact that usually initially large eddies are produced which then, due to the instability

of the system, decay to smaller ones which then again decay, and so on, until molecular viscosity stops the process. It should be mentioned that more formal definitions can be given in the context of mathematical physics [24–26] which, however, are not used in this work.

Due to the properties mentioned above a deterministic description of turbulence is not possible. Therefore one has to use statistical methods which will be presented in the following.

1.1.3.1 The Ensemble Average

One of the most important tools in statistical physics is the averaging process. In general, averaging some quantity a, i.e. finding its mean value, denoted by $\langle a \rangle$, has to obey the so-called Reynolds Conditions [27] in order to be well-defined. For some quantities a and b, to which the average operation may be applied, and a constant c it is

$$\langle a + b \rangle = \langle a \rangle + \langle b \rangle \,, \qquad \langle ca \rangle = c \langle a \rangle \,, \tag{1.102}$$

$$\left\langle \frac{\partial a}{\partial t} \right\rangle = \frac{\partial}{\partial t} \langle a \rangle \,, \quad \left\langle \frac{\partial a}{\partial x_i} \right\rangle = \frac{\partial}{\partial x_i} \langle a \rangle \,, \tag{1.103}$$

$$\langle \langle a \rangle \, b \rangle = \langle a \rangle \langle b \rangle \,, \tag{1.104}$$

where the first line means linearity and the second one denotes commutativity of the average operator and the time or gradient derivative.

There is, of course, a large range of different methods of averaging. In the following, however, the so-called ensemble average is used which, for some given boundary conditions, takes into account all possible (Gaussian distributed) realizations $a^{(i)}$ of a given turbulent quantity a, such that it is defined by [28]

$$\langle a \rangle = \lim_{n \to \infty} \frac{1}{n} \sum_{i=1}^{n} a^{(i)} \,. \tag{1.105}$$

In this work, unless noted otherwise, chevrons ($\langle ... \rangle$) indicate the ensemble average.

It should be noted, however, that in reality it is of course impossible to measure an infinite number of possible realizations – even in the laboratory their number is limited, while the situation for astrophysics is even more problematic since here the boundary conditions cannot be controlled at all. Hence, the solution here is to use some other, more accessible kind of average, like the one taken over time or over space, and assume that at some point it converges towards the ensemble average. Whether this assumption, known as the Ergodic Hypothesis, is valid, is a non-trivial question in statistical physics which cannot be answered easily and often not at all. In the following, however, it is assumed to be true as usually done in this context.

1.1.3.2 Homogeneous Isotropic Turbulence

The impact of the claim of both homogeneity and isotropy can be seen best for the correlation function which, for some quantity $\mathbf{a}$, in the most general case is given by the ensemble average

$$\mathcal{C}_{ijk\ldots}\left(\mathbf{r}', \mathbf{r}'', \mathbf{r}''', ...\right) = \left\langle a_i(\mathbf{r}') a_j(\mathbf{r}'') a_k(\mathbf{r}''') ... \right\rangle \,, \tag{1.106}$$

where the a_i are the components of $\mathbf{a}$. In the following the simplest case, given by

$$\mathcal{C}_{ij}\left(\mathbf{r}', \mathbf{r}''\right) = \left\langle a_i(\mathbf{r}') a_j(\mathbf{r}'') \right\rangle \,, \tag{1.107}$$

will be used and furthermore the divergence-free case, i.e. $\nabla \cdot \mathbf{a} = 0$, is assumed. Now homogeneity has the consequence that $\mathcal{C}$ can only depend on $\mathbf{r} \equiv \mathbf{r}'' - \mathbf{r}'$, the difference between the two coordinates, while isotropy puts even stricter constraints, namely that $\mathcal{C}$ may only depend on $r = |\mathbf{r}| = |\mathbf{r}'' - \mathbf{r}'|$, where r is called the correlation length of the turbulence [29]. Therefore one can write

$$\mathcal{C}_{ij}\left(\mathbf{r}', \mathbf{r}''\right) = \mathcal{C}_{ij}\left(r\right) = \left\langle a_i(\mathbf{r}') a_j(\mathbf{r}'') \right\rangle \tag{1.108}$$

and, since it is $\nabla \cdot \mathbf{a} = 0$, also

$$\frac{\partial \mathcal{C}_{ij}}{\partial r_i} = \frac{\partial \mathcal{C}_{ij}}{\partial r_j} = \frac{\partial \left\langle a_i(\mathbf{r}') a_j(\mathbf{r}' + \mathbf{r}) \right\rangle}{\partial r_j} = \left\langle a_i(\mathbf{r}') \frac{\partial a_j(\mathbf{r}' + \mathbf{r})}{\partial r_j} \right\rangle = 0\,. \tag{1.109}$$

According to Noether's Theorem, isotropy may also be interpreted as the claim for rotation invariance. This can be achieved by describing $\mathbf{a}$ with respect to some arbitrary directions, given by some unit vectors $\mathbf{u}$ and $\mathbf{w}$, rather than by fixed coordinate axes. Therefore the correlation has now to be calculated for the quantities $\mathbf{u} \cdot \mathbf{a}$ and $\mathbf{w} \cdot \mathbf{a}$, i.e.

$$\begin{aligned} \mathcal{C}(\mathbf{r}, \mathbf{u}, \mathbf{w}) &= \left\langle \left(\mathbf{u} \cdot \mathbf{a}(\mathbf{r}')\right) \left(\mathbf{w} \cdot \mathbf{a}(\mathbf{r}'')\right) \right\rangle = \left\langle u_i a_i(\mathbf{r}') w_j a_j(\mathbf{r}'') \right\rangle \\ &\overset{(1.102)}{=} u_i w_j \left\langle a_i(\mathbf{r}') a_j(\mathbf{r}'') \right\rangle = u_i w_j \mathcal{C}_{ij}(r)\,. \end{aligned} \tag{1.110}$$

Now, in order to be isotropic, this relation should not change under rotations or, more general, under orthogonal transformations. To be more formal [30], if the vectors $\mathbf{u}$, $\mathbf{w}$ and $\mathbf{r}$ are all transformed by some orthogonal matrix O, i.e.

$$\mathbf{r}^{\mathrm{rot}} = O^{\dagger}\mathbf{r}\,,\ \mathbf{u}^{\mathrm{rot}} = O^{\dagger}\mathbf{u}\,,\ \mathbf{w}^{\mathrm{rot}} = O^{\dagger}\mathbf{w}\,, \tag{1.111}$$

then the claim for isotropy means that

$$\mathcal{C}(\mathbf{r}, \mathbf{u}, \mathbf{w}) = \mathcal{C}(\mathbf{r}^{\mathrm{rot}}, \mathbf{u}^{\mathrm{rot}}, \mathbf{w}^{\mathrm{rot}})\,. \tag{1.112}$$

Applying this to (1.110) means that now rotation invariant quantities have to be constructed of combinations of $\mathbf{r}$, $\mathbf{u}$ and $\mathbf{w}$. All these combinations can, however, be reduced to elementary ones: Taking into account only one vector would lead to the expressions $\mathbf{u}^2 = 1$, $\mathbf{w}^2 = 1$ and $\mathbf{r}^2$, i.e. the trivial ones. The combination of two vectors of the set leads to products, i.e. $\mathbf{r} \cdot \mathbf{u}$, $\mathbf{r} \cdot \mathbf{w}$ and $\mathbf{u} \cdot \mathbf{w}$, and, finally, three vectors can form a triple product, i.e. $\mathbf{u} \cdot (\mathbf{w} \times \mathbf{r})$. Therefore, the most general ansatz for $\mathcal{C}$ is given by

$$\begin{aligned} \mathcal{C}(\mathbf{r}, \mathbf{u}, \mathbf{w}) &= \alpha(r)\left(\mathbf{r} \cdot \mathbf{u}\right)\left(\mathbf{r} \cdot \mathbf{w}\right) + \beta(r)\left(\mathbf{u} \cdot \mathbf{w}\right) + \gamma(r)\mathbf{u} \cdot (\mathbf{w} \times \mathbf{r}) \\ &= \alpha(r) r_i u_i r_j w_j + \beta(r) u_i w_i + \gamma(r) \epsilon_{ijn} u_i w_j r_n \end{aligned} \tag{1.113}$$

Comparing this expression to (1.110) then finally gives the generic form of the general approach for the correlation function [31, 32]:

$$\mathcal{C}_{ij} = \alpha(r) r_i r_j + \beta(r)\delta_{ij} + \gamma(r)\epsilon_{ijn} r_n\,. \tag{1.114}$$

This relation may be decomposed into a longitudinal ("l") and an transversal ("t") part by keeping in mind that for a fixed r it is $r_{\mathrm{l}} = r$ and $r_{\mathrm{t}} = 0$ and therefore

$$\mathcal{C}_{\mathrm{l}} \equiv \mathcal{C}_{\mathrm{ll}} = \alpha(r) r^2 + \beta(r)\,,\ \mathcal{C}_{\mathrm{t}} \equiv \mathcal{C}_{\mathrm{tt}} = \beta(r)\,, \tag{1.115}$$

such that (1.114) can be rewritten as

$$\mathcal{C}_{ij} = \frac{\mathcal{C}_{\mathrm{l}} - \mathcal{C}_{\mathrm{t}}}{r^2} r_i r_j + \mathcal{C}_{\mathrm{t}}\delta_{ij} + \gamma(r)\epsilon_{ijn} r_n\,, \tag{1.116}$$

where for the divergence-free case considered here $\mathcal{C}_\mathrm{l}$ and $\mathcal{C}_\mathrm{r}$ are related by

$$\mathcal{C}_\mathrm{t} = \mathcal{C}_\mathrm{l} + \frac{1}{2} r \frac{\mathrm{d}\mathcal{C}_\mathrm{l}}{\mathrm{d}r} = \frac{1}{2r} \frac{\mathrm{d}}{\mathrm{d}r} \left(r^2 \mathcal{C}_\mathrm{l} \right) . \tag{1.117}$$

After deriving this result, the next step is to calculate the power spectrum. Since $\mathcal{C}_{ij}$ depends only on the separation r, in Fourier space, given by the Fourier Transform (A.21), for uncorrelated modes it has the form

$$\left\langle \hat{a}_i(\mathbf{k}, t) \cdot \hat{a}_j(\mathbf{k}', t')^* \right\rangle = \frac{(2\pi)^3}{V} \delta_{tt'} \delta^{(3)}(\mathbf{k}' - \mathbf{k}) \mathcal{P}_{ij}(k') \,, \tag{1.118}$$

where, according to the Wiener-Khinchin-Kolmogorov Theorem (cf. Sec. A.3), it is $P(k') \propto \mathcal{F}_{\mathbf{rk}} \left\{ \mathcal{C}_{ij}(r) \right\}$ [32]. Writing this down in a more general way, one gets

$$\mathcal{P}_{ij}(k) = \mathcal{F}_{\mathbf{rk}} \{ \mathcal{C}_{ij}(r) \} = \frac{1}{(2\pi)^{\frac{3}{2}}} \int \mathcal{C}_{ij}(r) e^{-i\mathbf{k}\cdot\mathbf{r}} \mathrm{d}^3 r \,. \tag{1.119}$$

Now, due to similar symmetry arguments as before, $\mathcal{P}_{ij}$ for (1.114) is given by

$$\mathcal{P}_{ij}(k) = \mathcal{P}_1(k) k_i k_j + \mathcal{P}_2(k) \delta_{ij} + \mathcal{P}^\mathrm{H}(k) \epsilon_{ijn} k_n \,, \tag{1.120}$$

which can be further simplified by taking into account (1.109) in Fourier space,

$$k_i \mathcal{P}_{ij}(k) = k_j \mathcal{P}_{ij} = 0 \,. \tag{1.121}$$

Since $\epsilon_{ijn} k_i k_n = \epsilon_{ijn} k_j k_n = 0$ and $k_i k_i = k_j k_j = k^2$, multiplying (1.120) by k_i or k_j and then using (1.121) gives

$$\mathcal{P}_1 k^2 + \mathcal{P}_2 = 0 \tag{1.122}$$

and therefore finally, renaming $\mathcal{P}_2$ into $\mathcal{P}$, (1.120) may be written as

$$\mathcal{P}_{ij}(k) = \left(\delta_{ij} - \frac{k_i k_j}{k^2} \right) \mathcal{P}(k) + \epsilon_{ijn} k_n \mathcal{P}^\mathrm{H}(k) \tag{1.123}$$

which is the most general form of the correlation function for homogeneous and isotropic turbulence in Fourier space.

After this general discussion now the correlators will be related to actual quantities of MHD, namely the velocity and the magnetic fields, $\mathbf{v}$ and $\mathbf{B}$. This is done for the latter by writing down the ensemble average of M_k and $\mathcal{H}_k$,

$$\begin{aligned} \langle M_k \rangle &\overset{(1.64)}{=} \left\langle \frac{k^2}{2\rho} |\hat{\mathbf{B}}(\mathbf{k})|^2 \right\rangle = \frac{k^2}{2\rho} \left\langle \hat{B}_i(\mathbf{k}) \hat{B}_i(\mathbf{k})^* \right\rangle \overset{(1.119)}{=} \frac{k^2}{2\rho} \mathcal{P}^B_{ii}(k) \\ &\overset{(1.123)}{=} \frac{k^2}{2\rho} \left[\left(\delta_{ii} - \frac{k_i k_i}{k^2} \right) \mathcal{P}_B(k) + \epsilon_{iin} k_n \mathcal{P}^\mathrm{H}_B(k) \right] \overset{(A.15)}{=} \frac{k^2}{\rho} \mathcal{P}_B(k) \end{aligned} \tag{1.124}$$

and

$$\begin{aligned} \langle \mathcal{H}_k \rangle &\overset{(1.73)}{=} \left\langle \frac{4\pi i}{\rho} \left(\mathbf{k} \times \hat{\mathbf{B}}(\mathbf{k}) \right) \cdot \hat{\mathbf{B}}(\mathbf{k})^* \right\rangle = \frac{4\pi i}{\rho} \epsilon_{ijn} k_j \left\langle \hat{\mathbf{B}}_n(\mathbf{k}) \hat{\mathbf{B}}_i(\mathbf{k})^* \right\rangle \\ &\overset{(1.119)}{=} \frac{4\pi i}{\rho} \epsilon_{ijn} k_j \mathcal{P}^B_{ni}(k) \overset{(1.123)}{=} \frac{4\pi i}{\rho} \epsilon_{ijn} k_j \left[\left(\delta_{ni} - \frac{k_n k_i}{k^2} \right) \mathcal{P}_B(k) + \epsilon_{nim} k_m \mathcal{P}^\mathrm{H}_B(k) \right] \\ &\overset{(A.14),(A.17)}{=} \frac{4\pi i}{\rho} 2 \delta_{jm} k_j k_m \mathcal{P}^\mathrm{H}_B(k) = \frac{8\pi i}{\rho} k^2 \mathcal{P}^\mathrm{H}_B(k) \,, \end{aligned} \tag{1.125}$$

such that the spectral correlation function (1.123) can be written as

$$\mathcal{P}_{ij}^{\mathrm{B}}(k) = \frac{\rho}{k^2}\left[\left(\delta_{ij} - \frac{k_i k_j}{k^2}\right)\langle M_k\rangle - \frac{i}{8\pi}\epsilon_{ijn}k_n\langle\mathcal{H}_k\rangle\right] \tag{1.126}$$

or, in the full form as in (1.118),

$$\left\langle \hat{B}_i(\mathbf{k},t)\hat{B}_j(\mathbf{k}',t')^*\right\rangle = \frac{(2\pi)^3}{V}\delta_{tt'}\delta^{(3)}(\mathbf{k}'-\mathbf{k})\frac{\rho}{k^2}\left[\left(\delta_{ij} - \frac{k_i k_j}{k^2}\right)\langle M_k\rangle - \frac{i}{8\pi}\epsilon_{ijn}k_n\langle\mathcal{H}_k\rangle\right]. \tag{1.127}$$

In an equivalent way this can also be done for the kinetic energy: Here the ensemble averages are

$$\begin{aligned}\langle U_k\rangle &\overset{(1.65)}{=} \left\langle 2\pi k^2|\hat{\mathbf{v}}(\mathbf{k})|^2\right\rangle = 2\pi k^2\langle\hat{v}_i(\mathbf{k})\hat{v}_i(\mathbf{k})^*\rangle \overset{(1.119)}{=} 2\pi k^2\mathcal{P}_{ii}^{\mathrm{K}}(k)\\ &\overset{(1.123)}{=} 2\pi k^2\left[\left(\delta_{ii} - \frac{k_i k_i}{k^2}\right)\mathcal{P}_{\mathrm{K}}(k) + \epsilon_{iin}k_n\mathcal{P}_{\mathrm{K}}^{H}(k)\right] \overset{(A.15)}{=} 4\pi k^2\mathcal{P}_{\mathrm{K}}(k)\end{aligned} \tag{1.128}$$

and

$$\begin{aligned}\left\langle\mathcal{H}_k^{\mathrm{K}}\right\rangle &\overset{(1.74)}{=} \left\langle\frac{4\pi i k^2}{\rho}\left(\mathbf{k}\times\hat{\mathbf{v}}(\mathbf{k})\right)\cdot\hat{\mathbf{v}}(\mathbf{k})^*\right\rangle = \frac{4\pi i k^2}{\rho}\epsilon_{ijn}k_j\langle\hat{\mathbf{v}}_n(\mathbf{k})\hat{\mathbf{v}}_i(\mathbf{k})^*\rangle\\ &\overset{(1.119)}{=} \frac{4\pi i k^2}{\rho}\epsilon_{ijn}k_j\mathcal{P}_{ni}^{\mathrm{K}}(k) \overset{(1.123}{=} \frac{4\pi i k^2}{\rho}\epsilon_{ijn}k_j\left[\left(\delta_{ni} - \frac{k_n k_i}{k^2}\right)\mathcal{P}_{\mathrm{K}}(k) + \epsilon_{nim}k_m\mathcal{P}_{\mathrm{K}}^{\mathrm{H}}(k)\right]\\ &\overset{(A.14),(A.17)}{=} \frac{4\pi i k^2}{\rho}2\delta_{jm}k_j k_m\mathcal{P}_{\mathrm{K}}^{\mathrm{H}}(k) = \frac{8\pi i}{\rho}k^4\mathcal{P}_{\mathrm{K}}^{\mathrm{H}}(k),\end{aligned} \tag{1.129}$$

such that the spectral correlation function (1.123) is given by

$$\mathcal{P}_{ij}^{\mathrm{K}}(k) = \frac{1}{4\pi k^2}\left[\left(\delta_{ij} - \frac{k_i k_j}{k^2}\right)\langle U_k\rangle - \frac{i\rho}{2k^2}\epsilon_{ijn}k_n\left\langle\mathcal{H}_k^{\mathrm{K}}\right\rangle\right] \tag{1.130}$$

or, in the full form as in (1.118),

$$\left\langle\hat{v}_i(\mathbf{k},t)\hat{v}_j(\mathbf{k}',t')^*\right\rangle = \frac{(2\pi)^3}{V}\delta_{tt'}\delta^{(3)}(\mathbf{k}'-\mathbf{k})\frac{1}{4\pi k^2}\left[\left(\delta_{ij} - \frac{k_i k_j}{k^2}\right)\langle U_k\rangle - \frac{i\rho}{2k^2}\epsilon_{ijn}k_n\left\langle\mathcal{H}_k^{\mathrm{K}}\right\rangle\right] \tag{1.131}$$

The equations (1.127) and (1.131) therefore give the remarkable result that the correlation functions of the magnetic and kinetic fields are in their first part directly related to the corresponding spectral energies and in the second part to the corresponding spectral helicities.

1.1.3.3 The Kolmogorov Spectrum

Having the equations from the last sections by hand, the question arises which relation should be plugged in for the initial distribution of velocities depending on the scale k. Usually it is assumed that it follows a power law, i.e.

$$v_{\mathrm{eff}}^2(k) = v_0^2\left(\frac{k}{k_0}\right)^{\alpha}, \tag{1.132}$$

where k_0 corresponds to some scale $L_0 = \frac{2\pi}{k_0}$ on which $v_{\text{eff}} = v_0$ and at which the velocity distribution peaks, such that for $k < k_0$ it is $\alpha > 0$ and for $k > k_0$ it is $\alpha < 0$. There is, however, no final and consistent theory regarding the value of α (cf. Sec. 3.1.3.1). One simple way is to set $\alpha = 3$ for $k < k_0$ which would correspond to a white noise spectrum.

For $k > k_0$ there is a (still unproven) choice for α giving the so-called Kolmogorov spectrum. The basic ideas of this concept have been developed in [33, 34] and [35, 36]. Here [14] is used to give a general overview. It should be noted that the following considerations, due to a lack of a full theory, are just presenting some reasonable arguments which, although partly being confirmed by experiments, by no means claim to give a full consistent explanation of the topic.

In general, due to a large Reynolds Number $\mathcal{R}$, for large turbulences dissipation is not relevant and therefore the main mechanism at work is the cascading of the energy from bigger eddies to smaller ones. There is, however, a lower limit for the size of the eddies, given by the condition that the Reynolds Number is becoming of the order unity, i.e. it is, using (1.10),

$$\nu \simeq v_{\text{s}} L_{\text{s}} \,, \tag{1.133}$$

where L_{s} is the length scale and v_{s} the velocity scale of the smallest eddies. The energy of eddies below this size is dissipated by viscosity.

The main idea of [33–36] is that energy is fed at some rate $\mathcal{E}$ to the largest eddies which are characterized by the velocity v_{l} and the size L_{l}, connected by the relation

$$\mathcal{R} \sim \frac{L_{\text{l}} v_{\text{l}}}{\nu} \gg 1 \,, \tag{1.134}$$

which follows directly from (1.10). The energy then "cascades down", passing the smaller eddies, to those given by (1.133), where the energy is dissipated by the same rate, $\mathcal{E}$, in order to maintain equilibrium. Therefore, the energy transmission rate $\mathcal{E}$ is common to all eddies and it should be possible to express it in terms of the two quantities which characterize an eddy: The size L and the velocity v. For dimensional reasons it can be postulated that the only way to do this is given by

$$\mathcal{E} \sim \frac{v^3}{L} \tag{1.135}$$

or

$$v \sim (\mathcal{E} L)^{\frac{1}{3}} \,. \tag{1.136}$$

This is Kolmogorov's scaling law which states that the velocity scale of a particular eddy is proportional to the cube root of its size. Since this is now regarded as a general law, it is also

$$\mathcal{E} \sim \frac{v_{\text{s}}^3}{L_{\text{s}}} \tag{1.137}$$

for the smallest eddies and therefore, together with (1.133),

$$L_{\text{s}} \sim \left(\frac{\nu^3}{\mathcal{E}}\right)^{\frac{1}{4}} \,, \; v_{\text{s}} \sim (\nu \mathcal{E})^{\frac{1}{4}} \,. \tag{1.138}$$

Combining (1.135) for the largest eddies, i.e. $\mathcal{E} \sim v_{\text{l}}^3 / L_{\text{l}}$, with (1.134) and (1.138), one can now write

$$\frac{L_{\text{l}}}{L_{\text{s}}} \sim \mathcal{R}^{\frac{3}{4}} \,, \; \frac{v_{\text{l}}}{v_{\text{s}}} \sim \mathcal{R}^{\frac{1}{4}} \,, \tag{1.139}$$

which gives a direct relation between the scales of the largest and the smallest eddies with respect to the Reynolds Number $\mathcal{R}$.

Looking at the situation in k-space, one sees that the same way the sizes between L_s and L_l define the range of eddy sizes one is interested in, so the corresponding wavenumbers $k_\mathrm{l} = 2\pi/L_\mathrm{l}$ and $k_\mathrm{s} = 2\pi/L_\mathrm{s}$ do after applying the Fourier Transform. This range is also called the inertial range. Here, the energy transmission is again given by $\mathcal{E}$, however performing the energy transport from the smaller k_l to k_s.

Again, due to dimensional considerations, one can postulate that the spectra of kinetic (U_k) and magnetic (M_k) energies in a turbulent setting are given by

$$U_k \sim M_k \sim \mathcal{E}^{\frac{2}{3}} k^{-\frac{5}{3}} \,. \tag{1.140}$$

The exponent $-5/3$ is the so-called Kolmogorov exponent and is generally regarded as *the* generic exponent for turbulent energy cascading.

However, as mentioned before, this is a rather empirical hypothesis – there is no real proof whether this reasoning is valid or not. Just to give an impression of the controversy it should be mentioned here that, as argued by [37, 38], in a magnetized medium the exponent could be $-3/2$, i.e.

$$U_k \sim M_k \sim \mathcal{E}^{\frac{1}{2}} k^{-\frac{3}{2}} \,. \tag{1.141}$$

1.1.3.4 Isserlis' Theorem

In the previous sections the methods to treat two-point correlation functions, i.e. correlation functions of the type (1.108), have been developed. However, for the following calculations it is also necessary to consider the more general case given by (1.107). The basic idea here is to reduce this more complicated form to the simpler case using Isserlis' Theorem [39, 40] (being a generalization of Wick's Theorem [41] used especially in physics for operator expressions) which states that for a zero-mean multivariate Gaussian distribution vector $(x_1, ..., x_k)$ and linear functions $f_1, ..., f_n$ of $x_1, ..., x_k$ the following expression holds:

$$E(f_1 ... f_n) = \begin{cases} 0, \ n \text{ odd}, \\ \Sigma \left[E(f_{p_1} f_{q_1}) ... E(f_{p_{n/2}} f_{q_{n/2}}) \right], \ n \text{ even}, \end{cases} \tag{1.142}$$

where E denotes the operation of taking the average and in the second case (n even) the sum is understood to be taken over all distinct pairs of x_{p_i}, x_{q_i}, i.e. for all $p_1 < ... < p_{n/2}$ with $p_i < q_i$ for all i. This is a very important result since it means that one can reduce any average of an even number of functions f_i to a product of pair averages.

In order to relate this to the work presented in this thesis one can take E to be the ensemble average, i.e. $E(...) \to \langle ... \rangle$, and then apply this to (1.107) for a four-point correlation function (as this is the most important case in the following) which gives

$$\langle a_i a_j a_k a_l \rangle = \langle a_i a_j \rangle \langle a_k a_l \rangle + \langle a_i a_k \rangle \langle a_j a_l \rangle + \langle a_i a_l \rangle \langle a_j a_k \rangle \,. \tag{1.143}$$

1.2 Cosmology

Cosmology describes the evolution of structures at the largest scales and of the Universe itself. Since under these premises gravity is by far the dominating interaction, General Relativity is the most accepted underlying theory and thus will be presented in Sec. 1.2.1.

Hereafter it is applied in order to derive the dynamics of the Universe over different phases of its evolution, first in a more general and abstract way in Sec. 1.2.2 and then by recapitulating its actual development since the Big Bang in Sec. 1.2.3. The discussion is concluded by a somewhat more detailed discussion of phase transitions in the Early Universe (Sec. 1.2.4) as they may play a major role in the magnetogenesis of Primordial Magnetic Fields.

1.2.1 Basics of General Relativity

In this section the aim is to give some basic information on General Relativity (GR) as far as it is used in this work. For further reference and a more exhaustive treatment see, for example, [42].

The first step from classical theories to GR is to introduce the concept of spacetime coming from Special Relativity by combining both space and time into a single description represented, for example, as a 4-vector, defined as

$$x^\mu = \begin{pmatrix} x^0 \\ x^1 \\ x^2 \\ x^3 \end{pmatrix} = \begin{pmatrix} ct \\ \mathbf{x} \end{pmatrix} . \tag{1.144}$$

This concept is not restricted only to spacetime but can be also used to describe various physical quantities in a compact way, e.g. momentum and energy.

In this formalism an event is a point in the four-dimensional space. In order to measure the separation $\mathrm{d}s$ of two such events, one has to take into account that in general the spacetime is not flat but has a certain structure which is described by the metric tensor g such that it is

$$\mathrm{d}s^2 = c^2\mathrm{d}\tau^2 = g_{\alpha\beta}\mathrm{d}x^\alpha\mathrm{d}x^\beta \,, \tag{1.145}$$

where τ is the so-called proper time, i.e. the time measured by the observer. Here the Einstein Sum Convention is used, for which Greek indices have a range of 0...3, while Latin indices have a range of 1...3.

Now, due to the so-called Relativity Principle, this separation (or interval) has to be the same for all observers, independent of their reference frame, i.e. $\mathrm{d}s^2$, as defined in (1.145), has to stay invariant after switching to a set of coordinates x' given by

$$x'^\mu = \frac{\partial x'^\mu}{\partial x^\nu} x^\nu \,. \tag{1.146}$$

The quantity $g_{\alpha\beta}$ is not a vector as defined before since it has got two indices and is therefore a different geometrical object – a tensor. An even more general object can be therefore defined by a tensor T of rank (m,n) with a total of $m+n$ indices and a behavior under coordinate transformations given by

$$T'^{\alpha_1\ldots\alpha_m}{}_{\beta_1\ldots\beta_n} = \frac{\partial x'^{\alpha_1}}{\partial x^{\mu_1}} \cdots \frac{\partial x'^{\alpha_m}}{\partial x^{\mu_m}} \frac{\partial x^{\nu_1}}{\partial x'^{\beta_1}} \cdots \frac{\partial x^{\nu_n}}{\partial x'^{\beta_n}} T^{\mu_1\ldots\mu_m}{}_{\nu_1\ldots\nu_n} \,. \tag{1.147}$$

As one can see, one has to distinguish between the covariant (lower index) and the contravariant (upper index) components of a tensor due to different kinds of transformations.

As mentioned before, an important tensor in GR is the metric tensor since it directly enters into the definition of the so-called (torsionless) Christoffel Symbols

$$\Gamma^{\alpha}_{\beta\gamma} = \frac{1}{2} g^{\alpha\mu} \left(\frac{\partial g_{\gamma\mu}}{\partial x^{\beta}} + \frac{\partial g_{\beta\mu}}{\partial x^{\gamma}} - \frac{\partial g_{\gamma\beta}}{\partial x^{\mu}} \right) \tag{1.148}$$

in terms of which the main dynamic equation, also known as the Geodesic Equation, may be written in a compact form:

$$\frac{\mathrm{d}^2 x^{\alpha}}{\mathrm{d}\tau^2} + \Gamma^{\alpha}_{\mu\nu} \frac{\mathrm{d}x^{\mu}}{\mathrm{d}\tau} \frac{\mathrm{d}x^{\nu}}{\mathrm{d}\tau} = 0 \,. \tag{1.149}$$

The importance of the metric tensor becomes even more clear since one, as it has been said before, can connect it to the structure of spacetime, more precisely to its curvature. To do so, first one has to define the Riemann Tensor $R^{\alpha}{}_{\beta\gamma\delta}$, given by

$$R^{\alpha}{}_{\beta\gamma\delta} = \frac{\partial \Gamma^{\alpha}_{\beta\delta}}{\partial x^{\gamma}} - \frac{\partial \Gamma^{\alpha}_{\beta\gamma}}{\partial x^{\delta}} + \Gamma^{\alpha}_{\mu\gamma} \Gamma^{\mu}_{\delta\beta} - \Gamma^{\alpha}_{\mu\delta} \Gamma^{\mu}_{\gamma\beta} \,, \tag{1.150}$$

the Ricci Tensor,

$$R_{\alpha\beta} = R^{\mu}{}_{\alpha\beta\mu} \,, \tag{1.151}$$

and the curvature scalar,

$$R = R_{\mu}{}^{\mu} \,, \tag{1.152}$$

using which it is finally possible to write down the Einstein Equations describing the curvature of spacetime by the energy content:

$$G^{\mu\nu} = -\frac{8\pi G}{c^4} T^{\mu\nu} - \Lambda g^{\mu\nu} \tag{1.153}$$

with

$$G^{\mu\nu} \equiv R^{\mu\nu} - \frac{1}{2} g^{\mu\nu} R \tag{1.154}$$

being the so-called Einstein Tensor, G Newton's Gravitational Constant, c the speed of light and $T^{\mu\nu}$ the energy-momentum (or stress-energy) tensor. Assuming that the Universe can be seen as a perfect fluid with density ρ, pressure p and 4-velocity field $v^{\mu} = \mathrm{d}x^{\mu}/\mathrm{d}\tau$, it is given by

$$T^{\mu\nu} = \left(\rho + \frac{p}{c^2} \right) v^{\mu} v^{\nu} - p g^{\mu\nu} \,. \tag{1.155}$$

Finally, Λ is the Cosmological Constant which accounts for the Vacuum Energy as can be seen by defining

$$T^{\mu\nu}_{\mathrm{vac}} \equiv \frac{\Lambda c^4}{8\pi G} g^{\mu\nu} \tag{1.156}$$

such that one can rewrite (1.153) as

$$G^{\mu\nu} \equiv -\frac{8\pi G}{c^4} \left(T^{\mu\nu} + T^{\mu\nu}_{\mathrm{vac}} \right) \,. \tag{1.157}$$

$T^{\mu\nu}_{\mathrm{vac}}$ therefore indeed can be interpreted as an effective energy-momentum tensor for which, comparing it with (1.156), it has to be

$$p = -\rho c^2 \,. \tag{1.158}$$

Since $T^{\mu\nu}_{\mathrm{vac}}$ is proportional to $g^{\mu\nu}$, it is unaltered by Lorentz Transformations and is therefore the same for all observers in Special Relativity. This, in fact, is exactly the requirement for the vacuum and therefore the aforementioned claim is indeed true.

1.2.2 Friedmann Universe

As discussed previously, the Universe is assumed to be homogeneous and isotropic. Therefore, also the treatment in General Relativity and Cosmology has to be in agreement with this assumption. This can be expressed by the structure of the metric which in its general form reads

$$\mathrm{d}s^2 = c^2\mathrm{d}\tau^2 = c^2\mathrm{d}t^2 - a^2(t)\left[\frac{\mathrm{d}r_\mathrm{c}^2}{1-kr_\mathrm{c}^2} + r_\mathrm{c}^2\left(\mathrm{d}\theta^2 + \sin^2\theta\mathrm{d}\phi^2\right)\right] \tag{1.159}$$

and is called the Friedmann-Lemaître-Robertson-Walker (FLRW) metric for which now spherical coordinates are used. r_c is a comoving coordinate and k the parameter of curvature which can have the values -1 (negative curvature, hyperbolic), 0 (vanishing curvature, flat) and $+1$ (positive curvature, spheric).

A quantity of crucial importance is the scale factor a which describes the dynamical evolution of the Universe. In particular, (1.159) is invariant under simultaneous transformations of the type

$$a \to \frac{a}{\lambda}\,,\ r_\mathrm{c} \to \lambda r_\mathrm{c}\ \ k \to \frac{k}{\lambda^2}\,, \tag{1.160}$$

such that usually a is chosen to be dimensionless and equal to 1 at some specific time, e.g. the present. Speaking more descriptively, a relates the *physical* distance r, i.e. the distance between two astrophysical objects which an observer would actually measure, to the so-called *comoving* distance r_c which is defined such that it does not change due to the time evolution (since all explicit time dependence of the metric has been moved to the scale factor) and therefore is cosmologically invariant. This relation is given by

$$r = a(t)r_\mathrm{c}\,. \tag{1.161}$$

In order to derive the time evolution of a, usually, originating from the idea of recession velocities of cosmological objects, the so-called Hubble Parameter H is defined as

$$H \equiv \frac{\partial_t a}{a}\,. \tag{1.162}$$

Some recently measured values of H are, for example, given by $H = 74.3 \pm 2.1\,\mathrm{km\,s^{-1}Mpc^{-1}}$ [43] and $H = 67.3 \pm 1.2\,\mathrm{km\,s^{-1}Mpc^{-1}}$ [44] of which the latter will be used as the default value in calculations. As one can see, these values already differ to some extent which is also true for other measurements due to different techniques but also rather large uncertainties. It should be noted here that sometimes in the literature the so-called Hubble Time $t_H = H^{-1}$ or the so-called Hubble Radius $r_H = cH^{-1}$ are used. Furthermore, the reduced Hubble Parameter h is defined by

$$h = \frac{H}{100\,\frac{\mathrm{km}}{\mathrm{s\,Mpc}}}\,. \tag{1.163}$$

Finally, the scale factor can be related to observations via the redshift z. It is defined by the relation of the frequency f_emit of a signal emitted by an object to the frequency observed, f_obs:

$$\frac{f_\mathrm{emit}}{f_\mathrm{obs}} \equiv 1 + z\,. \tag{1.164}$$

Now the cause of the cosmological redshift is Expansion of the Universe itself, therefore one should look at the comoving distance r_c a signal has travelled, which, from (1.159), is given by

$$r_\mathrm{c} = \int_{t_\mathrm{emit}}^{t_\mathrm{obs}} \frac{c\,\mathrm{d}t}{a(t)} \tag{1.165}$$

and is closely connected to the so-called conformal time η, given by

$$\eta = \int_{t_\mathrm{emit}}^{t_\mathrm{obs}} \frac{\mathrm{d}t}{a(t)}\,. \tag{1.166}$$

As r_c is constant throughout the time, its value should be independent of the emission/observation time (t_{emit}/t_{obs}) of the signal, meaning that

$$\frac{\mathrm{d}t_\mathrm{emit}}{\mathrm{d}t_\mathrm{obs}} = \frac{a(t_\mathrm{emit})}{a(t_\mathrm{obs})} \tag{1.167}$$

and therefore for the frequencies, from (1.164),

$$1 + z = \frac{f_\mathrm{emit}}{f_\mathrm{obs}} = \frac{a(t_\mathrm{obs})}{a(t_\mathrm{emit})}\,. \tag{1.168}$$

Coming back to the discussion of the FLRW metric, one can now plug it into the Einstein Equations (1.153) which results in the Friedmann Equations [42, 45]

$$H^2 \quad = \left(\tfrac{\partial_t a}{a}\right)^2 = \tfrac{8\pi G}{3}\rho - \tfrac{kc^2}{a^2}\,, \tag{1.169}$$

$$\partial_t H + H^2 \quad = \tfrac{\partial_t^2 a}{a} = -\tfrac{4\pi G}{3}\left(\rho + \tfrac{3p}{c^2}\right)\,, \tag{1.170}$$

where a is the scale factor, H the Hubble Parameter (1.162), G Newton's Gravitational Constant, k the parameter of curvature from (1.159), p the pressure and ρ the energy density of the Universe. The latter is usually expressed in terms of a critical density ρ_crit, namely by the definition

$$\Omega \equiv \frac{\rho}{\rho_\mathrm{crit}} = \frac{8\pi G\rho}{3H^2}\,, \tag{1.171}$$

where ρ_crit is obtained by plugging $k = 0$ into (1.169), i.e.

$$\rho_\mathrm{crit} = \frac{3H^2}{8\pi G}\,. \tag{1.172}$$

The total value of Ω is assumed to consist of three contributions: relativistic (hot) matter/radiation (Ω_r), non-relativistic (cold) matter (Ω_m) and vacuum energy (Ω_Λ). While the present value for the contribution from radiation is negligible ($\Omega_\mathrm{r}^\mathrm{pres} \simeq 5.45 \times 10^{-5}$), most recent observations show that for cold (dark and ordinary) matter and vacuum energy they are given by [44] $\Omega_\mathrm{m}^\mathrm{pres} = 0.315^{+0.018}_{-0.016}$ and $\Omega_\Lambda^\mathrm{pres} = 0.685^{+0.016}_{-0.018}$, respectively.

Now it is important to know the scale factor dependence of these three contributions as this will govern the evolution of the Universe itself. According to the First Law of Thermodynamics the expansion of the Universe is an adiabatic process which, under the assumption of thermal equilibrium, obeys the equation

$$T\frac{\mathrm{d}S}{\mathrm{d}t} = \frac{\mathrm{d}U}{\mathrm{d}t} + p\frac{\mathrm{d}V}{\mathrm{d}t} = 0\,, \tag{1.173}$$

where T ist the temperature, S the entropy, U the total energy and V the voulme. If one now takes some value $a = a_0 = 1$ for the scale factor at a given initial time, the relation between the total energy and the energy density is given by the state equation

$$U = \epsilon V \overset{(1.161)}{=} \epsilon V_c a^3 \,, \tag{1.174}$$

where the index 'c', as before, denotes comoving quantities. Therefore (1.174) becomes

$$\frac{\mathrm{d}\left(\epsilon a^3\right)}{\mathrm{d}t} + p\frac{\mathrm{d}a^3}{\mathrm{d}t} = 0 \,. \tag{1.175}$$

In general the relation between the energy density and the pressure for a medium is given by

$$p = \eta\epsilon = \eta\rho c^2 \,, \tag{1.176}$$

where η, in the simplest case, is constant and depends on the scenario one looks at. Plugging this into (1.175) gives

$$\frac{\mathrm{d}\left(\epsilon a^3\right)}{\mathrm{d}t} + \eta\epsilon\frac{\mathrm{d}a^3}{\mathrm{d}t} = \frac{\mathrm{d}}{\mathrm{d}t}\left(\epsilon a^{3(1+\eta)}\right) = 0 \,, \tag{1.177}$$

which means that $\epsilon a^{3(1+\eta)}$ is constant in time and one therefore can write

$$p \propto \epsilon \propto \rho \propto \Omega \propto a^{-3(1+\eta)} \,. \tag{1.178}$$

Now it is known from thermodynamics that for a relativistic gas the relation

$$\epsilon = 3p = 3nk_B T \,, \tag{1.179}$$

where n is the particle number density, holds, meaning $\eta = \frac{1}{3}$, while for cold matter it is $p = 0$ and therefore $\eta = 0$. Finally, for Vacuum Energy the energy density is constant, such that (1.177) in this case results in $\epsilon = -p = \text{const}$ or $\eta = -1$ which also can be directly seen from (1.158). To summarize these considerations it is finally possible to write down (1.178) as

$$p \propto \epsilon \propto \rho \propto \Omega \propto a^{-3(1+\eta)} = \begin{cases} a^{-4} \,, & \text{radiation,} \\ a^{-3} \,, & \text{matter,} \\ a^{0} \,, & \text{Vacuum Energy.} \end{cases} \tag{1.180}$$

Assuming $k = 0$, i.e. a flat Universe, (1.169) gives the time dependence for the scale factor,

$$a \propto \begin{cases} t^{\frac{1}{2}} \,, & \text{radiation,} \\ t^{\frac{2}{3}} \,, & \text{matter,} \\ e^{H_\Lambda t} \,, & \text{Vacuum Energy.} \end{cases} \tag{1.181}$$

with $H_\Lambda \equiv \left(\Lambda c^2/3\right)^{\frac{1}{2}}$ and therefore, again from (1.169), for the Hubble Parameter

$$H \propto \begin{cases} a^{-2} \propto t^{-1} \,, & \text{radiation,} \\ a^{-\frac{3}{2}} \propto t^{-1} \,, & \text{matter,} \\ \text{const} \,, & \text{Vacuum Energy.} \end{cases} \tag{1.182}$$

The latter of these solutions, i.e. the case $a \propto e^{H_\Lambda t}$ and $H = \text{const}$ for Vacuum Energy domination is also known as de Sitter Space.

1.2.3 Evolution of the Early Universe

All observations point towards the conclusion that 13.817 ± 0.048 Gyr [44] before the present spacetime and energy have been created in a process known as the Big Bang. In the following the most important states of the Universe are named and discussed, the time designation always to be understood as the time elapsed after the Big Bang. However, these times are in many cases only estimates with controversial opinions on their exact values.

The **Planck Epoch** has lasted from the Big Bang until one Planck Time $t_{\mathrm{Pl}} = \left(\hbar G/c^5\right)^{\frac{1}{2}} \simeq 5.39 \times 10^{-44}\,\mathrm{s}$ (corresponding to an approximate energy of $T \simeq 10^{28}$ eV) has passed. There can be only very little said about this epoch as the laws of conventional physics are not valid. This is due to the fact that time is assumed to lose its property of being a continuum for times below the Planck Time, therefore resulting in a structure which has to be described in terms of a full Quantum Gravity theory which until the present day has not been found. At the transition to the succeeding epoch gravitation separates from the other three forces. During the following **Grand Unification Epoch** ($t = t_{\mathrm{Pl}}$ to $t \simeq 10^{-36}\,\mathrm{s}$ or $T \simeq 10^{28}\,\mathrm{eV}$ to $T \simeq 10^{24}\,\mathrm{eV}$) the strong, weak and electromagnetic forces were united in the so-called electronuclear force. Here the physics is described by a Great Unified Theory (GUT), such that in particular the particle Lagrangian obeys a GUT symmetry, e.g. SU(5). It should be noted here that no consistent theory exists for both the Planck and the GUT Epochs. Especially in light of inflationary cosmology (see below) the picture becomes highly complex. Therefore, only the description hereafter may be considered as reasonable to greater extent.

The concept of the subsequent phase, **Inflation**, was first introduced by [46] in order to solve the so-called Horizon and Flatness Problems. The former describes the, on first sight, paradox observation that regions of the observable Universe which, according to classical cosmology, have *not* been ever casually connected with each other (due to the fact that the distance between them is larger than the distance light could have travelled over the corresponding age of the Universe) in fact *do* share common global properties (like the CMB temperature) which cannot be explained by sheer coincidence. At the same time the Flatness Problem refers to the fact that the observed Universe appears to be flat, i.e. $k = 0$ in (1.159) or, equivalently, $\Omega = 1$ in (1.171). This, however, would require an extraordinary fine tuning of the initial parameters, such that it again seems unlikely that this could have happened within the scope of classical cosmology.

Inflation solves these and other problems in a rather elegant way [47]. Although there are several different models of Inflation in existence, the basic common idea is that it is given by the de Sitter solution of the Einstein Equations, which means, as derived in Sec. 1.2.2, $a \propto e^{H_\Lambda t}$ and $H = \mathrm{const}$, implying an exponential expansion of the Universe. This can directly solve the Flatness Problem since after $\propto 60$ e-folds [47], basically independent of the initial curvature, it is $\Omega \to 1$ and therefore $k = 0$. The same number of e-folds is also required to solve the Horizon Problem – two regions of the Universe which were casually connected before Inflation do not necessarily have to be so after the exponential (and superluminous) expansion while at the same time sharing common initial properties. Most recent measurements associate Inflation with an upper limit for the energy scale of approximately $1.94 \times 10^{25}\,\mathrm{eV}$ [44].

A field theoretical treatment of Inflation is provided by introducing a new scalar field, the inflaton, which undergoes a phase transition causing the exponential expansion described above. Assuming it to be a first order phase transition (cf. Sec. 1.2.4), latent heat is released at the end of the process which raises the temperature of the, due to the

rapid expansion, supercooled Universe (almost) to the value it had prior Inflation. This stage is called **Reheating** and might have resulted in a massive production of Standard Model particles in a way that after Reheating the energy content of the Universe is dominated by radiation. It should be noted here that both Inflation and Reheating are not well understood up to the present day such that various different theories exist – see, e.g., [48].

Hereafter the Universe enters the Electroweak Unification Epoch. In the beginning the remaining GUT gauge bosons, if present, quickly decay due to the low temperature. Once thermal equilibrium has been restored, the Universe can be seen as filled with an ideal gas of leptons and quarks (as well as their anti-particles), W and Z bosons, photons and gluons. The Electroweak Unification Epoch ends with the **Electroweak Phase Transition** which takes place at a temperature of $T \simeq 10^{11}\,\mathrm{eV}$ ($z \simeq 4 \times 10^{14}$), when the spontaneous breaking of $SU(2)_L \otimes U(1)_Y$ occurs. It is followed by the **QCD Phase Transition**, i.e. the confinement of free quarks into hadrons, which happens at roughly $T \simeq 2 \times 10^8\,\mathrm{eV}$ ($z \simeq 8.5 \times 10^{11}$). Since both these phase transitions are considered as possible important processes to generate Primordial Magnetic Fields, they will be discussed in more detail in the corresponding dedicated sections (Secs. 1.2.4.1 and 1.2.4.2).

A crucial particle physics event happening subsequently is **Neutrino Decoupling**: Before that the reaction $e^- + e^- \leftrightarrow \nu_e + \overline{\nu}_e$ is in thermal equilibrium, having the mean free path $L_{\nu,\mathrm{mfp}}$ for neutrinos approximately given by [49]

$$L_{\nu,\mathrm{mfp}} \simeq \frac{1}{\sigma_\nu n} = \frac{1}{(G_\mathrm{F}T)^2\,(n_\mathrm{l} + n_\mathrm{q})} \simeq 10^9 \left(\frac{T}{10^6\,\mathrm{eV}}\right)^{-5} \left(\frac{g_\mathrm{l} + g_\mathrm{q}}{8.75}\right)^{-1} \mathrm{m} \propto a^5\,, \quad (1.183)$$

where G_F is the Fermi Constant, $(G_\mathrm{F}T)^2$ a typical cross section for the electroweak interaction, n_l and n_q are number densities and g_l and g_q are the statistical weights for leptons and quarks at the considered epoch, respectively. Once the mean free path exceeds the Hubble Radius r_H, i.e. the interaction rate becomes bigger than the Hubble rate, the neutrinos practically do not interact with the charged leptons anymore, thus decoupling from the aforementioned reaction. More elaborate calculations [50] then give the temperatures of the decoupling for the different neutrino species: $T_{\nu_e} \simeq 1.34 \times 10^6\,\mathrm{eV}$ and $T_{\nu_\mu} \simeq T_{\nu_\tau} \simeq 1.5 \times 10^6\,\mathrm{eV}$, which correspond to a redshift of $z \simeq 6 \times 10^9$.

Being not able to interact with photons anymore, the dominant reaction for neutrinos are nuclear, therefore being the starting point for **Big Bang (or Primordial) Nucleosynthesis** which takes place at temperatures between $\mathcal{O}(10^6)\,\mathrm{eV}$ and $(6...7) \times 10^4\,\mathrm{eV}$ [51]. In terms of nuclear physics during that period of time the dominant reactions are $p + e^- \leftrightarrow n + \nu$ and $p + \overline{\nu} \leftrightarrow n + e^+$. However, at approximately $T \simeq (6...7) \times 10^5\,\mathrm{eV}$, the rate for this reaction drops below the Hubble rate H as well, thus fixing (or "freezing out") the number ratio between neutrons and protons to $N_n/N_p \simeq 1/7$ which quickly changes in favor of the protons since free neutrons decay with a mean life time of $\tau_n \simeq 887\,\mathrm{s}$. This free decay stops, rather abruptly, at roughly $T \simeq 6.5 \times 10^4\,\mathrm{eV}$ when the formation of different isotopes of light elements, preferably deuterium, helium and lithium, proceeds, therefore binding all free neutrons. The details of this process are highly sensitive to various parameters, such as the baryon-to-photon ratio, the reaction rates and the nature of neutrinos.

Soon afterwards the **transition from the radiation-dominated regime to the matter-dominated one** takes place. The time at which this happens is given by the

formula [52]

$$t_{\mathrm{rm}} = \frac{4}{3}\left(1 - 2^{-\frac{1}{2}}\right) \frac{\left(\Omega_{\mathrm{r}}^{\mathrm{pres}}\right)^{\frac{3}{2}}}{\left(\Omega_{\mathrm{m}}^{\mathrm{pres}}\right)^{2}} H_{\mathrm{pres}}^{-1}\,, \tag{1.184}$$

which gives $t_{\mathrm{rm}} \simeq 23\,000$ years for the parameters used in this work, corresponding to a redshift $z \simeq 5\,000$ or a temperature of $T \simeq 1.2\,\mathrm{eV}$.

Recombination denotes the moment in the evolution of the Early Universe when protons first bind free electrons to form neutral hydrogen atoms or, to give a more precise definition following [53], the point in time when 90% of all electrons have combined with protons. The temperature at which this happens may be calculated from the Saha Equation knowing the photon/baryon ratio which, taking into account additional aspects of the physics at that epoch, gives a redshift of $z = 1\,078 \pm 11$ [54] which agrees very well with the most recent observations [44] of $z = 1\,090.43 \pm 0.54$ and corresponds to a temperature of $T_{\mathrm{Rec}} \simeq 0.25\,\mathrm{eV}$.

Since Recombination dramatically reduces the number of free electrons for photons to scatter with, the mean free path for the latter dramatically increases such that for $T \simeq T_{\mathrm{Rec}}$ it is given by [49]

$$L_{\gamma,\mathrm{mfp}} \simeq \frac{1}{\sigma_{\mathrm{T}} n_e} \simeq 10^{20} X_e \left(\frac{\Omega_{\mathrm{b}} h^2}{0.0125}\right)^{-1} \left(\frac{T}{0.25\,\mathrm{eV}}\right)^{-3} \mathrm{m} \propto a^3\,, \tag{1.185}$$

where Ω_{b} is the relative baryon density as defined in (1.171), h the normalized Hubble Parameter $h = H/(100\,\mathrm{km\,s^{-1}\,Mpc^{-1}})$ and X_e the ionization fraction, i.e. the number of free electrons per baryon, having the values $X_e \simeq 1$ before and $X_e \simeq 10^{-5}$ during Recombination. This means that shortly after Recombination, once the photon mean free path exceeds the size of the Universe, i.e. when $L_{\gamma,\mathrm{mfp}} \simeq H^{-1}$, **Photon Decoupling** takes place – from that time on photons can travel through the Universe practically undisturbed.

This relic radiation therefore survives until the present day, only affected by the Expansion of the Universe which decreases its temperature. In its nature it is, as confirmed by various experiments (see, e.g., [44, 55]), a highly isotropic black body radiation, i.e. the ambient photon density per photon energy is given by

$$\frac{dN_{\mathrm{CMB}}(\epsilon)}{dV\,d\epsilon} = \frac{1}{\pi^2} \frac{\epsilon^2}{e^{\frac{\epsilon}{k_B T}} - 1}\,, \tag{1.186}$$

where ϵ is the photon energy and the temperature at present is given by [56] $T = 2.7255 \pm 0.0006\,\mathrm{K} = (2.3487 \pm 0.0005) \times 10^{-4}\,\mathrm{eV}$. Due to this value for the temperature this relic radiation is also known as **Cosmic Microwave Background (CMB)**.

The last phase of the Early Universe are the so-called **Dark Ages**. Basically all protons recombine with electrons, such that nearly all the primordial medium consists of neutral hydrogen which therefore is the main source of radiation. However, hydrogen only can absorb and emit photons of specific wavelengths which are dominated by the so-called 21-cm line concerning photon energies of $\epsilon \simeq 6 \times 10^{-6}\,\mathrm{eV}$ which are far below the mean energy of the CMB, so that such emissions are rather rare, hence the name Dark Ages. The Dark Ages end at $z \gtrsim 6$ ($T \simeq 1.6 \times 10^{-3}\,\mathrm{eV}$) [57] with the process of **Reionization** when first stars and Quasars formed, emitting high energy photons, thus providing a source of energy capable of ionizing the hydrogen atoms, thus converting the medium into a plasma which it remains to be up to the present day.

Another important transition which in particular has a great impact on the future development of the Universe is the **transition from a matter-dominated to a vacuum energy dominated energy content of the Universe**. The age of the Universe at which this takes place is given by [52]

$$t_{\mathrm{m}\Lambda} = \frac{2H_{\mathrm{pres}}^{-1}}{3\left(1-\Omega_{\mathrm{m}}^{\mathrm{pres}}\right)^{\frac{1}{2}}} \ln\left(1+2^{\frac{1}{2}}\right) \simeq 10.3\times10^{10}\,\mathrm{years}\,, \tag{1.187}$$

where $H_{\mathrm{pres}} = 67.3\,\mathrm{km\,Mpc^{-1}\,s^{-1}}$ and $\Omega_{\mathrm{m}}^{\mathrm{pres}} = 0.315$ have been used for the present values of the Hubble Parameter and the relative matter energy density, respectively. This would correspond to a redshift of $z \simeq 0.3$ or a temperature $T \simeq 3\times10^{-4}\,\mathrm{eV}$.

1.2.4 QCD and Electroweak Phase Transitions in the Early Universe

For many cases a given physical system has got multiple states or phases which are denoted by different forms of symmetries. In the simplest case there are two phases – the "ordered" ("more" symmetry) and the "disordered" ("less" symmetry) one. A phase transition therefore denotes the transition between these two states. To distinguish between them, a so-called order parameter is introduced, usually being zero in the disordered and non-zero in the ordered phase.

Following the Ehrenfest classification, phase transitions can be subdivided in different categories or orders, depending on the actual physics of the given system, of which the most interesting ones are the first and second order phase transitions. In general the order denotes the derivative of a thermodynamical potential which is discontinuous at a given phase transition. Taking, for example, the Free Energy $F = U - TS$, where U is the total energy of the system, T the temperature and S the entropy, this would mean that a first order phase transition will have a discontinuity in entropy which would result in the release of so-called latent heat. Phase transitions of second order are discontinuous in the second derivative of F. In the following these and higher order phase transitions will be also called continuous phase transitions. It should be noted here that at present there are also more sophisticated classification schemes than the one by Ehrenfest, however the latter is sufficient for the purpose here. Further reading is given in [58].

May now the ordering parameter be called ϕ. For a second order phase transition the considered potential V (for example the Free Energy, i.e. $V \equiv F$) can be approximated by [59]

$$V(\phi) = V_0 + \alpha\phi^2 + \beta\phi^4\,, \tag{1.188}$$

where V_0, α and $\beta > 0$ are factors which may depend on the parameters describing the system, here on the temperature T, in particular it is

$$\alpha = a\left(T - T_{\mathrm{crit}}\right) \tag{1.189}$$

for $a > 0$ and the critical temperature of the phase transition T_{crit}. Depending on whether it is $T > T_{\mathrm{crit}}$ or $T < T_{\mathrm{crit}}$, $V(\phi)$ has one of the two shapes shown in the left panel of Fig. 1.2. For $T > T_{\mathrm{crit}}$ $V(\phi)$ has one minimum at $\phi = 0$ while for $T < T_{\mathrm{crit}}$ there are two, located at $\phi = \pm\left[a\left(T_{\mathrm{crit}} - T\right)/\left(2\beta\right)\right]^{\frac{1}{2}}$, as well as now, in addition, a maximum at $\phi = 0$. This means that while for higher temperatures there is only one stable equilibrium of the system, once the temperature drops below T_{crit}, the $\phi = 0$ state becomes unstable such that a small perturbation causes a relaxation to one of the now stable (minimal) conditions which indicates a spontaneous symmetry breaking. Here also the nature of a second order phase transition can be seen since the expectation

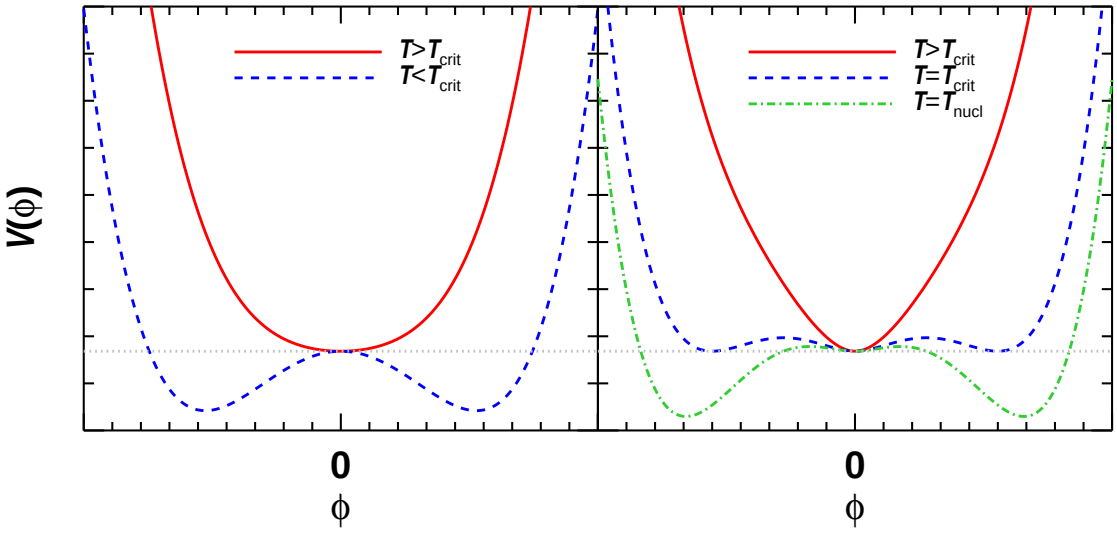

Figure 1.2: *Left panel*: The potential V above (solid, red) and below (dashed, blue) the critical temperature $T_{\rm crit}$ of a second order phase transition as introduced by (1.188). *Right panel*: The potential V above the critical temperature $T_{\rm crit}$ (solid, red), below it (dashed, blue) and at the nucleation temperature $T_{\rm nucl} < T_{\rm crit}$ (dot-dashed, green) for a first order phase transition, given by (1.190). In both panels the dotted gray line represents the value of $V = V_0$.

value of the ordering parameter has a continuous transition from a zero to a non-zero value.

For a first order phase transition the potential, in comparison to the one shown above, acquires an additional cubic term such that it has the form [59]

$$V(\phi) = V_0 + \alpha\phi^2 + \gamma\,|\phi|^3 + \beta\phi^4 \tag{1.190}$$

with $\gamma < 0$. Now, as shown in the right panel of Fig. 1.2, there are more possible configurations. Again, starting with a high temperature (i.e. $T > T_{\rm crit}$) on which now all the parameters α, β, γ may depend, there is only one minimum of the potential, namely at $\phi = 0$. However, as the temperature decreases below $T_{\rm crit}$, i.e. to the point at which the condition $\gamma^2 > 32\alpha\beta/9$ is fulfilled, V acquires two more minima (and, as a consequence, two additional maxima) situated at $\phi_\pm = \left[\mp 3\gamma \pm \left(9\gamma^2 - 32\alpha\beta\right)^{\frac{1}{2}}\right] / (8\beta)$ which, for the parameter configuration $\gamma^2 = 4\alpha\beta$, have the same value of V as the zero solution, namely $V(\phi_\pm) = V(0) = V_0$. This means that now the lowest state is degenerated while for lower temperatures the value of V for the asymmetric minima is lowered even more, making them the more preferable states, such that a spontaneous and discontinuous change of the equilibrium from a symmetric to an asymmetric one through tunneling becomes more and more probable. This discontinuous change of state is characteristic for a first order phase transition.

Further decrease of the temperature lowers $V(\phi_\pm)$, however the system may remain in the initial state, i.e. it supercools, until some typical nucleation temperature $T_{\rm nucl}$ when tunneling to an asymmetric state becomes probable enough such that both phases may now co-exist [60]. The nucleation seeds start to grow in form of bubbles, releasing latent heat into the medium and therefore reheating it which is a highly complex process. For cosmic phase transitions, however, in the end Expansion of the Universe decreases the temperature far enough such that only the low temperature phase is present.

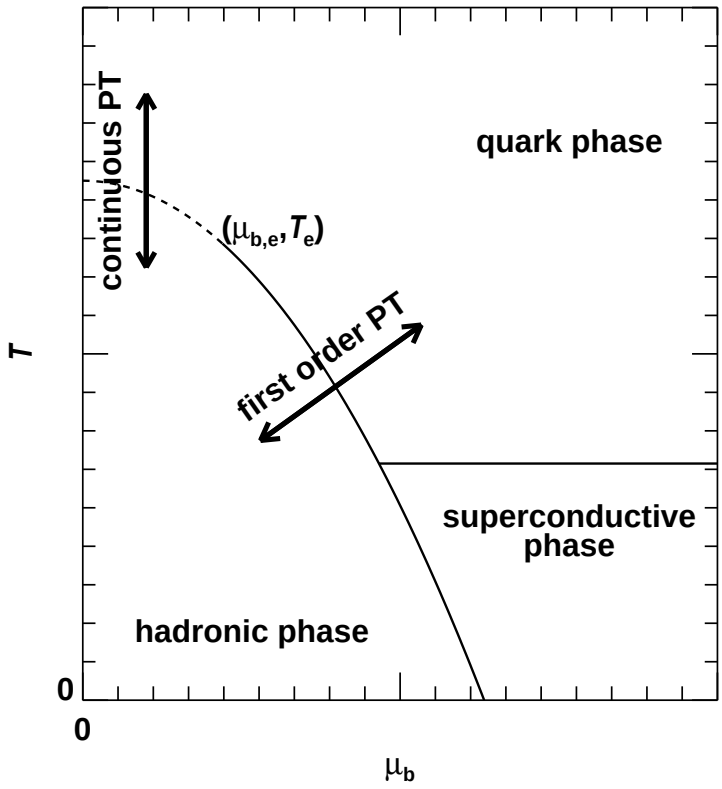

Figure 1.3: A qualitative sketch of the QCD phase diagram depending on the temperature T and the baryonic chemical potential μ_b [65]. If the phase transition takes place across the solid line, it is a first order QCD Phase Transition, the dashed line means a continuous phase transition. These two regimes are separated by the so-called endpoint $(\mu_{\mathrm{b,e}}, T_\mathrm{e})$. The superconductive phase is not discussed here, for further information on it see [65].

1.2.4.1 QCD Phase Transition

An important question is whether the QCD Phase Transition (QCDPT) has been of first or of second order. While earlier works (e.g. [61]) suggest that the former is the case, more recent publications claim, using lattice calculations, the latter one, or even a crossover, to be true [1, 62, 63]. This can be seen from Fig. 1.3: Assuming that the baryonic chemical potential μ_b vanishes, the system is clearly in the continuous regime where the transition takes place at T_QCD which is still not completely known as can be seen from the different results found in the literature, e.g. $T_\mathrm{QCD} = (1.64 \pm 0.02) \times 10^8\,\mathrm{eV}$ [62] or $T_\mathrm{QCD} = (1.92 \pm 0.07 \pm 0.04) \times 10^8\,\mathrm{eV}$ [64].

However, since not all cosmological parameters are known to the full extent, a first order cosmological QCD Phase Transition cannot be completely excluded. In fact, [65] claims that in general, like in the discussion presented above, μ_b is assumed to be equal to zero which, being one of the crucial assumptions for a continuous phase transition, not necessarily has to be true as the lepton asymmetry might be large and therefore cause μ_b to grow with temperature. Furthermore, also a non-vanishing leptonic chemical potential (e.g. for neutrinos) might influence the phase transition behavior and therefore open up a large and mostly unexplored parameter space.

Another possible scenario for the QCD Phase Transition to be of first order is that μ_b has been large *before* the phase transition, becoming smaller afterwards [66, 67]. In more detail this would mean that during the transition the system is trapped in a false metastable vacuum state for which the potential and therefore the energy density is

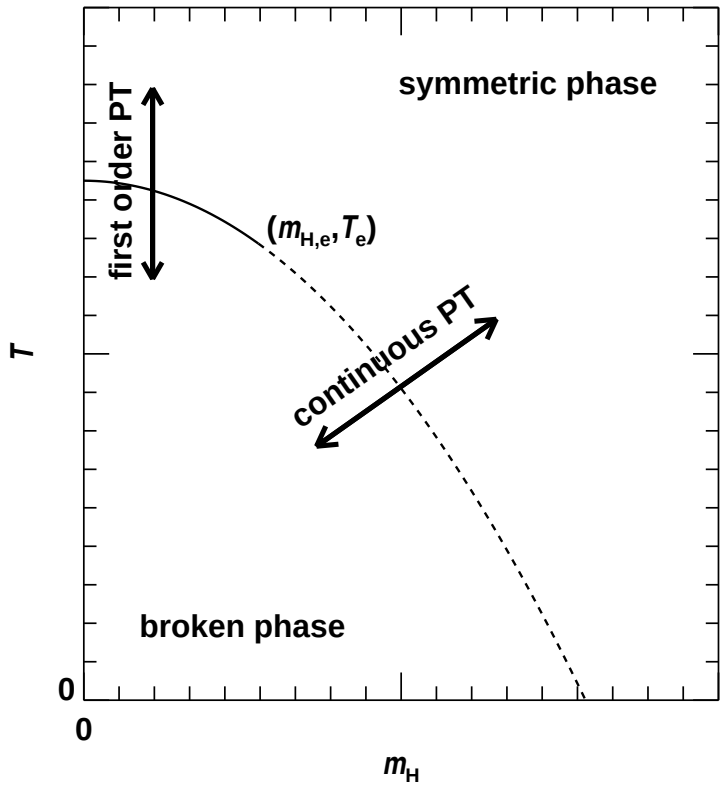

Figure 1.4: A qualitative sketch of the electroweak phase diagram for the Standard Model depending on the temperature T and the Higgs mass m_{H} [68]. If the phase transition takes place across the solid line, it is a first order Electroweak Phase Transition (EWPT), the dashed line means a continuous phase transition. These two regimes are separated by the so-called endpoint $(m_{\mathrm{H,e}}, T_{\mathrm{e}})$. The symmetric phase is the one where the $SU(2)_L \otimes U(1)_Y$ gauge group is valid, the broken phase has only got the $U(1)_Q$ symmetry.

constant. This, on the other hand, means that the Universe undergoes a so-called Little Inflation. At the end of this process the true vacuum state can be obtained such that the Universe reheats due to the released latent heat up to a temperature close to the one at the beginning of the Little Inflation. At the same time the chemical potential has decreased to the predicted values, however having crossed the first order transition line in Fig. 1.3. See also Fig. 2 in [67].

Furthermore, it is possible that while in equilibrium, which is usually assumed in QCD calculations, the continuous result is valid, out of equilibrium, which could be the case in the Early Universe, the situation changes such that at least a weak first order phase transition has to be considered (for an overview see [69]). Finally it should be noted that there are also more recent results from lattice calculations which claim that the standard scenario presented here is not necessarily true [70]. Motivated by all these findings therefore the QCD Phase Transition will be assumed to be a first order one since, as shown in Sec. 2.1.2.1, this may be an origin for Primordial Magnetic Fields.

1.2.4.2 Electroweak Phase Transition

The effect of the Electroweak Phase Transition (EWPT) can be understood best in terms of the gauge symmetry of the Universe [53]. While before the transition, in the symmetric phase, the underlying symmetry group is $SU(2)_L \otimes U(1)_Y$, where the index L means the transformation of left-handed fermions and Y is the hypercharge, after the

transition it is broken down to the $U(1)_Q$ group of the electromagnetic charge Q. The physical consequence of this process is that the complex Higgs field ϕ, given by

$$\phi = \frac{1}{\sqrt{2}} \begin{pmatrix} \phi_1 + i\phi_2 \\ \phi_3 + i\phi_4 \end{pmatrix} \tag{1.191}$$

and having the potential

$$V(\phi) = -m^2 \phi^\dagger \phi + \lambda \left(\phi^\dagger \phi \right)^2 , \tag{1.192}$$

may gain a non-zero (false) vacuum expectation value σ by a spontaneous symmetry breaking due to the form of the potential described above. With $\sigma = \frac{m^2}{\lambda} \neq 0$ the W and Z bosons as well as fermions acquire masses since they are proportional to σ. An important parameter here is the mass m_H of the particle associated with the field ϕ, the so-called Higgs Boson. This mass is usually used, together with the temperature T, to describe the phase transition parameter space.

The mass of the Higgs Boson at the endpoint (s. Fig. 1.4) has been found to have a value inside the Higgs mass range of roughly $m_\mathrm{H,e} \simeq 60...80\,\mathrm{GeV}$ [71–73], the latter reference even giving an estimate for the temperature T_e at the endpoint, $T_\mathrm{e} = 129.6\,\mathrm{GeV}$. These results have been found under the assumption of the validity of the Standard Model (SM) which therefore would mean that if the Higgs-like particle with a mass of approximately $m_\mathrm{H} \simeq 125\,\mathrm{GeV}$ recently observed at the LHC [74, 75] turns out to be the predicted Standard Model Higgs Boson, then it can be seen from Fig. 1.4 that a first order Electroweak Phase Transition is excluded.

However, several modifications and extensions of the SM have been proposed in order to circumvent this constraint. One possibility is to consider higher orders of the Higgs Boson operator [76, 77]. This would then directly change the effective Higgs potential which, for appropriate parameter values, can maintain a first order EWPT even for Higgs masses as high as 125 GeV. An experimental proof would be an altered Higgs Boson self-coupling.

Much attention has been also put into the analysis of the modification of the EWPT by supersymmetric models (e.g. [78–80]). Although the details of the different models and of the corresponding consequences are rather different, the basic idea is that due to the existence of the so-called stop quark in supersymmetric theories either the effective potential itself is modified, for example by the enhancement of a specific term, or higher order (QCD) corrections become relevant and hence affect the phase transition.

Of course this list of effects resulting in an first order EWPT is by far not complete, however, as for the QCDPT, the aim is to give a short overview and to motivate the considerations later on. Further reading, especially in light of the recent LHC results, may be, for example, found in [81].

Chapter 2

Extragalactic Magnetic Fields

Движенья нет, сказал мудрец брадатый.
Другой смолчал и стал пред ним ходить.
Сильнее бы не мог он возразить;
Хвалили все ответ замысловатый.
Но, господа, забавный случай сей
Другой пример на память мне приводит:
Ведь каждый день пред нами солнце ходит,
Однако ж прав упрямый Галлилей
— A. S. Pushkin, *Движение* [*Motion*] (1826)

There is clear evidence that both galaxies and galaxy clusters are filled with magnetic fields of μG strength. However, little is known about the origin of these fields and furthermore about the existence and structure of magnetic fields in the extragalactic voids. Nevertheless, there is a number of approaches which try to deduce the properties of these Extragalactic Magnetic Fields (EGMF). Therefore, first, possible origins of EGMF are discussed in Sec. 2.1, followed by the analysis of recent observations to find constraints on their parameters in Sec. 2.2, especially focussing on a lower limit of the magnetic field strength.

2.1 Origin of Cosmic Magnetic Fields

An important but still unsolved question concerns the origin of Galactic and Extragalactic Magnetic Fields. As a summary one can say that there are mainly two scenarios being discussed: On the one hand the Astrophysical Scenario, where small seed magnetic fields are created at cosmologically late times inside galaxies and then amplified by a dynamo effect, and, on the other hand, the Cosmological Scenario, where so-called Primordial (or pre-galactic) Magnetic Fields are created in the Early Universe by some global mechanism having rather large magnitudes. Both cases are discussed in the following, the former in Sec. 2.1.1 and the latter in Sec. 2.1.2.

2.1.1 Astrophysical Scenario of Magnetogenesis

The Astrophysical Scenario describes the theory that cosmic magnetic fields have their origin in rather late times, when structures like stars, galaxies or galaxy clusters already have formed to some extent and are themselves responsible for the magnetogenesis. Therefore in this case the resulting scales of the seed fields are rather small and the magnitude weak. Furthermore, in contrast to the Cosmological Scenario described below, magnetogenesis here can be regarded to be a rather local event, focussed on the structure in question.

Once such a seed field, for example on galactic scales, is created, a dynamo mechanism is assumed to take over and amplify it to strengths of up to the μG scale, such that it can account for the observed galactic magnetic field (for a review of possible dynamo mechanisms see, for example, [82]). Subsequently, these magnetic fields may be then transported to the intergalactic space by one of the various mechanisms discussed in literature, like the dragging of magnetic fields outside the galaxy due to magnetized galactic winds from stellar activity [83–85] or jets from Black Holes/Active Galactic Nuclei [86–89].

Therefore, a crucial question concerns the origin of the seed magnetic fields for which different possible approaches will be discussed in the following. The list is, of course, by far non-exhaustive but rather should give an idea of possible physical processes which might be involved, also referring the reader to the references within the given literature. In addition, a more comprehensive overview can be found in [82, 90, 91]

2.1.1.1 The Biermann Battery Mechanism

Independent of the actual magnetogenesis epoch, one crucial question arises: Where did the initial seed magnetic fields actually come from? If one assumes that initially the magnetic field strength has been $\mathbf{B} = \mathbf{0}$, (1.13) would result in $\partial_t \mathbf{B} = \mathbf{0}$ which means that with no initial magnetic fields no magnetic fields would have been created at all.

A possible solution to solve the problem of the creation of magnetic fields "from scratch" is nowadays known as the Biermann Battery [82, 92, 93]. Although it is listed in the section of the Astrophysical Scenarios, the underlying principle is relevant for the Cosmological Scenario as well. Therefore here this generic principle is first discussed following [82] and then applied to particular astrophysical settings.

The main idea is that the form of Ohm's Law presented as (1.1) is not the generic and therefore not the most general one. In fact, one has to consider the actual movement of charges which for electrons in the medium (ions are not considered here as they are much slower) is given by

$$n_e m_e \partial_t \mathbf{v} = -n_e e \left(\mathbf{E} + \mathbf{v} \times \mathbf{B}\right) - \nabla p_e + \mathbf{F} \,, \tag{2.1}$$

where n_e is the electron number density, m_e and e are the mass and the charge of the electron, respectively, and p_e is the electron pressure, while $\mathbf{F}$ represents any additional forces which are neglected in the following (as they are small either due to the small electron mass or, for the ion friction force, due to the fact that it is associated with $\mathbf{j}/\sigma$ which is small as well). Now one can drop all terms featuring m_e, as it is considered to be much smaller than the energies involved, and therefore obtain

$$\mathbf{E} + \mathbf{v} \times \mathbf{B} = -\frac{\nabla p_e}{n_e e} \,. \tag{2.2}$$

Applying the curl to this expression and using (1.4) on the left hand side, one gets

$$\partial_t \mathbf{B} = \nabla \times (\mathbf{v} \times \mathbf{B}) + \nabla \times \left(\frac{\nabla p_e}{n_e e}\right) \overset{(A.3),(A.8)}{=} \nabla \times (\mathbf{v} \times \mathbf{B}) - \frac{\nabla n_e \times \nabla p_e}{n_e^2 e} \,. \tag{2.3}$$

Now, assuming local charge neutrality, i.e.

$$n_e \simeq n_p \equiv \frac{\chi \rho}{m_p} \,, \tag{2.4}$$

where χ is the ionization fraction, m_p is the proton mass and ρ is the mass density, and thermal equilibrium, i.e.

$$p_e \simeq \frac{n_e}{n_p + n_e} p \overset{(2.4)}{\simeq} \frac{\chi}{1+\chi} p \,, \tag{2.5}$$

with the initial condition $\mathbf{B} = \mathbf{0}$ one can transform (2.3) to

$$\partial_t \mathbf{B} = -\alpha \frac{\nabla\rho \times \nabla p}{\rho^2} \tag{2.6}$$

with $\alpha = \frac{m_p}{(1+\chi)e}$. Comparing (2.6) with (1.34), it can be written as

$$\partial_t \mathbf{B} = \alpha \partial_t \boldsymbol{\zeta} \tag{2.7}$$

and therefore

$$\mathbf{B} = \alpha \boldsymbol{\zeta} \,, \tag{2.8}$$

where $\boldsymbol{\zeta} = \nabla \times \mathbf{v}$ is the vorticity as defined in Sec. 1.1.1.3.

As mentioned above, the Biermann Battery may be applied to different scenarios of astrophysical magnetic field generation. One of the earliest possibilities for magnetogenesis are the so-called Population III stars which formed during the period of Reionization. This has been investigated by various authors (see e.g. [94, 95]) with the result that magnetic field strengths of up to $10^{-12}\,\mathrm{G}$ might be produced. Another approach is to consider early stages of galaxy formation itself, namely prior [96] or during [97] the collapse of protogalactic density perturbations, giving seed magnetic field strengths of $B \simeq 10^{-21}\,\mathrm{G}$ and $B \simeq 10^{-17}\,\mathrm{G}$, respectively.

2.1.1.2 Vorticity of the Radiation-Dominated Era

One of the first mechanisms to explain the origin of the magnetic fields has been suggested by [98] (see also [82, 99]). Starting with (1.7), setting $\lambda = \mu = 0$, one can write down the equation of motion for a fluid of charged particles [82]:

$$\rho_i \left[\partial_t \mathbf{v}_i + (\mathbf{v}_i \cdot \nabla)\, \mathbf{v}_i\right] = -\nabla p_i + \mathbf{F}_i \,, \tag{2.9}$$

where $i = e, p$ denotes the kind of particles considered (electrons and protons, respectively) and $\mathbf{F}_i$ is the corresponding force density, given by

$$\mathbf{F}_i = e n_i \left(\mathbf{E} + \mathbf{v}_i \times \mathbf{B}\right) \pm e n_i \frac{\mathbf{j}}{\sigma} - \rho_i \nabla \phi_g + \mathbf{P}_{i\gamma} \tag{2.10}$$

with the number density n_i and the gravitational potential ϕ_g. The upper sign is valid for electrons, the lower for protons. The four terms on the right hand side of (2.10) represent, in the given order, the Lorentz Force, the momentum transfer from electrons to protons (hence the different signs), the gravitational force and the momentum transfer from the corresponding particle to photons (which is usually only relevant for electrons), respectively. For photons, the third important total fluid component, the Navier-Stokes Equations are not valid. Dealing with radiation, one has to take into account relativistic effects which leads to the relation [100]

$$\frac{4}{3}\rho_\gamma \left[\partial_t \mathbf{v}_\gamma + (\mathbf{v}_\gamma \cdot \nabla)\, \mathbf{v}_\gamma\right] + \frac{1}{3}\mathbf{v}_\gamma \left[\partial_t \rho_\gamma + (\mathbf{v}_\gamma \cdot \nabla)\, \rho_\gamma\right] = -\nabla p_\gamma - \frac{4}{3}\rho_\gamma \nabla \phi_g - \mathbf{P}_{e\gamma} \,. \tag{2.11}$$

Applying the curl operator to (2.9) for protons, i.e. $i = p$ as in (1.34), and using (A.8) gives, with a vanishing pressure gradient due to homogeneity,

$$\partial_t \boldsymbol{\zeta}_p - \nabla \times (\mathbf{v}_p \times \boldsymbol{\zeta}_p) = \frac{e}{m_p} \left[\nabla \times \mathbf{E} + \nabla \times (\mathbf{v}_p \times \mathbf{B}) - \frac{1}{\sigma} \nabla \times \mathbf{j} \right] \tag{2.12}$$

or, with (1.3)-(1.5), (A.6), (A.7) and (A.9),

$$\begin{aligned} &\partial_t \boldsymbol{\zeta}_p + \boldsymbol{\zeta}_p \left(\nabla \cdot \mathbf{v}_p \right) - \left(\boldsymbol{\zeta}_p \cdot \nabla \right) \mathbf{v}_p + \left(\mathbf{v}_p \cdot \nabla \right) \boldsymbol{\zeta}_p \\ &= \frac{e}{m_p} \left[-\partial_t \mathbf{B} - \mathbf{B} \left(\nabla \cdot \mathbf{v}_p \right) + \left(\mathbf{B} \cdot \nabla \right) \mathbf{v}_p - \left(\mathbf{v}_p \cdot \nabla \right) \mathbf{B} + \frac{1}{4\pi\sigma} \Delta \mathbf{B} \right] . \end{aligned} \tag{2.13}$$

For a protogalaxy the proton velocity $\mathbf{v}_p$ can be decomposed into two components,

$$\mathbf{v}_p = \mathbf{v}_{p,\mathrm{rot}} + \mathbf{r} \frac{\partial_t a}{a} , \tag{2.14}$$

the first term being the rotation velocity and the second one the expansion velocity which depends on the comoving spatial coordinate $\mathbf{r}$ and the scale factor a. With $\nabla \cdot \mathbf{v}_{p,\mathrm{rot}} = 0$ one can write down the relations

$$\nabla \cdot \mathbf{v}_p = 3 \frac{\partial_t a}{a}, \; \left(\mathbf{B} \cdot \nabla \right) \mathbf{v}_p = \mathbf{B} \frac{\partial_t a}{a}, \; \left(\boldsymbol{\zeta}_p \cdot \nabla \right) \mathbf{v}_p = \boldsymbol{\zeta}_p \frac{\partial_t a}{a} , \tag{2.15}$$

of which the latter two are valid exactly only for a specific angle [99]. (2.13) therefore finally becomes

$$\partial_t \boldsymbol{\zeta}_p + 2 \frac{\partial_t a}{a} \boldsymbol{\zeta}_p + \left(\mathbf{v}_p \cdot \nabla \right) \boldsymbol{\zeta}_p = \frac{e}{m_p} \left[-\partial_t \mathbf{B} - 2 \frac{\partial_t a}{a} \mathbf{B} - \left(\mathbf{v}_p \cdot \nabla \right) \mathbf{B} + \frac{1}{4\pi\sigma} \Delta \mathbf{B} \right] . \tag{2.16}$$

Multiplying by a^2 and rearranging gives

$$\left[a^2 + 2a \partial_t a + a^2 \left(\mathbf{v}_p \cdot \nabla \right) \right] \left(\boldsymbol{\zeta}_p + \frac{e}{m_p} \mathbf{B} \right) = a^2 \frac{e}{m_p} \left(\frac{1}{4\pi\sigma} \Delta \mathbf{B} \right) \tag{2.17}$$

or

$$\left[\partial_t + \left(\mathbf{v}_p \cdot \nabla \right) \right] \left[a^2 \left(\boldsymbol{\zeta}_p + \frac{e}{m_p} \mathbf{B} \right) \right] = \frac{1}{4\pi\sigma} \frac{e}{m_p} a^2 \Delta \mathbf{B} . \tag{2.18}$$

The operator on the left hand side being the convective (and therefore total) derivative with respect to time t, the integration of this equation over t, starting from some initial time t_0 with vanishing magnetic field, i.e. $\mathbf{B}(t_0) = \mathbf{0}$, gives

$$\left[a(t)^2 \left(\boldsymbol{\zeta}_p(t) + \frac{e}{m_p} \mathbf{B}(t) \right) \right] - a(t_0)^2 \boldsymbol{\zeta}_p(t_0) = \mathbf{0} , \tag{2.19}$$

where again conductivity has been assumed to be very large, i.e. $\sigma \to \infty$. This can be finally rearranged to a conservation law,

$$\boldsymbol{\zeta}_p(t) + \frac{e}{m_p} \mathbf{B}(t) = \left(\frac{a(t_0)}{a(t)} \right)^2 \boldsymbol{\zeta}_p(t_0) . \tag{2.20}$$

The next step consists of an analysis of (2.9) for electrons, for which the inertial and gravitational forces may be neglected, hence giving

$$\mathbf{0} = e n_e \left(\mathbf{E} + \mathbf{v}_e \times \mathbf{B} \right) + e n_e \frac{\mathbf{j}}{\sigma} + \mathbf{P}_{e\gamma} . \tag{2.21}$$

Dividing this equation by n_e and taking the curl gives, using the same method as for the case of protons above,

$$\rho_p \left[\partial_t + (\mathbf{v}_e \cdot \nabla)\right] \left(a^2 \frac{e}{m_p} \mathbf{B}\right) = -a^2 \nabla \times \mathbf{P}_{e\gamma} \,. \tag{2.22}$$

The last relation to be considered is the one for photons, (2.11). As motivated above, only the third term on the right hand side does not vanish for the situation described here. On the other hand, for the left hand side, due to homogeneity, it is $(\mathbf{v}_\gamma \cdot \nabla)\, \rho_\gamma = 0$ and, since for photons it is $\rho_\gamma \propto a^{-4}$ (see Sec. 1.2.2), one gets $\partial_t \rho_\gamma = -4\rho_\gamma \frac{\partial_t a}{a}$, i.e. (2.11) becomes

$$\frac{4}{3}\rho_\gamma \left(\partial_t \mathbf{v}_\gamma + (\mathbf{v}_\gamma \cdot \nabla)\, \mathbf{v}_\gamma\right) - \frac{4}{3}\rho_\gamma \mathbf{v}_\gamma \frac{\partial_t a}{a} = -\mathbf{P}_{e\gamma} \,. \tag{2.23}$$

Taking the curl of this equation, using the same relations as for the derivation of (2.13) and

$$\nabla \cdot \mathbf{v}_\gamma = 3\frac{\partial_t a}{a},\ (\boldsymbol{\zeta}_\gamma \cdot \nabla)\, \mathbf{v}_\gamma = \boldsymbol{\zeta}_\gamma \frac{\partial_t a}{a} \,, \tag{2.24}$$

results in

$$\partial_t \boldsymbol{\zeta}_\gamma + (\mathbf{v}_\gamma \cdot \nabla)\, \boldsymbol{\zeta}_\gamma + \frac{\partial_t a}{a}\boldsymbol{\zeta}_\gamma = -\frac{3}{4}\frac{1}{\rho_\gamma} \nabla \times \mathbf{P}_{e\gamma} \,. \tag{2.25}$$

Multiplied by a this can be simplified to

$$\left[\partial_t + (\mathbf{v}_\gamma \cdot \nabla)\right] (a\boldsymbol{\zeta}_\gamma) = -\frac{3}{4}\frac{a}{\rho_\gamma} \nabla \times \mathbf{P}_{e\gamma} \,. \tag{2.26}$$

Solving both (2.22) and (2.26) for $\nabla \times \mathbf{P}_{e\gamma}$ and then equating them gives

$$\frac{e}{m_p} \left[\partial_t + (\mathbf{v}_e \cdot \nabla)\right] \left(a^2 \mathbf{B}\right) = \frac{4}{3}\rho_\gamma a \left[\partial_t + (\mathbf{v}_\gamma \cdot \nabla)\right] (a\boldsymbol{\zeta}_\gamma) \tag{2.27}$$

or, using (2.18),

$$\rho_p \left[\partial_t + (\mathbf{v}_e \cdot \nabla)\right] \left(a^2 \boldsymbol{\zeta}_p\right) + \frac{4}{3}\rho_\gamma a \left[\partial_t + (\mathbf{v}_\gamma \cdot \nabla)\right] (a\boldsymbol{\zeta}_\gamma) = 0 \,, \tag{2.28}$$

which can be rearranged to

$$\left[\partial_t + (\mathbf{v}_e \cdot \nabla)\right] \left[a^5 \left(4\rho_\gamma \boldsymbol{\zeta}_\gamma + 3\rho_p \boldsymbol{\zeta}_p\right)\right] = 0 \,, \tag{2.29}$$

as can be proven by taking the derivative. Integrating this expression over t gives

$$\left[a^5 \left(4\rho_\gamma(t)\boldsymbol{\zeta}_\gamma(t) + 3\rho_p(t)\boldsymbol{\zeta}_p(t)\right)\right] - \left[a^5 \left(4\rho_\gamma(t_0) + 3\rho_p(t_0)\right)\right] \boldsymbol{\zeta}_p(t_0) = 0 \tag{2.30}$$

since $\boldsymbol{\zeta}_p(t_0) = \boldsymbol{\zeta}_\gamma(t_0)$. The situation considered here taking place during the radiation-dominated era, one can set $\rho_\gamma \gg \rho_p$ and furthermore, with $\rho_\gamma(t_0)/\rho_\gamma(t) = a^4$ (as mentioned above), it is possible to rewrite (2.30) as

$$\boldsymbol{\zeta}_p(t_0) = \frac{a(t)}{a(t_0)} \boldsymbol{\zeta}_\gamma(t) \,. \tag{2.31}$$

Finally, inserting this into (2.20), one obtains the result

$$\mathbf{B}(t) = \frac{m_p}{e} \left(\frac{a(t_0)}{a(t)} - 1\right) \boldsymbol{\zeta}_p(t) \,. \tag{2.32}$$

As can be seen from this expression, it is therefore possible to create magnetic fields if initially vorticity is present. With the parameters of the protogalaxies during the radiation-dominated era they can reach values of up to $10^{-16}\,\mathrm{G}$ [98] and may serve as seed fields which are amplified later on by a dynamo mechanism.

However, the calculations have been carried out under idealized conditions – one of the main points of criticism here is that in the Early Universe the fast vorticity decay due to Expansion of the Universe prevents the mechanism described above to work in an efficient way [86]. Still, it may serve as a toy model and, if true nevertheless, reveal a connection between primordial vorticity and magnetic seed fields.

2.1.1.3 Magnetic Fields from Active Galactic Nuclei

Due to the physics of Active Galactic Nuclei (AGN) one expects them to gain a magnetic field [91] which finally would produce a galactic seed field. [87, 101] were able to give an estimate for the resulting field strength by parametrizing the rotation energy of the central dense AGN power source with mass M_c as $E_\mathrm{rot} = fM_\mathrm{c}$ for $f < 1$. Assuming equipartition between rotational and magnetic energy $E_\mathrm{mag} = B_\mathrm{c}/(8\pi)V_\mathrm{c}$ for the average magnetic field strength B_c over the central region volume V, the magnetic field is given by

$$B_\mathrm{c} = \left(\frac{8\pi f M_\mathrm{c}}{V_\mathrm{c}}\right)^{\frac{1}{2}} . \tag{2.33}$$

Because of the high conductivity of the plasma [87] the magnetic field is frozen in (cf. Sec. 1.1.1.1), such that it expands adiabatically, i.e. on a galactic scale the magnetic field is given by $B_\mathrm{g} = B_\mathrm{c}(V_\mathrm{c}/V_\mathrm{g})^{\frac{2}{3}}$ which for typical parameters gives [101] $B_\mathrm{c} \simeq 10^9\,\mathrm{G}$ and $B_\mathrm{g} \simeq 10^{-5}\,\mathrm{G}$.

2.1.1.4 Magnetic Fields from Cosmic Ray Currents

A rather different approach to the origin of seed fields for cosmic magnetic fields was used by [102]. The authors consider GeV Cosmic Rays (assumingly mostly protons) which escape from a galaxy and propagate through the Intergalactic Medium. This corresponds to a small but non-negligible current $\mathbf{j}_\mathrm{CR}$. Due to charge imbalance this induces an electric field $\mathbf{E}$ which causes a return current $\mathbf{j}_\mathrm{t}$ inside the intergalactic plasma given by the relation $|\mathbf{E}| = \eta_\mathrm{Sp}\,|\mathbf{j}_\mathrm{t}|$, where η_Sp is the Spitzer Resistivity which has a temperature dependence of $\eta_\mathrm{Sp} \propto T^{-\frac{2}{3}}$.

Since the IGM is not uniform, it is possible for $\mathbf{j}_\mathrm{t}$ and therefore for $\mathbf{E}$ to have a non-vanishing curl which, according to (1.4), gives rise to a magnetic field if the primary and the return currents are separated. The time dependence of this magnetic field is estimated by [102]

$$\partial_t B \simeq |\nabla \times (\eta_\mathrm{Sp}\mathbf{j}_\mathrm{CR})| \overset{(A.3)}{=} |\eta_\mathrm{Sp}\nabla \times \mathbf{j}_\mathrm{CR} - \mathbf{j}_\mathrm{CR} \times \nabla\eta_\mathrm{Sp}| \simeq |\mathbf{j}_\mathrm{CR} \times \nabla\eta_\mathrm{Sp}| \simeq \frac{\mathbf{j}_\mathrm{CR}\eta_\mathrm{Sp}}{L_T} , \tag{2.34}$$

where $L_T = \nabla T/T$ is the typical scale of temperature inhomogeneities. Plugging in the typical parameters during Reionization, the cosmological epoch which this mechanism is assumed to operate at, the result, further investigated by numerical simulations, is that Cosmic Rays are able to generate magnetic fields with strengths of $B \simeq 10^{-17} ... 10^{-16}\,\mathrm{G}$ on time scales of 10^9 years.

2.1.2 Cosmological Scenario of Magnetogenesis

The Cosmological Scenario of cosmic magnetogenesis describes the generation of magnetic fields in the Early Universe, approximately prior to or during Recombination, i.e. $T > T_{\mathrm{Rec}} \simeq 0.25\,\mathrm{eV}$. In contrast to the Astrophysical Scenario the magnetic fields are not created by local objects (like stars, galaxies, etc.) and then spread into the IGM, but rather by a global incident like, for example, a cosmological phase transition (cf. Secs. 1.2.3 and 1.2.4) which therefore would generate magnetic fields all over the Universe simultaneously. In other words, just as, for example, the CMB is the observable trace of Photon Decoupling, one would expect that a global, omnipresent magnetic field is the characteristic signature of the aforementioned cosmological incident. Therefore, once they can be measured, such magnetic fields would reveal information about the magnetogenesis event itself.

Magnetic fields which are created this way are also known as Primordial Magnetic Fields (PMF). There is a large number of possible events which are regarded as candidates for primordial magnetogenesis of which the most promising up to now seem to be the Electroweak and the QCD Phase Transitions for which the different scenarios will be discussed in more detail in the following, however also presenting other possible models hereafter without the claim of completeness. For further reading and additional possible mechanisms the reviews [1, 103, 104] should be consulted.

2.1.2.1 Magnetic Fields from the QCD Phase Transition

Apart from the general discussion of the QCD Phase Transition (QCDPT) in Sec. 1.2.4, a more demonstrative presentation of the processes during a first order QCDPT may be extracted from [61]: As soon as the temperature decreases below the critical temperature T_{QCD} by a certain amount, small nucleation sites of the hadronic phase appear with an average distance of $L_{\mathrm{QCD}} \simeq 10^{0\pm1}\,\mathrm{m}$ between them. These "seeds" start to grow slowly (with velocities of the order $v \simeq 0.1c$) via deflagration in form of spherical bubbles of the hadronic phase. The latent heat released due to this growth is transported via supersonic shock fronts which finally collide at the time when the bubble itself has a radius of approximately $\frac{L_{\mathrm{QCD}}}{10}$. After that the latent heat release is balanced with respect to Expansion of the Universe, such that the temperature is kept at T_{QCD} until Expansion becomes dominant and the temperature is lowered below the critical value which results in a quick transformation of all the quarks into baryons and mesons.

One possible scenario to create magnetic fields during this phase transition is to consider the quark and leptonic components of the primordial medium as two fluids with a net positive and negative charge, respectively [105]. The release of latent heat as described above creates a pressure gradient up to the shock front which, due to charge separation of the two components, generates a radial electric field given by [105, 106]

$$\mathbf{E} \simeq \frac{(\rho_{\mathrm{q}} + p_{\mathrm{q}})\,\nabla p_{\mathrm{l}} - (\rho_{\mathrm{l}} + p_{\mathrm{l}})\,\nabla p_{\mathrm{q}}}{e n_{\mathrm{l}}\,(\rho + p)}\,, \tag{2.35}$$

where ρ is the energy density and p the pressure density of quarks (index 'q'), leptons (index 'l') and in total (no index), respectively. Although this computation does not take into account many details, such as the specific contributions by the different types of leptons and quarks, it gives a good estimate of the resulting electric field for the given parameters of the QCD Phase Transition from numerical simulations, $\mathbf{E} \simeq 1.5{\times}10^{6}\,\mathrm{V/m}$.

Furthermore, also the currents created by the process may be calculated. Taking (1.5) including the displacement current, one can set the magnetic field to zero, therefore

reducing the equation to

$$\mathbf{0} = 4\pi\mathbf{j} + \partial_t \mathbf{E} \simeq 4\pi\mathbf{j} + \frac{v}{L_{QCD}}\mathbf{E}\,, \tag{2.36}$$

where v is the magnitude of the fluid velocity, hence giving

$$|\mathbf{j}| \simeq \frac{v}{4\pi L_{QCD}} |\mathbf{E}| \ . \tag{2.37}$$

After the shocks collide, the system becomes turbulent, therefore giving rise to a generation of magnetic fields in a similar way as the Biermann Battery mechanism (cf. Sec. 2.1.1.1). With (1.5), this time neglecting the displacement current, (2.37) gives the estimate

$$\frac{B}{L_{\mathrm{QCD}}} \simeq 4\pi\,|\mathbf{j}| \overset{(2.37)}{\simeq} \frac{v}{L_{\mathrm{QCD}}}\,|\mathbf{E}| \tag{2.38}$$

and therefore values for B of approximately $B(L_{\mathrm{QCD}}) \simeq v\,|\mathbf{E}| \simeq 5\,\mathrm{G}$ for velocities of $v \simeq 0.1c$ (see above). For scales L different than the QCD transition scale L_{QCD} the magnetic field may be obtained by the power law rule $B \propto L^{-\frac{\alpha}{2}}$ as described in Sec. 3.1.3.1.

A different approach is to look at the coexistence phase of the QCDPT [107], based on the difference of the baryon number densities $n_{\mathrm{b}}^{\mathrm{q}}$ and $n_{\mathrm{b}}^{\mathrm{h}}$ of the quark and the hadronic phase, respectively, in chemical equilibrium, given by the ratio $R = n_{\mathrm{b}}^{\mathrm{q}}/n_{\mathrm{b}}^{\mathrm{h}}$, which depends on the phase transition temperature T_{QCD}. However, as the bubbles of the hadronic phase continue to grow, this equilibrium cannot be maintained anymore since diffusion becomes less effective. Therefore the growing bubbles "push" the quarks at their walls ahead of themselves, thus increasing R there by orders of magnitude up to values of $R \simeq 10^2 ... 10^4$, with an upper limit of $R \simeq 10^6$. The thickness d of such a layer with a baryon excess is given by [108]

$$d \simeq \frac{L_{\mathrm{diff}}^2}{L_{\mathrm{QCD}}}\,, \tag{2.39}$$

where L_{diff} is the diffusion length, which depends also on T_{QCD}, and, for example, is given by $L_{\mathrm{diff}} \simeq 4.4 \times 10^{-6}\,\mathrm{m}$ for $T_{\mathrm{QCD}} = 100\,\mathrm{MeV}$. The baryon number density therefore has a sharp discontinuity at the boundary of the two phases, falling off exponentially inside the quark phase.

Together with the baryon number excess comes also a net charge excess which, due to the high quark concentration, is positive on the quark side and, due to leptons, negative at the bubble wall, again decreasing exponentially with the distance from it. The positive charge density ρ_{ch}^{+} is given by

$$\rho_{\mathrm{ch}}^{+} = e\overline{n}_{\mathrm{b}} R\beta\,, \tag{2.40}$$

where β accounts for the different quark masses and can attain values of up to 0.28, while the overline denotes the spatial average.

This net charge distribution produces currents via a peculiar velocity field. The magnitude of this velocity field may be estimated by demanding a constant entropy density for which the continuity equation gives $\nabla \cdot \mathbf{v}_{\mathrm{q}} = \nabla \cdot \mathbf{v}_{\mathrm{h}} = 0$ for the total velocity field. By decomposing these velocities into the component due to the velocity of the Hubble expansion and the peculiar one ($\mathbf{v}^{\mathrm{p}}$),

$$\mathbf{v}_i = \mathbf{v}_i^{\mathrm{p}} + \mathbf{r}\frac{\partial_t a}{a}\,, \tag{2.41}$$

where $i = \mathrm{q}, \mathrm{h}$ denote the two phases of the transition, this can be rewritten as

$$\nabla \cdot \mathbf{v}_i^{\mathrm{p}} = -\nabla \cdot \left(\mathbf{r} \frac{\partial_t a}{a} \right) \overset{(1.162)}{=} -3H_{\mathrm{QCD}} \,, \tag{2.42}$$

where H_{QCD} is the Hubble parameter at the QCDPT. A rough estimate therefore gives the value for the peculiar velocity,

$$v_i^{\mathrm{p}} \simeq L_{\mathrm{QCD}} H_{\mathrm{QCD}} \,. \tag{2.43}$$

Having all these considerations at hand, it is finally possible to give a value for the generated magnetic field. This can be done by representing the charged layer of the hadronic phase bubble of radius r by a charged spherical shell of charge $q = 4\pi r^2 d\rho_{\mathrm{ch}}^+$ rotating at speed $v = v_{\mathrm{h}}^{\mathrm{p}}$. The magnetic moment μ_{cs} for such an object is given by [12]

$$\mu_{\mathrm{cs}} = \frac{qvr}{3} \tag{2.44}$$

while, from (1.50), for $\mathbf{r} \parallel \boldsymbol{\mu}$ and $|\mathbf{r}| = r$, the magnetic field at the surface can be estimated to be

$$\begin{aligned} B_{\mathrm{QCD}} &= \left| 3\frac{(\boldsymbol{\mu}_{\mathrm{cs}} \cdot \mathbf{r})\,\mathbf{r}}{r^5} - \frac{\boldsymbol{\mu}_{\mathrm{cs}}}{r^3} \right| = \left| 3\frac{(\mu_{\mathrm{cs}} r)\,\mathbf{r}}{r^5} - \frac{\boldsymbol{\mu}_{\mathrm{cs}}}{r^3} \right| = 2\frac{\mu_{\mathrm{cs}}}{r^3} \overset{(2.44)}{=} 2\frac{qv}{r^2} \\ &= \frac{2}{3} \left(4\pi d\rho_{\mathrm{ch}}^+ \right) \left(v_{\mathrm{h}}^{\mathrm{p}} \right) \overset{(2.39),(2.40)}{\simeq} \frac{8\pi}{3} e\overline{n}_{\mathrm{b}} R\beta L_{\mathrm{diff}}^2 H_{QCD} \,. \end{aligned} \tag{2.45}$$

With the values of the parameters motivated above, namely $\overline{n}_{\mathrm{b}} \simeq 10^{33} m^{-3}$, $L_{\mathrm{diff}} \simeq 4 \times 10^{-6}\,\mathrm{m}$ and $\beta R \simeq 0.1...10$, the estimated magnetic field is given by $B_{\mathrm{QCD}} \simeq 10^6...10^8\,\mathrm{G}$, which exceeds the one found in [105] by several orders of magnitude.

In addition to this "direct" magnetogenesis due to bubble growth itself, also hydrodynamic instabilities during this process may play a role in the generation of magnetic fields [109]. Such a growth is assumed to be possible in an efficient way if the condition [110]

$$v \leq v_{\mathrm{crit}} \equiv \left(\frac{T_{\mathrm{QCD}}^2 - T_{\mathrm{q}}^2}{2T_{\mathrm{QCD}}^2} \right)^{\frac{1}{2}} \,, \tag{2.46}$$

where T_{q} is the temperature in the quark phase, is fulfilled which seems to be the case for the QCDPT. The growth rate Γ_{inst} for such instabilities is given by

$$\Gamma_{\mathrm{inst}} \simeq (v_{\mathrm{h}} - v_{\mathrm{q}}) \frac{k}{2} \tag{2.47}$$

for appropriate values of k, where v_{h} and v_{q} are the hadron and the quark phase velocities in the bubble wall rest frame, respectively. In the same frame, looking at a small section of the bubble wall, it can be regarded as planar, located at $y = 0$ in a Cartesian coordinate system with its perturbation y_{w} given by

$$y_{\mathrm{w}}(x,t) = y_0 \exp\left(\Gamma_{\mathrm{inst}} t + ikx \right) \,. \tag{2.48}$$

Using this, the authors of [109] were able to derive that the velocity perturbations on both sides of the wall, oriented parallel to it (i.e., for example, in the direction of the x-axis), suffer a discontinuity described by the equation

$$\left| v'_{\mathrm{q},x} - v'_{\mathrm{h},x} \right| = (v_{\mathrm{q}} - v_{\mathrm{h}}) k y_{\mathrm{w}}(x,t) \tag{2.49}$$

for perturbation of velocities in both phases, $v'_{\mathrm{q},x}$ and $v'_{\mathrm{h},x}$, which results in a current which, using (1.5), gives a magnetic field. The latter might be further amplified by MHD effects resulting in magnetic field strengths of $B \simeq 1...10\,\mathrm{G}$ right at the QCD phase transition on a comoving scale of 10 Mpc. This would result in $B \simeq 10^{-20}\,\mathrm{G}$ today if no Inverse Cascade is operating (cf. Sec 3.1).

2.1.2.2 Magnetic Fields from the Electroweak Phase Transition

One possible mechanism to create magnetic fields during the Electroweak Phase Transition (EWPT) is based on a similar idea as for the QCDPT described above, i.e., for a first order phase transition, on the nucleation of the low-temperature phase [111]. In particular, during such a phase transition bubbles of the spontaneously broken phase (cf. Sec. 1.2.4.2) form and start to expand at subsonic speeds, converting the false vacuum energy into kinetic energy. The expansion of these bubbles is preceded by a supersonic shock front. Once these shock fronts collide, they produce turbulence approximately of the size of the bubbles given by R_{bubble} since the Reynolds Number has been estimated to be sufficiently high, namely of the order of $\mathcal{R} \simeq 10^{12}$ [111]. Assuming, furthermore, as shown in Sec. 3.1.2, that the conductivity is rather high and therefore the magnetic fields follow the fluid motions, this would moreover mean that strong magnetic turbulence is produced as well and, being in equipartition with the kinetic turbulent flow, has the energy

$$B^2(R_{\mathrm{bubble}}) \simeq \epsilon\,(T_{\mathrm{EW}})\,v^2 \simeq g_* T_{\mathrm{EW}}^4 v^2\,, \tag{2.50}$$

where $\epsilon\,(T_{\mathrm{EW}}) \simeq g_* T_{\mathrm{EW}}^4$ (with $g_* \simeq 10^2$ being the number of degrees of freedom that scatter by electroweak processes and $T_{\mathrm{EW}} \simeq 10^{11}\,\mathrm{GeV}$ the critical temperature of EWPT) is the energy density of the electroweak plasma and $v \simeq 10^{-1}$ is the typical fluid velocity.

In order to derive the magnetic field strength on scales larger than R_{bubble}, one can treat it as a superposition of randomly oriented magnetic dipoles of the size R_{bubble}, each having a strength as described above. By making a continuum approximation of randomly Gaussian distributed magnetic moments $\boldsymbol{\mu}_i$ pointing in the ith direction, their correlation function is given by (cf. Sec. 1.1.3.2)

$$\langle \boldsymbol{\mu}_i(\mathbf{r})\boldsymbol{\mu}_j(\mathbf{0})\rangle = \kappa\delta_{ij}\delta^{(3)}(\mathbf{r})\,, \tag{2.51}$$

such that, using the fact that the magnetic field produced by a magnetic dipole is given by $B \propto e\mu/\left|\mathbf{r}-\mathbf{r}_{\mathrm{d}}\right|^3$ (cf. Sec. 1.1.1.5), $\mathbf{r}_{\mathrm{d}}$ being the position of the dipole, the correlation function for the superposition mentioned above is

$$\langle \mathbf{B}(\mathbf{r})\mathbf{B}(\mathbf{0})\rangle \simeq \kappa e^2 \int \frac{1}{|\mathbf{r}-\mathbf{r}_{\mathrm{d}}|}\frac{1}{|\mathbf{r}_{\mathrm{d}}|}\mathrm{d}^3 r_{\mathrm{d}}\,. \tag{2.52}$$

Now one can cut off the logarithmic divergence of this integral at a typical dipole size, i.e. at R_{bubble}, given by

$$R_{\mathrm{bubble}} \simeq f_{\mathrm{b}} H_{\mathrm{EW}}^{-1} \tag{2.53}$$

where $H_{\mathrm{EW}}^{-1} \simeq 10\,\mathrm{cm}$ is the typical horizon size at the EWPT and $f_{\mathrm{b}} \simeq 10^{-3}...\,10^{-2}$ is the typical fractional size. This therefore gives for (2.52)

$$\langle \mathbf{B}(\mathbf{r})\mathbf{B}(\mathbf{0})\rangle \simeq \frac{e^2\kappa}{r^3}\ln\left(\frac{H_{\mathrm{EW}} r}{f_{\mathrm{b}}}\right)\,. \tag{2.54}$$

Now, averaging over a domain of the size R and using the assumption of equipartition, i.e. (2.50), one arrives at

$$\overline{B_R^2} \simeq v^2 g_* T_{\mathrm{EW}}^4 \left(\frac{f_\mathrm{b}}{H_{\mathrm{EW}} R}\right)^3 \ln^2\left(\frac{H_{\mathrm{EW}} R}{f_\mathrm{b}}\right) . \tag{2.55}$$

Taking the upper limit for the diffusion length as the significant length scale, i.e. $R \simeq L_{\mathrm{diff}} \simeq 10^{-5}\,\mathrm{pc}$, one finally gets an estimate of

$$B(L_{\mathrm{diff}}) \simeq 10^{-9} ... \, 10^{-7}\,\mathrm{G} \tag{2.56}$$

for the EGMF field strength. Again, taking into account plasma instabilities as has been described in the previous section based on [109], magnetic fields strength as high as $B \simeq 1 ... \, 10\,\mathrm{G}$ on a comoving scale of $10\,\mathrm{Mpc}$ might be created (corresponding to $B \simeq 10^{-29}\,\mathrm{G}$ today) although for EWPT the physics of instabilities is not entirely certain, in the best case having them operating at later stages of the phase transition.

However, even for a second order EWPT the creation of magnetic fields is predicted to happen [103, 112]. When the temperature approaches T_{EW} (the temperature of the EWPT), domains of the false vacuum with broken symmetry emerge due to thermal fluctuations (cf. Sec. 1.2.4.2). The size of these domains is estimated to be roughly the correlation length of the Higgs field at the temperature T_G (the so-called Ginsburg Temperature at which the domains' Free Energy becomes larger than the corresponding thermal energy, therefore making them stable against thermal fluctuations), thus forcing the system out of thermal equilibrium in favor of the broken phase. It turns out that that $T_\mathrm{G} \simeq T_{\mathrm{EW}}$, such that the size of a broken phase domain is given by the correlation length $L_{\mathrm{corr}}^{\mathrm{EW}}$ given by [112] $L_{\mathrm{corr}}^{\mathrm{EW}} \simeq 10/T_\mathrm{G}$. Now, the different vacuum expectation values of the two phases result in a gradient between them which, once the EWPT is complete, will result in a current of W bosons and thus in a magnetic field. The conceptual difficulty which has to be overcome here is the definition of the electromagnetic field in the presence of an inhomogeneous Higgs background which, however, may be done [113], giving a magnetic field with a strength of $B \simeq 10^{23}\,\mathrm{G}$ on length scales $L_{\mathrm{corr}}^{\mathrm{EW}}$ which, neglecting effects of magnetic helicity, would result in magnetic field strengths of $B \simeq 10^{-30}\,\mathrm{G}$ on length scales of $100\,\mathrm{kpc}$. In a similar way, however using a different statistical approach, [114] finds $B \simeq 10^{-19}\,\mathrm{G}$.

2.1.2.3 Magnetic Fields from Inflation

One of the first publications to consider Inflation as the magnetogenesis epoch for Primordial Magnetic Fields has been [115]. The basic idea is to couple the electromagnetic field to gravitation by adding terms of the form $RA_\mu A^\mu$, $R_{\mu\nu} A^\mu A^\nu$, $R_{\mu\nu\lambda\kappa} F^{\mu\nu} F^{\lambda\kappa}/m^2$, $R_{\mu\nu} F_{\mu\kappa} F^\nu_\kappa / m^2$ or $R F^{\mu\nu} F_{\mu\nu} / m^2$, where A^μ is the electromagnetic 4-potential given by

$$A^\mu = \begin{pmatrix} \phi \\ \mathbf{A} \end{pmatrix} \tag{2.57}$$

and $F^{\mu\nu}$ the electromagnetic field tensor,

$$F_{\mu\nu} = \partial_\mu A_\nu - \partial_\nu A_\mu \, . \tag{2.58}$$

Taking, for simplicity, only additional terms of the form $RA_\mu A^\mu$ and $R_{\mu\nu} A_\mu A^\nu$, the resulting Lagrangian for electromagnetic fields therefore would have the form

$$\mathcal{L} = -\frac{1}{4} F_{\mu\nu} F^{\mu\nu} - \frac{b}{2} R A_\mu A^\mu - \frac{c}{2} R_{\mu\nu} A^\mu A^\nu \, , \tag{2.59}$$

where b and c are constants describing the coupling, where the case $b = c = 0$ corresponds to the classical Lagrangian of electromagnetism. This equation may be transformed into a time evolution equation for $\mathbf{B}$, given by [115]

$$\frac{1}{a^2}\partial_\eta^2\left(a^2\mathbf{B}\right) - \Delta\mathbf{B} + \frac{n}{\eta^2}\mathbf{B} = 0\,, \tag{2.60}$$

where a is the scale factor, η the conformal time, (1.166), and n is defined as

$$n \equiv \eta^2\left\{6b\frac{\partial_\eta^2 a}{a} + c\left[\frac{\partial_\eta^2 a}{a} + \left(\frac{\partial_\eta a}{a}\right)^2\right]\right\}\,. \tag{2.61}$$

Following the rules for Fourier Transforms given in Sec. A.3, (2.60) can be rewritten in terms of $\tilde{\mathbf{B}}_\mathbf{k} \equiv a^2\mathcal{F}_{\mathbf{rk}}\{\mathbf{B}\}$ as

$$\partial_\eta^2\tilde{\mathbf{B}}_\mathbf{k} + k^2\tilde{\mathbf{B}}_\mathbf{k} + \frac{n}{\eta^2}\tilde{\mathbf{B}}_\mathbf{k} = 0\,. \tag{2.62}$$

For $n = 0$, i.e. the classical electromagnetic theory, the magnetic energy denisty would have the dependence on the scale factor given by $\epsilon_B \overset{(1.60)}{\propto} \left|\tilde{\mathbf{B}}_\mathbf{k}\right|^2/a^4 \propto a^{-4}$ as expected (cf. Ch. 3).

However, in the case $b = -1/6$ and $c = 0$ (the so-called minimal coupling case) for an electromagnetic mode outside the horizon, i.e. a mode with $|k\eta| \ll 1$, it is $\left|\tilde{\mathbf{B}}_\mathbf{k}\right| \propto a$ and therefore $\epsilon_B \propto a^{-2}$, such that one can say that once the mode becomes greater than the horizon it is "frozen in" such that the corresponding magnetic energy density decays more slowly than for modes inside the horizon. This continues until the mode reenters the horizon (due to further Expansion) which happens much later, during the radiation-dominated regime. Therefore, assuming that during Inflation a quantum fluctuation of the electromagnetic field which exceeds the Hubble Radius is excited, they store the electromagnetic energy such that the resulting magnetic fields might be relevant. However, the corresponding energy content is highly dependent on the particular Inflation model as well as on the choice of the parameters b and c, the values given in [115] having a range of $\epsilon_B/\rho_\mathrm{r} \simeq 10^{-57}...10^{-8}$, where ρ_r is the radiation energy density. It should be noted here that this model has a number of issues like the not well-motivated introduction of the values for b and c and the breaking of gauge variance by the terms added to the Lagrangian.

2.1.2.4 Magnetic Fields from Density Perturbations

The general idea of this mechanism of magnetogenesis originates in the suggestion by [98] as described in Sec. 2.1.1.2 and is based on magnetogenesis from vorticity in protogalaxies. However, as claimed by [116, 117], vorticity might originate from density perturbations and therefore have a cosmological cause. The idea is to treat the cosmic medium as a fluid of three intensely interacting components (photons, electrons and protons) during the radiation-dominated era. Then, from $T \simeq m_e = 5.1 \times 10^5\,\mathrm{eV}$ to $T \simeq T_\mathrm{Rec}$, small differences in the different interaction strengths and masses of the particles cause small differences in the rotation velocities, giving rise to currents and therefore magnetic fields. The crucial assumption here is that these rotation velocities are caused by scalar density perturbations [116] which are omnipresent in the Early Universe. By

taking into account perturbations of the metric up to the second order, the authors were able to derive a magnetic field of

$$B(\lambda) \simeq 10^{-23} \left(\frac{\lambda}{1\,\mathrm{Mpc}} \right)^{-2} \mathrm{G} \tag{2.63}$$

on a scale λ at Recombination. In [117] the authors claim that in addition also the anisotropic stress of photons might play a role and find a somewhat stronger field of $B \simeq 10^{-19}\,\mathrm{G}$ at $\lambda = 10\,\mathrm{Mpc}$.

2.1.2.5 Magnetic Fields from Neutrino Decoupling

The concept of magnetogenesis during Neutrino Decoupling, as introduced by [118], assumes that before Neutrino Decoupling the net neutrino lepton number, $N_\nu - N_{\overline{\nu}}$, varied in space on some scale λ. Since the Weak Interaction cross section of neutrinos and electrons on the one hand and of neutrinos and positrons on the other hand are different, in the presence of an interacting neutrino flux the two charged components experience different forces leading to different drift velocities which results in an electric current of [118]

$$|\mathbf{j}| \simeq 4 \times 10^{-20} e \left(\frac{T}{1\,\mathrm{MeV}} \right)^3 \left(\frac{\delta n_\nu}{n_\nu} \right) , \tag{2.64}$$

where T is the temperature and $\delta n_\nu / n_\nu$ is the relative excess in neutrino number density. According to the authors this would give a seed magnetic field of $B \simeq 10^{-22}\,\mathrm{G}$.

2.2 Lower Limits for the Magnetic Field Strength

First, standard constraints on EGMF, derived from cosmological and astrophysical observations, are given in Sec. 2.2.1. Since, as will be shown there, they do not give lower limits on the magnetic field strength, the remainder of the present section will be dedicated to the discussion of recent ideas on the derivation of such limits due to observations of far away sources since photons emitted by such objects are thought to develop electromagnetic cascades (Sec. 2.2.2) which are affected by EGMF (Sec. 2.2.3). Finally, in Secs. 2.2.4 and 2.2.5, an alternative approach to explain the aforementioned observations, namely the interaction of the cascade electrons and positrons with the Intergalactic Medium (IGM), is presented.

2.2.1 Current Observational Status of Extragalactic Magnetic Fields

Up to the present day it is not possible to detect Extragalactic Magnetic Fields (EGMF) by direct observation, but rather only to set limits on them. The resulting value for the field strength B, together with the information about the correlation length L_B, in the simplest case describes the configuration of EGMF. By different observation techniques it is then possible to exclude some of the ranges for these quantities.

Apart from these methods described in Secs. 2.2.1.1-2.2.1.4, there are further possibilities to probe EGMF [103, 119] which, however, currently still require further refinement or more observational data. Two of them shall be mentioned here briefly: On the one hand, the propagation of Ultra High Energy Cosmic Rays (UHECR) with energies of up to $10^{21}\,\mathrm{eV}$ [120] from which EGMF strengths of up to $10^{-9}\,\mathrm{G}$ may be deduced due to specific features in the spectrum of gamma rays produced during UHECR propagation. On the other hand, constraints from BBN may be derived as the presence of strong

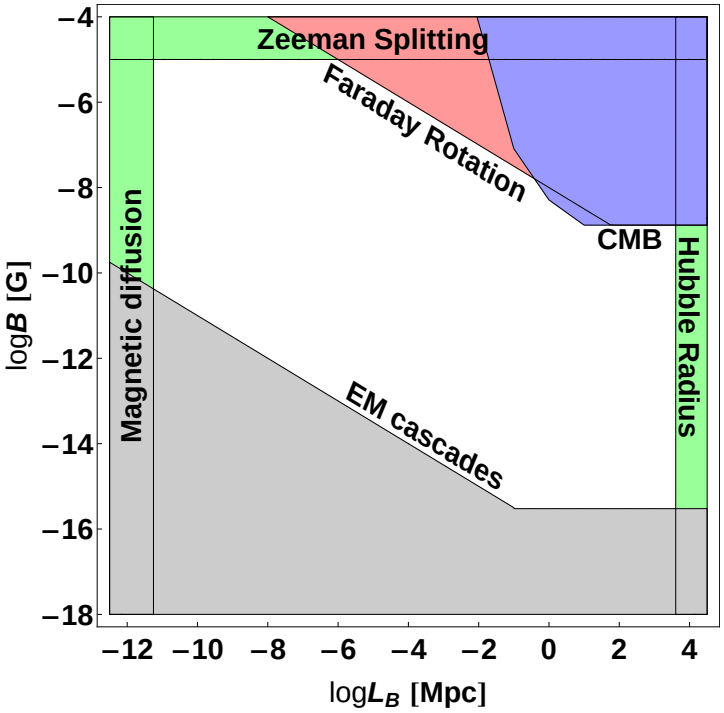

Figure 2.1: Constraints on the field strength B and the correlation length L_B for Extragalactic Magnetic Fields: Zeeman Splitting (Sec. 2.2.1.1), Non-observation of Faraday Rotation for Quasars (Sec. 2.2.1.2), limits from the distortions of the CMB spectrum (Sec. 2.2.1.3), upper and lower generic constraints on the correlation length from small scale magnetic decay and the size of the Universe, respectively (Sec. 2.2.1.4), and observations of electromagnetic cascades (Sec. 2.2.3).

magnetic fields should have increased the β decay rate of neutrons due to the enlargement of the electron phase space, resulting in fewer neutrons available to be bound into helium and thus a lower relic abundance of the latter [121, 122]. Furthermore, magnetic fields might have also influenced the BBN freeze-out temperature because of modifications of the Expansion rate of the Universe due to the additional provided energy, hence again varying the abundance of the light elements [123]. Comparing that to actual BBN predictions then might give limits somewhere in the range $B \lesssim 10^{-6}...10^{-9}$ G [103].

2.2.1.1 Zeeman Splitting

A first upper limit for B can be derived from the Zeeman Splitting of the 21-cm-hydrogen-line [124]: The Zeeman Effect describes the impact of magnetic fields on the spectral lines of atoms due to the interaction between the magnetic moment of the electrons and the magnetic field [125]. In general, the potential energy of a magnetic dipole, characterized by a magnetic moment $\boldsymbol{\mu}$, is given by its orientation in an external magnetic field $\mathbf{B}$ along, without loss of generality, the z-axis, expressed by

$$E_\mu = \boldsymbol{\mu} \cdot \mathbf{B} = \mu_z B \,. \tag{2.65}$$

Since in the classical picture the magnetic moment of an atom is parallel to the angular momentum, in terms of quantum mechanics this can be rewritten as an additional potential to the Hamilton Operator,

$$V_\mu = g \frac{e\hbar}{2m_e} m B \,, \tag{2.66}$$

where g is the Landé g-Factor associated with the angular momentum considered – either the orbital angular momentum for the normal or the total angular momentum from the LS-Coupling for the anomalous Zeeman Effect. Furthermore, m is the corresponding angular momentum projection quantum number.

The observed Zeeman Effect for radiation from distant quasars corresponds to a field strength of the order of $B \simeq 1 - 100\ \mu\mathrm{G}$ which usually is assumed to be the field of the Milky Way and other galaxies [126]. Therefore, as a conclusion, the EGMF cannot be stronger than this value, which places an upper constraint of $B \lesssim 10^{-5}\,\mathrm{G}$. This constraint is shown in Fig. 2.1, labeled "Zeeman Splitting".

2.2.1.2 Faraday Rotation

The second phenomenon which can be used to detect EGMF is Faraday Rotation. It describes the effect that the polarization plain of an electromagnetic wave with a wavelength λ rotates by an angle β if it passes a medium which is under the influence of an magnetic field. The relation which describes this process is given by [11]

$$\beta = \lambda^2 RM \propto \lambda^2 \int_0^d n_e B_{||} dl\,, \tag{2.67}$$

where the so-called rotation measure RM depends on the integral along the line of sight of n_e, the number density of the electrons, and $B_{||}$, the component of the magnetic field parallel to the direction of photon propagation.

Although the exact value of n_e is not known, it is possible to set well-motivated constraints. Assuming it to be close to the critical density of the Universe and to be distributed homogeneously, the obtained limit is given by [127, 128]

$$B L_B^{\frac{1}{2}} \lesssim 10^{-8}\,\mathrm{G\,Mpc}^{\frac{1}{2}} \tag{2.68}$$

and can be seen in Fig. 2.1 with the label "Faraday Rotation". To derive this constraint the authors performed a statistical analysis over a large data sample of rotation measures of quasars and their dependence on the redshift z from which they concluded that only the galactic medium and the source itself give a significant contribution, while the Intergalactic Medium is not magnetized up to the level of sensitivity. Taking more complex models of the electron distribution into account, like the dependence of the observables on the Lyα data and therefore inhomogeneities, the constraints in general become weaker [129, 130].

2.2.1.3 CMB Anisotropies

The simplest approach to derive limits on the EGMF from CMB anisotropies is to assume the former to be a homogeneous magnetic field along, without loss of generality, the z-axis. The consequence is an anisotropic energy-momentum tensor and, following from the Einstein Equations (1.153), therefore an anisotropic expansion law. To be more specific, the most general form of the metric belonging to this setting is [131]

$$\mathrm{d}s^2 = \mathrm{d}t^2 - a^2(t)\left(\mathrm{d}x^2 + \mathrm{d}y^2\right) - b^2(t)^2 \mathrm{d}z^2\,, \tag{2.69}$$

where a and b are two different scale factors accounting for the anisotropic expansion. Introducing the quantities $\alpha = \frac{\partial_t a}{a}$, $\beta = \frac{\partial_t b}{b}$ and the anisotropy measure $\mathfrak{s} = \alpha - \beta$, the Einstein Equations may be rewritten as [132]

$$\partial_t \left(\frac{\mathfrak{s}}{H}\right) = \frac{1}{(\eta+1)\,t}\left(\frac{\mathfrak{s}}{H}(\eta - 1) + 4\frac{\epsilon_B}{\rho}\right)\,, \tag{2.70}$$

$$\partial_t \left(\frac{\epsilon_B}{\rho} \right) = -\frac{2}{9\,(\eta+1)\,t} \frac{\epsilon_B}{\rho} \left(4\frac{\mathfrak{s}}{H} + 9\,(\eta+1) - 12 \right) , \tag{2.71}$$

where $8\pi G$ has been set equal to 1 and ϵ_B is the magnetic energy density. Here H is the Hubble Parameter which, as the isotropy is assumed to be small, is close to its isotropic value given by (1.162), and η the characteristic factor introduced in (1.176). It is visible from (2.70) that for a vanishing magnetic field the anisotropy would rapidly decay for $\eta < 1$.

In the asymptotic case, i.e. $t \to \infty$, $\frac{\mathfrak{s}}{H}$ has to be constant and therefore one can read off from (2.70) that then it is $\frac{\mathfrak{s}}{H} \to \frac{4}{1-\eta}\frac{\epsilon_B}{\rho}$. Using this relation and, in addition, $\eta = \frac{1}{3}$ for the radiation-dominated era, (2.71) reduces to

$$\partial_t \left(\frac{\epsilon_B}{\rho} \right) = -4 \left(\frac{\epsilon_B}{\rho} \right)^2 , \tag{2.72}$$

for which the solution is given by

$$\frac{\epsilon_B}{\rho} \to \frac{C}{1 + 4C \ln\left(\frac{t}{t_0}\right)} , \tag{2.73}$$

where C is an integration constant.

In order to relate this to temperature anisotropies, one can calculate, under the assumption that the temperature at Recombination has been equal to T_{Rec} throughout the Universe, the different temperatures of photons coming from either the x-/y- or the z-direction:

$$T_x = T_y = T_{\mathrm{Rec}} \frac{a_{\mathrm{Rec}}}{a_{\mathrm{pres}}} = T_{\mathrm{Rec}} \exp\left(-\int_{t_{\mathrm{Rec}}}^{t_{\mathrm{pres}}} \alpha \mathrm{d}t \right) , \tag{2.74}$$

$$T_z = T_{\mathrm{Rec}} \frac{b_{\mathrm{Rec}}}{b_{\mathrm{pres}}} = T_{\mathrm{Rec}} \exp\left(-\int_{t_{\mathrm{Rec}}}^{t_{\mathrm{pres}}} \beta \mathrm{d}t \right) , \tag{2.75}$$

where the indices 'Rec' and 'pres' indicate quantities at the Recombination era and at the present, respectively. Hence, the temperature anisotropy is given by

$$\begin{aligned} \frac{\Delta T}{T} &= \frac{T_x - T_z}{T_{\mathrm{Rec}}} \overset{(2.74),(2.75)}{=} 1 - \exp\left(-\int_{t_{\mathrm{Rec}}}^{t_{\mathrm{pres}}} (\alpha - \beta)\, \mathrm{d}t \right) \simeq \int_{t_{\mathrm{Rec}}}^{t_{\mathrm{pres}}} (\alpha - \beta)\, \mathrm{d}t \\ &= \int_{t_{\mathrm{Rec}}}^{t_{\mathrm{pres}}} \mathfrak{s} \mathrm{d}t = \int_{t_{\mathrm{Rec}}}^{t_{\mathrm{pres}}} \frac{\mathfrak{s}}{H} H \mathrm{d}t \simeq \int_{t_{\mathrm{Rec}}}^{t_{\mathrm{pres}}} \frac{\mathfrak{s}}{H} \frac{1}{2t} \mathrm{d}t = \frac{1}{2} \int_{\ln t_{\mathrm{Rec}}}^{\ln t_{\mathrm{pres}}} \frac{\mathfrak{s}}{H} \mathrm{d} \ln t \,, \end{aligned} \tag{2.76}$$

where the relation $H \simeq 1/(2t)$ for the radiation-dominated era has been used. The last term can be, for $\mathfrak{s}/H = \mathrm{const}$, simplified to

$$\frac{\Delta T}{T} = \frac{1}{2} \int_{\ln t_{\mathrm{Rec}}}^{\ln t_{\mathrm{pres}}} \frac{\mathfrak{s}}{H} \mathrm{d} \ln t \simeq \frac{1}{2} \frac{\mathfrak{s}}{H} \ln\left(\frac{t_{\mathrm{pres}}}{t_{\mathrm{Rec}}} \right) \simeq 5 \frac{\mathfrak{s}}{H} \simeq 30 \frac{\epsilon_B}{\rho_{\mathrm{r}}} . \tag{2.77}$$

Setting $\Delta T/T < 10^{-6}$, the authors of [131] derived an upper limt on the magnetic field strength given by $B < 10^{-10} ... 10^{-9}\,\mathrm{G}$. A further refinement of this method using the CMB anisotropy measurements of COBE [55], which determined the CMB anisotropies to be of the order of $\Delta T/T \simeq 10^{-5}$, gives an upper bound of $B \leq 4 \times 10^{-9}\,\mathrm{G}$ [132] for large correlation lengths of the order of the Hubble Radius as shown in Fig. 2.1, denoted as "CMB anisotropies". More recent measurements [44], using a slightly different approach, give the limit $B < 3.4 \times 10^{-9}\,\mathrm{G}$ at scales of around 1 Mpc.

More realistic models take into account the stochastic nature of magnetic fields and look at particular physical mechanisms. An important idea is to use the effect first derived by [133, 134] which describes the impact of energy injection on the CMB spectrum. The possible consequences are twofold [134]: If the injection happens at redshifts $z \lesssim 4 \times 10^4$, an anisotropic energy injection results, via Compton Scattering, in a photon spectrum which may be described by a superposition of many black body distributions with slightly different temperatures, also known as Compton Distortions. For higher redshifts the photon distribution has enough time to evolve into an equilibrium state which, under the assumption of a constant photon number, changes from a Planck distribution to a Bose-Einstein one, characterized by a chemical potential μ.

In terms of magnetic fields it has been shown [135] that the magnetic energy dissipated away at small scales [49] may be transferred to the heat bath which then can distort the CMB spectrum. The authors were then able to calculate the resulting chemical potential and its time evolution. From recent constraints on the CMB chemical potential, $|\mu| < 9 \times 10^{-5}$ [136], magnetic fields are limited to $B \lesssim 3 \times 10^{-8}\,\mathrm{G}$ on scales of the order of 400 pc for the case of early energy deposit and on scales of approximately 0.6 Mpc for the late energy injection case.

2.2.1.4 Generic Bounds of the Correlation Length

A generic lower limit on the correlation length can be found using (1.16). The diffusion time τ_{diff} is approximately the time it takes magnetic fields to decay on a length scale L. Due to the proportionality $\tau_{\mathrm{diff}} \propto L^2$, after a given time, all magnetic fields on length scales smaller than the corresponding length already will have decayed, therefore giving the relation $L_B \simeq L(\tau_{\mathrm{diff}})$. Hence, to have a lower constraint on the correlation length, one has to use $\tau_{\mathrm{diff}} \simeq H^{-1}$ as the generic time scale with a conductivity of $\sigma \simeq 10^{11}\,\mathrm{s}^{-1}$ (see Sec. 3.1.2), such that rearranging (1.16) gives

$$L_B \geq L(\tau_{\mathrm{diff}}) = (4\pi\sigma H)^{-\frac{1}{2}} \ , \tag{2.78}$$

which results in $L_B \geq 2 \times 10^{11}\,\mathrm{m} \simeq 6 \times 10^{-12}\mathrm{Mpc}$.

However, no distinguished *upper* bounds on L_B could be found. The only possible statement which can be made is that it cannot be larger than the Hubble Radius, i.e. $L_B \leq H^{-1}$. These two generic limits are shown in Fig. 2.1, marked as "Magnetic diffusion" and "Hubble Radius", respectively.

2.2.2 Electromagnetic Cascades from High Energy Gamma Rays

Up to this point only lower and upper limits on the correlation length and a upper constraint for the magnetic field B have been stated. However, it is a crucial question whether also a *lower* limit on B can be given since this would be an important additional motivation to investigate Primordial Magnetic Fields.

Before relating it to concrete observations of EGMF, the general properties of an electromagnetic cascade should be discussed. Gamma rays emitted by a blazar are subject to reactions with the so-called Extragalactic Background Light (EBL) which, among other contributions, consists of the CMB and the Cosmic Infrared Background (CIB). While the former is a well-known and -studied phenomenon (cf. Sec. 1.2.3), the latter is still not entirely understood and therefore a source of uncertainty.

Usually CIB is defined to be the diffuse radiation from outside the Milky Way at a energy range of about 10^{-3} to 1 eV or even up to 10 eV [137]. The spectrum is

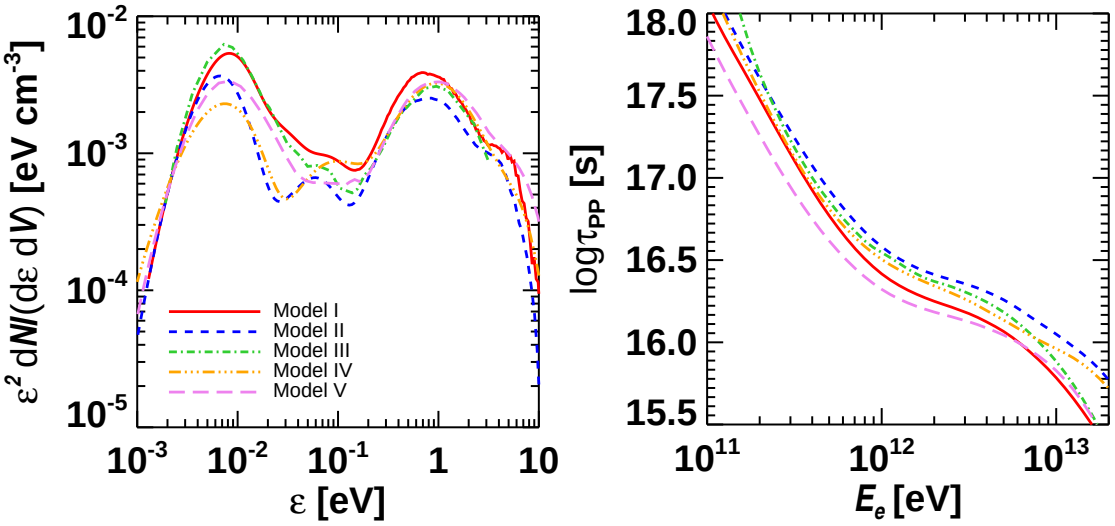

Figure 2.2: *Left panel*: The energy density of the Cosmic Infrared Background at redshift $z = 0$ versus the background photon energy ϵ for the various models (I-V) listed in Sec. 2.2.2. *Right panel*: The interaction time for Pair Production on the EBL for the same infrared backgrounds.

typically subdivided into two parts, each of them dominated by an intensity maximum (s. left panel of Fig. 2.2): First, the near infrared, having the peak at about 1 eV, which originates mostly from diffuse starlight having its frequency decreased by redshift. Second, the far infrared (with its maximum at approximately 10^{-2} eV), which mainly consists of light from stars which has been absorbed and then re-emitted at lower energies by intergalactic dust during its propagation. Since observations of the CIB are rather challenging [137], a large number of different models exist, five of which are presented as an example in the left panel of Fig. 2.2 and will be used for the calculations later on: The best-fit model of [138] (Model I), the lower-limit model of [139] (Model II), the model presented in [140] (Model III), model C of [141] (Model IV) and finally the semi-analytic model of [142] (Model V).

The dominating reaction of a high energy photon γ with a background photon $\gamma_{\rm EBL}$ is Pair Production (PP) [143–146] ($\gamma + \gamma_{\rm EBL} \rightarrow e^+ + e^-$) although there are several other possible reactions (such as [147] Double Pair Production ($\gamma + \gamma_{\rm EBL} \rightarrow e^+ + e^- + e^+ + e^-$), photon-photon scattering ($\gamma + \gamma_{\rm EBL} \rightarrow \gamma + \gamma$), direct photon interactions with the magnetic field (e.g. $\gamma + B \rightarrow e^+ + e^-$), the process $\gamma + \gamma_{\rm EBL} \rightarrow e^+ + e^- + \gamma$, muon Pair Production ($\gamma + \gamma_{\rm EBL} \rightarrow \mu^+ + \mu^- + \gamma$) and others) which, however, are usually negligible in the context of the development of an electromagnetic cascade. The threshold gamma ray energy $E_{\rm PP,thr}$ for PP is given by [147]

$$E_{\rm PP,thr} = \frac{m_e^2}{\epsilon} \simeq 2.6 \times 10^{11} \left(\frac{\epsilon}{\rm eV}\right)^{-1} \text{eV}\,, \tag{2.79}$$

where m_e is the electron mass and ϵ the energy of the EBL photon. In the high energy limit, i.e. $s \gg m_e^2$, the PP cross section is approximately

$$\sigma_{\rm PP} \simeq \frac{3}{2}\sigma_{\rm T}\frac{m_e^2}{s}\ln\left(\frac{s}{2m_e^2}\right)\,, \tag{2.80}$$

where s is the squared center of mass energy for the reaction and $\sigma_{\rm T}$ is the Thomson Scattering cross section

$$\sigma_{\rm T} = \frac{8\pi}{3}\frac{\alpha^2}{m_e^2} \simeq 6.65 \times 10^{-25}\,\text{cm}^2 \tag{2.81}$$

for the electromagnetic fine-structure constant α. On the other hand, for smaller energies σ_{PP} peaks close the threshold energy given by (2.79) such that the most efficient targets for Pair Production are EBL photons with an energy of $\epsilon \simeq m_e^2/E_\gamma$ which for TeV photons would give $\epsilon \simeq 10^{-1}\mathrm{eV}$, i.e. in the CIB range.

In general, one can calculate the interaction time τ (or, after multiplying it by c, the interaction length, or mean free path, λ) for a reaction of ultrarelativistic particles using the general formula [148]

$$\tau^{-1} = \frac{c}{\lambda} = \frac{1}{2}\int_{\epsilon_{\mathrm{thr}}}^{\infty} \frac{\mathrm{d}N_{\mathrm{EBL}}}{\mathrm{d}\epsilon \mathrm{d}V} \int_{-1}^{1} \sigma(s)\,(1-\cos\theta)\,\mathrm{d}\,(\cos\theta)\,\mathrm{d}\epsilon\,, \tag{2.82}$$

where $\mathrm{d}N_{\mathrm{EBL}}/\left(\mathrm{d}\epsilon \mathrm{d}V\right)$ is the ambient photon density per photon energy of the EBL, θ the angle between the directions of the incident particle and the EBL photon, σ the cross section of the reaction in question and ϵ_{thr} the threshold energy for the background photons.

For PP the incoming particle is a high energy photon with an energy E_γ, $\sigma = \sigma_{\mathrm{PP}}$ and, following (2.79), $\epsilon_{\mathrm{thr}} = m_e^2/E_\gamma$. Calculating the PP interaction time, it turns out that the estimate for the energy of the EBL photons scattering the incoming photons most efficiently to lie in the CIB range is indeed reasonable since the value for τ is highly sensitive to the particular CIB model [148] as can be also seen in the right panel of Fig. 2.2. Its approximate value is given by [119]

$$\tau_{\mathrm{PP}} \simeq 8 \times 10^{16} \kappa (1+z)^{-2} \left(\frac{E_\gamma}{10^{12}\,\mathrm{eV}}\right)^{-1} \mathrm{s}\,, \tag{2.83}$$

where $\kappa \simeq 1$ accounts for the EBL model uncertainties described above.

An electron or positron produced during PP typically has an energy of $E_e \simeq E_\gamma/2$ (however, in the so-called Klein-Nishina limit, i.e. $s \gg m_e^2$, *one* of the particles carries most of the high energy photon's energy [147]), thus still being in the ultrarelativistic regime and therefore having an energy high enough to be able to react with the EBL as well. The by far dominating reaction here is Inverse Compton (IC) scattering ($e^\pm + \gamma_{\mathrm{EBL}} \rightarrow e^\pm + \gamma_{\mathrm{EBL}}$) [149, 150] during which the electron up-scatters a background field photon to higher energies. It should be noted that, in principle, also higher order processes, like double IC scattering ($e^\pm + \gamma_{\mathrm{EBL}} \rightarrow e^\pm + \gamma + \gamma$), are possible but, due to their minor contribution, can be neglected in the following [147].

For energies below $E_e \simeq 10^{13}\,\mathrm{eV}$ the IC cross section is basically given by the Thomson Cross Section, $\sigma_{\mathrm{IC}} \simeq \sigma_{\mathrm{T}}$, i.e. the scattering process is elastic. This can be used to calculate the interaction time by plugging it into (2.82) for σ, i.e. $\sigma(s) = \sigma_{\mathrm{T}}$, and setting $\epsilon_{\mathrm{thr}} = 0$ since IC does not have a threshold energy. The result is a constant interaction time (except for effects of Expansion) for $E < 10^{13}\,\mathrm{eV}$ [148]. Now, however, the EBL component with energies most relevant for the scattering is CMB such that τ_{IC} does not depend on the CIB model and may be calculated explicitly, giving

$$\tau_{\mathrm{IC}} \simeq 1.2 \times 10^{11} (1+z)^{-3}\,\mathrm{s}\,, \tag{2.84}$$

where z is the cosmological redshift. Another important time scale to be used in the following is the cooling time $\tau_{\mathrm{IC,cool}}$ (or, equivalently, since $v \simeq c$, the cooling or energy loss length $\lambda_{\mathrm{IC,cool}} = c\tau_{\mathrm{IC,cool}}$) which is defined as

$$\tau_{\mathrm{IC,cool}} = \frac{\lambda_{\mathrm{IC,cool}}}{c} = \frac{E_e}{\mathrm{d}E_e/\mathrm{d}t} \simeq 3.87 \times 10^{13} \left(\frac{E_e}{10^{12}\,\mathrm{eV}}\right)^{-1} (1+z)^{-4}\,\mathrm{s} \tag{2.85}$$

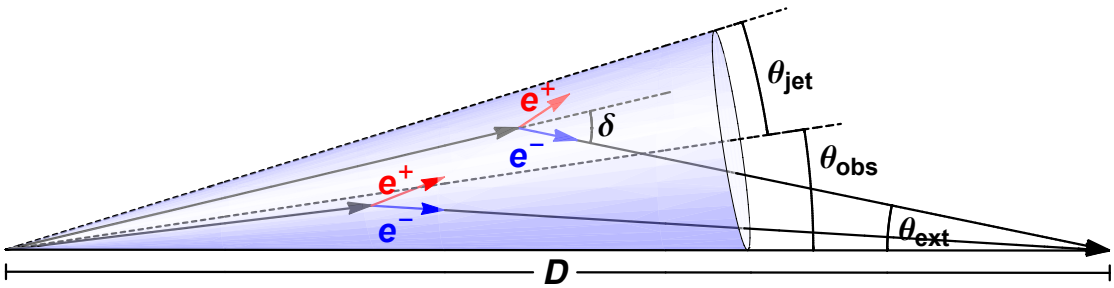

Figure 2.3: Gamma rays (black) emitted from a blazar on the left develop an electromagnetic cascade due to interactions with the Extragalactic Background Light (EBL) via Pair Production, producing electrons (blue) as well as positrons (red), and Inverse Compton (IC) scattering. The interaction of this cascade with the EGMF results in several observational features. Here θ_{obs} is the angle under which the jet emission of the source is observed at Earth on the right, θ_{jet} is the jet half opening angle, θ_{ext} describes the angular size of the extended emission and δ is the deviation angle of a Pair Production product reaching the observer (situated at a distance D from the source) from the initial gamma ray direction.

and is directly related to the electron's energy loss. Both τ_{IC} and $\tau_{\text{IC,cool}}$ are shown in the left panel of Fig. 2.5. Photons produced in an IC scattering on average have an energy of [11]

$$E_\gamma \simeq \frac{4}{3}\epsilon_{\text{CMB}} \left(\frac{E_e}{m_e}\right)^2 \simeq 4 \times 10^9 \left(\frac{E_e}{10^{12}\,\text{eV}}\right)^2 \text{eV}\,, \tag{2.86}$$

where in the second step a typical energy for a CMB photon, $\epsilon_{\text{CMB}} \simeq 7 \times 10^{-4}\,\text{eV}$, has been plugged in.

Dealing with magnetic fields, one should of course also mention synchrotron radiation, i.e. photons emitted by charged particles (electrons and positrons in this work) due to the radial acceleration inside a magnetic field. However, the cooling time $\tau_{\text{synch,cool}}$ for this process is given by [11]

$$\tau_{\text{synch,cool}} \simeq 2.5 \times 10^{20} \left(\frac{E_e}{10^{12}\,\text{eV}}\right)^{-1} \left(\frac{B}{10^{-9}\,\text{G}}\right)^{-2} \text{s}\,, \tag{2.87}$$

such that for EGMF it is, from (2.85), $\tau_{\text{IC,cool}} \ll \tau_{\text{synch,cool}}$ and therefore, compared to IC, the effect of synchrotron radiation is negligible.

The above discussion of PP and IC scattering shows that an initial photon emitted by a source will produce a electron/positron pair which, in turn, upscatters CMB photons to high energies. This recurs as long as the energies of the participating particles are well above the PP threshold and therefore results in an electromagnetic cascade which is schematically presented in Fig. 2.3. For $z \ll 1$ one expects the primary gamma ray either to reach the observer without reacting with the EBL or to undergo, at most, one PP process while the gamma ray produced by the resulting short-living pair has a mean free path large enough to reach the Earth.

2.2.3 Limits on the EGMF Strength from Gamma Ray Data

The idea and methodology to derive lower limits on the strength of EGMF from observations of gamma rays from blazars was first proposed by [4] and further developed by [119]. Both are based on the idea that electrons and positrons produced during the cascade are deflected by the EGMF which alters the observation of a gamma ray source. To summarize what follows, one can say that the three main effects consist of a visible

halo around point sources, modified time delays and the suppression of gamma ray flux at low (i.e. GeV) energies.

The former idea, i.e. that point sources appear extensive due to magnetic fields, has been investigated by various authors [151–156]. For the deflection of charged leptons in the EGMF one can distinguish two opposite cases depending on the relation between the magnetic field correlation length L_B of the EGMF and the energy loss length for IC scattering (2.85) [119]: For $L_B \gg \lambda_{\mathrm{IC,cool}}$ the motion of the electrons and positrons can be approximated by the propagation in an homogeneous magnetic field and therefore the angle δ in Fig. 2.3 is given by

$$\delta = \frac{\lambda_{\mathrm{IC,cool}}}{r_{\mathrm{L}}} \simeq 3 \times 10^{-4} (1+z)^{-2} \left(\frac{B}{10^{-18}\,\mathrm{G}}\right) \left(\frac{E_e}{10^{12}\,\mathrm{eV}}\right)^{-2} , \tag{2.88}$$

where B is the comoving magnetic field strength, which is assumed, in the simplest case, to be related to the physical value B_{phys} by $B_{\mathrm{phys}} = B(1+z)^2$, and r_{L} is the Larmor Radius given by

$$r_{\mathrm{L}} = \frac{E_e}{eB} \simeq 10^3 (1+z)^{-2} \left(\frac{B}{10^{-18}\,\mathrm{G}}\right)^{-1} \left(\frac{E_e}{10^{12}\,\mathrm{eV}}\right) \mathrm{Mpc}\,. \tag{2.89}$$

On the other hand, if the correlation length is small compared to the IC cooling distance, i.e. $L_B \ll \lambda_{\mathrm{IC,cool}}$, the deflection of the electron/positron can be seen as a diffusion process, such that δ is given by

$$\delta = \frac{(\lambda_{\mathrm{IC,cool}} L_B)^{\frac{1}{2}}}{r_{\mathrm{L}}} \simeq 2 \times 10^{-5} (1+z)^{-\frac{1}{2}} \left(\frac{E_e}{10^{12}\,\mathrm{eV}}\right)^{-\frac{3}{2}} \left(\frac{B}{10^{-18}\,\mathrm{G}}\right) \left(\frac{L_B}{1\,\mathrm{kpc}}\right) , \tag{2.90}$$

where both B and $L_B = L_B^{\mathrm{phys}}(1+z)$ are comoving quantities. Now from geometrical considerations in Fig. 2.3 one can see that

$$\frac{\sin\delta}{\sin\theta_{\mathrm{ext}}} \simeq \frac{\delta}{\theta_{\mathrm{ext}}} = \frac{\lambda_{\mathrm{PP}}^{\mathrm{phys}}(E_{\gamma,0})}{D^{\mathrm{phys}}} \equiv \tau_\theta(E_{\gamma,0}, z)\,, \tag{2.91}$$

where D is the distance to the source and $E_{\gamma,0}$ is the energy of the initial photon emitted by the source. In the first step it has been assumed that the first PP takes place close to the source, i.e. $\delta, \theta_{\mathrm{ext}} \ll 1$. This is a reasonable assumption due to the decrease of the interaction time (and therefore the mean free path) with energy as seen from (2.83). Therefore, one can now write down an expression for θ_{ext}, the extension angle of the source [119]:

$$\theta_{\mathrm{ext}} \simeq \begin{cases} 0.5^\circ\,(1+z)^{-2} \left(\frac{\tau_\theta}{10}\right)^{-1} \left(\frac{E_\gamma}{10^{11}\,\mathrm{eV}}\right)^{-1} \left(\frac{B}{10^{-14}\,\mathrm{G}}\right), \; L_B \gg \lambda_{\mathrm{IC,cool}}\,, \\ 0.07^\circ\,(1+z)^{-\frac{1}{2}} \left(\frac{\tau_\theta}{10}\right)^{-1} \left(\frac{E_\gamma}{10^{11}\,\mathrm{eV}}\right)^{-\frac{3}{4}} \left(\frac{B}{10^{-14}\,\mathrm{G}}\right) \left(\frac{L_B}{1\,\mathrm{kpc}}\right)^{\frac{1}{2}}, \; L_B \ll \lambda_{\mathrm{IC,cool}}\,, \end{cases} \tag{2.92}$$

where the dependence on the observed gamma ray energy E_γ rather than on E_e could be achieved by using (2.86). This is a rather important result since one can see that the (observed) extension of the source shrinks with increasing energy which, for sufficiently large magnetic fields, provides a possibility to derive a lower limit on the magnetic field directly from images of gamma ray sources. However, this is only possible if $\theta_{\mathrm{ext}} > \theta_{\mathrm{PSF}}$, i.e. the extension angle exceeds the Point Spread Function angle θ_{PSF} of the instrument. Since the latter usually decreases with photon energy, hence limiting the resolution, it

is a challenging task to perform such an analysis, so probably only future experiments might be able to make it possible. Another problem is given by the fact that the considered source has to be distinguished from the diffuse gamma ray background [155]. Overcoming these issues, in principle, would then make it possible to obtain a measure for magnetic fields as low as $B \gtrsim 10^{-15}\,\mathrm{G}$ even from blazar remnants [155].

The second possibility to derive constraints from below on the magnetic field strength is the analysis of time delays for gamma ray sources [157–163]. To be more precise, if a source emits a flare of gamma rays, then it is expected that at Earth one will observe this initial flare as well as a secondary, delayed one. This is due to the fact that, while a primary photon travels straight forward from the source to the observer, photons from the cascade have a longer way as can be seen in Fig. 2.3: It first propagates under some angle away from the line of sight, produces a short-living electron/positron which then, via IC, produces another photon for which, due to the ultrarelativistic nature of the charged lepton, has the same direction as the lepton producing it, namely, in order to be observable, pointed at Earth. The primary photons therefore correspond to the first, the latter secondary photons to the second flare.

The resulting time delay, i.e. the time between these two flares, is given by

$$t_{\mathrm{delay}} = \left(\tau_{\mathrm{PP}}(E_{\gamma,0}, z) + t_{\mathrm{casc}}\right) - D\,, \tag{2.93}$$

where $\tau_{\mathrm{PP}}(E_{\gamma,0}, z)$ is the average time the initial photon passes from the source to the first PP (while the corresponding length scale is given by $D_\gamma \equiv c\tau_{\mathrm{PP}}(E_{\gamma,0}, z)$). The unknown time (and length) scale is t_{casc} (and D_{casc}), i.e. the period from the first PP until the cascade reaches the observer. From geometrical considerations in Fig. 2.3 one can use the law of cosines, which gives

$$\begin{aligned}
D_{\mathrm{casc}} &= \left(D^2 + D_\gamma^2 - 2DD_\gamma\cos\left(\delta - \theta_{\mathrm{ext}}\right)\right)^{\frac{1}{2}} = D\left(1 + \left(\frac{D_\gamma}{D}\right)^2 - 2\frac{D_\gamma}{D}\cos\left(\delta - \theta_{\mathrm{ext}}\right)\right)^{\frac{1}{2}} \\
&\overset{D_\gamma \ll D}{\simeq} D\left(1 - 2\frac{D_\gamma}{D}\cos\left(\delta - \theta_{\mathrm{ext}}\right)\right)^{\frac{1}{2}} \simeq D\left(1 - \frac{D_\gamma}{D}\cos\left(\delta - \theta_{\mathrm{ext}}\right)\right) = D \\
&- D_\gamma\cos\left(\delta - \theta_{\mathrm{ext}}\right) \simeq D - D_\gamma\left(1 - \frac{\left(\delta - \theta_{\mathrm{ext}}\right)^2}{2}\right) \overset{(2.91)}{\simeq} D - D_\gamma\left(1 - \frac{\delta^2\left(1 - \tau_\theta^{-1}\right)^2}{2}\right),
\end{aligned} \tag{2.94}$$

where the Taylor Series $(1-x)^{\frac{1}{2}} = 1 - x/2 + \mathcal{O}(x^2)$ and $\cos x = 1 - \frac{x^2}{2} + \mathcal{O}(x^4)$ have been used. (2.93) may now be rewritten as

$$\begin{aligned}
t_{\mathrm{delay}} &\simeq D_\gamma + D_{\mathrm{casc}} - D \overset{(2.94)}{\simeq} D_\gamma + D - D_\gamma\left(1 - \frac{\delta^2\left(1 - \tau_\theta^{-1}\right)^2}{2}\right) - D \\
&= D_\gamma\frac{\delta^2}{2}\left(1 - \tau_\theta^{-1}\right)^2 .
\end{aligned} \tag{2.95}$$

Using (2.88) and (2.90) for the corresponding cases, plugging in (2.83) and, furthermore, taking into account expansion of the Universe, this finally gives [119]

$$t_{\mathrm{delay}} \simeq \begin{cases} 2\times 10^4\kappa\left(1 - \tau_\theta^{-1}\right)^2(1+z)^{-5}\left(\frac{E_\gamma}{10^{12}\,\mathrm{eV}}\right)^{-\frac{5}{2}}\left(\frac{B}{10^{-18}\,\mathrm{G}}\right)^2\,\mathrm{s}\,, & L_B \gg \lambda_{\mathrm{IC,cool}}\,, \\ 10^2\kappa\left(1 - \tau_\theta^{-1}\right)^2(1+z)^{-2}\left(\frac{E_\gamma}{10^{12}\,\mathrm{eV}}\right)^{-2}\left(\frac{B}{10^{-18}\,\mathrm{G}}\right)^2\left(\frac{L_B}{1\,\mathrm{kpc}}\right)^{-\frac{1}{2}}\,\mathrm{s}, & L_B \ll \lambda_{\mathrm{IC,cool}}\,. \end{cases} \tag{2.96}$$

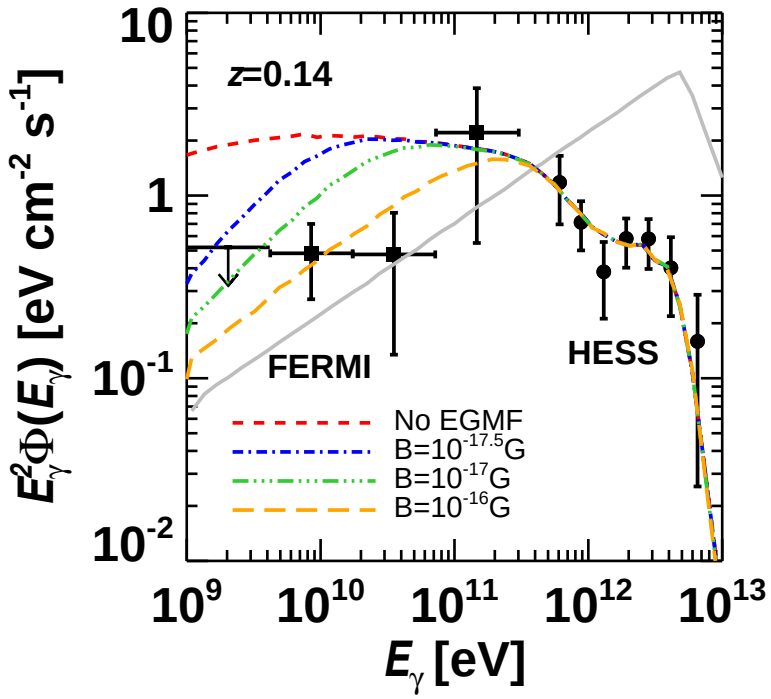

Figure 2.4: Effect of EGMF on the photon spectrum neglecting the plasma effects of the IGM. Data points are shown for both HESS (circle) and Fermi LAT (square) while the curves show the best fit of a Monte Carlo simulation for the HESS data. In addition to the observed spectra for the magnetic fields indicated in the legend the intrinsic spectrum of the source is given (solid, gray).

However, this time delay is only observable if it is large enough: Even without EGMF, pairs are already initially produced with a direction inside, for ultrarelativistic particles, a rather narrow cone around the line of sight with an opening angle $\theta_0 \simeq m_e/E_e$. This results in a tail of the actual flare which, for a very small magnetic field, might "hide" its effect. If, however, the signal of the secondary flare is detectable, then an energy dependent time delay observation might indeed, following (2.96), make it possible to deduce information about magnetic fields down to field strengths of $B \gtrsim 10^{-21} ... 10^{-19}$ G [119, 162].

Finally, the third possible method to detect EGMF using gamma ray data is the non-detection [2, 164] or suppression [163, 165–167] of photon flux at GeV energies. In contrast to the time delay method described above it is much less sensitive to variability of the source since it makes use of cumulative observational data. This method can be derived from (2.88) and (2.90): In both cases the deflection angle δ has a dependence $\delta \propto E_e^{-\Delta} B$, where it is $\Delta > 0$, such that δ increases with the magnetic field strength but decreases with the electron energy, i.e. less energetic particles are deflected more. Therefore, assuming sufficiently strong magnetic fields, even for $\mathcal{O}$(TeV) electrons and positrons produced during PP the deflection angle might be large enough such that during an IC scattering process the secondary photons which, according to (2.86), have GeV energies, are emitted in a narrow cone (see above) with the observer being outside of it. Therefore one expects that the detected flux of gamma rays in the GeV range is much lower than in the case if no significant magnetic field is present.

The general procedure can be described as follows: One has to use objects emitting TeV gamma rays for which both GeV and TeV gamma ray data is available (the former from the Fermi Large Area Telescope (LAT) and the latter from HESS or other Imaging Atmospheric Cherenkov Telescopes). By now this is the case for various sources, usually

blazars or BL Lac at redshifts of $z < 1$ – see, e.g., [166, 168–170]. If no GeV flux has been detected for the given object, one may use the upper limits in this energy range. Then, assuming reasonable values for the object's internal parameters – such as the intrinsic slope, the high energy cutoff and the luminosity – one can run numerical simulations to calculate the expected observable flux which is then to be compared with actual observational data.

This has been carried out for several objects in the references given above, all giving qualitatively similar results, for which a representative example, taken from the work of the author of the present thesis [10], is shown in Fig. 2.4 for the BL Lac 1ES 0229+200 (see below) where a uniform magnetic field is assumed. Here, the source is taken to have an intrinsic spectrum with $\mathrm{d}N/\mathrm{d}E \propto E^{-\Gamma}$, $\Gamma = 1.5$ and an energy cutoff at $E_{\mathrm{cut}} = 5 \times 10^{12}\,\mathrm{eV}$.

As one can see, fitting the simulated results to the high energy data does only satisfy the limits for GeV energies if one assumes a relevant magnetic field strength which is in agreement with [167]. A thorough statistical analysis has been therefore performed in [2] by looking at various different sources, giving, in the most optimistic case,

$$B \gtrsim \begin{cases} 10^{-14}\,\left(\frac{L_B}{100\,\mathrm{pc}}\right)^{\frac{1}{2}}\,\mathrm{G},\; L_B \ll \lambda_{\mathrm{IC,cool}}\,, \\ 3 \times 10^{-16}\,\mathrm{G},\; L_B \gg \lambda_{\mathrm{IC,cool}}\,. \end{cases} \tag{2.97}$$

However, it should be noted here, as also has been done in [2], that, due to the various uncertainties, these results should be regarded as order of magnitude estimates rather than solid limits.

In fact, the results from all three methods to derive lower bounds on B described above have been subject to a general criticism due to the statistical methods used. In particular, the authors of [171, 172] claim that with a refined procedure they do *not* find any evidence that the zero EGMF hypothesis is false. To explain the contradiction to the results presented above they name three reasons: First, they use more up-to-date data from Fermi LAT, therefore having higher statistics and thus more reliable data. Second, they claim that the modulation of the source spectrum has not been refined enough which they improved by fitting a broken power law to the source parameters. And last, the authors assert that they use a more robust statistical analysis regarding the binning of the data and its connection to the cascade flux.

2.2.4 Plasma Instabilities and Gamma Rays from Distant Blazars

Apart from the criticism of the statistical and therefore methodical procedure to derive lower limits on B presented in the previous section, there have been objections against it from the physical point of view [5, 6, 173]: Up to now only interactions of the gamma rays and electrons/positrons with the EBL have been taken into account. However, it is possible that the charged leptons interact with the Intergalactic Medium (IGM) as well, which might result in plasma instabilities for which the growth time is smaller than τ_{IC} and $\tau_{\mathrm{IC,cool}}$, making them the dominant energy loss mechanism. After a brief discussion of plasma instabilities in general the implications of these assumptions are presented in the following.

Plasma instabilities are a well-known phenomenon which arises due to plasma oscillations [174]: The time dependence of the propagation of electromagnetic waves is given by $\mathbf{E}, \mathbf{B} \propto \exp(i\omega t)$. While for vacuum solutions of the Maxwell Equations the angular frequency ω is always real, propagation inside a medium may change the dispersion relation in such a way that also complex values for ω are possible. In particular,

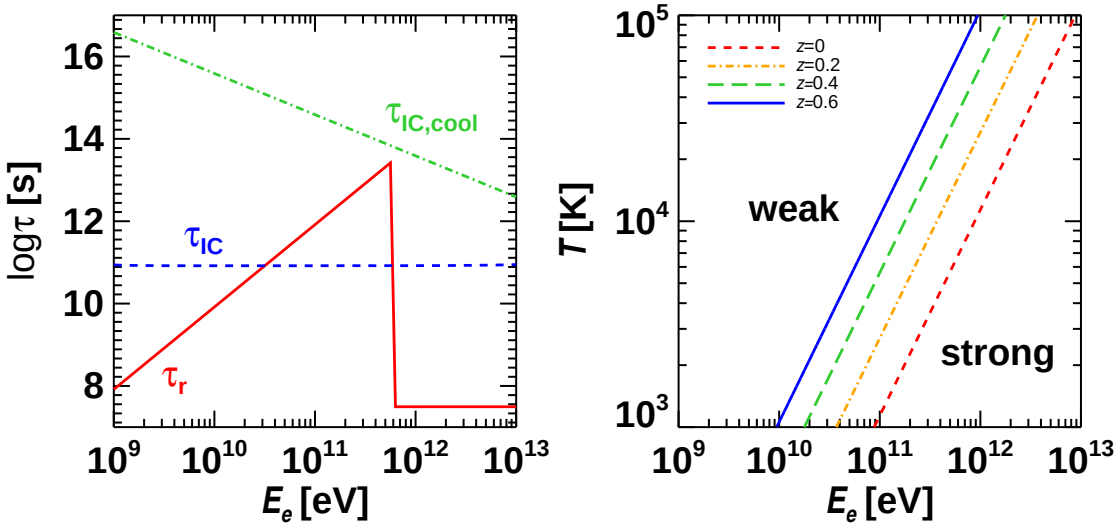

Figure 2.5: *Left panel*: The interaction time $\tau_{\rm IC}$ (dashed, blue) and the cooling time $\tau_{\rm IC,cool}$ (dot-dashed, green) for Inverse Compton scattering and the relaxation time $\tau_{\rm r}$ for electrons due to plasma effects (solid, red). The parameters used here are $n_{\rm IGM} = 10^{-7}\,{\rm cm}^{-3}$, $T = 10^4\,{\rm K}$, $z = 0.14$ and $n_{\rm beam}$ according to (2.113) with $\mathcal{L} = 10^{37.5}\,{\rm W}$. Note the transition for $\tau_{\rm r}$ between the weak and the strong blazar regime at $E_e \simeq 6 \times 10^{11}\,{\rm eV}$. *Right panel*: Transition between the weak and the strong blazar regime (denoted by 'weak' and 'strong', respectively) given by the condition in (2.109) for different redshifts with $n_{\rm IGM} = 10^{-7}\,{\rm cm}^{-3}$ and the beam density as for the left panel. For parameters forming the region below a given line the system is in the strong blazar regime with the Modulation Instability dominating, the region above the line gives the weak regime, where Non-Linear Landau Damping is most important.

if $\mathfrak{Im}\,(\omega) < 0$, the expression $\exp\,(i\omega t)$ obtains an exponentially growing term which makes the setting unstable. This is denoted as a plasma instability.

Following the formalism developed in [6] here and later on, the electron/positron beam with the number density $n_{\rm beam}$ and the Intergalactic Medium with the number density $n_{\rm IGM}$ are regarded as two streams of medium with different velocities. Here $n_{\rm beam}$ is given by the development of the electromagnetic cascade described above. Such conditions may give rise to the so-called two-stream-like instabilities, which then grow on a characteristic time scale τ due to both linear and non-linear effects. Considering the former, in the situation of interest here the linear oblique electrostatic instability has been found to be the dominant one. Since a two-stream setting is present, the dispersion relation is given by [6, 175]

$$1 = \frac{\omega_{p,e}^2}{\omega^2} + \frac{\omega_{\rm beam}^2}{\left(\omega - k_\parallel v\right)^2}\,, \tag{2.98}$$

where $\omega_{p,e}^2 = 4\pi e^2 n_{\rm IGM}/m_e$ is the plasma frequency, $k_\parallel$ the wavenumber parallel to the direction of propagation, v the velocity of the beam electrons and positrons and

$$\omega_{\rm beam}^2 = \omega_\parallel^2 \cos^2\theta + \omega_\perp^2 \sin^2\theta \tag{2.99}$$

an effective angular frequency depending on the longitudinal ($\omega_\parallel^2 = 4\pi e^2 m_e^2 n_{\rm beam} E_e^{-3}$) and transversal ($\omega_\perp^2 = 4\pi e^2 n_{\rm beam} E_e^{-1}$) angular frequency, respectively, as well as on the angle θ between the wave vector and the direction of the flow, i.e. $\cos\theta = k_\parallel/k$.

(2.98) corresponds to the general form of the dispersion relation of a plasma carrying a current of electrons with velocity v, wavenumber k as well as the ion and electron

plasma angular frequencies $\omega_{p,i}$ and $\omega_{p,e}$, respectively. This general form is given by

$$1 = \frac{\omega_{p,i}^2}{\omega^2} + \frac{\omega_{p,e}^2}{(\omega - kv)^2}\,, \tag{2.100}$$

for which a solution for $\omega = \omega_{\max}$, the angular frequency at maximum growth rate of the instability, is known to be [174]

$$\omega_{\max} = \frac{kv}{1 + \alpha \exp\left(i\frac{\pi}{3}\right)} = \frac{kv}{\alpha^2 + \alpha + 1}\left[\left(\frac{\alpha}{2} + 1\right) - i\frac{3^{\frac{1}{2}}\alpha}{2}\right], \tag{2.101}$$

where α has to fulfill the conditions

$$\frac{2\alpha + 1}{\alpha^3(\alpha + 2)} = \frac{\omega_{p,i}^2}{\omega_{p,e}^2},\ 1 + \frac{3\alpha^2 + 2\alpha + 1}{\alpha^3(\alpha + 2)} = \frac{(kv)^2}{\omega_{p,e}^2}\,, \tag{2.102}$$

i.e. for (2.98) it is

$$\frac{2\alpha + 1}{\alpha^3(\alpha + 2)} = \frac{\omega_{p,e}^2}{\omega_{\text{beam}}^2},\ 1 + \frac{3\alpha^2 + 2\alpha + 1}{\alpha^3(\alpha + 2)} = \frac{\left(k_\parallel v\right)^2}{\omega_{\text{beam}}^2}\,. \tag{2.103}$$

Since $\omega_{p,e} \gg \omega_{\text{beam}}$, it is $\omega_{p,e}^2/\omega_{\text{beam}}^2 \gg 1$ and therefore it follows from the first expression of (2.103) that α has to be small, such that, via a Taylor Expansion, (2.103) may be rewritten as

$$\frac{1}{2\alpha^3} \simeq \frac{\omega_{p,e}^2}{\omega_{\text{beam}}^2},\ \frac{1}{2\alpha^3} \simeq \frac{\left(k_\parallel v\right)^2}{\omega_{\text{beam}}^2}\,, \tag{2.104}$$

which means that

$$k_\parallel v \simeq \omega_{p,e}\,. \tag{2.105}$$

Performing a Taylor Expansion in α on (2.101) and plugging it into (2.105) gives

$$\begin{aligned}
\mathfrak{Im}\left(\omega_{\max}\right) &\simeq \frac{3^{\frac{1}{2}}}{2}\omega_{p,e}\alpha \overset{(2.104)}{\simeq} 3^{\frac{1}{2}}2^{-\frac{4}{3}}\omega_{p,e}^{\frac{1}{3}}\omega_{\text{beam}}^{\frac{2}{3}} \\
&= 3^{\frac{1}{2}}2^{-\frac{4}{3}}\left(\frac{4\pi e^2 n_{\text{IGM}}}{m_e}\right)^{\frac{1}{6}}\left(\omega_\parallel^2\cos^2\theta + \omega_\perp^2\sin^2\theta\right)^{\frac{1}{3}} \\
&= 3^{\frac{1}{2}}2^{-\frac{4}{3}}\left(\frac{4\pi e^2 n_{\text{IGM}}}{m_e}\right)^{\frac{1}{6}}\left[\omega_\perp^2\left(1 - v^2\cos^2\theta\right)\right]^{\frac{1}{3}} \\
&= \frac{3^{\frac{1}{2}}2^{-\frac{4}{3}}(4\pi)^{\frac{1}{2}}e}{m_e^{\frac{1}{6}}}n_{\text{IGM}}^{\frac{1}{6}}n_{\text{beam}}^{\frac{1}{3}}E_e^{-\frac{1}{3}}\left(1 - v^2\cos^2\theta\right)^{\frac{1}{3}}\,.
\end{aligned} \tag{2.106}$$

Finally, taking into account the approximation in (2.105) and considering ultrarelativistic electron/positron beams (i.e. $v \simeq 1$), it can be shown that (2.106) becomes maximal for $\cos\theta = (3/5)^{\frac{1}{2}}$ [6].

Using this solution for the astrophysical setting presented in this work, the electrostatic growth time is found to be

$$\tau_{\text{e}} \simeq 1.1 \times 10^6 \left(\frac{E_e}{10^{12}\,\text{eV}}\right)^{\frac{1}{3}}\left(\frac{n_{\text{beam}}}{10^{-22}\,\text{cm}^{-3}}\right)^{-\frac{1}{3}}\left(\frac{n_{\text{IGM}}}{10^{-7}\,\text{cm}^{-3}}\right)^{-\frac{1}{6}}\,\text{s}\,, \tag{2.107}$$

where E_e is the energy of the electrons/positrons.

However, as mentioned above, non-linear effects have to be considered as well. This is done by calculating the total relaxation time τ_r as [6, 176]

$$\tau_\mathrm{r} = 100\tau_\mathrm{e}\xi^{-1}\,\mathrm{s}\,, \tag{2.108}$$

introducing a dimensionless parameter $\xi \leq 1$ which has got a characteristic value for a particular non-linear effect and therefore accounts for its influence as discussed in the following.

The dominating effect in the present case is the Modulation Instability [6]. It can be explained by the fact that in a turbulent medium ions scatter the oscillations caused by the beam such that they are transferred from the resonance to smaller wavenumbers. This, on the other hand, means that the energy is shifted to higher phase speeds [177]. However, this effect occurs only if the beam density n_beam lies above a critical density n_crit, i.e. if it is $n_\mathrm{beam} > n_\mathrm{crit}$, where n_crit is given by

$$n_\mathrm{crit} = 2.5\times10^{-25}\left(\frac{E_e}{10^{12}\,\mathrm{eV}}\right)^{-1}\left(\frac{n_\mathrm{IGM}}{10^{-7}\,\mathrm{cm}^{-3}}\right)\left(\frac{T}{10^4\,\mathrm{K}}\right)^2\,\mathrm{cm}^{-3}\,, \tag{2.109}$$

where T is the temperature of the IGM. The dissipation time scale here is given by

$$\begin{aligned}\tau_\mathrm{M} = 8.3\times10^6\,\mathrm{s}&\left[1+\frac{5}{4}\ln\left(\frac{T}{10^4\,\mathrm{K}}\right)-\frac{1}{4}\ln\left(\frac{n_\mathrm{IGM}}{10^7\,\mathrm{cm}^{-3}}\right)\right]\\ &\times\left(\frac{E_e}{10^{12}\,\mathrm{eV}}\right)^{\frac{1}{3}}\left(\frac{n_\mathrm{beam}}{10^{-22}\,\mathrm{cm}^{-3}}\right)^{-\frac{1}{3}}\left(\frac{n_\mathrm{IGM}}{10^{-7}\,\mathrm{cm}^{-3}}\right)^{-\frac{1}{6}}\,.\end{aligned} \tag{2.110}$$

If, however, one looks at a weak blazar, i.e. n_beam lies below n_crit, then another, less efficient mechanism suppresses the cascade evolution, namely the Non-Linear Landau Damping (NLD). For this process the rate is known [178], so the factor ξ in (2.108) can be explicitly calculated, resulting in

$$\xi = 2.1\times10^{-7}\times\left(\frac{E_e}{10^{12}\,\mathrm{eV}}\right)^{-\frac{4}{3}}\left(\frac{n_\mathrm{beam}}{10^{-22}\,\mathrm{cm}^{-3}}\right)^{-\frac{2}{3}}\left(\frac{n_\mathrm{IGM}}{10^{-7}\,\mathrm{cm}^{-3}}\right)^{\frac{2}{3}}\left(\frac{T}{10^4\,\mathrm{K}}\right)^2\,, \tag{2.111}$$

which, plugged into (2.108), gives

$$\tau_\mathrm{NLD} \simeq 5.2\times10^{14}\,\mathrm{s}\left(\frac{E_e}{10^{12}\,\mathrm{eV}}\right)^{\frac{5}{3}}\left(\frac{n_\mathrm{beam}}{10^{-22}\,\mathrm{cm}^{-3}}\right)^{\frac{1}{3}}\left(\frac{n_\mathrm{IGM}}{10^{-7}\,\mathrm{cm}^{-3}}\right)^{-\frac{5}{6}}\left(\frac{T}{10^4\,\mathrm{K}}\right)^{-2}\,. \tag{2.112}$$

In order to evaluate the impact of these damping effects on the development of an electromagnetic cascade, the corresponding time scales, τ_M and τ_NLD, have to be compared to τ_IC, the IC interaction time scale, which is given by (2.84), and to the IC cooling time (2.85).

The comparison of time scales is shown in the left panel of Fig. 2.5 for some typical parameter values. It can be seen that in the strong blazar regime, i.e. for $n_\mathrm{beam} > n_\mathrm{crit}$, the electromagnetic cascade is completely suppressed since τ_r is several orders of magnitude smaller than τ_IC. This means that, due to the Modulation Instability, almost all electrons have been relaxed to a rather non-interactive state long way before they can produce a high energy photon by Inverse Compton interaction. However, for electron/positron beams fulfilling $n_\mathrm{beam} < n_\mathrm{crit}$ (the weak blazar condition) a cascade can still develop, even though it is partially suppressed by NLD.

After giving the definition for n_beam in (2.113), it is shown on the right hand side of Fig. 2.5 how the transition energy between the weak and strong blazar regimes changes

as function of the IGM temperature for sources with a given luminosity $\mathcal{L}$ placed at different redshifts.

It should be noted that the ideas and conclusions which have been presented in this section are in the focus of an ongoing debate. In particular in [179] it has been argued that the kind of analysis used here is not applicable to electromagnetic cascades in voids. By performing a kinetic treatment the authors claim to find that the instability growth is severely suppressed and therefore the relaxation time for the electrons/positrons inside the beam remains much larger than the IC interaction time. However, in a more recent paper [173] these objections have been addressed by refining the analysis and concluding that the results from [6] are still valid. Furthermore, the discussion in this section is true only for an unmagnetized medium while even for rather small magnetic fields the arguments may not be valid anymore. And since, for example magnetic outflow from Galaxies might, at least locally, "pollute" the voids with magnetic fields, this assumption is rather unrealistic and therefore still awaits a well-motivated upper limit of the permitted field strength B in order to be able to make more reliable predictions.

2.2.5 Suppression of Low Energy Photon Flux in Observed Spectra of Blazars due to interactions with the Intergalactic Medium

After the general discussion of plasma instabilities and their influence on the propagation of gamma rays in extragalactic space, the formalism will be now applied to an actual setting following the procedure in [10]. The object of choice here is the BL Lac 1ES 0229+200 with the observational parameters being listed in [180] of which the ones of interest here are the redshift $z = 0.140$ and the luminosity $\mathcal{L} = 10^{37.5}\,\mathrm{W}$. Furthermore, the source is taken to have an intrinsic spectrum with $\mathrm{d}N/\mathrm{d}E \propto E^{-\Gamma}$, where, in order to check the reliability of the procedure, it has been performed for spectral indices with different values, namely $\Gamma = 1.2$, $\Gamma = 1.5$ and $\Gamma = 1.8$, while the high energy cutoff is set to be $E_{\mathrm{cut}} = 5 \times 10^{12}\,\mathrm{eV}$. This source is particularly interesting for the analysis performed below since, on the one hand, both high energy data from HESS [180] as well as a GeV data analysis from Fermi LAT [167] are available and, on the other hand, since in [167] it has been used to derive lower limits on EGMF as described above such that afterwards a direct comparison to the corresponding results is possible.

For the numerical simulations the ELMAG code [181] (version 2.01) has been used. This software uses the Monte Carlo approach for single particles to simulate the propagation of electromagnetic cascades. This is done by taking into account the interaction of electrons, positrons and photons with the EBL as described above and, in addition, synchrotron energy losses and deflections in the small angle approximation. The latter means that, while considering one-dimensional propagation and therefore not being able to treat deflections (which are a three-dimensional phenomenon) to full extent, for each time step the deflection angle is calculated and then accumulated, such that in the end a reasonable value for the total deflection is obtained as long as the magnetic fields in question are not too strong.

In order to account for the interactions with the IGM, i.e. to model the effect of plasma instabilities, the code has been modified by implementing the following scheme: Each time an electron or positron either performs an IC scattering or enters the cascade due to a PP reaction of a photon, both the time until the next IC scattering takes place (as done for the Monte Carlo propagation in any case) and the relaxation time τ_{r} as described above are calculated and then compared – if the latter is smaller, one can assume that before it can produce another photon most of the electron's energy is

already dissipated away such that it does not further contribute to the development of the cascade as can be seen in the left panel of Fig. 2.5: At small energies their interaction is dominated by plasma effects such that IC reactions play a role of negligible importance.

However, in order to actually calculate τ_{r}, i.e., depending on which blazar regime is operating, τ_{M} from (2.110) or τ_{NLD} from (2.112), it is necessary to have values for T, n_{IGM} and n_{beam}. For the former one can say that, although the IGM is not completely homogeneous, but is rather traversed by voids and overdensities, on average one can set $n_{\mathrm{IGM}} \simeq 10^{-7}\,\mathrm{cm}^{-3}$ and $T \simeq 10^4\,\mathrm{K}$. However, since the measurement of T is subject to various uncertainties, in the following values of the range $T = 10^3\,\mathrm{K}...10^5\,\mathrm{K}$, which have been shown to be reasonable estimates for low-redshift IGM [6, 182], are investigated as well.

The problem which occurs while one tries to give an estimate for n_{beam} is given by the fact that it is a dynamical quantity which depends on the actual state of the cascade such that for a Monte Carlo approach, where one particle at a time is propagated, this cannot be done to full extent. Therefore one has to find a well-motivated estimate based on the knowledge of the interaction length of the cascade particles which has been done, as an upper limit, by [5], giving

$$n_{\mathrm{beam}} \simeq 7.4 \times 10^{-22} \left(\frac{\mathcal{L}}{10^{38}\,\mathrm{W}}\right) \left(\frac{E_e}{10^{12}\,\mathrm{eV}}\right) \left(\frac{1+z}{2}\right)^{3\zeta-4} \mathrm{cm}^{-3}\,, \tag{2.113}$$

where $\mathcal{L}$ is the isotropic-equivalent luminosity and $\zeta = 4.5$ for $z < 1$ is a parameter that can be inferred from the analysis of the star formation rate in the local Universe [138].

As it has been shown in the previous section, neglecting the effects of interactions with the IGM but including magnetic fields may account for the suppression of GeV signals. However, as presented in Fig. 2.7, even for a vanishing magnetic field the plasma effects itself give a suppression of the flux in agreement with Fermi LAT observations. It should be stressed here that this does not prove the non-existence of EGMF, but rather possibly weakens the role of GeV suppression for probing the lower limits on the magnetic field strength.

As discussed above, in the following the temperature T of the Intergalactic Medium, bringing the largest uncertainties into the calculations, will be considered as a "free" parameter inside the range $T = 10^3\,\mathrm{K}...10^5\,\mathrm{K}$ such that varying it will help to obtain more robust results. Its actual value plays a major role since it does not just change the value of the relaxation time continuously, but, according to (2.109), determines whether, for a given electron energy E_e, the plasma interactions take place in the strong or the weak blazar regime.

For low temperatures, in fact, n_{crit} is rather low such that most of the influence of the IGM is set inside the strong blazar regime, the relaxation due to plasma effects therefore taking place rather fast which means that cascade development is almost completely suppressed. This can be seen in the upper panels of Fig. 2.7 since the observed signal reproduces the intrinsic slope quite well which means that only primary low energy photons, having a rather large mean free path, reach the observer, while no intermediate pairs from PP are able to contribute since, having lost most of their energy, the energy of the photons they produce is also below the energy range interesting here.

The higher the temperature gets, the higher also n_{crit} becomes, thus increasing the influence of the weak blazar regime. In addition, once being inside this regime, according to (2.112), τ_{NLD} decreases, such that the impact of NLD increases even more. The feature resulting from that in the spectrum is an additional peak which for $T = 10^5\,\mathrm{K}$ even dominates the spectrum as, compared to the low energy case discussed before, the

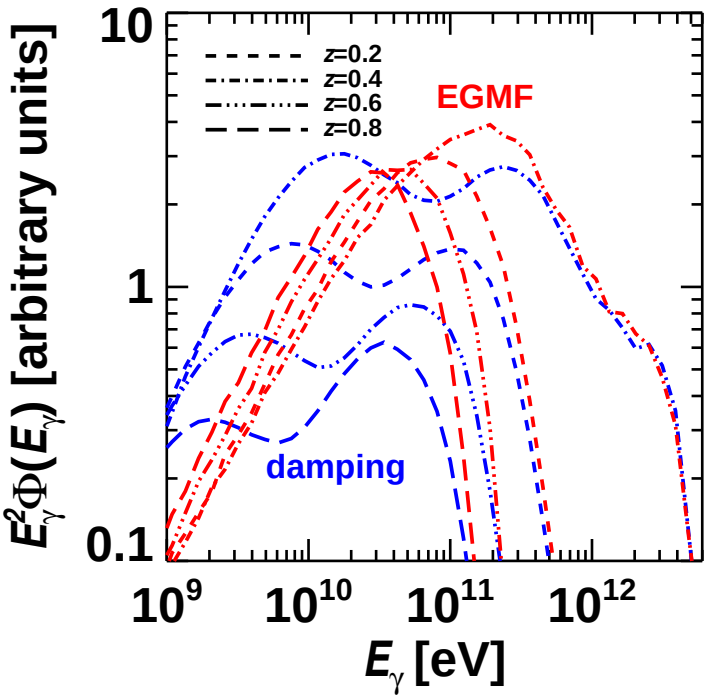

Figure 2.6: The dependence of the observed blazar spectrum on the source redshift. The intrinsic spectrum has been chosen to have $\Gamma = 1.2$. The blue lines give the case including only the plasma effects for $T = 5 \times 10^4$, red lines show the case in which particles are deflected by a magnetic field with $B = 10^{-16}$ G, neglecting the role of IGM.

observed slope does not correspond to the intrinsic one anymore but rather hardens, thus moving towards the undisturbed IC spectrum, which means that now the electromagnetic cascade develops at least partially.

Furthermore, also the energy corresponding to the aforementioned additional high temperature peak shows that IC is operating and now plays a significant role: As can be seen from Fig. 2.5, $E_{\rm crit}$, the energy at which the transition between the two regimes takes place, increases with temperature, such that all electrons with energies $E \leq E_{\rm crit}$ may contribute to the cascade directly via IC. In particular, taking $T = 5 \times 10^4$ eV, for 1ES 0229+200 it is $E_{\rm crit} \simeq 2 \times 10^{12}$ eV and therefore, according to (2.86), the average energy of photons produced via IC is given by $E_\gamma \simeq 2 \times 10^{10}$ eV, the approximate energy of the additional peak as confirmed in Fig. 2.7 in the panel corresponding to $T = 5 \times 10^4$ eV. In conclusion, the peak as well as the hardening of the spectrum for small energies may be explained due to photons up-scattered by IC.

As can be seen in Fig. 2.7, overall a lower IGM temperature is preferred which means that the development of the electromagnetic cascade is severely suppressed, i.e., as argued by [5, 6], the strong blazar regime is dominating. As mentioned above, this has been checked for intrinsic spectrum index values of $\Gamma = 1.2$, $\Gamma = 1.5$ and $\Gamma = 1.8$ of which the former two are presented in Fig. 2.7 and for which these conclusions hold. The rather extreme case of $\Gamma = 1.8$ has been checked as well, however, giving rather large flux at low energies, it may be excluded, giving additional constraints for the modeling of the source spectrum.

In order to be able to make a more general statement, of course the analysis of more sources at different redshifts is needed. As a basis for more detailed future work this is done in Fig. 2.6 for both the case of deflection by EGMF and for the case of energy dissipation due to IGM effects, where the parameters giving the best fit for 1ES

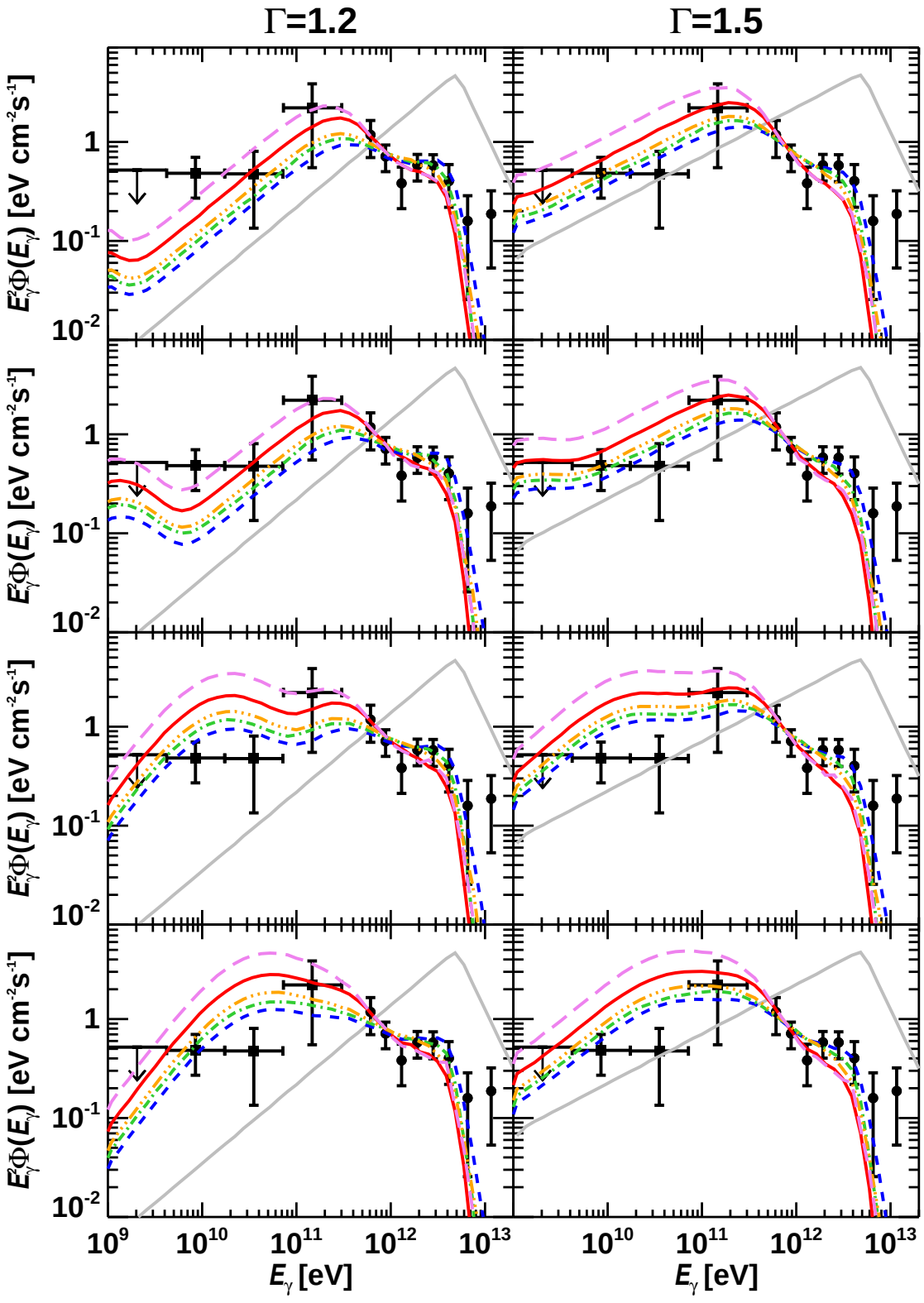

Figure 2.7: Gamma ray spectra of 1ES 0229+200 at $z = 0.14$ for different temperatures and EBL models with the slope of the intrinsic spectrum (grey, solid) given by $\Gamma = 1.2$ (left) and $\Gamma = 1.5$ (right) in case IGM effects are taken into account and magnetic fields are supposed to be negligible. The temperatures used here are $T = 5 \times 10^3$ K, $T = 10^4$ K, $T = 5 \times 10^4$ K and $T = 10^5$ K (from top to bottom). The different line styles correspond to the EBL models I-V introduced in Sec. 2.2.2 in the same way as in Fig. 2.2.

0229+200 with the EBL Model II (cf. Figs. 2.4 and 2.7) are used. In both cases the high energy cutoff is the same, however, regarding the suppression at GeV energies, the two scenarios differ dramatically: For EGMF deflection the flux at GeV energies increases compared to the peak of the spectrum. This is due to the fact that TeV electrons are not affected much by deflections because of their large Larmor Radius and therefore may contribute to the cascade development which might be enhanced for large distances to the source as then it is possible that PP happens more than once (and therefore, in the end, more photons might be produced). Plasma instabilities, however, are rather effective at TeV energies such that their influence "accumulates" over time, therefore reducing the overall gamma ray production more over larger distances.

Summarizing this section, it may be said that apart from EGMF which, as discussed in Sec. 2.2.3, deflect electrons inside electromagnetic cascades from the line of sight, also interactions with the IGM due to plasma instabilities might explain the suppression of gamma rays on GeV scales observed at Earth. The outcome of the corresponding analysis for the specific object 1ES 0229+200 shows that the best fit values give $B \gtrsim 10^{-16}\,\mathrm{G}$ and $T \lesssim 5 \times 10^4\,\mathrm{K}$, respectively, such that both should be taken into account in order to explain spectra of far away blazars in general. The crucial statement is therefore that the existence of EGMF is not required (but also not excluded) to explain the given features, such that the derivation of lower limits for the magnetic field strength has to be reanalyzed under these premises. Still, further observations with higher sensitivity are necessary to distinguish between the two possibilities which, due to a rather distinct feature of a second peak in the spectrum in the case of the IGM scenario, might be indeed possible once upcoming observations by, for example, HESS-II [183] or CTA [184], will have been performed.

Chapter 3

Time Evolution of Primordial Magnetic Fields

> Es beugen alle sich dem Zepter der Notwendigkeit, und seufzen unter dem Fluch der Zeit, die nichts bestehen lässt.
> — F. Schleiermacher, *Monologen* (1800)

Ever since it has been proposed that magnetic fields have been created in the Early Universe (as discussed in Sec. 2.1.2), much effort has been put into the analysis of their evolution up to the present day, both numerically and (semi-)analytically [49, 185–200]. However, numerical simulations encounter a major problem: They do not have the resolution required to handle the magnetic fields over the large range of length scales present in the Universe. At the same time analytical studies up to now were not taking into account all aspects of the involved physics like, e.g., the backreaction of the turbulent medium onto the magnetic field.

In this chapter the results of a full semi-analytic analysis of the time evolution of Primordial Magnetic Fields generated in the Early Universe, based on [8, 9], are presented. After, in Sec. 3.1, giving an overview of the additional effects coming into play when dealing with MHD in the Early Universe, compared to the generic situation of Sec. 1.1, the main initial equations are presented before proceeding to the derivation of the Master Equations (3.52)-(3.52), from which the evolution of Primordial Magnetic Fields may be obtained, in Sec. 3.2. The chapter is concluded by showing the results of simulations using these equations and presenting additional constrains on present day EGMF in Sec. 3.3.

3.1 Magnetohydrodynamics in the Early Universe

In the following some basic concepts of MHD in the Early Universe are presented. Before doing so, some introductory remarks should be made. The main quantities to deal with are connected to the spectral energy content, i.e. the spectral magnetic energy density M_k and the spectral kinetic energy density U_k introduced in Sec. 1.1.1.6, as well as the spectral magnetic helicity density $\mathcal{H}_k$ introduced in Sec. 1.1.2. The standard assumption then is that the spectral energy is concentrated on a specific scale L_I (or $k_\mathrm{I} = 2\pi/L_\mathrm{I}$ as the corresponding wavenumber) which in the following will be called the integral or coherence scale. Therefore, M_I, U_I and $\mathcal{H}_\mathrm{I}$, as well as other quantities with an index 'I', are to be understood as the corresponding values at the integral scale.

Furthermore, it should be noted that the index '0' denotes the value of a quantity

right at the magnetogenesis epoch considered. In particular, to have a time measure, the scale factor a is used which, in contrast to the standard definition, is set to be $a_0 = 1$ initially, i.e. it is unity at magnetogenesis.

3.1.1 Expansion of the Universe

In order to take into account Expansion of the Universe, it has been pointed out by [185] that to obtain physically relevant results it is necessary to consider comoving quantities, which have been introduced in Sec. 1.2.2 and will be marked by an index 'c' in the following, rather than by the physical ones. The crucial point here is that the transition between these two can be done by simple rescaling while the *fundamental equations of motion may still be used in their generic form presented in Sec.* 1.1.1. The corresponding scaling laws are given by [194]

$$\epsilon = \epsilon_{\mathrm{c}} a^{-4},\ \rho = \rho_{\mathrm{c}} a^{-4},\ p = p_{\mathrm{c}} a^{-4},\ \mathbf{B} = \mathbf{B}_{\mathrm{c}} a^{-2},\ \mathbf{v} = \mathbf{v}_{\mathrm{c}}, \mathrm{d}t = \mathrm{d}t_{\mathrm{c}} a, L = L_{\mathrm{c}} a,\ k = k_{\mathrm{c}} a^{-1} \tag{3.1}$$

for the radiation-dominated regime, while for the matter-dominated regime the so-called super-comoving variables are used:

$$\epsilon = \epsilon_{\mathrm{c}} a^{-3}, \rho = \rho_{\mathrm{c}} a^{-3}, p = p_{\mathrm{c}} a^{-3}, \mathbf{B} = \mathbf{B}_{\mathrm{c}} a^{-2}, \mathbf{v} = \mathbf{v}_{\mathrm{c}} a^{-\frac{1}{2}}, \mathrm{d}t = \mathrm{d}t_{\mathrm{c}} a^{\frac{3}{2}}, L = L_{\mathrm{c}} a, k = k_{\mathrm{c}} a^{-1} \tag{3.2}$$

For both expressions ρ is the mass/energy density, p the pressure, $\mathbf{B}$ the magnetic field, $\mathbf{v}$ the velocity field, t the time, L a length scale and k an inverse length scale (or wavenumber) involved.

3.1.2 Conductivity

The conductivity of the IGM, i.e. the conductivity of the Universe on large scales throughout its evolution, can be estimated in a rather general way as done by [115]. The average time τ_i between particle interactions for a particle species i is given by

$$\tau_i \simeq \min\left[\frac{1}{n_i \sigma_i}, t_H\right], \tag{3.3}$$

where n_i is the number density of the particle in question, σ_i is the interaction cross section and t_H is the Hubble Time (since it is the maximal possible time scale). With τ_i it is then possible to estimate the drift velocity

$$v_i \simeq \frac{q_i |\mathbf{E}| \tau_i}{E_i} \overset{(3.3)}{\simeq} \frac{q_i |\mathbf{E}|}{E_i} \min\left[\frac{1}{n_i \sigma_i}, t_H\right] \tag{3.4}$$

for the particle energy E_i and charge q_i, respectively, and an electric field $\mathbf{E}$. Therefore, following Ohm's Law, (1.1), an approximate value for the conductivity is given by

$$\sigma = \frac{|\mathbf{j}_i|}{|\mathbf{E}|} = \frac{n_i q_i v_i}{|\mathbf{E}|} \simeq \min\left[\frac{q_i^2}{E_i \sigma_i}, \frac{n_i q_i^2 t_H}{E_i}\right]. \tag{3.5}$$

During the beginning of the radiation-dominated regime most of the relativistic particles are charged such that the interaction time τ_i is smaller than the age of the Universe as the mean distance between the particles is rather small while the interaction is mediated by a massless gauge boson, giving therefore

$$\sigma_i \simeq \frac{q_i^4}{T^2}, \tag{3.6}$$

while the particle energy is mainly given by $E_i \simeq T$. Plugging all this into (3.5) gives

$$\sigma \simeq \frac{T}{q_i^2}\,, \tag{3.7}$$

i.e. a direct proportionality of the conductivity to the temperature T. Even after the electron-positron annihilation, when the number density of charged particles, mainly electrons and ions, is given by $10^{-10} n_\gamma$, due to the fact that the interactions are mainly given by Thomson Scattering, the conductivity still manages to remain very high. In a more sophisticated analysis, taking into account the scatterings of leptons, antileptons and quarks in more detail, the conductivity is found to be [201]

$$\sigma \simeq \frac{1}{\alpha \ln\left(1/\alpha\right)} T\,, \tag{3.8}$$

where α is the coupling constant. As one can see this result is close to the simple estimate presented above and, the prefactor $1/\left[\alpha \ln\left(1/\alpha\right)\right]$ having values of the order $\simeq 50...150$ in the Early Universe, the conductivity still can be seen as very large if, as done in [115], the value it has is compared to $\sigma \simeq H$.

In the matter-dominated regime, more specifically after Recombination [103], the main scattering process is again Thomson Scattering of the electrons on background photons, therefore (3.3) becomes equal to (2.84). Having the electron number density being given by [53]

$$n_e \simeq 3 \times 10^{-10}\,\mathrm{cm}^{-3} \Omega_{\mathrm{pres}} h \left(1+z\right)^3\,, \tag{3.9}$$

where Ω_{pres} is the present day density parameter and h the reduced Hubble Parameter, one can plug this into (3.5), obtaining, since the energy of the non-relativistic electrons is given by $E_e \simeq m_e$,

$$\sigma = \frac{|\mathbf{j}|}{|\mathbf{E}|} = \frac{n_e e v_e}{|\mathbf{E}|} \overset{(2.84),(3.4)}{\simeq} \frac{n_e e^2}{m_e n_\gamma \sigma_{\mathrm{T}}} \simeq 10^{11}\,\Omega_{\mathrm{pres}} h\,\mathrm{s}^{-1}\,. \tag{3.10}$$

The two most remarkable features are, on the one hand, the fact that now the conductivity is constant, in contrast to the radiation-dominated regime, and, on the other hand, it is still remarkably large taking the same measure as before.

3.1.3 Turbulent and Viscous Phases of Magnetohydrodynamics in the Early Universe

During the Evolution of the Early Universe there are two regimes which are relevant from the point of view of MHD and which can be distinguished by the corresponding Reynolds Number $\mathcal{R}$ (cf. (1.10)): On the one hand the turbulent phase for $\mathcal{R} \gg 1$ and on the other hand the viscous phase for $\mathcal{R} \ll 1$. Another way to express this is to look at (1.27), repeated here for convenience:

$$\partial_t \mathbf{v} = -\left(\mathbf{v}\cdot\nabla\right)\mathbf{v} + \frac{1}{4\pi\rho}\left(\nabla\times\mathbf{B}\right)\times\mathbf{B} + \mathbf{f}\,. \tag{3.11}$$

While for the case of turbulence the second term on the right hand side is balanced by the first one, for viscosity this is the case between the second and the third term. Therefore a simple estimate may be given for the relation describing the magnetic field (or the Alfvén velocity) of the system. For the turbulent phase it is given by

$$v \simeq \frac{B}{4\pi\rho} \overset{(1.29)}{=} v_{\mathrm{A}}\,, \tag{3.12}$$

whereas for the viscous phase one gets

$$|\mathbf{f}| \simeq \frac{B^2}{4\pi\rho L} \overset{(1.29)}{=} \frac{v_\mathrm{A}}{L}\,. \tag{3.13}$$

In the following these two cases will be discussed based on [194] (the content of which, in more detail, is presented in [202]) in order to motivate the basic framework for Primordial Magnetic Fields.

3.1.3.1 The Turbulent Phases

A turbulent phase is characterized by a generic energy cascading mechanism as described in Sec. 1.1.3. This is a further motivation for the existence of the integral scale L_I described above since, due to the resulting decay of modes with high wavenumbers, there indeed should be one scale at which the spectral energy peaks. Furthermore, it is even possible by some simple arguments to get an estimate on the time evolution of both L_I and M_I, the two quantities which later can be related to the parameters describing present day EGMF.

First, it should be noted that, since the typical velocity of the fluid is equal to the Alfvén velocity, it follows that the magnetic and the kinetic energy densities should be equal, i.e. equipartition between these two is expected. Going one step further, this would mean that even when in the beginning equipartition is not true, i.e. the magnetic energy is smaller, after a rather short time it will be the case.

Furthermore, it is important to remark that, as a turbulent phase is discussed here, usually ensemble averaged quantities are the topic of discussion. Since on large scales the Universe can be regarded as homogeneous and isotropic, the formalism of Sec. 1.1.3.2 is applicable, in particular the correlators (1.127) and (1.131), where in the presented scenario kinetic helicity is set to be zero.

Now some effective quantities for a given scale k may be defined. For the effective magnetic field B_k^eff (or the corresponding Alfvén velocity $v_{\mathrm{A},k}^\mathrm{eff}$) this can be done by taking the average energy density, (1.60),

$$\epsilon_B = \int \rho M_k \,\mathrm{d}k = \int \rho k M_k \,\mathrm{d}\ln k \equiv \int \frac{\left(B_k^\mathrm{eff}\right)^2}{8\pi}\,\mathrm{d}\ln k\,, \tag{3.14}$$

where the form of the last term has been defined in accordance to the general form of magnetic energy density (1.58). Therefore the effective magnetic field and the effective Alfvén velocity are related to the magnetic spectral energy by

$$M_k = \frac{\left(B_k^\mathrm{eff}\right)^2}{8\pi\rho k} \overset{(1.29)}{=} \frac{\left(v_{\mathrm{A},k}^\mathrm{eff}\right)^2}{2k}\,. \tag{3.15}$$

In a similar way this can be done for the kinetic component, i.e. one uses the kinetic energy density (1.60) to define the effective velocity v_k^eff as

$$\epsilon_\mathrm{K} = \int \rho U_k \,\mathrm{d}k = \int \rho k U_k \,\mathrm{d}\ln k \equiv \int \frac{\rho}{2}\left(v_k^\mathrm{eff}\right)^2 \,\mathrm{d}\ln k \tag{3.16}$$

and therefore

$$U_k = \frac{\left(v_k^\mathrm{eff}\right)^2}{2k}\,. \tag{3.17}$$

As for the general shape of M_k during the turbulent phase, one can say that both for scales larger and smaller than the integral scale one expects a power law, i.e.

$$M_k \propto \left(\frac{k}{k_\mathrm{I}}\right)^{\alpha-1} \propto \left(\frac{L}{L_\mathrm{I}}\right)^{1-\alpha} . \tag{3.18}$$

For $k > k_\mathrm{I}$ (or, equivalently, $L < L_\mathrm{I}$) it is the situation as described in Sec. 1.1.3.3, therefore it is $\alpha = -2/3$ (Kolmogorov) or $\alpha = -1/2$ (Iroshnikov/Kraichnan).

However, for $k < k_\mathrm{I}$ (or $L > L_\mathrm{I}$) no generic value for α could be given up to now, especially since it seems to depend on the initial conditions [194]. One suggestion in order to predict it was introduced by [203]: To find the magnetic field strength B_L averaged over some scale $L > L_B$, it is necessary to realize that the total volume considered, $V_L = L^3$, contains $N = V_L/V_B = (L/L_B)^3$ uncorrelated magnetic domains of size $V_B = L_B^3$, each having a randomly directed average magnetic field with a strength of B_dom. Therefore, the magnetic field strength, averaged over the total volume, is reduced by a factor of $N^{\frac{1}{2}}$ which gives

$$B_L = \frac{B_\mathrm{dom}}{N^{\frac{1}{2}}} = B_\mathrm{dom}\left(\frac{V_B}{V_L}\right)^{\frac{1}{2}} = B_\mathrm{dom}\left(\frac{L_B}{L}\right)^{\frac{3}{2}} , \tag{3.19}$$

i.e. a $B_L \propto L^{-\frac{3}{2}} \propto k^{\frac{3}{2}}$ dependence. Since from (3.15) one can see that $M_k \propto B^2/k \propto B^2 L$, it follows that it is $\alpha = 3$, i.e. a white noise spectrum. The same value for α also has been obtained in [113, 114, 199, 204]

Still, [205] claims that this is not true since the argumentation above does not take causality into account properly. The authors argue that for the reasonable assumption of a finite correlation length, the correlation function $\mathcal{C}_{ij}$ of the type (1.114) for magnetic fields (where for now vanishing helicity is assumed, i.e. $\gamma(r) = 0$) will have a compact support which therefore, according to the Paley-Wiener-Theorem, implies that its Fourier Transform is analytical, i.e. it can be locally given by a converging power series. Since the said Fourier Transform is given by (1.123) (where again the helical term is omitted for now), one can approximate $\mathcal{P}(k)$ by a power law, i.e. $\mathcal{P} \simeq \mathcal{P}_0 k^n$, such that (1.123) dictates that $\left(\delta_{ij} - k_i k_j/k^2\right) k^n$ has to be analytic and therefore $n \geq 2$. In order to calculate the magnetic fields on a scale L, one can take the volume average, which can be estimated by [204]

$$\left\langle B_L^2 \right\rangle \propto k^3 \left\langle B_k^2 \right\rangle_{k=2\pi/L} \propto k^3 \mathcal{P}(k) \propto k^{n+3} . \tag{3.20}$$

Therefore the relation between n and α would be $\alpha = n + 3$, such that $n = 2$, the lowest possible value for n, which may be assumed if no further restrictions are present [205], would correspond to $\alpha = 5$, i.e. a violet noise spectrum which is also known as Batchelor or von Kármán spectrum. The same value for α has also been found in different analytical [206] and numerical [198] discussions.

Based on these findings now a general picture of the time evolution of the spectral energy can be drawn. The key quantity here is the scale-dependent relaxation time τ_L, being at the same time the eddy turn over time at scale L, which for (3.12) is given by

$$\tau_L \simeq \frac{L}{v^\mathrm{eff}_{k=2\pi/L}} \simeq \frac{L}{v^\mathrm{eff}_{\mathrm{A},k=2\pi/L}} \overset{(3.15)}{=} \frac{L}{(2kM_k)^{\frac{1}{2}}} \overset{(3.18)}{\propto} \frac{L}{(L^{-\alpha})^{\frac{1}{2}}} \propto L^{\frac{\alpha+2}{2}} . \tag{3.21}$$

For $L \geq L_\mathrm{I}$, i.e. for positive α, this means that τ_L grows with the scale size L. Therefore, after a relaxation time τ_L the energy on scale L and, due to its power law dependence

described above, also on all smaller scales, has decayed, thus making it the new integral scale such that it gradually moves to larger scales (i.e. smaller values of k). This phenomenon is also known as selective decay of modes in k-space [194].

Solving (3.21) for L therefore gives the time development of the integral scale L_I starting from L_0, the initial value of the integral scale at time t_0,

$$L_\mathrm{I} \simeq L_0 \left(\frac{t}{t_0}\right)^{\frac{2}{\alpha+2}}, \; k_\mathrm{I} \simeq k_0 \left(\frac{t}{t_0}\right)^{-\frac{2}{\alpha+2}} \tag{3.22}$$

and, plugged into (3.18), for M_k it gives

$$M_\mathrm{I} \simeq M_0 \left(\frac{L_\mathrm{I}}{L_0}\right)^{1-\alpha} \simeq M_0 \left(\frac{k_\mathrm{I}}{k_0}\right)^{\alpha-1} \simeq M_0 \left(\frac{t}{t_0}\right)^{-2\frac{\alpha-1}{\alpha+2}} . \tag{3.23}$$

By including magnetic helicity in this setting, the situation changes dramatically as now the behavior of the spectral quantities is determined mainly by the requirement of magnetic helicity conservation as described in Sec. 1.1.2.2: Assuming that at some point the system reaches (and afterwards stays in) the state of maximal helicity, given by the equality sign in (1.101), one can say that, again due to the fact that also most of the spectral helicity density is concentrated at the integral scale, it is

$$\mathrm{const} \overset{(1.83)}{=} \frac{h_B}{\rho} \overset{(1.71)}{=} \int \mathcal{H}_k \,\mathrm{d}k \simeq k_\mathrm{I} \mathcal{H}_\mathrm{I} \overset{(1.101)}{\simeq} k_\mathrm{I} \left(\frac{8\pi}{k_\mathrm{I}} M_\mathrm{I}\right) = 8\pi M_\mathrm{I} \tag{3.24}$$

and therefore $M_\mathrm{I} = \mathrm{const}$. This means that the decay of the energy now depends on the behavior of k_I with time which can be estimated, taking into account the selective decay, i.e. assuming that the scale L of the decay time τ_L is the integral scale, by

$$\frac{\mathrm{d}k_\mathrm{I}}{\mathrm{d}t} \simeq \frac{k_\mathrm{I}}{\tau_L} \overset{(3.21)}{\simeq} \frac{k_\mathrm{I}}{L_\mathrm{I}/\left(2k_\mathrm{I}M_\mathrm{I}\right)^{\frac{1}{2}}} \overset{(3.24)}{\propto} k_\mathrm{I}^{\frac{5}{2}} , \tag{3.25}$$

which gives $k_\mathrm{I} \simeq t^{-\frac{2}{3}}$, having therefore

$$L_\mathrm{I} \simeq L_0 \left(\frac{t}{t_0}\right)^{\frac{2}{3}}, \; k_\mathrm{I} \simeq k_0 \left(\frac{t}{t_0}\right)^{-\frac{2}{3}}, \; \mathcal{H}_\mathrm{I} \overset{(1.71)}{\simeq} \mathcal{H}_0 \left(\frac{t}{t_0}\right)^{\frac{2}{3}} . \tag{3.26}$$

This is a remarkable result as now the time development is independent of the slope, but rather obeys a power law with an universal index of $\pm 2/3$.

In order to make these general considerations describe an actual cosmological setting, one has to take into account the Expansion of the Universe. In particular, one has to compare τ_L, the typical time scale at L, with the Hubble time t_H. Usually one assumes that at the magnetogenesis epoch they are the same, i.e.

$$\tau_L \simeq \frac{L}{v(L)} \simeq \frac{L}{v_\mathrm{A}(L)} \simeq H^{-1} = t_H \,. \tag{3.27}$$

For the matter- and the radiation-dominated regime, the Hubble Time, according to (1.182), grows as $t_H \propto a^2$ and $t_H \propto a^{\frac{3}{2}}$, respectively. Therefore, relative to the Hubble Time, the proper value of τ_L scales as

$$\frac{\tau_L}{t_H} \overset{(3.1)}{\propto} \frac{a}{a^2} \propto a^{-1} \tag{3.28}$$

for the radiation-dominated and

$$\frac{\tau_L}{t_H} \overset{(3.2)}{\propto} \frac{a^{\frac{3}{2}}}{a^{\frac{3}{2}}} \propto a^0 \tag{3.29}$$

for the matter-dominated regime, respectively. This means that in comoving coordinates for the former case a growth of the integral scale is allowed since τ_L grows slower than the Universe expands, whereas for the latter these rates are equal such that only a logarithmic growth may take place. This means that, for a turbulent medium, while during the radiation-dominated era the integral scale and the energy content behave as derived earlier in this section, during the matter-dominated era they remain constant. Due to decoupling of the electrons after Recombination the medium may be assumed to be turbulent [194], which means that *in order to investigate the impact of Primordial Magnetic Fields on today's EGMF in general it is sufficient to follow their evolution up to the point when (cold) matter becomes the dominating energy component of the Universe which can be roughly taken to happen at Recombination.*

3.1.3.2 The Viscous Phases

Viscous phases are characterized by a specific dissipation force which enters into the Euler Equations (1.27) and is of the form [194]

$$\mathbf{f} = \begin{cases} \eta \Delta \mathbf{v},\, L_{\mathrm{mfp}} \ll L\,, \\ -\alpha \mathbf{v},\, L_{\mathrm{mfp}} \gg L\,, \end{cases} \tag{3.30}$$

where L is some typical scale of the MHD system and L_{mfp} is the mean free path of the particle in question, which scatters with the fluid particles and therefore causes viscosity in the first place. Following the argumentation above, namely that in a viscous phase the balance between the second and the third terms on the right hand side of (1.27) governs the behavior of that equation (which symbolically may be written as $\left|B^2/(4\pi\rho L)\right| \simeq \left|v_{\mathrm{A}}^2/L\right| \simeq |v|$ for a given scale L), and, using (3.30) one obtains

$$v \simeq \begin{cases} \frac{v_{\mathrm{A}}^2 L}{\eta},\, L_{\mathrm{mfp}} \ll L\,, \\ \frac{v_{\mathrm{A}}^2}{\alpha L},\, L_{\mathrm{mfp}} \ll L\,. \end{cases} \tag{3.31}$$

The two kinds of particles in question to trigger a viscous phase in the Early Universe as described above are neutrinos and photons. Therefore this occurs twice – shortly before Neutrino Decoupling and shortly before Photon Decoupling (at $T \simeq 10^6$ eV and at $T \simeq 0.25\,\mathrm{eV}$, respectively – cf. Sec. 1.2.3) while otherwise a turbulent environment may be assumed. The reason that neutrinos dominate during the first viscous phase is given by the fact that between the Electroweak Phase Transition and their decoupling they have the longest mean free path of all particles and therefore give the major contribution to the momentum and heat transport [49]. A similar argument also holds later on for photons as well.

The two possible cases considered in (3.30) are, on the one hand, dissipation due to diffusion of the particles, as can be seen directly from the form of $\mathbf{f}$ and from the fact that the mean free path is smaller than the typical length scale, and, on the other hand, due to the so-called free streaming background component for which only occasional scatterings occur. Here η and α are the corresponding dissipation coefficients which are given, apart from numerical factors, by [194]

$$\eta_\nu \propto L_{\nu,\mathrm{mfp}}\,,\ \alpha_\nu \propto L_{\nu,\mathrm{mfp}}^{-1} \tag{3.32}$$

for neutrinos and

$$\eta_\gamma \propto L_{\gamma,\mathrm{mfp}}\,,\ \alpha_\gamma \propto \frac{\rho_\gamma}{\rho_\mathrm{b}} L^{-1}_{\gamma,\mathrm{mfp}} \tag{3.33}$$

for photons, where ρ_γ and ρ_b are the photon and baryon energy densities, respectively.

With these relations at hand and the expressions for the mean free paths for neutrinos, (1.183), and photons, (1.185), with $L_{\nu,\mathrm{mfp}} \propto a^5$ and $L_{\gamma,\mathrm{mfp}} \propto a^3$, one can now, using (3.32) and (3.33), write down the behavior of the coefficients η and α, for both the free streaming and the diffusive regimes, in an expanding Universe:

$$\eta_\nu \propto a^5\,,\ \alpha_\nu \propto a^{-5}\,,\ \eta_\gamma \propto a^3\,,\ \alpha_\gamma \propto a^{-4}\,. \tag{3.34}$$

This can be directly used to make conclusions about the eddy turnover time τ_L in a similar way as it has been done for the turbulent case:

$$\frac{\tau_L}{t_H} \simeq \frac{L/v}{t_H} \overset{(3.31)}{\simeq} \frac{\eta/v_\mathrm{A}^2}{t_H} \propto \begin{cases} \frac{a^5/a^0}{a^2} \propto a^3\,, \text{ diffusive neutrino regime,} \\ \frac{a^3/a^0}{a^2} \propto a^1\,, \text{ diffusive photon regime} \end{cases} \tag{3.35}$$

and

$$\frac{\tau_L}{t_H} \simeq \frac{L/v}{t_H} \overset{(3.31)}{\simeq} \frac{\left(\alpha L^2\right)/v_\mathrm{A}^2}{t_H} \propto \begin{cases} \frac{\left(a^{-5}a^2\right)/a^{-1}}{a^2} \propto a^{-4}\,, \text{ free streaming neutrino regime,} \\ \frac{\left(a^{-4}a^2\right)/a^{-1}}{a^{\frac{3}{2}}} \propto a^{-\frac{5}{2}}\,, \text{ free streaming photon regime,} \end{cases} \tag{3.36}$$

where for the first three cases radiation domination and for the last case (free streaming photon regime), as it takes place at rather late times, matter domination has been assumed.

The expressions (3.35) and (3.36) give a rather important result: During the viscous diffusive regime (both for neutrinos and photons) the dissipation time scale τ_L grows faster than the Hubble time, therefore preventing further dissipation of energy on scales bigger than the integral scale L_I from the transition between a turbulent and a viscous phase which implies that also the integral scale itself does not change. On the other hand, during the free streaming regime, since α has a strong dependence on the scale factor, both the growth of the integral scale and the corresponding dissipation of energy takes place faster than in the turbulent regime.

After a thorough investigation of these phenomena, [194] came to the crucial conclusion that, considering the integral scale and the corresponding energy content before Recombination, the viscous phases, each consisting of a diffusive and a free streaming regime, *has a very small net effect*. That means that while evolution stops during the former, it "catches up" during the successive latter regime, such that at the end of viscosity the relevant quantities approximately obtain values very close to the ones they would have gained if only the turbulent phase would have been active all the time. Other authors, such as [200], assume that a viscous phase might change the result compared to the case neglecting it, claiming at the same time that considering the "only turbulent" scenario gives a reasonable upper limit for the integral scale and the energy content.

3.2 Master Equations for the Time Evolution of the Energy Content of Magnetic Fields

In this section the Master Equations for the time evolution of the energy content of Primordial Magnetic Fields will be derived. Here a similar procedure as the one which already has been applied to solar winds [207, 208] and the galactic magnetic field [209] is used, adapting it to the set requirements, also by extending former works [197, 210].

3.2.1 Full Derivation of the Master Equations

In order to derive the time evolution of the magnetic spectral energy M_q, the kinetic energy U_q and the spectral magnetic helicity $\mathcal{H}_q$, one has to, as can be seen from the defining equations (1.64), (1.65) and (1.73), respectively, find an expression for the Fourier Transform of the time evolution equation for both $\mathbf{B}$ and $\mathbf{v}$. This can be done by applying (A.21) to (1.13) and (1.27), respectively. Using the general rules for Fourier Transforms given in Sec. A.3 for the former this gives

$$\partial_t \hat{\mathbf{B}}(\mathbf{q}) = \frac{1}{4\pi\sigma}(i\mathbf{q})^2 \hat{\mathbf{B}}(\mathbf{q}) + i\mathbf{q} \times \frac{V^{\frac{1}{2}}}{(2\pi)^{\frac{3}{2}}} \int \hat{\mathbf{v}}(\mathbf{q}-\mathbf{k}) \times \hat{\mathbf{B}}(\mathbf{k}) \, \mathrm{d}^3k \,. \tag{3.37}$$

Here for the last term on the right hand side the Convolution Theorem, (A.24), has been used. Performing further simplifications one obtains

$$\begin{aligned}
\partial_t \hat{\mathbf{B}}(\mathbf{q}) &= -\frac{1}{4\pi\sigma} q^2 \hat{\mathbf{B}}(\mathbf{q}) + \frac{iV^{\frac{1}{2}}}{(2\pi)^{\frac{3}{2}}} \mathbf{q} \times \int \hat{\mathbf{v}}(\mathbf{q}-\mathbf{k}) \times \hat{\mathbf{B}}(\mathbf{k}) \, \mathrm{d}^3k \\
&= -\frac{1}{4\pi\sigma} q^2 \hat{\mathbf{B}}(\mathbf{q}) + \frac{iV^{\frac{1}{2}}}{(2\pi)^{\frac{3}{2}}} \int \mathbf{q} \times \left(\hat{\mathbf{v}}(\mathbf{q}-\mathbf{k}) \times \hat{\mathbf{B}}(\mathbf{k}) \right) \mathrm{d}^3k \\
&\overset{(A.1)}{=} -\frac{q^2 \hat{\mathbf{B}}(\mathbf{q})}{4\pi\sigma} + \frac{iV^{\frac{1}{2}}}{(2\pi)^{\frac{3}{2}}} \int \left[\left(\mathbf{q} \cdot \hat{\mathbf{B}}(\mathbf{k}) \right) \cdot \hat{\mathbf{v}}(\mathbf{q}-\mathbf{k}) - (\mathbf{q} \cdot \hat{\mathbf{v}}(\mathbf{q}-\mathbf{k})) \cdot \hat{\mathbf{B}}(\mathbf{k}) \right] \mathrm{d}^3k \,.
\end{aligned} \tag{3.38}$$

For the differential equation of $\mathbf{v}$, (1.27), the procedure is similar, giving, again using the Convolution Theorem,

$$\begin{aligned}
\partial_t \hat{\mathbf{v}}(\mathbf{q}) &= -\frac{iV^{\frac{1}{2}}}{(2\pi)^{\frac{3}{2}}} \int \left(\hat{\mathbf{v}}(\mathbf{q}-\mathbf{k}) \cdot \mathbf{k} \right) \hat{\mathbf{v}}(\mathbf{k}) \, \mathrm{d}^3k \\
&+ \frac{iV^{\frac{1}{2}}}{(2\pi)^{\frac{3}{2}}} \frac{1}{4\pi\rho} \int \left(\mathbf{k} \times \hat{\mathbf{B}}(\mathbf{k}) \right) \times \hat{\mathbf{B}}(\mathbf{q}-\mathbf{k}) \, \mathrm{d}^3k \overset{(A.1)}{=} -\frac{iV^{\frac{1}{2}}}{(2\pi)^{\frac{3}{2}}} \int \left(\hat{\mathbf{v}}(\mathbf{q}-\mathbf{k}) \cdot \mathbf{k} \right) \hat{\mathbf{v}}(\mathbf{k}) \, \mathrm{d}^3k \\
&+ \frac{iV^{\frac{1}{2}}}{(2\pi)^{\frac{3}{2}}} \frac{1}{4\pi\rho} \int \left[\left(\hat{\mathbf{B}}(\mathbf{q}-\mathbf{k}) \cdot \mathbf{k} \right) \hat{\mathbf{B}}(\mathbf{k}) - \left(\hat{\mathbf{B}}(\mathbf{q}-\mathbf{k}) \cdot \hat{\mathbf{B}}(\mathbf{k}) \right) \mathbf{k} \right] \mathrm{d}^3k \,.
\end{aligned} \tag{3.39}$$

In order to solve these ordinary differential equations, the Runge-Kutta method described in Sec. A.4 is used, more precisely the Midpoint Method, i.e. for the parameters introduced in (A.35) it is $s = 2$, $a_{21} = 1/2$, $b_1 = 0$, $b_2 = 1$, $c_1 = 0$ and $c_2 = 1/2$. Therefore, in order to approximate the corresponding value at a time $t_2 = t_0 + \Delta t$ (where t_0 is the initial time), one inserts an intermediate step at $t_1 = t_0 + 1/2\Delta t$. Introducing the notation $y(t_i) \equiv {}^{(i)}y$ for the quantities in (A.33) it is

$${}^{(1)}y = {}^{(0)}y + \tfrac{1}{2}\Delta t f\left(t_0, {}^{(0)}y\right) \,, \tag{3.40}$$

$${}^{(2)}y = {}^{(1)}y + \Delta t f\left(t_1, {}^{(1)}y\right) \tag{3.41}$$

and therefore (3.38) and (3.39) first become

$$\begin{aligned}
{}^{(1)}\hat{\mathbf{B}}_{\mathbf{q}} = {}^{(0)}\hat{\mathbf{B}}_{\mathbf{q}} + \frac{1}{2}\Delta t \Bigg\{ &- \frac{q^2 \, {}^{(0)}\hat{\mathbf{B}}_{\mathbf{q}}}{4\pi\sigma} \\
&+ \frac{iV^{\frac{1}{2}}}{(2\pi)^{\frac{3}{2}}} \int \left[\left(\mathbf{q} \cdot {}^{(0)}\hat{\mathbf{B}}_{\mathbf{k}} \right) \cdot {}^{(0)} \hat{\mathbf{v}}_{\mathbf{q}-\mathbf{k}} - \left(\mathbf{q} \cdot {}^{(0)} \hat{\mathbf{v}}_{\mathbf{q}-\mathbf{k}} \right) \cdot {}^{(0)}\hat{\mathbf{B}}_{\mathbf{k}} \right] \mathrm{d}^3k \Bigg\}
\end{aligned} \tag{3.42}$$

and

$$
\begin{aligned}
{}^{(1)}\hat{\mathbf{v}}_{\mathbf{q}} = {}^{(0)}\hat{\mathbf{v}}_{\mathbf{q}} + \frac{1}{2}\Delta t \Bigg\{ & - \frac{iV^{\frac{1}{2}}}{(2\pi)^{\frac{3}{2}}} \int \left(\hat{\mathbf{v}}_{\mathbf{q}-\mathbf{k}} \cdot \mathbf{k}\right) \hat{\mathbf{v}}_{\mathbf{k}} \, \mathrm{d}^3 k \\
& + \frac{iV^{\frac{1}{2}}}{(2\pi)^{\frac{3}{2}}} \frac{1}{4\pi\rho} \int \left[\left(\hat{\mathbf{B}}_{\mathbf{q}-\mathbf{k}} \cdot \mathbf{k} \right) \hat{\mathbf{B}}_{\mathbf{k}} - \left(\hat{\mathbf{B}}_{\mathbf{q}-\mathbf{k}} \cdot \hat{\mathbf{B}}_{\mathbf{k}} \right) \mathbf{k} \right] \mathrm{d}^3 k \,,
\end{aligned}
\tag{3.43}
$$

and then

$$
\begin{aligned}
{}^{(2)}\hat{\mathbf{B}}_{\mathbf{q}} = {}^{(0)}\hat{\mathbf{B}}_{\mathbf{q}} + \Delta t \Bigg\{ & - \frac{q^2 \, {}^{(1)}\hat{\mathbf{B}}_{\mathbf{q}}}{4\pi\sigma} \\
& + \frac{iV^{\frac{1}{2}}}{(2\pi)^{\frac{3}{2}}} \int \left[\left({}^{(1)}\hat{\mathbf{B}}_{\mathbf{k}} \cdot \mathbf{q} \right) {}^{(1)}\hat{\mathbf{v}}_{\mathbf{q}-\mathbf{k}} - \left({}^{(1)}\hat{\mathbf{v}}_{\mathbf{q}-\mathbf{k}} \cdot \mathbf{q} \right) {}^{(1)}\hat{\mathbf{B}}_{\mathbf{k}} \right] \mathrm{d}^3 k \Bigg\}
\end{aligned}
\tag{3.44}
$$

and

$$
\begin{aligned}
{}^{(2)}\hat{\mathbf{v}}_{\mathbf{q}} = {}^{(0)}\hat{\mathbf{v}}(\mathbf{q}) + \Delta t \Bigg\{ & \frac{iV^{\frac{1}{2}}}{(2\pi)^{\frac{3}{2}}} \int \Big[- \left({}^{(1)}\hat{\mathbf{v}}_{\mathbf{q}-\mathbf{k}} \cdot \mathbf{k} \right) {}^{(1)}\hat{\mathbf{v}}_{\mathbf{k}} \\
& + \frac{1}{4\pi\rho} \left({}^{(1)}\hat{\mathbf{B}}_{\mathbf{q}-\mathbf{k}} \cdot \mathbf{k} \right) {}^{(1)}\hat{\mathbf{B}}_{\mathbf{k}} - \frac{1}{4\pi\rho} \left({}^{(1)}\hat{\mathbf{B}}_{\mathbf{q}-\mathbf{k}} \cdot \, {}^{(1)}\hat{\mathbf{B}}_{\mathbf{k}} \right) \mathbf{k} \Big] \mathrm{d}^3 k \Bigg\} \,,
\end{aligned}
\tag{3.45}
$$

respectively. Here the abbreviations $\hat{\mathbf{B}}_{\mathbf{k}} \equiv \hat{\mathbf{B}}(\mathbf{k})$ and $\hat{\mathbf{v}}_{\mathbf{k}} \equiv \hat{\mathbf{v}}(\mathbf{k})$ for some wavenumber $\mathbf{k}$ have been introduced. The final step now is to insert both (3.42) and (3.43) into (3.44) and (3.45), respectively, which gives two lengthy expressions presented in the Appendix as (B.1) and (B.2). There and from here on the superscript ${}^{(0)}$ is dropped.

As has been stated before, the main aim is to find the time evolution of the main spectral quantities, therefore it is necessary to calculate the respective time derivatives, namely

$$
\partial_t M_q \overset{(1.64)}{=} \partial_t \left(\frac{q^2}{2\rho} |\hat{\mathbf{B}}_{\mathbf{q}}|^2 \right) = \frac{q^2}{\rho} \left(\partial_t \hat{\mathbf{B}}_{\mathbf{q}} \right) \cdot \hat{\mathbf{B}}^*_{\mathbf{q}} = \frac{q^2}{\rho} \left(\partial_t \hat{B}_{\mathbf{q},i} \right) \hat{B}^*_{\mathbf{q},i} \,, \tag{3.46}
$$

$$
\partial_t U_q \overset{(1.65)}{=} \partial_t \left(2\pi q^2 |\hat{\mathbf{v}}_{\mathbf{q}}|^2 \right) = 4\pi q^2 \left(\partial_t \hat{\mathbf{v}}_{\mathbf{q}} \right) \cdot \hat{\mathbf{v}}^*_{\mathbf{q}} = 4\pi q^2 \left(\partial_t \hat{v}_{\mathbf{q},i} \right) \hat{v}^*_{\mathbf{q},i} \,, \tag{3.47}
$$

$$
\begin{aligned}
\partial_t \mathcal{H}_q \overset{(1.73)}{=} \partial_t \left[\frac{4\pi i}{\rho} \left(\mathbf{q} \times \hat{\mathbf{B}}_{\mathbf{q}} \right) \cdot \hat{\mathbf{B}}^*_{\mathbf{q}} \right] &= \frac{8\pi i}{\rho} \left(\mathbf{q} \times \partial_t \hat{\mathbf{B}}_{\mathbf{q}} \right) \cdot \hat{\mathbf{B}}^*_{\mathbf{q}} \\
&= \frac{8\pi i}{\rho} \epsilon_{ijl} q_j \left(\partial_t \hat{B}_{\mathbf{q},l} \right) \hat{B}^*_{\mathbf{q},i} \,,
\end{aligned}
\tag{3.48}
$$

where, for all three equations, in the last step the index behind the wavenumber in the subscript is indicating the corresponding Cartesian component of $\mathbf{B}$ and $\mathbf{v}$, respectively, and, in addition, the Einstein Sum Convention has been used.

As one can see, in order to calculate these time derivatives, one needs $\hat{\mathbf{B}}_{\mathbf{k}}$, $\partial_t \hat{\mathbf{B}}_{\mathbf{k}}$, $\hat{\mathbf{v}}_{\mathbf{k}}$ and $\partial_t \hat{\mathbf{v}}_{\mathbf{k}}$. Since it is $\hat{\mathbf{B}}_{\mathbf{k}}(t) \simeq {}^{(2)}\hat{\mathbf{B}}_{\mathbf{k}}$ and $\hat{\mathbf{v}}_{\mathbf{k}}(t) \simeq {}^{(2)}\hat{\mathbf{v}}_{\mathbf{k}}$, one can directly use (B.1) and (B.2). Looking at the structure of these equations, it is clear that plugging this into (3.46)-(3.48) will give a large number of terms consisting of the various wavenumbers as well as of products of up to four expressions of both $\hat{\mathbf{B}}$ and $\hat{\mathbf{v}}$ (with different arguments and in different combinations) if one takes into account terms of up to the first order in Δt in the final form.

Since the interest lies in the statistical description of the time derivatives, the ensemble average, as defined in Sec. 1.1.3.1, is applied. The values of the magnetic and kinetic fields are assumed to obey a Gaussian distribution, such that Isserlis' Theorem (1.142), especially in the form (1.143), may be applied to simplify the expressions. Furthermore, it is assumed that $\hat{\mathbf{B}}$ and $\hat{\mathbf{v}}$ are uncorrelated, i.e. $\left\langle \hat{\mathbf{B}} \cdot \hat{\mathbf{v}} \right\rangle = 0$ for any combination of arguments. Finally, in order to have a differential equation for the time evolution of the spectral quantities, one has to use the correlation functions (1.127) and (1.131). Since the procedure described in this paragraph is a rather long calculation, it is presented in Appendix B, Section B.2, while here and in the following the resulting simplified time evolution equations are shown and analyzed.

From here on, as has been motivated in Sec. 3.1.2, the conductivity is assumed to be very large, such that in the limit $\sigma \to \infty$ the Master Equations for the time evolution of magnetic fields are given by

$$\begin{aligned}\langle \partial_t M_q \rangle = \int_0^\infty \Bigg(\Delta t \Bigg\{ &- \frac{2}{3} q^2 \langle M_q \rangle \langle U_k \rangle - \frac{4}{3} q^2 \langle M_q \rangle \langle M_k \rangle + \frac{1}{3} \frac{q^2 k^2}{(4\pi)^2} \langle \mathcal{H}_q \rangle \langle \mathcal{H}_k \rangle \\ &+ \int_0^\pi \left[\frac{1}{2} \frac{q^4}{k_1^4} \left(q^2 + k^2 - qk\cos\theta \right) \sin^3\theta \langle M_k \rangle \langle U_{k_1} \rangle \right] \mathrm{d}\theta \Bigg\} \Bigg) \mathrm{d}k \,,\end{aligned} \tag{3.49}$$

$$\begin{aligned}\langle \partial_t U_q \rangle = \int_0^\infty \Bigg(\Delta t \Bigg\{ &- \frac{2}{3} q^2 \langle M_k \rangle \langle U_q \rangle - \frac{2}{3} q^2 \langle U_q \rangle \langle U_k \rangle + \int_0^\pi \Bigg[\frac{1}{4} \frac{q^3 k}{k_1^4} \big(qk \sin^2\theta \\ &+ 2k_1^2 \cos\theta \big) \sin\theta \langle M_k \rangle \langle M_{k_1} \rangle + \frac{1}{4} \frac{q^4 k}{k_1^4} \left(3k - q\cos\theta \right) \sin^3\theta \langle U_k \rangle \langle U_{k_1} \rangle \\ &+ \frac{1}{(16\pi)^2} \frac{q^3 k^2}{k_1^2} \left(-2q - q\sin^2\theta + 2k\cos\theta \right) \sin\theta \langle \mathcal{H}_k \rangle \langle \mathcal{H}_{k_1} \rangle \Bigg] \mathrm{d}\theta \Bigg\} \Bigg) \mathrm{d}k\end{aligned} \tag{3.50}$$

and

$$\begin{aligned}\langle \partial_t \mathcal{H}_q \rangle = \int_0^\infty \Bigg(\Delta t \Bigg\{ &\frac{4}{3} k^2 \langle M_q \rangle \langle \mathcal{H}_k \rangle - \frac{4}{3} q^2 \langle M_k \rangle \langle \mathcal{H}_q \rangle \\ &- \frac{2}{3} q^2 \langle U_k \rangle \langle \mathcal{H}_q \rangle + \int_0^\pi \left[\frac{1}{2} \frac{q^4 k^2}{k_1^4} \sin^3\theta \langle U_{k_1} \rangle \langle \mathcal{H}_k \rangle \right] \mathrm{d}\theta \Bigg\} \Bigg) \mathrm{d}k \,,\end{aligned} \tag{3.51}$$

as can be seen from (B.41)-(B.41) for (k, θ)-coordinates, where θ is the angle between $\mathbf{q}$ and $\mathbf{k}$, i.e. $\mathbf{q} \cdot \mathbf{k} = qk\cos\theta$, and $\mathbf{k}_1 \equiv |\mathbf{q} - \mathbf{k}|$, while $k_1 \equiv |\mathbf{k}_1|$ is its magnitude.

These equations can be reformulated in terms of the (k, k_1)-coordinates. From (B.38)-(B.40) one can see that this gives

$$\begin{aligned}\langle \partial_t M_q \rangle = \int_0^\infty \Bigg(\Delta t \Bigg\{ &- \frac{2}{3} q^2 \langle M_q \rangle \langle U_k \rangle - \frac{4}{3} q^2 \langle M_q \rangle \langle M_k \rangle + \frac{1}{3} \frac{1}{(4\pi)^2} q^2 k^2 \langle \mathcal{H}_q \rangle \langle \mathcal{H}_k \rangle \\ &+ \int_{|q-k|}^{q+k} \Bigg[\Bigg(- \frac{q^7}{16k^3 k_1^3} + \frac{q^5}{16k^3 k_1} + \frac{q^5}{16k k_1^3} + \frac{q^3 k}{16 k_1^3} + \frac{3q^3}{8kk_1} + \frac{q^3 k_1}{16k^3} - \frac{qk^3}{16k_1^3} + \frac{qk}{16k_1} \\ &+ \frac{qk_1}{16k} - \frac{qk_1^3}{16k^3} \Bigg) \langle M_k \rangle \langle U_{k_1} \rangle \Bigg] \mathrm{d}k_1 \Bigg\} \Bigg) \mathrm{d}k\end{aligned} \tag{3.52}$$

and

$$\begin{aligned}\langle\partial_t U_q\rangle = \int_0^\infty \Bigg(\Delta t\Bigg\{ &-\frac{2}{3}q^2\langle M_k\rangle\langle U_q\rangle - \frac{2}{3}q^2\langle U_q\rangle\langle U_k\rangle + \int_{|q-k|}^{q+k}\Bigg[\Bigg(-\frac{q^5}{16kk_1^3}+\frac{q^3k}{8k_1^3}\\ &+\frac{3q^3}{8kk_1}-\frac{qk^3}{16k_1^3}+\frac{3qk}{8k_1}-\frac{5qk_1}{16k}\Bigg)\langle M_k\rangle\langle M_{k_1}\rangle + \Bigg(\frac{q^7}{32k^3k_1^3}-\frac{7q^5}{32kk_1^3}-\frac{3q^5}{32k^3k_1}+\frac{11q^3k}{32k_1^3}\\ &+\frac{5q^3}{16kk_1}+\frac{3q^3k_1}{32k^3}-\frac{5qk^3}{32k_1^3}+\frac{9qk}{32k_1}-\frac{3qk_1}{32k}-\frac{qk_1^3}{32k^3}\Bigg)\langle U_k\rangle\langle U_{k_1}\rangle\\ &+\frac{1}{(8\pi)^2}\Bigg(\frac{q^5}{16kk_1}-\frac{3q^3k}{8k_1}-\frac{q^3k_1}{8k}+\frac{5qk^3}{16k_1}-\frac{3qkk_1}{8}+\frac{qk_1^3}{16k}\Bigg)\langle\mathcal{H}_k\rangle\langle\mathcal{H}_{k_1}\rangle\Bigg]\mathrm{d}k_1\Bigg\}\Bigg)\mathrm{d}k\end{aligned} \tag{3.53}$$

as well as

$$\begin{aligned}\langle\partial_t\mathcal{H}_q\rangle = \int_0^\infty \Bigg(\Delta t\Bigg\{&\frac{4}{3}k^2\langle M_q\rangle\langle\mathcal{H}_k\rangle - \frac{4}{3}q^2\langle M_k\rangle\langle\mathcal{H}_q\rangle - \frac{2}{3}q^2\langle U_k\rangle\langle\mathcal{H}_q\rangle\\ &+\int_{|q-k|}^{q+k}\Bigg[\Bigg(-\frac{q^5}{8kk_1^3}+\frac{q^3k}{4k_1^3}+\frac{q^3}{4kk_1}-\frac{qk^3}{8k_1^3}+\frac{qk}{4k_1}-\frac{qk_1}{8k}\Bigg)\langle U_{k_1}\rangle\langle\mathcal{H}_k\rangle\Bigg]\mathrm{d}k_1\Bigg\}\Bigg)\mathrm{d}k\,.\end{aligned} \tag{3.54}$$

3.2.2 Checks for Consistency

As several assumptions have been made during the derivation of the Master Equations presented in the previous section, it is important to make sure that they fulfill the basic requirements from the physics point of view, such that a reasonable interpretation of the results is possible.

Before examining the conservation of both energy and magnetic helicity, it is important whether the Master Equations, representing the MHD description, give the purely hydrodynamic equations if no magnetic energy (and no magnetic helicity) is injected for the initial conditions, i.e. $M_q = 0\,\forall\,q$ and $\mathcal{H}_q = 0\,\forall\,q$. This can be tested directly with (3.49) and (3.50). Since in both every term contains at least one product with M or $\mathcal{H}$, the total is zero, such that if the initial magnetic energy vanishes, it will remain zero, the same also being true for magnetic helicity. (3.50), on the other hand, reduces to

$$\langle\partial_t U_q\rangle = \int\Bigg(\Delta t\Bigg\{-\frac{2}{3}q^2\langle U_q\rangle\langle U_k\rangle + \int_0^\pi\Bigg[\frac{q^4k}{4k_1^4}(3k-q\cos\theta)\sin^3\theta\langle U_k\rangle\langle U_{k_1}\rangle\Bigg]\mathrm{d}\theta\Bigg\}\Bigg)\mathrm{d}k \tag{3.55}$$

which therefore may be seen as the time evolution of the spectral kinetic energy in the hydrodynamic regime.

3.2.2.1 Energy Conservation

As has been pointed out in Sec. 1.1.1.6, more specifically in (1.54), if the ideal turbulent regime is considered, i.e. neglecting any dissipative outer forces and setting $\sigma \to \infty$, the total energy of the system has to be conserved. This means, according to (1.60) and (1.61),

$$\langle\partial_t(\epsilon_K+\epsilon_B)\rangle = \rho\int_0^\infty(\langle\partial_t M_q\rangle + \langle\partial_t U_q\rangle)\,\mathrm{d}q = 0\,. \tag{3.56}$$

In order to evaluate this expression it can be shown, in a similar way as for (B.36), that an even more general rule for the exchange of integration limits apply, namely, for some function $f(q,k,k_1)$,

$$\begin{aligned}\int_0^\infty \int_0^\infty \int_{|q-k|}^{q+k} f(q,k,k_1)\,\mathrm{d}k_1\mathrm{d}k\mathrm{d}q &= \int_0^\infty \int_0^\infty \int_{|q-k_1|}^{q+k_1} f(q,k,k_1)\,\mathrm{d}k\mathrm{d}q\mathrm{d}k_1 \\ &= \int_0^\infty \int_0^\infty \int_{|k-k_1|}^{k+k_1} f(q,k,k_1)\,\mathrm{d}q\mathrm{d}k_1\mathrm{d}k\,.\end{aligned} \tag{3.57}$$

Therefore, using the representations (3.52) and (3.53), transforming the integrals as given by (3.57) and then calculating, if applicable, the respective innermost of the three integrals, (3.56) may be rewritten as

$$\begin{aligned}&\rho\int_0^\infty \left(\langle\partial_t M_q\rangle + \langle\partial_t U_q\rangle\right)\mathrm{d}q = \rho\Delta t\Bigg\{\int_0^\infty\int_0^\infty\Bigg(-\frac{2}{3}q^2\langle M_q\rangle\langle U_k\rangle \\ &-\frac{4}{3}q^2\langle M_q\rangle\langle M_k\rangle + \frac{1}{3}\frac{1}{(4\pi)^2}q^2k^2\langle\mathcal{H}_q\rangle\langle\mathcal{H}_k\rangle\Bigg)\mathrm{d}k\mathrm{d}q \\ &+\int_0^\infty\int_0^\infty\left[\frac{2}{3}\left(k^2+k_1^2\right)\langle M_k\rangle\langle U_{k_1}\rangle\right]\mathrm{d}k\mathrm{d}k_1 + \int_0^\infty\int_0^\infty\Bigg(-\frac{2}{3}q^2\langle M_k\rangle\langle U_q\rangle \\ &-\frac{2}{3}q^2\langle U_q\rangle\langle U_k\rangle\Bigg)\mathrm{d}k\mathrm{d}q + \int_0^\infty\int_0^\infty\Bigg(\frac{4}{3}k^2\langle M_k\rangle\langle M_{k_1}\rangle + \frac{2}{3}k^2\langle U_k\rangle\langle U_{k_1}\rangle \\ &-\frac{1}{3}\frac{1}{(4\pi)^2}k^2k_1^2\langle\mathcal{H}_k\rangle\langle\mathcal{H}_{k_1}\rangle\Bigg)\mathrm{d}k\mathrm{d}k_1\Bigg\}\,.\end{aligned} \tag{3.58}$$

By renaming the dummy integration variable from k_1 to q in the fourth, seventh, eighth and the ninth terms, one can directly see that the following terms (denoted by roman numbers I-IX in the order they appear in (3.58)) cancel each other: II and VII, III and IX, VI and VIII as well as IV which cancels I and V taken together. Therefore the total of (3.58) is zero such that the energy is indeed conserved.

3.2.2.2 Conservation of Magnetic Helicity

Similar to the total energy also the total magnetic helicity is conserved in the limit of $\sigma\to\infty$ as has been shown in Sec. 1.1.2.2. Again, to make sure that the Master Equations are consistent they also have to fulfill this requirement which can be expressed as

$$\langle\partial_t h_\mathrm{B}\rangle \overset{(1.71)}{=} \rho\int\langle\partial_t\mathcal{H}_q\rangle\,\mathrm{d}q = 0\,. \tag{3.59}$$

This may be calculated using (3.57) for the last term, such that one obtains

$$\begin{aligned}\langle\partial_t\mathcal{H}_q\rangle = \Delta t\Bigg[&\int_0^\infty\int_0^\infty\left(\frac{4}{3}k^2\langle M_q\rangle\langle\mathcal{H}_k\rangle - \frac{4}{3}q^2\langle M_k\rangle\langle\mathcal{H}_q\rangle - \frac{2}{3}q^2\langle U_k\rangle\langle\mathcal{H}_q\rangle\right)\mathrm{d}k\mathrm{d}q \\ &+\int_0^\infty\int_0^\infty\frac{2}{3}k^2\langle U_{k_1}\rangle\langle\mathcal{H}_k\rangle\,\mathrm{d}k\mathrm{d}k_1\Bigg]\,.\end{aligned} \tag{3.60}$$

Here again, due to the symmetry of the integrations, one can see that the first with the second as well as the third with the fourth term give zero, respectively, therefore fulfilling (3.59) and confirming that magnetic helicity is conserved.

3.2.3 The Master Equations in an Expanding Universe

In order to apply the Master Equations to the time evolution of magnetic fields from the Early Universe to now, Expansion of the Universe has to be taken into account. In the following, as motivated above, this will be done for the radiation-dominated regime for which the essential transformation rules from physical to comoving coordinates are given by (3.1). These rules can be used to obtain the transformation of M_q, U_q and $\mathcal{H}_q$. In order to do so, first, from (A.19) and (A.21), one can see that the normalized Fourier Transform $\hat{f}$ of a function $f(\mathbf{r})$ can be related to the comoving length scales by

$$\hat{f} = \frac{1}{(2\pi)^{\frac{n}{2}}} \frac{1}{V^{\frac{1}{2}}} \int f\, e^{-i\mathbf{k}\cdot\mathbf{r}}\, \mathrm{d}^3 r = a^{\frac{3}{2}} \frac{1}{(2\pi)^{\frac{n}{2}}} \frac{1}{V_{\mathrm{c}}^{\frac{1}{2}}} \int f\, e^{-i\mathbf{k}_{\mathrm{c}}\cdot\mathbf{r}_{\mathrm{c}}}\, \mathrm{d}^3 r_{\mathrm{c}}\,, \tag{3.61}$$

where the index 'c' again denotes comoving quantities. Plugging this into the relations $\mathbf{B} = \mathbf{B}_c a^{-2}$ and $\mathbf{v} = \mathbf{v}_c$ from (3.1) therefore gives

$$\hat{\mathbf{B}} = \hat{\mathbf{B}}_{\mathrm{c}} a^{-\frac{1}{2}}\,,\ \hat{\mathbf{v}} = \hat{\mathbf{v}}_{\mathrm{c}} a^{\frac{3}{2}} \tag{3.62}$$

and therefore, from (1.64), (1.65) and (1.73),

$$M_q = M_q^{\mathrm{c}} a\,,\ U_q = U_q^{\mathrm{c}} a\,,\ \mathcal{H}_q = \mathcal{H}_q^{\mathrm{c}} a^2\,, \tag{3.63}$$

such that the comoving energy densities ϵ_B^{c} and $\epsilon_{\mathrm{K}}^{\mathrm{c}}$ are constant during the Expansion of the Universe if dynamical evolution is excluded.

With this one can finally show that the Master Equations are invariant under the transformation from physical to comoving coordinates, i.e. if the symbolic replacements

$$\begin{gathered} \partial_t \to \partial_{t_{\mathrm{c}}} a^{-1}\,,\ \Delta t \to \Delta t_{\mathrm{c}} a\,,\ k \to k_{\mathrm{c}} a^{-1}\,,\ \mathrm{d}k \to \mathrm{d}k_{\mathrm{c}} a^{-1}\,, \\ M_k \to M_k^{\mathrm{c}} a\,,\ U_k \to U_k^{\mathrm{c}} a\,,\ \mathcal{H}_k \to \mathcal{H}_k^{\mathrm{c}} a^2\,, \end{gathered} \tag{3.64}$$

where k is representing any wavenumber in question, are made, the Master Equations exactly keep their form, now, however, being expressed in comoving coordinates.

In addition, since the time evolution described in the following is taking place over many orders of magnitude in time, it is beneficial to express it in terms of the scale factor a rather than in terms of the time t. Therefore the time derivative $\partial_{t_{\mathrm{c}}}$ may be rewritten as

$$\partial_{t_{\mathrm{c}}} = \frac{\partial \ln a}{\partial t_{\mathrm{c}}} \frac{\partial}{\partial \ln a} = \frac{1}{a} \frac{\partial a}{\partial t_{\mathrm{c}}} \frac{\partial}{\partial \ln a} \overset{(3.64)}{=} \frac{\partial a}{\partial t} \frac{\partial}{\partial \ln a} \overset{(1.162)}{=} Ha \frac{\partial}{\partial \ln a} \overset{(1.182)}{=} \frac{H_0}{a} \frac{\partial}{\partial \ln a}\,, \tag{3.65}$$

where H_0 is is the Hubble Parameter at the time of the magnetogenesis scenario considered. Furthermore, from here on, every quantity with an index '0' is meant to be its corresponding value at magnetogenesis as well, in particular it is $a_0 \equiv a(t = t_0) = 1$, i.e. the scale factor is taken to be 1 at this initial epoch.

With this the Master Equations, from here on dropping the index 'c', i.e. all quantities are meant to be comoving unless noted otherwise, can be rewritten as

$$\left\langle \frac{\partial M_q}{\partial \ln a} \right\rangle = \frac{a}{H_0} \int \Big(... \Big) \mathrm{d}k\,, \tag{3.66}$$

$$\left\langle \frac{\partial U_q}{\partial \ln a} \right\rangle = \frac{a}{H_0} \int \Big(... \Big) \mathrm{d}k\,, \tag{3.67}$$

$$\left\langle \frac{\partial \mathcal{H}_q}{\partial \ln a} \right\rangle = \frac{a}{H_0} \int \Big(... \Big) \mathrm{d}k \,, \tag{3.68}$$

where the parenthesis (...) in (3.66)-(3.68) correspond to the parenthesis in (3.49)-(3.51) or (3.52)-(3.52).

The only quantity still to be identified is the time step Δt. The generic choice would be to set it to a constant value, however here, following methods known from molecular chaos, it is chosen to correspond to the eddy turnover time present since for a turbulent scenario it is the same as the correlation time. The two characteristic velocities of the setting are the effective fluid and Alfvén velocities which are given by (3.17) and (3.15), respectively. The value of Δt used in this work is

$$\Delta t \simeq \min \left[t_H, \frac{L}{v_L^{\mathrm{eff}}}, \frac{L}{v_{\mathrm{A}}^{\mathrm{eff}}(L)} \right] \simeq \min \left[\frac{a}{H_0}, \frac{2\pi}{k \left(2k \left\langle U_k \right\rangle\right)^{\frac{1}{2}}}, \frac{2\pi}{k \left(3/2k \left\langle M_k \right\rangle\right)^{\frac{1}{2}}} \right] , \tag{3.69}$$

where requirement of causality sets the constraint that Δt cannot be larger than t_H. This choice is rather general as it takes into account directly the fact that the eddy turnover time is different on different scales.

However, it is important to test to which extent the results presented below depend on the choice of Δt. This has been done by executing additional simulations. First, a rather basic possibility would be to set $\Delta t = a/H_0$, i.e. to make the rather rough assumption for the correlation time to have the maximally attainable value due to causality. This is still a reasonable assumption as it corresponds to the initial conditions given by (3.27) and also the results obtained by simulations with this different Δt are in agreement with the ones for (3.69).

Another reasonable possibility would be to find a time scale which would characterize the spectrum and therefore has the greatest impact on the time evolution. Since (as motivated in Sec. 3.1.3.1) it is $M_q \ll M_{\mathrm{I}}$ and $U_q \ll U_{\mathrm{I}}$ for both $q \ll k_{\mathrm{I}}$ and $q \gg k_{\mathrm{I}}$, for these values of q it turns out that L/v_L^{eff} and $L/v_{\mathrm{A}}^{\mathrm{eff}}(L)$ will be much bigger than t_H and thus it has to be reduced to a/H_0 due to causality. Therefore the generic choice would be to use $\Delta t \simeq \min\{a/H_0, 2\pi/[k_{\mathrm{I}} \left(2k_{\mathrm{I}} \left\langle U_{\mathrm{I}} \right\rangle\right)^{\frac{1}{2}}], 2\pi/[k_{\mathrm{I}} \left(3/2k \left\langle M_{\mathrm{I}} \right\rangle\right)^{\frac{1}{2}}]\}$ which also does not alter the results too much. In fact, as has been shown in Sec. 3.1.3.1, both for the helical and the non-helical case one has

$$\frac{2\pi}{k_{\mathrm{I}} \left(2k_{\mathrm{I}} \left\langle U_{\mathrm{I}} \right\rangle\right)^{\frac{1}{2}}} \propto \frac{2\pi}{k_{\mathrm{I}} \left(3/2k_{\mathrm{I}} \left\langle M_{\mathrm{I}} \right\rangle\right)^{\frac{1}{2}}} \begin{cases} \overset{(3.22),(3.23)}{\propto} \dfrac{1}{t^{-\frac{2}{\alpha+2}} \left(t^{-\frac{2}{\alpha+2}} t^{-2\frac{\alpha-1}{\alpha+2}} \right)^{\frac{1}{2}}} \propto t \,, \text{non-helical}, \\ \overset{(3.26),(3.24)}{\propto} \dfrac{1}{t^{-\frac{2}{3}} \left(t^{-\frac{2}{3}} t^{0} \right)^{\frac{1}{2}}} \propto t \,, \text{helical}, \end{cases} \tag{3.70}$$

which means, as for the comoving time scales t it is $t \propto a$ in the radiation-dominated regime, that this selection of Δt gives the same dependence on the scale factor, once again confirming the robustness of the results. Therefore, (3.69) indeed may be used in the following.

3.3 Time Evolution of of Primordial Magnetic Fields in the Early Universe

Using the tools developed in the last sections, it is now finally possible to describe the behavior of the spectral densities for the magnetic field energy and helicity as well as

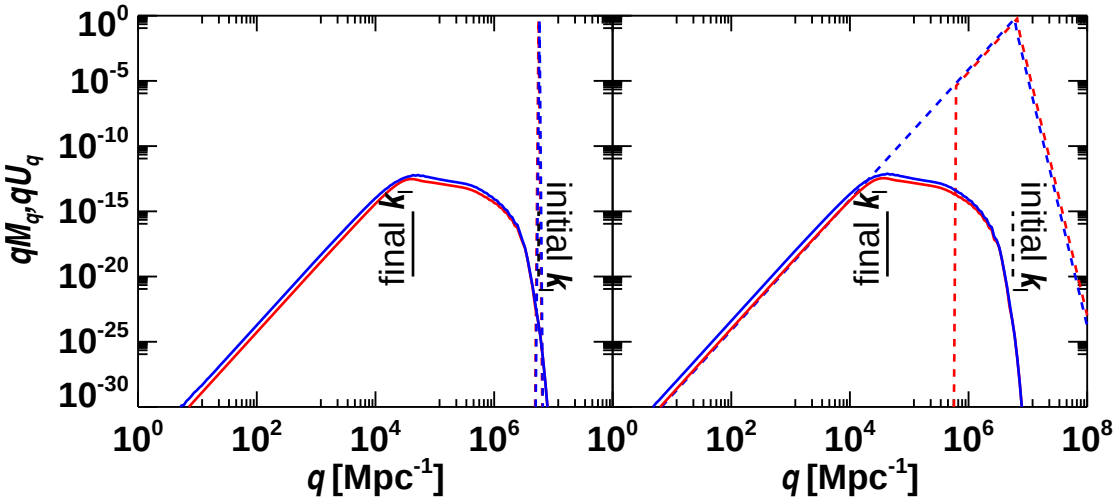

Figure 3.1: Time evolution of magnetic (red) and kinetic (blue) spectral energies according to (3.66) and (3.67), respectively. Dashed lines denote the initial conditions (i.e. at $a = 1$) while the solid lines represent the situation for $a = 10^8$, i.e. magnetogenesis at the QCDPT is assumed. *Left panel*: Starting at some time where both spectral energies were concentrated on the same scale (which, in [109], has been shown to be a reasonable assumption) they evolve close to equipartition, building up a $M_q \sim q^4$ slope *ab initio*. *Right panel*: Starting at some time when the turbulence has already built up a $M_q \sim q^4$ slope, after some time the magnetic spectral energy reaches equipartition with the same slope fairly well. It should be noted that for both cases the actual value for k_I from the simulation is in good agreement with the one predicted by (3.72), denoted by the vertical lines labeled "initial k_I" and "final k_I", respectively.

for the kinetic energy. To do so, in the following it is assumed that magnetogenesis took place during a phase transition as described in Sec. 2.1.2. Since the general procedures and conclusions for both the Electroweak and the QCD Phase Transitions are rather similar, the latter will be discussed in more detail, commenting, however, on the differences to the former as well.

The results presented in the following have been obtained by numerically solving the Master Equations in the form (3.52)-(3.54) together with the transformations from Sec. 3.2.3 with the semi-implicit Midpoint Rule [211].

3.3.1 Non-Helical Primordial Magnetic Fields

First, the case without helicity, i.e. $\mathcal{H}_q = 0 \,\forall\, q$, is discussed, based on [8]. Considering the arguments in Sec. 3.1, one has to keep in mind that in general both the magnetic and the kinetic spectral energy density follow a power law with respect to the wavenumber (i.e. inverse scale) q, namely

$$\langle E_q \rangle \simeq E_0 \left(\frac{q}{k_0} \right)^{\alpha - 1} , \tag{3.71}$$

with $\alpha > 1$ for $q < k_\mathrm{I}$ and $\alpha < 1$ for $q > k_\mathrm{I}$, where k_I is the integral scale, i.e. the scale which most of the energy is concentrated on. E here and later on stands for either M or U, while E_0 (i.e. M_0 or U_0) is the normalization factor given by the corresponding initial value at k_0, where k_0 is the initial value of k_I at magnetogenesis.

The goal now is to find the behavior of the magnetic (and kinetic) spectral energy densities for small $q < k_0$ as this would correspond to large scales and therefore EGMF. It has been shown with general considerations in Sec. 3.1 that the integral scale follows

$$k_\mathrm{I} \simeq k_0 a^{-\frac{2}{\alpha+2}} , \tag{3.72}$$

where k_0 is determined by [197]

$$k_0 \simeq \frac{2\pi H_0}{v_0} = \left(\frac{2\pi^2 H_0^2}{U_0}\right)^{\frac{1}{3}} \tag{3.73}$$

and the time dependence of E_I (the value of E at k_I, i.e. $E_\mathrm{I} \equiv E_{k_\mathrm{I}}$) is given by

$$E_\mathrm{I} \simeq E_0 a^{-2\frac{\alpha-1}{\alpha+2}} \tag{3.74}$$

for the value of the corresponding spectral energy at k_I. Here, for initial equipartition with $v_0 \simeq 1$, it has been assumed that $E_0 = M_0 = U_0 = (2k_0)^{-1}$.

Now, using the Master Equations, it is possible for the first time to verify these predictions by a full semi-analytical calculation and, furthermore, to derive a definite value for α. As can be seen from Fig. 3.1, both spectral energy densities and the integral scale follow the relation predicted by (3.74) and (3.72), respectively, very well.

Furthermore, the figure shows that for small q it is $\alpha = 5$. This can also be derived analytically from (3.52) and (3.53): For large scales, i.e. $q \ll k_\mathrm{I} \simeq k$, one can assume $\langle U_q \rangle \ll \langle U_k \rangle$ and $\langle M_q \rangle \ll \langle M_k \rangle$ and therefore neglect the terms containing $\langle M_q \rangle$ and $\langle U_q \rangle$ in (3.52) and (3.53), leaving the $\langle M_k \rangle \langle U_{k_1} \rangle$ term in the former and both the $\langle M_k \rangle \langle M_{k_1} \rangle$ and $\langle U_k \rangle \langle U_{k_1} \rangle$ terms in the latter one.

From (3.71) it is known that $\langle M_k \rangle \sim k^{\alpha_1 - 1}$ and $\langle U_k \rangle \sim k^{\alpha_2 - 1}$, where in general one has to consider the possibility that $\alpha_1 \neq \alpha_2$, i.e. that the small scale slope for the magnetic and the kinetic spectral energies might be different. Using this it is possible to calculate the remaining k_1-integrals of (3.52) and (3.53) which, after a Taylor Expansion, give

$$\left\langle \frac{\partial M_q}{\partial \ln a} \right\rangle \simeq q^4 \frac{a}{H_0} \int \frac{\Delta t}{k^2} \left[\frac{2}{3} \langle M_k \rangle \langle U_k \rangle + \mathcal{O}\left(\left(\frac{q}{k} \right)^2 \right) \right] \mathrm{d}k \tag{3.75}$$

and

$$\left\langle \frac{\partial U_q}{\partial \ln a} \right\rangle \simeq q^4 \frac{a}{H_0} \int \mathrm{d}k \frac{\Delta t}{k^2} \left[\langle U_k \rangle \langle U_k \rangle - \frac{\alpha_2 - 4}{3} \langle M_k \rangle \langle M_k \rangle + \mathcal{O}\left(\left(\frac{q}{k} \right)^2 \right) \right], \tag{3.76}$$

where one can see that for both q^4 is the leading order term in q. Therefore for $q \ll k_\mathrm{I}$ both the magnetic and the kinetic spectral energies have a steep spectrum which is proportional to q^4 or L^{-4}, i.e. $\alpha = \alpha_1 = \alpha_2 = 5$ (where L is the considered scale) which, following (3.15), corresponds to a scaling of the form $B \sim L^{-\frac{5}{2}}$ and $v \sim L^{-\frac{5}{2}}$ for the scale dependence of the magnetic and the turbulence fields on large scales, respectively. This would be in good agreement with the results in [198, 205, 206] as mentioned before. For the turbulent field this is a crucial statement, confirmed by simulation: Independent of the initial conditions, even starting off with the total energy being concentrated on only one scale, a q^4 slope for the spectral energies forms, $\alpha = 5$ being an universal power law exponent for MHD turbulence. This is demonstrated in Fig. 3.1.

However, even more information of similar importance may be extracted from the large scale version of the Master Equations, (3.75) and (3.76). Since it has been found that $\alpha = \alpha_1 = \alpha_2 = 5$, (3.76) may be rewritten as

$$\left\langle \frac{\partial U_q}{\partial \ln a} \right\rangle \simeq q^4 \frac{a}{H_0} \int \mathrm{d}k \frac{\Delta t}{k^2} \left[\langle U_k \rangle \langle U_k \rangle - \frac{1}{3} \langle M_k \rangle \langle M_k \rangle + \mathcal{O}\left(\left(\frac{q}{k} \right)^2 \right) \right] \tag{3.77}$$

which, with the above assumption of initial equipartition, i.e. $M_k \simeq U_k \simeq E_k$, has exactly the same form as (3.75), such that (3.75) and (3.76) can be approximated by one equation, namely

$$\left\langle \frac{\partial E_q}{\partial \ln a} \right\rangle \simeq q^4 \frac{a}{H_0} \int \mathrm{d}k \left(\frac{2\Delta t}{3k^2} \left\langle E_k \right\rangle \left\langle E_k \right\rangle \right) . \tag{3.78}$$

This, therefore, gives the crucial result that, assuming initial equipartition between the turbulent kinetic and magnetic energies (which, as has been shown in Sec. 3.1.3.1, is reasonable), this equipartition is also kept up in later times. This has been also confirmed by simulation as again may be seen in Fig. 3.1.

If, however, the initial conditions are not given by equipartition at large scales, but rather by a setting where the kinetic spectral energy has already built up a slope while the magnetic spectral energy did not, as shown in the right panel of Fig. 3.1, the question arises whether the latter can catch up with the former fast enough such that the argumentation is still valid. The limiting case to be discussed is given, on the one hand, by setting $\Delta t \simeq a/H_0$ at $a \gtrsim 1$ for Δt as causality condition, and, on the other hand, by a narrowly peaked shape for both M_k and U_k around k_0, for example

$$\langle M_k \rangle = \langle U_k \rangle \equiv \langle E_k \rangle = \begin{cases} E_0 \left(\frac{k}{k_0} \right)^{\gamma - 1} , \ k \leq k_0 \, , \\ E_0 \left(\frac{k}{k_0} \right)^{-(\gamma - 1)} , \ k > k_0 \, , \end{cases} \tag{3.79}$$

where the exponent $\gamma > 5$ is a measure for the width of the peak. Thus, (3.75) can be rewritten as

$$\left\langle \frac{\partial M_q}{\partial \ln a} \right\rangle = \left\langle \frac{\partial M_q}{\partial a} \right\rangle \frac{\partial a}{\partial \ln a} = a \left\langle \frac{\partial M_q}{\partial a} \right\rangle \overset{(3.78)}{\simeq} \frac{2}{3} \frac{q^4 a^2}{H_0^2} \int \frac{\mathrm{d}k}{k^2} \left\langle E_k \right\rangle^2 \overset{(3.79)}{\simeq} \frac{2}{3} \frac{a^2}{H_0^2} \frac{q^4 E_0^2}{(\gamma - 1) k_0} . \tag{3.80}$$

Integrating this equation up to the q^4 slope for $\left\langle \frac{\partial M_q}{\partial \ln a} \right\rangle$, i.e. $M_q \simeq E_0 \, (q/k_0)^4$, and up to the corresponding scale factor a_{LS} over a, i.e.

$$\int_0^{E_0 \left(\frac{q}{k_0} \right)^4} \mathrm{d} \left\langle M_q \right\rangle \simeq \frac{2}{3} \frac{1}{H_0^2} \frac{q^4 E_0^2}{(\gamma - 1) k_0} \int_1^{a_{LS}} a \mathrm{d}a \, , \tag{3.81}$$

it can be solved for a_{LS}, giving

$$a_{\mathrm{LS}} \lesssim \left[3 \frac{H_0^2}{k_0^3 E_0} (\gamma - 1) + 1 \right]^{\frac{1}{2}} \simeq \left[\frac{3}{2\pi^2} (\gamma - 1) + 1 \right]^{\frac{1}{2}} , \tag{3.82}$$

where the values introduced above, namely $E_0 = (2k_0)^{-1}$ and $H_0 = k_0/(2\pi)$, have been used. For a relative full width at half maximum of $\Delta_{\frac{1}{2}}/k_0 = 1/100$ one has $\gamma \simeq 15$, such that $a_{\mathrm{LS}} \lesssim 5$. This means that a Batchelor slope is indeed built up rather fast which, once again, confirms that the assumption of equipartition for non-helical fields is indeed well-motivated.

Finally, in order to relate the considerations of this section to actual observations, in particular to the constraints of Sec. 2.2.1, one has to calculate the correlation length and the magnetic field strength at present day resulting from the time evolution of Primordial Magnetic Fields. For the former this can be done by identifying it with the integral scale L_{I}, while for the latter the effective magnetic field strength, given by (3.15), i.e.

$$M_q = \frac{B^2(L)}{8\pi q \rho} \, , \tag{3.83}$$

is used. With (3.72)-(3.74) this results in [8]

$$B(L) = (8\pi q \rho M_q)^{\frac{1}{2}} = B_0 \, (2qM_q)^{\frac{1}{2}} \simeq B_0 \, (H_0 L)^{-\frac{\alpha}{2}} \ . \tag{3.84}$$

In order to derive an upper limit on B, the initial magnetic field strength, $B_0 = (4\pi\rho)^{\frac{1}{2}}$, as mentioned above, is set to have the same energy density as the CMB, i.e. $\rho = T^4/(120\pi) \simeq 2.6 \times 10^5 \, \mathrm{eV/m^3}$ and therefore $B_0 \simeq 3 \times 10^{-6} \, \mathrm{G}$. With (3.72) and (3.74) one therefore gets

$$B_\mathrm{I} \equiv B(L_\mathrm{I}) = B_0 \, (2k_\mathrm{I} M_\mathrm{I})^{\frac{1}{2}} = B_0 a^{-\frac{\alpha}{\alpha+2}} \, . \tag{3.85}$$

For the scenario discussed here, namely magnetogenesis at QCDPT, it is $a \simeq 10^8$, such that for the former it is $L_\mathrm{I} \simeq 200 \, \mathrm{pc}$ and hence $B(200\mathrm{pc}) \lesssim 5 \times 10^{-12} \, \mathrm{G}$. Unless the magnetic field possesses a significant helical component (s. below), (3.85) can be regarded as the generic upper limit for magnetic fields of cosmological origin.

3.3.2 Helical Primordial Magnetic Fields

As has been discussed in Sec. 1.1.2, magnetic helicity is an important quantity in magnetohydrodynamics and therefore it is important to include it into the discussion of Primordial Magnetic Fields. However, the origin of helicity is still not known. Since $\mathfrak{H}$ is odd in the P and CP symmetries, its generation has to involve a process which violates both of them. Therefore, the epochs in the Early Universe considered to be the most interesting ones in this context are Lepto- and Baryogenesis [212–215]. Although differing in the details, the common idea of these publications is that at some early stage non-Abelian fields obtain a non-vanishing Chern-Simons Number, the non-Abelian equivalent of helicity, which changes due to creation and dissipation of non-perturbative field configurations like, for example, sphalerons. After symmetry breaking it is then possible for the Chern-Simons Number, at least partially, to be converted to actual magnetic helicity.

It has been first found out by [216, 217] that magnetic helicity plays a major role in the evolution of magnetic fields, especially due to the so-called Inverse Cascade, i.e. the transport of energy from small to large scales in a turbulent setting due to non-linear terms which cause interactions between different length scales. Since it might be important for generation of EGMF on large scales today, the investigation of the effect of helicity onto Primordial Magnetic Fields has been an important approach in the recent years (see, for example, [190–192, 194, 200, 212]). In the following it will be shown that using the Master Equations an Inverse Cascade may be seen as well, thus confirming previous results, from which additional conclusions about present day EGMF can be drawn.

Therefore, after considering the case where no magnetic helicity is present, now, based on the findings from [9], a non-vanishing helical component is included into the calculation, limited by the condition (1.101), i.e. $|\mathcal{H}_k| \leq 8\pi M_k/k$ and, in particular, for the integral scale, $|\mathcal{H}_\mathrm{I}| \leq 8\pi M_\mathrm{I}/k_\mathrm{I}$. In order to determine the actual value of the spectral helicity density, the factor f is introduced, defined through the relation

$$\mathcal{H}_\mathrm{I} = f \frac{8\pi}{k_\mathrm{I}} M_\mathrm{I} \, , \tag{3.86}$$

which is especially useful to define the initial condition in the form

$$\mathcal{H}_0 = f_0 \frac{8\pi}{k_0} M_0 \, , \tag{3.87}$$

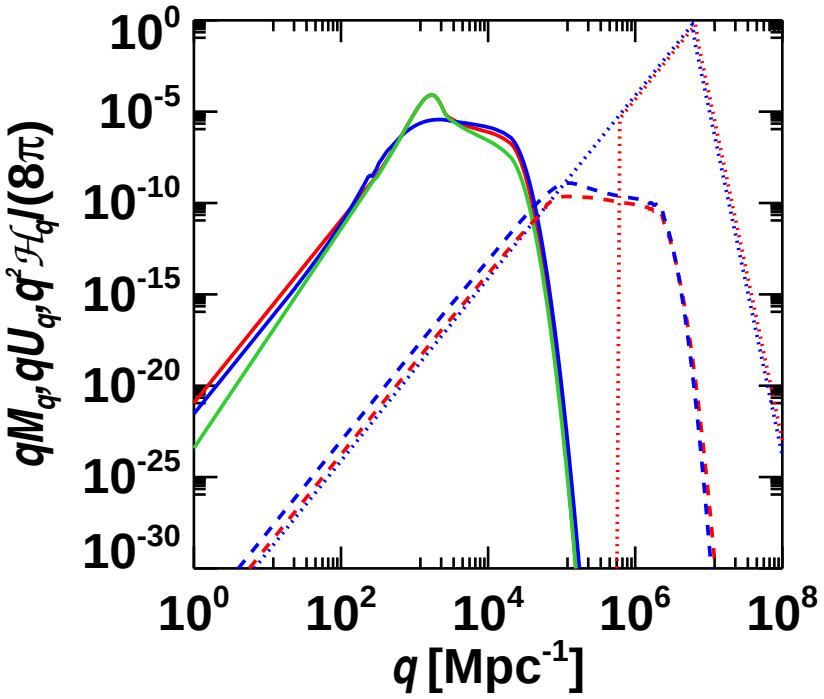

Figure 3.2: Time evolution of magnetic (red) and kinetic (blue) spectral energies as well as of the spectral magnetic helicity (green). Dotted lines denote the initial conditions (i.e. at $a = 1$) while for later times, namely $a = 10^6$, the dashed lines represent the situation for non-helical and the solid lines for the maximal helical case.

where again $k_0 \equiv k_\mathrm{I}(a = a_0)$ is the integral scale at magnetogenesis (hence the index '0') and $M_0 \equiv M_\mathrm{I}(a = a_0)$ as well as $\mathcal{H}_0 \equiv \mathcal{H}_\mathrm{I}(a = a_0)$ are the corresponding values of M_I and $\mathcal{H}_\mathrm{I}$, respectively. Therefore $f_0 = 0$ would represent the non-helical case while $f_0 = 1$ is the maximum helical one.

As can be seen qualitatively from Fig. 3.2, the time evolution for the integral scale as well as for the spectral energy densities changes dramatically once helicity is included. While the slope for small q still corresponds to an exponent $\alpha = 5$, the integral scale as well as M_I, U_I (and $\mathcal{H}_\mathrm{I}$) have a rather different behavior.

This is demonstrated in Fig. 3.3: Here one can see that helicity only has an influence on the magnetic and kinetic spectral energies if at the integral scale it has a value which is close to the maximal spectral helicity value $\mathcal{H}_{\mathrm{I,max}}$ given by (3.86). If, however, spectral helicity is small, M_I and k_I evolve as it has been calculated in the previous section, namely $k_\mathrm{I} \propto a^{-\frac{2}{\alpha+2}}$ and $M_\mathrm{I} \propto a^{-2\frac{\alpha-1}{\alpha+2}}$. Due to helicity conservation, as can be seen from (3.24), it is $\mathcal{H}_\mathrm{I} \propto k_\mathrm{I}^{-1} \propto a^{\frac{2}{\alpha+2}}$, such that the generic ratio between spectral helicity and spectral energy changes over time, in particular it is

$$\frac{\mathcal{H}_\mathrm{I}}{8\pi M_\mathrm{I}/k_\mathrm{I}} \propto \frac{a^{\frac{2}{\alpha+2}}}{a^{-2\frac{\alpha-1}{\alpha+2}}/a^{-\frac{2}{\alpha+2}}} \propto a^{2\frac{\alpha-1}{\alpha+2}} \propto a^{\frac{8}{7}}\,, \tag{3.88}$$

which means that it increases until the integral value of spectral helicity has reached its maximal value. Therefore, two different regimes of time evolution for helical magnetic fields can be distinguished – on the one hand prior the maximal helicity configuration and on the other hand once this configuration has been reached.

For the former regime, labeled as '1' in the following, basically the arguments from the previous section considering the non-helical case are valid such that for some initial

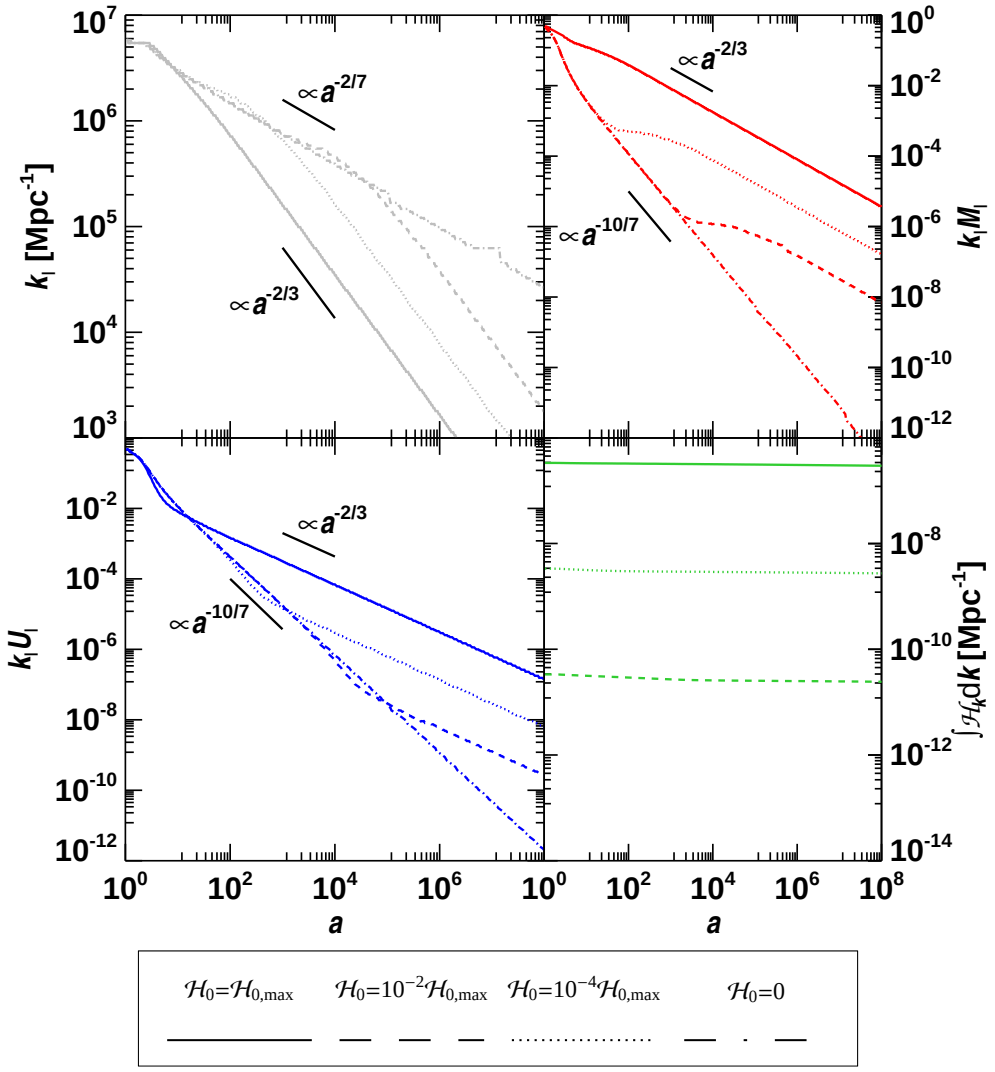

Figure 3.3: Time evolution of the integral scale (*upper left*) and the values at the integral scale of the magnetic spectral energy (*upper right*), the kinetic spectral energy (*lower left*), and the total normalized magnetic helicity density $h_B/\rho = \int \mathcal{H}_k \mathrm{d}k$ (*lower right*) for different values of the initial spectral helicity in fractions of its maximal value $\mathcal{H}_{0,\max} \equiv 8\pi M_0/k_0$. Here it is assumed that magnetogenesis took place at the QCD Phase Transition.

conditions at $a = a_0 \equiv 1$,

$$k_{\rm I} M_{\rm I} = k_0 M_0 \,, \; k_{\rm I} U_{\rm I} = k_0 U_0 \,, \; \frac{k_{\rm I}^2 \mathcal{H}_{\rm I}}{8\pi} = \frac{k_0^2 \mathcal{H}_0}{8\pi} = f_0 k_0 M_0 \,, \tag{3.89}$$

the time evolution may be described by

$$k_{\rm I} = k_0 a^{-\kappa_1} \,, \; k_{\rm I} M_{\rm I} = k_0 M_0 a^{-\mu_1} \,, \; \mathcal{H} = f_0 M_0 a^{\chi_1} \,, \tag{3.90}$$

where $\kappa_1 = 2/(\alpha+2) = 2/7$, $\mu_1 = 2\alpha/(\alpha+2) = 10/7$ and $\chi_1 = 2/(\alpha+1) = 2/7$ if one uses $\alpha = 5$ as derived above. This, in fact is well confirmed by simulations using the Master Equations since, for the QCD magnetogenesis scenario, one obtains $\kappa_1 \simeq 0.30$, $\mu_1 \simeq 1.4$ and $\chi_1 \simeq 0.30$ as can be seen in Fig. 3.3.

The regime denoted by the index '2', which commences once the system has reached maximal helicity, can be seen as the limiting case of regime 1 for which the condition

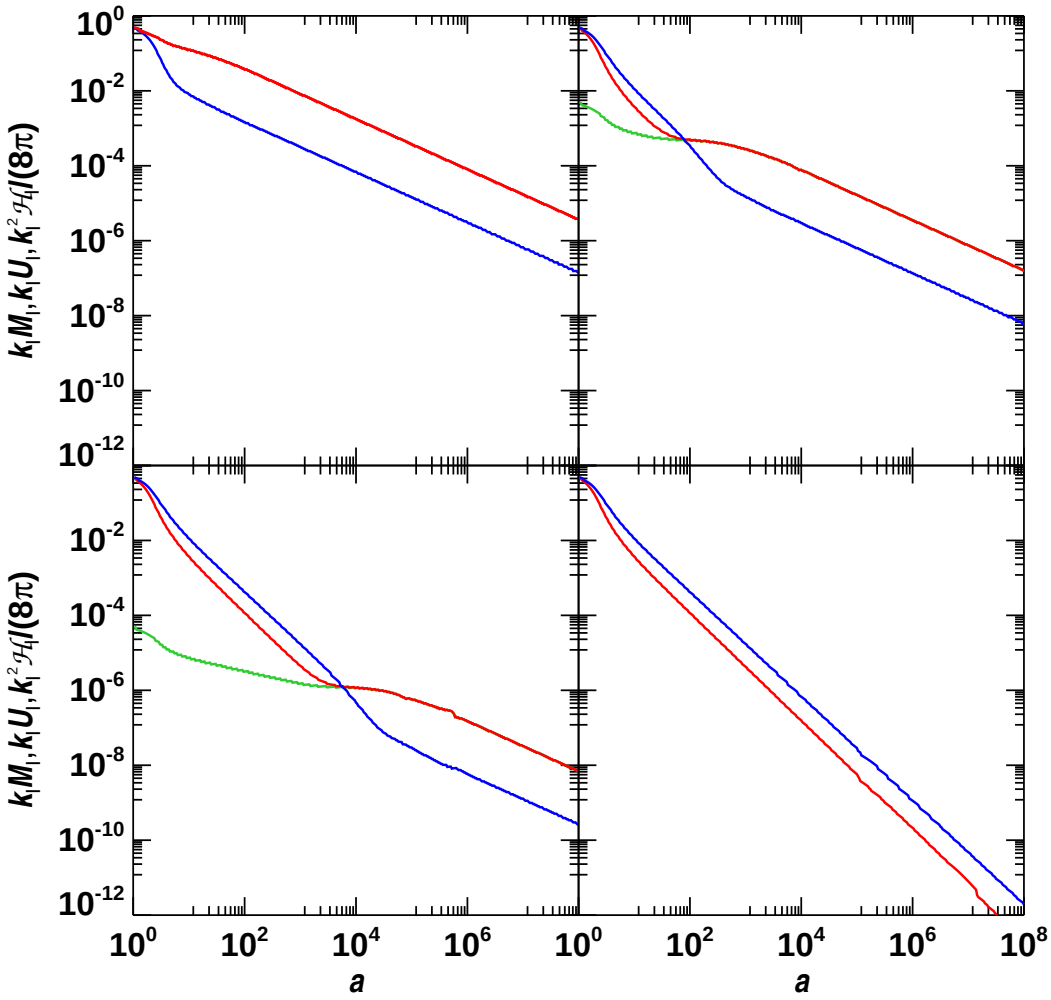

Figure 3.4: Time evolution of the values of the magnetic and kinetic spectral energies and the helical spectral density at the integral scale, i.e. $M_{\rm I}$ (red), $U_{\rm I}$ (blue) and $\mathcal{H}_{\rm I}$ (green), respectively. For convenience these quantities have been multiplied by $k_{\rm I}$ (for $M_{\rm I}$ and $U_{\rm I}$) and by $k_{\rm I}^2/(8\pi)$ (for $\mathcal{H}_{\rm I}$). The panels show the situation for different initial values of the helicity $\mathcal{H}_0$: maximal helicity, i.e. $\mathcal{H}_0 = \mathcal{H}_{0,\rm max}$ (*upper left*), $\mathcal{H}_0 = 10^{-2}\mathcal{H}_{0,\rm max}$ (*upper right*), $\mathcal{H}_0 = 10^{-4}\mathcal{H}_{0,\rm max}$ (*lower left*) and no helicity, i.e. $\mathcal{H}_0 = 0$ (*lower right*). Note that for the case of maximal helicity $k_{\rm I}^2\mathcal{H}_{\rm I}/(8\pi)$ has approximately the same value as $k_{\rm I}M_{\rm I}$ and is therefore not visible in the plot. Here it is assumed that magnetogenesis took place at the QCD Phase Transition.

(3.86) is fulfilled such that no processing as in (3.88) can take place anymore. The time evolution of the relevant quantities is now given by

$$k_{\rm I} = k_0 a^{-\kappa_2}\,,\; k_{\rm I}M_{\rm I} = k_0 M_0 a^{-\mu_2}\,,\; \mathcal{H} = f_0 M_0 a^{\chi_2}\,, \tag{3.91}$$

where, as helicity conservation is now the crucial condition, from the considerations in Sec. 3.1.3.1 and the transformation rules (3.1) it follows that $\kappa_2 = 2/3$, $\mu_2 = 2/3$ and $\chi_2 = 2/3$, to be compared to the values found numerically, $\kappa_2 \simeq 0.66$, $\mu_2 \simeq 0.67$ and $\chi_2 \simeq 0.66$ which again show excellent agreement.

The remaining question is how small the initial helicity can be in order to still play a relevant role for the time evolution of Primordial Magnetic Fields. This can be estimated by calculating the time at which the transition from regime 1 to regime 2 takes place and then check whether this happens before Recombination. If this is the case, helicity, at least for a small time window, might govern the time evolution. This check can be

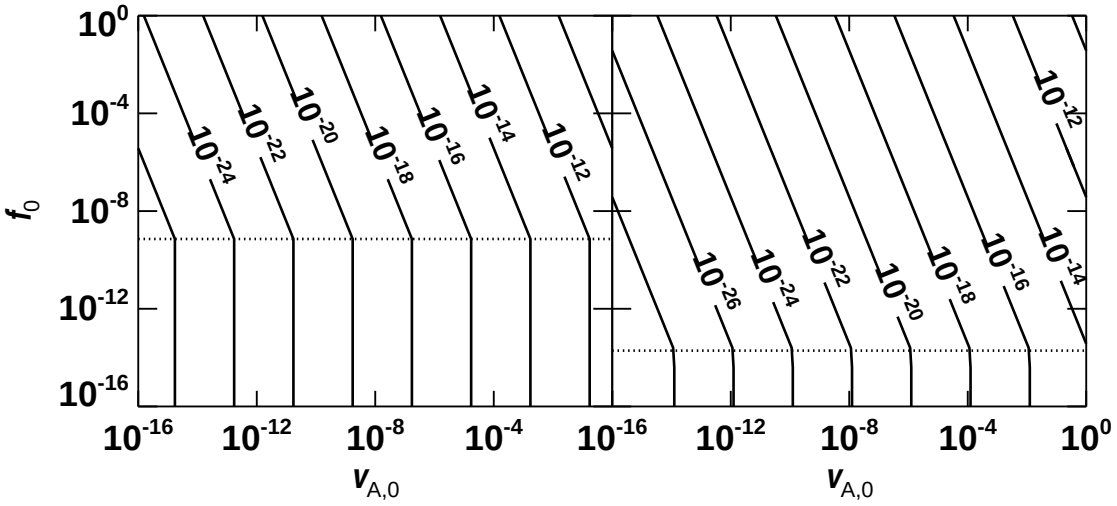

Figure 3.5: Present day magnetic field strength having survived dissipation during the evolution in the Early Universe, according to (3.98) as a function of initial Alfvén velocity $v_{\rm A,0}$ and helicity $\mathcal{H}_0 = f_0\mathcal{H}_{0,\rm max}$ for magnetogenesis occurring during the QCD Phase Transition (*left panel*) and the Electroweak Phase Transition (*right panel*), respectively, the numbers inside the figure giving the magnetic field strength in Gauss. Here all initial conditions above the dotted line lead to a maximally helical present day field. Note that $\epsilon_B \simeq \rho v_{\rm A}^2/2$. It is stressed that the magnetic field has to fulfill $v_{\rm A}/L \simeq H$ at the magnetogenesis epoch. For different initial conditions, the modified $v_{\rm A,0}$ and f_0 to be used in the figure may be deduced from (3.99).

done by solving the equation $k_{\rm I}M_{\rm I} = k_{\rm I}^2\mathcal{H}_{\rm I}/(8\pi)$, i.e., with (3.89), (3.90) and (3.91),

$$k_0 M_0 a^{-\mu_1} = f_0 k_0 M_0 a^{-\chi_1}\,, \tag{3.92}$$

for $a = a_{\rm tr}$, the scale factor corresponding to the transition, which gives

$$a_{\rm tr} = f_0^{-\frac{1}{\mu_1-\chi_1}} = f_0^{-\frac{1}{2}\frac{\alpha+2}{\alpha-1}} = f_0^{-\frac{7}{8}}\,. \tag{3.93}$$

Setting $a_{\rm tr} = a_{\rm Rec}$ therefore gives the minimal value $f_{0,\rm min}$ such that helicity plays a role in the overall time evolution,

$$f_{0,\rm min} \simeq a_{\rm Rec}^{\chi_1-\mu_1} = a_{\rm Rec}^{-2\frac{\alpha-1}{\alpha+2}} = a_{\rm Rec}^{-\frac{8}{7}}\,, \tag{3.94}$$

which is $f_{0,\rm min} \simeq 7\times10^{-10}$ for $a_{\rm Rec} \simeq 10^8$, i.e. the QCDPT scenario, and $f_{0,\rm min} \simeq 2\times10^{-14}$ for $a_{\rm Rec} \simeq 10^{12}$, i.e. the EWPT scenario. This shows that even if the initial helicity is several orders of magnitude smaller than its maximal value for a sufficient amount of time, it still may play a major role.

In fact, with the simulations based on the Master Equations it was possible to confirm the predictions that the time evolution is given by

$$k_{\rm I}(a) \simeq \begin{cases} k_0 a^{-\kappa_1},\ a \le a_{\rm tr}\,, \\ k_0 a_{tr}^{\kappa_2-\kappa_1} a^{-\kappa_2},\ a > a_{\rm tr} \end{cases} \tag{3.95}$$

with $\kappa_1 = 2/(\alpha+2)$ and $\kappa_2 = 2/3$ and

$$k_{\rm I}M_{\rm I}(a) \simeq \begin{cases} k_0 M_0 a^{-\mu_1},\ a \le a_{\rm tr}\,, \\ k_0 M_0 a_{tr}^{\mu_2-\mu_1} a^{-\mu_2},\ a > a_{\rm tr} \end{cases} \tag{3.96}$$

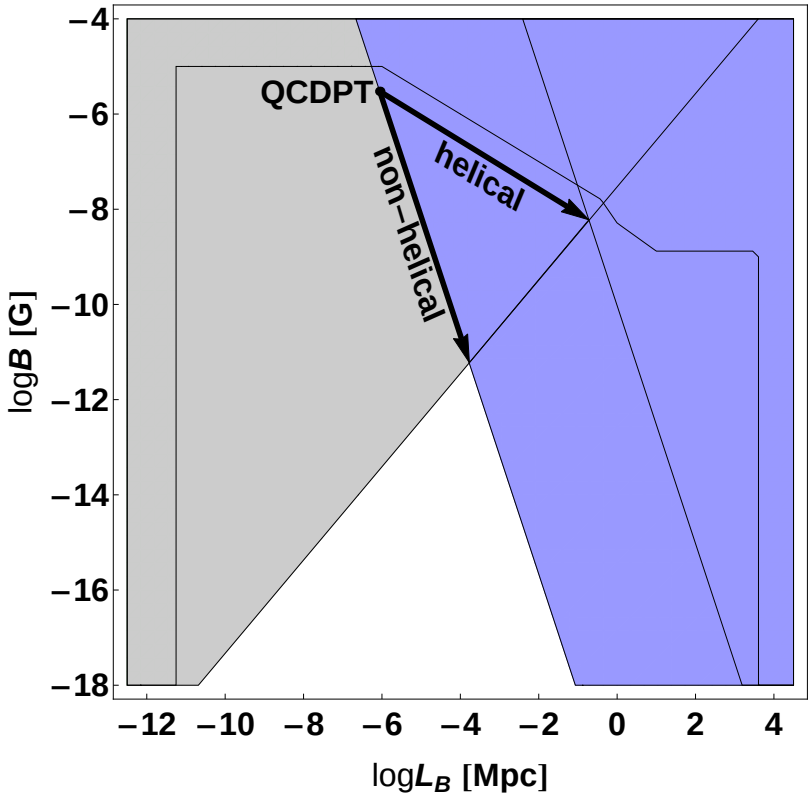

Figure 3.6: Constraints on EGMF due to time evolution of Primordial Magnetic Fields. The point labeled "QCDPT" denotes the initial configuration of magnetogenesis during the QCD Phase Transition while the arrows show their time evolution with maximal and with zero initial helicity. For comparison, constraints from Sec. 2.2.1 are shown as well.

with $\mu_1 = 2\alpha/(\alpha+2)$ and $\mu_2 = 2/3$. These results are also presented in Figs. 3.3 and 3.4.

This indeed shows that an Inverse Cascade is operating as will be derived in the following. For both regimes the dependence of $k_\mathrm{I} M_\mathrm{I}$, the quantity which basically describes the energy content, on k_I can be deduced from either (3.90) or (3.91), giving

$$k_\mathrm{I} M_\mathrm{I} = k_0 M_0 \left(\frac{k_\mathrm{I}}{k_0}\right)^{\frac{\mu_i}{\kappa_i}} . \tag{3.97}$$

For regime 1, i.e. $i = 1$ in this equation, it is $\mu_1/\kappa_1 = \alpha$, such that the spectral energy indeed decays "along" the generic slope, while for $i = 2$ one gets $\mu_2/\kappa_2 = 1 < \alpha$. This means that an Inverse Cascade is present which here could be confirmed for the first time directly from a full scale semi-analytic study. This therefore strengthens former findings that in order to explain the origin of EGMF from Primordial Magnetic Fields, one has to assume a non-negligible amount of magnetic helicity in the beginning.

Using again (3.84), one may then finally estimate the magnitude of the present day magnetic field depending on its initial value and the helicity,

$$\frac{B_\mathrm{today}}{3\times10^{-6}\mathrm{Gauss}} \simeq \begin{cases} v_{A,0} a_\mathrm{Rec}^{-5/7}, & f_0 \leq a_\mathrm{Rec}^{-8/7}, \\ v_{A,0} f_0^{1/3} a_\mathrm{Rec}^{-1/3}, & f_0 > a_\mathrm{Rec}^{-8/7}, \end{cases} \tag{3.98}$$

where $v_{A,0}$ is the initial Alfvén velocity at magnetogenesis, i.e., $v_{\mathrm{A},0}^2 \simeq 2\epsilon_B/\rho$, and $\alpha = 5$ has been assumed. For the upper limit of initial equipartition between the magnetic field

and CMB energy densities one has to set $v_{\mathrm{A},0} = 1$. One can see that, compared to the non-helical case, the present day value of the magnetic field is enhanced by a factor of $a_{\mathrm{Rec}}^{8/21} f_0^{1/3}$ which translates to $2.7 \times 10^3 f_0^{1/3}$ and $3.7 \times 10^4 f_0^{1/3}$ for magnetogenesis during the QCD and Electroweak Phase Transition, respectively, and therefore, for maximal helicity, i.e. $f_0 = 1$, 2.7×10^3 and 3.7×10^4. This is also visualized in Fig. 3.5 where the prediction of field strength is given depending on the initial conditions. As discussed above, the latter are assumed to be given by $v_{\mathrm{A}}/L \simeq H_0$ which, in case that this is not true, has to be altered to [9]

$$
\begin{aligned}
v_{\mathrm{A},0} &\simeq v_{\mathrm{A}}^{\mathrm{ini}} L_{\mathrm{ini}}^{\frac{\alpha}{\alpha+2}} \left(\frac{v_{\mathrm{A}}^{\mathrm{ini}}}{H} \right)^{-\frac{\alpha}{\alpha+2}} , \\
f_0 &\simeq f_{\mathrm{ini}} L_{\mathrm{ini}}^{2\frac{\alpha-1}{\alpha+2}} \left(\frac{v_{\mathrm{A}}^{\mathrm{ini}}}{H} \right)^{-2\frac{\alpha-1}{\alpha+2}} ,
\end{aligned}
\tag{3.99}
$$

unless $f_0 > 1$ or $v_{\mathrm{A},0} > v_{\mathrm{A}}^{\mathrm{ini}}$. Here $v_{\mathrm{A}}^{\mathrm{ini}}$, L_{ini}, and f_{ini} quantify the initial total magnetic field strength, coherence length and helicity.

Furthermore, in addition to the results from Sec. 2.2, additional limits on the main parameters of EGMF, i.e. the field strength and the correlation length, may be derived from the discussion presented above. These additional constraints are shown in Fig. 3.6 where, as the limiting case, magnetic fields from QCDTP are drawn in the two extreme cases of maximal and zero magnetic helicity. The additional constraints are given, on the one hand, by extrapolating the connecting line between end points of the two possible limiting cases (which is consistent with other scenarios of magnetogenesis as well) and, on the other hand, by scaling down the magnetic field strength with the correlation length as $B \sim L^{-\frac{5}{2}}$ according to the derivation above.

Chapter 4

Conclusions and Outlook

[S]tultorum [eventus] magister [est]
— T. Livius, *Ab urbe conditia XXII*

The current knowledge about Extragalactic Magnetic Fields (EGMF) is rather limited: Little is known about both their origin and structure which is mainly due to their small strength – "close by" they are overlaid by terrestrial, solar and galactic magnetic fields which are stronger by many orders of magnitude. Apart from that, even in the intergalactic voids, where magnetic fields may be assumed to exist in their generic form, their detection can only be performed indirectly via the analysis of features of particles they have been transversed by, which, however, is rather difficult as well, such that high sensitivity observations are required. Here, recently found lower limits on their field strength are reanalyzed in light of new results, before proceeding to the main topic of this work, namely the time evolution of Primordial Magnetic Fields which might be responsible for the EGMF.

The aforementioned lower limits on the magnetic field strength are derived from the suppression of gamma ray spectra of blazars in the GeV energy range. In fact, until now it has been related to the interaction of primary TeV photons from blazars with the Extragalactic Background Light, thus developing an electromagnetic cascade, the charged low energy component of which is deflected away from the line of sight due to the Lorentz Force. This kind of analysis, however, usually neglects any kind of interactions of the cascade with the Intergalactic Medium which recently have been claimed to be non-negligible, though, as the propagating electrons and positrons might induce plasma instabilities which, in turn, cause a rapid energy loss of the pairs such that they cannot contribute to the cascade evolution anymore.

Adopting these assumptions it has been possible in the present work to implement their effects in a Monte Carlo simulation of electromagnetic cascades for the case of the BL Lac 1ES 0229+200. By doing so it was possible for the first time to show *explicitly*, by calculating the corresponding expected spectra, that the aforementioned suppression might indeed be explained by fluid interactions, thus, if true, questioning the existence of the lower limits described above, however not necessarily making them completely invalid.

Still, much work has to be done in order to be able to draw final and fully consistent conclusions. First, on a rather basic, statistical level, the same analysis as has been presented before has to be applied to other relevant objects. Comparing the resulting simulations to actual observations would show whether the results derived for 1ES 0229+200 are confirmed and therefore turn out to be statistically significant overall. This, however, may still take time to accomplish as present day instruments lack the

statistics and are limited by the available technology, such that both have to be further improved in order to deliver sufficient observational results.

Furthermore, the underlying theory of plasma instability development due to propagation of ultrarelativistic particles through the Intergalactic Medium has been only derived analytically so far, this derivation being subject to criticism concerning in particular its applicability to the given astrophysical setting. For example, being performed for an unmagnetized plasma, the argumentation might break down once a magnetic field of sufficient strength is present. Deriving a limit on this field strength and comparing it to the various predictions is therefore necessary in order to have a full and consistent description.

The main focus of this thesis is laid on the analysis of the time evolution of Primordial Magnetic Fields. These are fields which are assumed to have been created in the framework of the so-called Cosmological Scenario, i.e. globally during a phase transition in the Early Universe. Apart from the fact that how this magnetogenesis took place exactly still remains a mystery, also the analysis of the time evolution of the resulting fields remains non-trivial up to the present day.

The author of the present work was able to shed light on this topic by assuming turbulence for which the correlators of both the magnetic and kinetic fields have been calculated. This, in turn, has been used to derive the corresponding power spectra as well as Master Equations which directly describe their time evolution. Here this has been done for the first time in a rather general way, especially by explicitly including the backreaction of the velocity fields onto the magnetic ones which has been neglected or only approximated in previous studies. These Master Equations are a set of differential equations which have to be solved numerically due to the presence of different non-linear terms.

The main results of this thorough semi-analytical calculation are the following: First, it was possible to derive that on large scales the magnetic fields behave as $B \sim L^{-\frac{5}{2}}$ with the actual length scale L. The exponent $-5/2$, which corresponds to a violet noise or Batchelor spectrum, turns out to be a universal factor which is fairly independent of the initial conditions and therefore also of the particular magnetogenesis scenario. Second, the assumption of equipartition between the magnetic and kinetic fields could be confirmed, which is important due to the fact that it is used in various numerical simulations as initial condition. Third, assuming the magnetogenesis event to be the QCD Phase Transition, i.e. happening at a rather late stage of the Early Universe and therefore providing a kind of upper limit, the present day Extragalactic Magnetic Fields were found to have a correlation length of $L_B \gtrsim 200\,\mathrm{pc}$ and a magnetic field strength of $B \lesssim 5 \times 10^{-12}\,\mathrm{G}$.

In a second stage of this work Primordial Magnetic Fields have been assumed to have non-vanishing initial magnetic helicity. This is insofar an important change of the initial conditions, as helicity is conserved, which now governs the overall time evolution. Therefore, in addition to the Master Equations for the development of the energetic spectra as described above, now also the time evolution of the magnetic helicity spectrum has been derived in order to fully take into account its impact, again including all kinds of non-linear interactions between the different components.

Here it has been found that the scaling of the magnetic field with L is the same as before, thus again underlining its universality. In addition an Inverse Cascade develops, therefore independently confirming previous numerical and analytical studies with the presented new semi-analytical approach, thus strengthening its relevance. An Inverse Cascade in this context denotes the phenomenon that due to helicity conservation a large

amount of the energy of the magnetic field is transferred to larger scales with a rather high rate. Hence, confirming that this is indeed true is of major relevance for present day Extragalactic Magnetic Fields since, as mentioned above, they operate on large scales and therefore an Inverse Cascade would increase their magnitude by several orders of magnitude, giving, for the scenario of QCD magnetogenesis, limits of $B \lesssim 10^{-8}\,\mathrm{G}$.

What has been not taken into account in this work is the effect of *kinetic* helicity. This is due to the fact that vorticity modes are predicted to decay because of the Expansion of the Universe, resulting, in turn, in the decay of kinetic helicity. However, it might still be interesting to calculate and implement the corresponding additional terms into the Master Equations in order to test this claim. Furthermore, at least at some period of time, it could still play a role since it might alter the character of the backreaction.

In order to support the results presented, it would be desirable to execute a full numerical simulation under the same assumptions and with the same initial conditions. Up to the present day for Extragalactic Magnetic Fields this has been a rather challenging task for the available computing systems, especially regarding their capability of spatial resolution in simulations, as one has to take into account a large range of spatial scales – from small ones, at which the magnetic fields are created, to galactic and intergalactic lengths, which the field energy is transferred to later on. However, with the ongoing increase of hardware performance on the one hand and the improvement of the corresponding software by, for example, its adaption for parallelized computing on the other hand, these limitations, although probably not being resolved in the near future, may be mastered to some extent, making better numerical simulations for this topic a realizable possibility. However, even in the short run it should be possible to accomplish numerical simulations on this topic by reducing the considered dynamic range to a smaller one, for example the vicinity of the integral scale.

An important aim is also to compare the results found in the present thesis with actual observational data. This, however, as described above, is a rather long-term objective due to instrumental limitations. Once these have been overcome, such that even rather small cosmic magnetic fields can be measured, this will give a unique opportunity to learn about the physics in the Early Universe: If Primordial Magnetic Fields are indeed remnants of a phase transition during that era, their present day state could, similar to the CMB for Photon Decoupling, give crucial insights into the nature of the corresponding incident. Therefore, once such data is available, the results of the work presented here may be used to trace back the Extragalactic Magnetic Fields to their origin in order to constrain its cosmological realization.

Finally, since the Master Equations have been derived under very general assumptions, it should be possible to apply them to other settings than the one of Primordial Magnetic Fields. As has been mentioned above, similar procedures have been used in order to analyze galactic and solar magnetic fields. With the Master Equations and the elaborate numerical method developed above in order to solve them numerically it sould be possible to refine these studies and thus gain new insights into the physics of the underlying processes.

Appendix A

Mathematical Tools

A.1 Vector Field Identities

The purpose of this section is to present (without proofs) important identities which are useful for dealing with products of vector fields and differential operators acting on them. For some three-dimensional vector fields $\mathbf{A}(\mathbf{r})$, $\mathbf{B}(\mathbf{r})$, $\mathbf{C}(\mathbf{r})$ and a scalar field $f(\mathbf{r})$ it is [218]

$$\mathbf{A} \times (\mathbf{B} \times \mathbf{C}) = (\mathbf{A} \cdot \mathbf{C})\,\mathbf{B} - (\mathbf{A} \cdot \mathbf{B})\,\mathbf{C}\,, \tag{A.1}$$

$$\nabla \cdot (f\mathbf{A}) = \mathbf{A} \cdot \nabla f + f \nabla \cdot \mathbf{A}\,, \tag{A.2}$$

$$\nabla \times (f\mathbf{A}) = f \nabla \times \mathbf{A} - \mathbf{A} \times \nabla f\,, \tag{A.3}$$

$$\nabla\,(\mathbf{A} \cdot \mathbf{B}) = \mathbf{A} \times (\nabla \times \mathbf{B}) + \mathbf{B} \times (\nabla \times \mathbf{A}) + (\mathbf{A} \cdot \nabla)\,\mathbf{B} + (\mathbf{B} \cdot \nabla)\,\mathbf{A}\,, \tag{A.4}$$

$$\nabla \cdot (\mathbf{A} \times \mathbf{B}) = \mathbf{B} \cdot (\nabla \times \mathbf{A}) - \mathbf{A} \cdot (\nabla \times \mathbf{B})\,, \tag{A.5}$$

$$\nabla \times (\mathbf{A} \times \mathbf{B}) = \mathbf{A}(\nabla \cdot \mathbf{B}) - \mathbf{B}(\nabla \cdot \mathbf{A}) + (\mathbf{B} \cdot \nabla)\mathbf{A} - (\mathbf{A} \cdot \nabla)\mathbf{B}\,, \tag{A.6}$$

$$\nabla \times (\nabla \times \mathbf{A}) = \nabla(\nabla \cdot \mathbf{A}) - \Delta\mathbf{A}\,, \tag{A.7}$$

$$\nabla \times (\nabla f) = 0\,, \tag{A.8}$$

$$\nabla \cdot (\nabla \times \mathbf{A}) = 0\,. \tag{A.9}$$

Furthermore, for an integration over an volume V with a surface S one gets

$$\int_V \mathbf{A}(\mathbf{r}) \mathrm{d}^3 r = \oint_S \mathbf{A}(\mathbf{r}) \cdot d\mathbf{S}\,, \tag{A.10}$$

known as Gauss' (divergence) Theorem, while for a surface integral over the surface S, which has a boundary ∂S, it is

$$\int_S (\nabla \times \mathbf{A}(\mathbf{r})) \cdot \mathrm{d}\mathbf{S} = \oint_{\partial S} \mathbf{A}(\mathbf{r}) \mathrm{d}\mathbf{r}\,, \tag{A.11}$$

which is (the special) Stokes' Theorem.

A.2 Kronecker and Levi-Civita Symbols

The Kronecker symbol in n dimensions is given by

$$\delta_{i_1 i_2 \ldots i_n} = \begin{cases} 1\,, \text{ if } i_1 = i_2 = \ldots = i_n\,, \\ 0\,, \text{ else.} \end{cases} \tag{A.12}$$

The general n-dimensional Levi-Civita symbol is defined as

$$\epsilon_{i_1 i_2 \dots i_n} = \begin{cases} 1, \text{ if } (i_1, i_2, ..., i_n) \text{ is an even permutation of } (1, 2, ..., n), \\ -1, \text{ if } (i_1, i_2, ..., i_n) \text{ is an odd permutation of } (1, 2, ..., n), \\ 0, \text{ else.} \end{cases} \tag{A.13}$$

In particular, in three dimensions the following rules apply

$$\epsilon_{ijk} = \epsilon_{jki} = \epsilon_{kij} = -\epsilon_{jik} = -\epsilon_{ikj} = -\epsilon_{kji}\,, \tag{A.14}$$

$$\epsilon_{iij} = \epsilon_{iji} = \epsilon_{jii} = \epsilon_{iii} = 0\,, \tag{A.15}$$

$$\epsilon_{ijk}\epsilon_{imn} = \delta_{jm}\delta_{kn} - \delta_{jn}\delta_{km}\,, \tag{A.16}$$

$$\epsilon_{imn}\epsilon_{jmn} = 2\delta_{ij}\,, \tag{A.17}$$

$$\epsilon_{ijk}\epsilon_{ijk} = 6\,. \tag{A.18}$$

A.3 Fourier Transform

The Fourier Transform is an important operation which is the basis for various methods in mathematics and physics to analyze the spectrum of a given function. Being more precise, for a given integrable function $f : \mathbb{R}^n \to \mathbb{C}$ the Fourier Transform, i.e. the frequency spectrum, is given by

$$\mathcal{F}_{\mathbf{rk}}\{f(\mathbf{r})\} \equiv \frac{1}{(2\pi)^{\frac{n}{2}}} \int f(\mathbf{r}) e^{-i\mathbf{k}\cdot\mathbf{r}}\, \mathrm{d}^n r\,, \tag{A.19}$$

where $\mathbf{k}$ is the new variable of the transform. One should note that the definition given here follows the "angular frequency and unitary" convention, while also other, equivalent ones, are possible. The advantage of the given form is, on the one hand, the fact that it is, as the name suggests, a unitary transform and, on the other hand, that its inverse,

$$\mathcal{F}^{-1}_{\mathbf{xk}}\{g(\mathbf{k})\} \equiv \frac{1}{(2\pi)^{\frac{n}{2}}} \int g(\mathbf{k}) e^{i\mathbf{k}\cdot\mathbf{r}} \mathrm{d}^n k\,, \tag{A.20}$$

is symmetric to it. Throughout this work it is $n = 3$ which also will be used in this section from now on. For convenience, furthermore a slightly modified form of the Fourier Transform, normalized by $V^{\frac{1}{2}}$, the square root of the considered volume V, denoted by a hat ($\hat{}$), i.e.

$$\hat{f}(\mathbf{k}) \equiv \frac{1}{V^{\frac{1}{2}}} \mathcal{F}_{\mathbf{xk}}\{f(\mathbf{r})\}\,, \tag{A.21}$$

is used. In the following the properties of Fourier Transforms which are important for this work are presented for an integrable function $f : \mathbb{R}^n \to \mathbb{C}$.

Linearity

The Fourier Transform is linear, i.e. for $a, b \in \mathbb{C}$ and two integrable functions $f, g : \mathbb{R}^n \to \mathbb{C}$ it is

$$\mathcal{F}_{\mathbf{xk}}\left\{af(\mathbf{r}) + bg(\mathbf{r})\right\} = a\mathcal{F}_{\mathbf{rk}}\left\{f(\mathbf{r})\right\} + b\mathcal{F}_{\mathbf{rk}}\left\{g(\mathbf{r})\right\}\,, \tag{A.22}$$

which can be seen directly from the properties of the integral.

Fourier Transform of a Derivative

Using integration by parts with mathematical induction, it can be shown that

$$\mathcal{F}_{\mathbf{rk}}\left\{\frac{\mathrm{d}^m}{\mathrm{d}r_j^m}f(\mathbf{r})\right\} = (ik_j)^m\,\mathcal{F}_{\mathbf{rk}}\left\{f(\mathbf{r})\right\}\,. \tag{A.23}$$

Convolution Theorem

The Convolution Theorem describes a basic property of the Fourier Transform. It reads

$$\mathcal{F}_{\mathbf{rk}}\{f(\mathbf{r})g(\mathbf{r})\} = \frac{1}{(2\pi)^{\frac{n}{2}}}\mathcal{F}_{\mathbf{rk}}\left\{f(\mathbf{r})\right\} * \mathcal{F}_{\mathbf{rk}}\left\{g(\mathbf{r})\right\}\,, \tag{A.24}$$

where the star, $*$, denotes a convolution of two functions which is given by

$$f(\mathbf{r}) * g(\mathbf{r}) \equiv \frac{1}{(2\pi)^{\frac{n}{2}}}\int f(\mathbf{r}-\mathbf{r}')g(\mathbf{r}')\mathrm{d}^n r'\,. \tag{A.25}$$

For some terms appearing in, for example, Sec. 1.1 it is important to calculate the Fourier Transform for terms of the form $(\mathbf{A}\cdot\nabla)\mathbf{C}$. For this purpose Cartesian coordinates for $n = 3$ and the Einstein Sum Convention are used in the following. The mth component of the Fourier Transform can be written as

$$\begin{aligned}
&\frac{1}{V}\left[\mathcal{F}_{\mathbf{rk}}\{(\mathbf{A}(\mathbf{r})\cdot\nabla)\mathbf{C}(\mathbf{r})\}\right]_m = \frac{1}{V}\mathcal{F}_{\mathbf{rk}}\{(A_j(\mathbf{r})\partial_j)C_m(\mathbf{r})\}\\
&= \frac{1}{V}\mathcal{F}_{\mathbf{rk}}\{A_j(\mathbf{r})\partial_j C_m(\mathbf{r})\} \overset{(A.24)}{=} \frac{1}{(2\pi)^{\frac{3}{2}}V^{\frac{1}{2}}}\hat{A}_j(\mathbf{k}) * \mathcal{F}_{\mathbf{rk}}\{\partial_n C_m(\mathbf{r})\}\\
&\overset{(A.23)}{=} \frac{1}{(2\pi)^{\frac{3}{2}}}\hat{A}_j(\mathbf{k}) * \left(ik_j\hat{C}_m(\mathbf{k})\right) = \frac{i}{(2\pi)^{\frac{3}{2}}}\int \hat{A}_j(\mathbf{k}-\mathbf{k}')k'_j\hat{C}_m(\mathbf{k}')\,\mathrm{d}^3k'\,,
\end{aligned} \tag{A.26}$$

i.e. it is

$$\frac{1}{V}\mathcal{F}_{\mathbf{rk}}\{(\mathbf{A}(\mathbf{r})\cdot\nabla)\mathbf{C}(\mathbf{r})\} = \frac{i}{(2\pi)^{\frac{3}{2}}}\int\left(\hat{\mathbf{A}}(\mathbf{k}-\mathbf{k}')\cdot\mathbf{k}'\right)\hat{\mathbf{C}}(\mathbf{k}')\mathrm{d}^3k'\,. \tag{A.27}$$

Wiener-Khinchin-Kolmogorov Theorem

The Wiener-Khinchin-Kolmogorov Theorem states that the so-called autocorrelation function C_f of a one-dimensional function $f(t)$ of a scalar t, defined as

$$C_f(t) = \lim_{T\to\infty}\int_{-T/2}^{T/2} f^*(t')f(t'-t)\mathrm{d}t'\,, \tag{A.28}$$

i.e. the average of $f^*(t')f(t'-t)$ over the whole range of t, is well defined and can be calculated as a (one-dimensional) inverse Fourier Transform

$$C_f(t) = \mathcal{F}^{-1}_{t\omega}\left\{\left|\mathcal{F}_{t\omega}\left\{f(t)\right\}\right|^2\right\} \tag{A.29}$$

and, on the other hand, the reverse transformation is given by

$$\left|\mathcal{F}_{t\omega}\left\{f(t)\right\}\right|^2 = \mathcal{F}^{-1}_{t\omega}\left\{C_f(t)\right\}\,. \tag{A.30}$$

These expressions therefore show that, for a given function, the autocorrelation function is directly related to the absolute square of the Fourier Transform.

Paley-Wiener Theorem

The Paley-Wiener Theorem in the form used in this thesis states that a function f has a compact support if and only if the Fourier Transform of $\mathcal{F}_{\mathbf{rk}}\{f\}$ is an analytic function, i.e. it can be expressed in terms of a converging power series in each point of its domain of definition. This is a rather specific formulation of the general Paley-Wiener Theorem which, however, is sufficient for the purpose of this work.

Parseval's Theorem

By applying the Convolution Theorem (A.24) a powerful relation can be derived, namely Parseval's Theorem which states that [219]

$$\int f(\mathbf{r})g(\mathbf{r})^* \,\mathrm{d}^3r = \int \mathcal{F}_{\mathbf{rk}}\{f(\mathbf{r})\}\mathcal{F}_{\mathbf{rk}}\{g(\mathbf{r})\}^* \,\mathrm{d}^3k = V\int \hat{f}(\mathbf{k})\hat{g}(\mathbf{k})^* \,\mathrm{d}^3k \tag{A.31}$$

or, more specific for $f = g$,

$$\int |f(\mathbf{r})|^2 \,\mathrm{d}^3r = \int |\mathcal{F}_{\mathbf{rk}}\{f(\mathbf{r})\}|^2 \,\mathrm{d}^3k = V\int \left|\hat{f}(\mathbf{k})\right|^2 \mathrm{d}^3k\,. \tag{A.32}$$

A.4 Runge-Kutta Methods

The purpose of this section is to summarize a possible method, introduced by [220–222], to obtain a numerical solution for ordinary differential equations (ODEs), i.e. differential equations of the form

$$\partial_t y(t) = f(t, y) \tag{A.33}$$

with the initial condition $y(t_0) = y_0$. One possibility is to use a one-step method. This means that in order to obtain the values of $y_j \equiv y(t_j)$ at a sequence of values for t_j, one defines the recursion rule

$$y_{j+1} = y_j + h_j\Phi\left(t_j, y_j, y_{j+1}, h_j\right)\,, \tag{A.34}$$

where $\Phi\left(t_j, y_j, y_{j+1}, h_i\right)$ is the so-called increment function which defines the particular method used and $h_j \equiv t_{j+1} - t_j$ is the jth step size. If Φ does not explicitly depend on y_{j+1}, i.e. it is $\Phi\left(t_j, y_j, y_{j+1}, h_j\right) = \Phi\left(t_j, y_j, h_j\right)$, it is called an explicit one-step method, otherwise an implicit one.

Of particular interest in the scope of this work are the s-stage Runge-Kutta methods which are defined by

$$\begin{aligned}
\Phi\left(t, y, h\right) &\equiv \sum_{i=1}^{s} b_i k_i\,,\\
k_1 &\equiv f(t, y)\,,\\
&\ldots\\
k_i &\equiv f\left(t + hc_i, y + h\sum_{j=1}^{s} a_{ij}k_j\right)\,,
\end{aligned} \tag{A.35}$$

where the parameters $a_{ij}, b_{ij} \in \mathbb{R}$, $c_i \in [0, 1]$ specify the particular Runge-Kutta method and have to obey

$$\sum_{i=1}^{s} b_i = 1\,. \tag{A.36}$$

In addition, if $a_{ij} = 0$ for all $j \geq i$, this will give an explicit method.

A helpful tool to characterize a particular Runge-Kutta method is the so-called Butcher Tableau which presents the parameters described above in a compact form:

$$\begin{array}{c|cccc} c_1 & a_{11} & a_{12} & ... & a_{1s} \\ c_2 & a_{21} & a_{22} & ... & a_{2s} \\ ... & \vdots & \vdots & \ddots & \vdots \\ c_s & a_{s1} & a_{s2} & ... & a_{ss} \\ \hline & b_1 & b_2 & ... & b_s \end{array}$$

It should be noted that for an explicit method only entries on and below the main diagonal are not equal zero.

To conclude this short overview, some examples for explicit Runge-Kutta methods shall be given. For explicit methods, in addition to the requirements on the parameters stated above, in order to be consistent, i.e. to match the Taylor Expansion of the exact solution for y in h to an order as high as possible, the parameters have to fulfill further relations which depend on s. For example, s being equal 2, they are given by

$$b_2 c_2 = \frac{1}{2},\ a_{21} b_2 = \frac{1}{2}\,. \tag{A.37}$$

The simplest Runge-Kutta method is the explicit Euler Method which is given by

$$\begin{array}{c|c} 0 & \\ \hline & 1 \end{array}$$

For $s = 2$ a large variety of different parameter combinations can be found, for example

$$\begin{array}{c|cc} 0 & & \\ 1 & 1 & \\ \hline & \frac{1}{2} & \frac{1}{2} \end{array} \qquad \begin{array}{c|cc} 0 & & \\ \frac{1}{2} & \frac{1}{2} & \\ \hline & 0 & 1 \end{array}$$

which are the Heun Method and the Midpoint Method, respectively, the latter also known as the "classical" second-order Runge-Kutta method or modified Euler Method. Finally, the probably most widely used method has to be mentioned as well: The "classical" fourth-order Runge-Kutta method which is represented by the Butcher Tableau

$$\begin{array}{c|cccc} 0 & & & & \\ \frac{1}{2} & \frac{1}{2} & & & \\ \frac{1}{2} & 0 & \frac{1}{2} & & \\ 1 & 0 & 0 & 1 & \\ \hline & \frac{1}{6} & \frac{1}{3} & \frac{1}{3} & \frac{1}{6} \end{array}$$

For a more exhaustive treatment of the topic see, e.g., [223] and, especially for electronic implementation, [224].

Appendix B

Supplementary Material for the Derivation of the Master Equations

B.1 Full Form of (3.44) and (3.45)

Performing the procedure described in Sec. 3.2.1, the full forms of (3.44) and (3.45), i.e. ${}^{(2)}\hat{\mathbf{B}}_{\mathbf{q}}$ and ${}^{(2)}\hat{\mathbf{v}}_{\mathbf{q}}$ in terms of ${}^{(0)}\hat{\mathbf{B}}$ and ${}^{(0)}\hat{\mathbf{v}}$, where in the following the superscript ${}^{(0)}$ is dropped, are given by

$$
\begin{aligned}
{}^{(2)}\hat{\mathbf{B}}(\mathbf{q}) = \hat{\mathbf{B}}_{\mathbf{q}} + \Delta t \Bigg\{ & -\frac{q^2 \hat{\mathbf{B}}_{\mathbf{q}}}{4\pi\sigma} + \frac{iV^{\frac{1}{2}}}{(2\pi)^{\frac{3}{2}}} \int \Big[\Big(\mathbf{q} \cdot \hat{\mathbf{B}}_{\mathbf{k}} \Big) \hat{\mathbf{v}}_{\mathbf{q}-\mathbf{k}} - (\mathbf{q} \cdot \hat{\mathbf{v}}_{\mathbf{q}-\mathbf{k}}) \hat{\mathbf{B}}_{\mathbf{k}} \Big] \mathrm{d}^3 k \Bigg\} + \frac{\Delta t^2}{2} \Bigg(\frac{q^4}{(4\pi\sigma)^2} \hat{\mathbf{B}}_{\mathbf{q}} + \iint \Bigg\{ -\frac{iV^{\frac{1}{2}}}{(2\pi)^{\frac{3}{2}}} \frac{k^2 + q^2}{4\pi\sigma} \Big[\Big(\mathbf{q} \cdot \hat{\mathbf{B}}_{\mathbf{k}} \Big) \hat{\mathbf{v}}_{\mathbf{q}-\mathbf{k}} \\
& - (\mathbf{q} \cdot \hat{\mathbf{v}}_{\mathbf{q}-\mathbf{k}}) \hat{\mathbf{B}}_{\mathbf{k}} \Big] + \frac{V}{(2\pi)^3} \Big[- (\mathbf{q} \cdot \hat{\mathbf{v}}_{\mathbf{k}-\mathbf{k}'}) \Big(\mathbf{k} \cdot \hat{\mathbf{B}}_{\mathbf{k}'} \Big) \hat{\mathbf{v}}_{\mathbf{q}-\mathbf{k}} + (\mathbf{q} \cdot \hat{\mathbf{v}}_{\mathbf{q}-\mathbf{k}}) \Big(\mathbf{k} \cdot \hat{\mathbf{B}}_{\mathbf{k}'} \Big) \hat{\mathbf{v}}_{\mathbf{k}-\mathbf{k}'} + \Big(\mathbf{q} \cdot \hat{\mathbf{B}}_{\mathbf{k}'} \Big) (\mathbf{k} \cdot \hat{\mathbf{v}}_{\mathbf{k}-\mathbf{k}'}) \hat{\mathbf{v}}_{\mathbf{q}-\mathbf{k}} - (\mathbf{q} \cdot \hat{\mathbf{v}}_{\mathbf{q}-\mathbf{k}}) (\mathbf{k} \cdot \hat{\mathbf{v}}_{\mathbf{k}-\mathbf{k}'}) \hat{\mathbf{B}}_{\mathbf{k}'} \\
& + \big(\mathbf{k}' \cdot \hat{\mathbf{v}}_{\mathbf{q}-\mathbf{k}-\mathbf{k}'} \big) \Big(\mathbf{q} \cdot \hat{\mathbf{B}}_{\mathbf{k}} \Big) \hat{\mathbf{v}}_{\mathbf{k}'} - \big(\mathbf{k}' \cdot \hat{\mathbf{v}}_{\mathbf{q}-\mathbf{k}-\mathbf{k}'} \big) (\mathbf{q} \cdot \hat{\mathbf{v}}_{\mathbf{k}'}) \hat{\mathbf{B}}_{\mathbf{k}} \Big] + \frac{V}{(2\pi)^3} \frac{1}{4\pi\rho} \Big[- (\mathbf{q} \cdot \mathbf{k}') \Big(\mathbf{B}_{\mathbf{q}-\mathbf{k}-\mathbf{k}'} \cdot \hat{\mathbf{B}}_{\mathbf{k}'} \Big) \hat{\mathbf{B}}_{\mathbf{k}} + \Big(\mathbf{q} \cdot \hat{\mathbf{B}}_{\mathbf{k}} \Big) \Big(\hat{\mathbf{B}}_{\mathbf{q}-\mathbf{k}-\mathbf{k}'} \cdot \hat{\mathbf{B}}_{\mathbf{k}'} \Big) \mathbf{k}' \\
& + \Big(\mathbf{q} \cdot \hat{\mathbf{B}}_{\mathbf{k}'} \Big) \Big(\mathbf{k}' \cdot \hat{\mathbf{B}}_{\mathbf{q}-\mathbf{k}-\mathbf{k}'} \Big) \hat{\mathbf{B}}_{\mathbf{k}} - \Big(\mathbf{q} \cdot \hat{\mathbf{B}}_{\mathbf{k}} \Big) \Big(\mathbf{k}' \cdot \hat{\mathbf{B}}_{\mathbf{q}-\mathbf{k}-\mathbf{k}'} \Big) \hat{\mathbf{B}}_{\mathbf{k}'} \Big] \Bigg\} \mathrm{d}^3 k' \mathrm{d}^3 k \Bigg)
\end{aligned}
\tag{B.1}
$$

and by

$$
\begin{aligned}
{}^{(2)}\hat{\mathbf{v}}(\mathbf{q}) = \hat{\mathbf{v}}_{\mathbf{q}} &+ \Delta t \frac{iV^{\frac{1}{2}}}{(2\pi)^{\frac{3}{2}}} \int \Big[-\left(\mathbf{k}\cdot\hat{\mathbf{v}}_{\mathbf{q}-\mathbf{k}}\right)\hat{\mathbf{v}}_{\mathbf{k}} + \frac{1}{4\pi\rho}\left(\mathbf{k}\cdot\hat{\mathbf{B}}_{\mathbf{q}-\mathbf{k}}\right)\hat{\mathbf{B}}_{\mathbf{k}} - \frac{1}{4\pi\rho}\left(\hat{\mathbf{B}}_{\mathbf{q}-\mathbf{k}}\cdot\hat{\mathbf{B}}_{\mathbf{k}}\right)\mathbf{k}\Big]\mathrm{d}^3k \\
&+ \frac{\Delta t^2}{2}\iint\Bigg\{ \frac{iV^{\frac{1}{2}}}{(2\pi)^{\frac{3}{2}}}\frac{1}{4\pi\sigma}\frac{1}{4\pi\rho}\left[k^2+(\mathbf{q}-\mathbf{k})^2\right]\left[\left(\hat{\mathbf{B}}_{\mathbf{q}-\mathbf{k}}\cdot\hat{\mathbf{B}}_{\mathbf{k}}\right)\mathbf{k} - \left(\mathbf{k}\cdot\hat{\mathbf{B}}_{\mathbf{q}-\mathbf{k}}\right)\hat{\mathbf{B}}_{\mathbf{k}}\right] \\
&+ \frac{V}{(2\pi)^3}\big[-\left(\mathbf{k}\cdot\hat{\mathbf{v}}_{\mathbf{q}-\mathbf{k}}\right)\left(\mathbf{k}'\cdot\hat{\mathbf{v}}_{\mathbf{k}-\mathbf{k}'}\right)\hat{\mathbf{v}}_{\mathbf{k}'} - \left(\mathbf{k}'\cdot\hat{\mathbf{v}}_{\mathbf{q}-\mathbf{k}-\mathbf{k}'}\right)\left(\mathbf{k}\cdot\hat{\mathbf{v}}_{\mathbf{k}'}\right)\hat{\mathbf{v}}_{\mathbf{k}}\big] \\
&+ \frac{V}{(2\pi)^3}\frac{1}{4\pi\rho}\Big[\left(\mathbf{k}\cdot\hat{\mathbf{v}}_{\mathbf{q}-\mathbf{k}}\right)\left(\mathbf{k}'\cdot\hat{\mathbf{B}}_{\mathbf{k}-\mathbf{k}'}\right)\hat{\mathbf{B}}_{\mathbf{k}'} - \left(\mathbf{k}\cdot\hat{\mathbf{v}}_{\mathbf{q}-\mathbf{k}}\right)\left(\hat{\mathbf{B}}_{\mathbf{k}-\mathbf{k}'}\cdot\hat{\mathbf{B}}_{\mathbf{k}'}\right)\mathbf{k}' \\
&- \left(\mathbf{k}\cdot\hat{\mathbf{B}}_{\mathbf{q}-\mathbf{k}}\right)\left(\mathbf{k}\cdot\hat{\mathbf{B}}_{\mathbf{k}'}\right)\hat{\mathbf{v}}_{\mathbf{k}-\mathbf{k}'} + \left(\mathbf{k}\cdot\hat{\mathbf{B}}_{\mathbf{q}-\mathbf{k}}\right)\left(\mathbf{k}\cdot\hat{\mathbf{v}}_{\mathbf{k}-\mathbf{k}'}\right)\hat{\mathbf{B}}_{\mathbf{k}'} - \left(\mathbf{q}\cdot\hat{\mathbf{B}}_{\mathbf{k}'}\right)\left(\mathbf{k}\cdot\hat{\mathbf{v}}_{\mathbf{q}-\mathbf{k}-\mathbf{k}'}\right)\hat{\mathbf{B}}_{\mathbf{k}} \\
&+ \left(\mathbf{k}\cdot\hat{\mathbf{B}}_{\mathbf{k}'}\right)\left(\mathbf{q}\cdot\hat{\mathbf{v}}_{\mathbf{q}-\mathbf{k}-\mathbf{k}'}\right)\hat{\mathbf{B}}_{\mathbf{k}} + \left(\mathbf{k}'\cdot\hat{\mathbf{B}}_{\mathbf{q}-\mathbf{k}-\mathbf{k}'}\right)\left(\mathbf{k}\cdot\hat{\mathbf{B}}_{\mathbf{k}'}\right)\hat{\mathbf{v}}_{\mathbf{k}} - \left(\mathbf{k}\cdot\mathbf{k}'\right)\left(\hat{\mathbf{B}}_{\mathbf{k}'}\cdot\hat{\mathbf{B}}_{\mathbf{q}-\mathbf{k}-\mathbf{k}'}\right)\hat{\mathbf{v}}_{\mathbf{k}} \\
&+ \left(\mathbf{k}\cdot\hat{\mathbf{B}}_{\mathbf{k}'}\right)\left(\hat{\mathbf{B}}_{\mathbf{q}-\mathbf{k}}\cdot\hat{\mathbf{v}}_{\mathbf{k}-\mathbf{k}'}\right)\mathbf{k} - \left(\mathbf{k}\cdot\hat{\mathbf{v}}_{\mathbf{k}-\mathbf{k}'}\right)\left(\hat{\mathbf{B}}_{\mathbf{q}-\mathbf{k}}\cdot\hat{\mathbf{B}}_{\mathbf{k}'}\right)\mathbf{k} + \left((\mathbf{q}-\mathbf{k})\cdot\hat{\mathbf{B}}_{\mathbf{k}'}\right)\left(\hat{\mathbf{B}}_{\mathbf{k}}\cdot\hat{\mathbf{v}}_{\mathbf{q}-\mathbf{k}-\mathbf{k}'}\right)\mathbf{k} \\
&- \left((\mathbf{q}-\mathbf{k})\cdot\hat{\mathbf{v}}_{\mathbf{q}-\mathbf{k}-\mathbf{k}'}\right)\left(\hat{\mathbf{B}}_{\mathbf{k}}\cdot\hat{\mathbf{B}}_{\mathbf{k}'}\right)\mathbf{k}\Big]\Bigg\}\mathrm{d}^3k'\mathrm{d}^3k\,.
\end{aligned}
\tag{B.2}
$$

B.2 Simplifications

The first expression to be calculated in order to evaluate (3.46) is of the form $\left(\partial_t\hat{\mathbf{B}}_{\mathbf{q}}\right)\cdot\hat{\mathbf{B}}^*_{\mathbf{q}}$. For this the time derivative of (B.1) has to be taken and then, due to numerical reasons, the substitution $\Delta t \to 1/2\Delta t$ has to be done, giving, using the Einstein Sum Convention,

$$
\begin{aligned}
&\left(\partial_t \hat{B}_{\mathbf{q},i}\right)\hat{B}^*_{\mathbf{q},i} = -\frac{q^2}{4\pi\sigma}\hat{B}_{\mathbf{q},i}\hat{B}^*_{\mathbf{q},i} + \frac{iV^{\frac{1}{2}}}{(2\pi)^{\frac{3}{2}}}\int\left(-q_a\hat{B}_{\mathbf{k},a}\hat{B}^*_{\mathbf{q},i}\hat{v}_{\mathbf{q}-\mathbf{k},i} + q_a\hat{B}_{\mathbf{k},i}\hat{B}^*_{\mathbf{q},i}\hat{v}_{\mathbf{q}-\mathbf{k},a}\right)\mathrm{d}^3k + \frac{\Delta t}{2}\Bigg\{2\frac{q^4}{(4\pi\sigma)^2}\hat{B}_{\mathbf{q},i}\hat{B}^*_{\mathbf{q},i}\\
&+\frac{q^2}{4\pi\sigma}\frac{iV^{\frac{1}{2}}}{(2\pi)^{\frac{3}{2}}}\int\left(q_a\hat{B}_{\mathbf{q},i}\hat{B}^*_{\mathbf{k},a}\hat{v}^*_{\mathbf{q}-\mathbf{k},i} - q_a\hat{B}_{\mathbf{q},i}\hat{B}^*_{\mathbf{k},i}\hat{v}^*_{\mathbf{q}-\mathbf{k},a} - q_a\hat{B}^*_{\mathbf{q},i}\hat{B}_{\mathbf{k},a}\hat{v}_{\mathbf{q}-\mathbf{k},i} + q_a\hat{B}_{\mathbf{k},i}\hat{B}^*_{\mathbf{q},i}\hat{v}_{\mathbf{q}-\mathbf{k},a}\right)\mathrm{d}^3k\\
&+\iint\Big[-\frac{1}{2}\frac{iV^{\frac{1}{2}}}{(2\pi)^{\frac{3}{2}}}\frac{k^2+q^2}{4\pi\sigma}\left(q_a\hat{B}_{\mathbf{k},a}\hat{B}^*_{\mathbf{q},i}\hat{v}_{\mathbf{q}-\mathbf{k},i} - q_a\hat{B}_{\mathbf{k},i}\hat{B}^*_{\mathbf{q},i}\hat{v}_{\mathbf{q}-\mathbf{k},a}\right) + \frac{V}{(2\pi)^3}\Big(q_aq_b\hat{B}_{\mathbf{k},a}\hat{B}^*_{\mathbf{k}',b}\hat{v}_{\mathbf{q}-\mathbf{k},i}\hat{v}^*_{\mathbf{q}-\mathbf{k}',i} - q_aq_b\hat{B}_{\mathbf{k},a}\hat{B}^*_{\mathbf{k}',i}\hat{v}_{\mathbf{q}-\mathbf{k},i}\hat{v}^*_{\mathbf{q}-\mathbf{k}',b}\\
&-q_aq_b\hat{v}_{\mathbf{q}-\mathbf{k},a}\hat{v}^*_{\mathbf{q}-\mathbf{k}',i}\hat{B}_{\mathbf{k},i}\hat{B}^*_{\mathbf{k}',b} + q_aq_b\hat{B}_{\mathbf{k},i}\hat{B}^*_{\mathbf{k}',i}\hat{v}_{\mathbf{q}-\mathbf{k},a}\hat{v}^*_{\mathbf{q}-\mathbf{k}',b} - q_ak_b\hat{B}_{\mathbf{k}',b}\hat{B}^*_{\mathbf{q},i}\hat{v}_{\mathbf{q}-\mathbf{k},i}\hat{v}_{\mathbf{k}-\mathbf{k}',a} + q_ak_b\hat{B}_{\mathbf{k}',b}\hat{B}^*_{\mathbf{q},i}\hat{v}_{\mathbf{q}-\mathbf{k},a}\hat{v}_{\mathbf{k}-\mathbf{k}',i}\\
&+q_ak_b\hat{B}_{\mathbf{k}',a}\hat{B}^*_{\mathbf{q},i}\hat{v}_{\mathbf{q}-\mathbf{k},i}\hat{v}_{\mathbf{k}-\mathbf{k}',b} - q_ak_b\hat{B}_{\mathbf{k}',i}\hat{B}^*_{\mathbf{q},i}\hat{v}_{\mathbf{q}-\mathbf{k},a}\hat{v}_{\mathbf{k}-\mathbf{k}',b} + k'_aq_b\hat{B}_{\mathbf{k},b}\hat{B}^*_{\mathbf{q},i}\hat{v}_{\mathbf{q}-\mathbf{k}-\mathbf{k}',a}\hat{v}_{\mathbf{k}',i} - q_bk'_a\hat{B}_{\mathbf{k},i}\hat{B}^*_{\mathbf{q},i}\hat{v}_{\mathbf{q}-\mathbf{k}-\mathbf{k}',a}\hat{v}_{\mathbf{k}',b}\Big)\\
&+\frac{V}{(2\pi)^3}\frac{1}{4\pi\rho}\big(-q_ak'_a\hat{B}_{\mathbf{q}-\mathbf{k}-\mathbf{k}',b}\hat{B}_{\mathbf{k}',b}\hat{B}_{\mathbf{k},i}\hat{B}^*_{\mathbf{q},i} + q_ak'_i\hat{B}_{\mathbf{k},a}\hat{B}_{\mathbf{q}-\mathbf{k}-\mathbf{k}',b}\hat{B}_{\mathbf{k}',b}\hat{B}^*_{\mathbf{q},i} + q_ak'_b\hat{B}_{\mathbf{k}',a}\hat{B}_{\mathbf{q}-\mathbf{k}-\mathbf{k}',b}\hat{B}_{\mathbf{k},i}\hat{B}^*_{\mathbf{q},i}\\
&-q_ak'_b\hat{B}_{\mathbf{k},a}\hat{B}_{\mathbf{q}-\mathbf{k}-\mathbf{k}',b}\hat{B}_{\mathbf{k}',i}\hat{B}^*_{\mathbf{q},i}\big)\Big]\mathrm{d}^3k'\mathrm{d}^3k\Bigg\}.
\end{aligned}
\tag{B.3}
$$

In the next step the ensemble average of this expression is taken. Since this results in several expressions of the (symbolic) type $\left\langle\hat{B}_i\hat{B}_j\right\rangle$, $\left\langle\hat{B}_i\hat{B}_j\hat{v}_k\right\rangle$, $\left\langle\hat{B}_i\hat{B}_j\hat{v}_k\hat{v}_l\right\rangle$ and $\left\langle\hat{B}_i\hat{B}_j\hat{B}_k\hat{B}_l\right\rangle$, Isserlis' Theorem (1.142) has to be used, giving, together with the condition $\left\langle\hat{v}\hat{B}\right\rangle = 0$ stated above,

$$
\left\langle\hat{B}_i\hat{B}_j\hat{v}_k\right\rangle = 0\,, \tag{B.4}
$$

$$
\left\langle\hat{B}_i\hat{B}_jv_k\hat{v}_l\right\rangle = \left\langle\hat{B}_i\hat{B}_j\right\rangle\langle\hat{v}_k\hat{v}_l\rangle\ , \tag{B.5}
$$

$$
\left\langle\hat{B}_i\hat{B}_j\hat{B}_k\hat{B}_l\right\rangle \overset{(1.143)}{=} \left\langle\hat{B}_i\hat{B}_j\right\rangle\left\langle\hat{B}_k\hat{B}_l\right\rangle + \left\langle\hat{B}_i\hat{B}_k\right\rangle\left\langle\hat{B}_j\hat{B}_l\right\rangle + \left\langle\hat{B}_i\hat{B}_l\right\rangle\left\langle\hat{B}_j\hat{B}_k\right\rangle\ . \tag{B.6}
$$

Furthermore, since $\mathbf{B}(\mathbf{r})$ and $\mathbf{v}(\mathbf{r})$ are real, the complex conjugate of their Fourier Transform is given by

$$
\hat{\mathbf{B}}^*_{\mathbf{q}} = \hat{\mathbf{B}}_{-\mathbf{q}}\,,\ \hat{\mathbf{v}}^*_{\mathbf{q}} = \hat{\mathbf{v}}_{-\mathbf{q}}\,, \tag{B.7}
$$

such that (B.3) becomes

$$\begin{aligned}
\left\langle \left(\partial_t \hat{B}_{\mathbf{q},i}\right) \hat{B}^*_{\mathbf{q},i} \right\rangle = &-\frac{q^2}{4\pi\sigma} \left\langle \hat{B}_{\mathbf{q},i} \hat{B}^*_{\mathbf{q},i} \right\rangle + \frac{\Delta t}{2} \Bigg\{ 2 \frac{q^4}{(4\pi\sigma)^2} \left\langle \hat{B}_{\mathbf{q},i} \hat{B}^*_{\mathbf{q},i} \right\rangle + \frac{V}{(2\pi)^3} \iint \Big[\Big(q_a q_b \left\langle \hat{B}_{\mathbf{k},a} \hat{B}^*_{\mathbf{k}',b} \right\rangle \left\langle \hat{v}_{\mathbf{q}-\mathbf{k},i} \hat{v}^*_{\mathbf{q}-\mathbf{k}',i} \right\rangle \\
&- q_a q_b \left\langle \hat{B}_{\mathbf{k},a} \hat{B}^*_{\mathbf{k}',i} \right\rangle \left\langle \hat{v}_{\mathbf{q}-\mathbf{k},i} \hat{v}^*_{\mathbf{q}-\mathbf{k}',b} \right\rangle - q_a q_b \left\langle \hat{B}_{\mathbf{k},i} \hat{B}^*_{\mathbf{k}',b} \right\rangle \left\langle \hat{v}_{\mathbf{q}-\mathbf{k},a} \hat{v}^*_{\mathbf{q}-\mathbf{k}',i} \right\rangle + q_a q_b \left\langle \hat{B}_{\mathbf{k},i} \hat{B}^*_{\mathbf{k}',i} \right\rangle \left\langle \hat{v}_{\mathbf{q}-\mathbf{k},a} \hat{v}^*_{\mathbf{q}-\mathbf{k}',b} \right\rangle \\
&- q_a k_b \left\langle \hat{B}_{\mathbf{k}',b} \hat{B}^*_{\mathbf{q},i} \right\rangle \left\langle \hat{v}_{\mathbf{q}-\mathbf{k},i} \hat{v}^*_{-\mathbf{k}+\mathbf{k}',a} \right\rangle + q_a k_b \left\langle \hat{B}_{\mathbf{k}',b} \hat{B}^*_{\mathbf{q},i} \right\rangle \left\langle \hat{v}_{\mathbf{q}-\mathbf{k},a} \hat{v}^*_{-\mathbf{k}+\mathbf{k}',i} \right\rangle + q_a k_b \left\langle \hat{B}_{\mathbf{k}',a} \hat{B}^*_{\mathbf{q},i} \right\rangle \left\langle \hat{v}_{\mathbf{q}-\mathbf{k},i} \hat{v}^*_{-\mathbf{k}+\mathbf{k}',b} \right\rangle \\
&- q_a k_b \left\langle \hat{B}_{\mathbf{k}',i} \hat{B}^*_{\mathbf{q},i} \right\rangle \left\langle \hat{v}_{\mathbf{q}-\mathbf{k},a} \hat{v}^*_{-\mathbf{k}+\mathbf{k}',b} \right\rangle + k'_a q_b \left\langle \hat{B}_{\mathbf{k},b} \hat{B}^*_{\mathbf{q},i} \right\rangle \left\langle \hat{v}_{\mathbf{q}-\mathbf{k}-\mathbf{k}',a} \hat{v}^*_{-\mathbf{k}',i} \right\rangle - q_b k'_a \left\langle \hat{B}_{\mathbf{k},i} \hat{B}^*_{\mathbf{q},i} \right\rangle \left\langle \hat{v}_{\mathbf{q}-\mathbf{k}-\mathbf{k}',a} \hat{v}^*_{-\mathbf{k}',b} \right\rangle \Big) \\
&+ \frac{1}{4\pi\rho} \Big(- q_a k'_a \left\langle \hat{B}_{\mathbf{q}-\mathbf{k}-\mathbf{k}',b} \hat{B}^*_{-\mathbf{k}',b} \right\rangle \left\langle \hat{B}_{\mathbf{k},i} \hat{B}^*_{\mathbf{q},i} \right\rangle - q_a k'_a \left\langle \hat{B}_{\mathbf{q}-\mathbf{k}-\mathbf{k}',b} \hat{B}^*_{-\mathbf{k},i} \right\rangle \left\langle \hat{B}_{\mathbf{k}',b} \hat{B}^*_{\mathbf{q},i} \right\rangle - q_a k'_a \left\langle \hat{B}_{\mathbf{q}-\mathbf{k}-\mathbf{k}',b} \hat{B}^*_{\mathbf{q},i} \right\rangle \left\langle \hat{B}_{\mathbf{k}',b} \hat{B}^*_{-\mathbf{k},i} \right\rangle \\
&+ q_a k'_i \left\langle \hat{B}_{\mathbf{q}-\mathbf{k}-\mathbf{k}',b} \hat{B}^*_{-\mathbf{k},a} \right\rangle \left\langle \hat{B}_{\mathbf{k}',b} \hat{B}^*_{\mathbf{q},i} \right\rangle + q_a k'_i \left\langle \hat{B}_{\mathbf{k},a} \hat{B}^*_{-\mathbf{k}',b} \right\rangle \left\langle \hat{B}_{\mathbf{q}-\mathbf{k}-\mathbf{k}',b} \hat{B}^*_{\mathbf{q},i} \right\rangle + q_a k'_i \left\langle \hat{B}_{\mathbf{k},a} \hat{B}^*_{\mathbf{q},i} \right\rangle \left\langle \hat{B}_{\mathbf{q}-\mathbf{k}-\mathbf{k}',b} \hat{B}^*_{-\mathbf{k}',b} \right\rangle \\
&+ q_a k'_b \left\langle \hat{B}_{\mathbf{q}-\mathbf{k}-\mathbf{k}',b} \hat{B}^*_{-\mathbf{k}',a} \right\rangle \left\langle \hat{B}_{\mathbf{k},i} \hat{B}^*_{\mathbf{q},i} \right\rangle + q_a k'_b \left\langle \hat{B}_{\mathbf{k}',a} \hat{B}^*_{-\mathbf{k},i} \right\rangle \left\langle \hat{B}_{\mathbf{q}-\mathbf{k}-\mathbf{k}',b} \hat{B}^*_{\mathbf{q},i} \right\rangle + q_a k'_b \left\langle \hat{B}_{\mathbf{k}',a} \hat{B}^*_{\mathbf{q},i} \right\rangle \left\langle \hat{B}_{\mathbf{q}-\mathbf{k}-\mathbf{k}',b} \hat{B}_{\mathbf{k},i} \right\rangle \\
&- q_a k'_b \left\langle \hat{B}_{\mathbf{q}-\mathbf{k}-\mathbf{k}',b} \hat{B}^*_{-\mathbf{k},a} \right\rangle \left\langle \hat{B}_{\mathbf{k}',i} \hat{B}^*_{\mathbf{q},i} \right\rangle - q_a k'_b \left\langle \hat{B}_{\mathbf{k},a} \hat{B}^*_{-\mathbf{k}',i} \right\rangle \left\langle \hat{B}_{\mathbf{q}-\mathbf{k}-\mathbf{k}',b} \hat{B}^*_{\mathbf{q},i} \right\rangle - q_a k'_b \left\langle \hat{B}_{\mathbf{k},a} \hat{B}^*_{\mathbf{q},i} \right\rangle \left\langle \hat{B}_{\mathbf{q}-\mathbf{k}-\mathbf{k}',b} \hat{B}^*_{-\mathbf{k}',i} \right\rangle \Big) \Big] \mathrm{d}^3k' \mathrm{d}^3k \Bigg\} .
\end{aligned} \tag{B.8}$$

As the aim is to find an expression in terms of M_q, U_q and $\mathcal{H}_q$, the relations (1.127) and (1.131) have to be used, assuming, however, vanishing kinetic helicity in (1.131). Since this involves the evaluation of Delta Functions, it has to be stated that the Delta Functions used here are not to be regarded as Dirac Delta Functions, but rather the integral expansion of the Kronecker Delta (cf. Sec. A.2), therefore, also taking into account the normalization, fulfilling the relations

$$\int \delta^{(3)}(\mathbf{q}-\mathbf{k}) f(\mathbf{k}) \, \mathrm{d}^3k = \int \delta^{(3)}(\mathbf{k}-\mathbf{q}) f(\mathbf{k}) \mathrm{d}^3k = f(\mathbf{q}) \,, \tag{B.9}$$

$$\int \delta^{(3)}(\mathbf{q}-\mathbf{k}) \delta^{(3)}(\mathbf{k}'-\mathbf{k}) f(\mathbf{k}) \, \mathrm{d}^3k = \delta^{(3)}(\mathbf{k}'-\mathbf{q}) f(\mathbf{q}) = \delta^{(3)}(\mathbf{q}-\mathbf{k}') f(\mathbf{q}') \,, \tag{B.10}$$

$$\int \delta^{(3)}(\mathbf{q}-\mathbf{k}) \delta^{(3)}(\mathbf{q}-\mathbf{k}) f(\mathbf{k}) \, \mathrm{d}^3k = \frac{V}{(2\pi)^3} f(\mathbf{q}) \,. \tag{B.11}$$

Taking all this into account, (B.8) may be further simplified: Looking at the first parenthesis inside the double integral, one can see that for all terms the helical terms vanish and, furthermore, the fifth and sixth terms cancel each other, while the fourth, the ninth and the tenth

terms average to zero. In a similar way also the second parenthesis inside the double integral may be simplified, contributing, however, helical components as well. Taken together, (B.8) can be expressed as

$$\begin{aligned}\left\langle \left(\partial_t \hat{B}_{\mathbf{q},i}\right) \hat{B}^*_{\mathbf{q},i} \right\rangle = &-\frac{2\rho}{4\pi\sigma} \langle M_q \rangle + \frac{\Delta t}{2} \Bigg\{ \frac{4q^2\rho}{(4\pi\sigma)^2} \langle M_q \rangle + \int \Big[-\frac{\rho}{2\pi} \frac{k^2}{k_1^4} \sin^2\theta \langle M_q \rangle \langle U_{k_1} \rangle + \frac{\rho}{2\pi} \frac{q^2}{k_1^2 k^2} \sin^2\theta \frac{q^2+k^2-qk\cos\theta}{q^2+k^2-2qk\cos\theta} \langle M_k \rangle \langle U_{k_1} \rangle \\ &+ \frac{\rho}{4\pi} \frac{1}{k^2} \left(-3+\cos^2\theta\right) \langle M_k \rangle \langle M_q \rangle + \frac{\rho}{32(2\pi)^3} \left(-2\frac{q}{k}\cos\theta + 2 + \sin^2\theta\right) \mathcal{H}_q \mathcal{H}_k \Big] \mathrm{d}^3k \Bigg\}.\end{aligned} \tag{B.12}$$

Here the Delta Functions have been evaluated with the d^3k' integral according to (B.9)-(B.11). Furthermore, several definitions have been introduced: The vector $\mathbf{k}_1$ is given by $\mathbf{k}_1 = \mathbf{q} - \mathbf{k}$, while q, k and k_1 denote the magnitude of the vectors $\mathbf{q}$, $\mathbf{k}$ and $\mathbf{k}_1$, respectively. In addition, the angle θ is defined to be situated between $\mathbf{q}$ and $\mathbf{k}$, i.e. $\mathbf{q} \cdot \mathbf{k} = qk\cos\theta$. Therefore, for $\langle \partial_t M_q \rangle$ one can finally write down the expression

$$\begin{aligned}\langle \partial_t M_q \rangle \overset{(3.46)}{=} \frac{q^2}{\rho} \left\langle \left(\partial_t \hat{B}_{\mathbf{q},i}\right) \hat{B}^*_{\mathbf{q},i} \right\rangle = &-\frac{2q^2}{4\pi\sigma} \langle M_q \rangle + \frac{\Delta t}{2} \Bigg\{ \frac{4q^4}{(4\pi\sigma)^2} \langle M_q \rangle + \int \Big[-\frac{1}{2\pi} \frac{q^2k^2}{k_1^4} \sin^2\theta \langle M_q \rangle \langle U_{k_1} \rangle \\ &+ \frac{1}{2\pi} \frac{q^4}{k_1^2 k^2} \sin^2\theta \frac{q^2+k^2-qk\cos\theta}{q^2+k^2-2qk\cos\theta} \langle M_k \rangle \langle U_{k_1} \rangle + \frac{1}{4\pi} \frac{q^2}{k^2} \left(-3+\cos^2\theta\right) \langle M_k \rangle \langle M_q \rangle + \frac{q^2}{32(2\pi)^3} \left(-2\frac{q}{k}\cos\theta + 2 + \sin^2\theta\right) \mathcal{H}_q \mathcal{H}_k \Big] \mathrm{d}^3k \Bigg\}.\end{aligned} \tag{B.13}$$

Rewriting the integration as $\mathrm{d}^3k = k^2 \sin\theta \mathrm{d}k\mathrm{d}\phi\mathrm{d}\theta = 2\pi k^2 \sin\theta \mathrm{d}k\mathrm{d}\theta$, since the integrand is independent of ϕ, and evaluating the θ-integral for the last two terms of (B.13) gives the final result for $\langle \partial_t M_q \rangle$, namely

$$\begin{aligned}\langle \partial_t M_q \rangle \overset{(3.46)}{=} \frac{q^2}{\rho} \left\langle \left(\partial_t \hat{B}_{\mathbf{q},i}\right) \hat{B}^*_{\mathbf{q},i} \right\rangle = &-\frac{2q^2}{4\pi\sigma} \langle M_q \rangle + \Delta t \Bigg\{ \frac{2q^4}{(4\pi\sigma)^2} \langle M_q \rangle + \iint \Big[-\frac{q^2k^4}{2k_1^4} \sin^3\theta \langle M_q \rangle \langle U_{k_1} \rangle \\ &+ \frac{q^4}{2k_1^2} \sin^3\theta \frac{q^2+k^2-qk\cos\theta}{q^2+k^2-2qk\cos\theta} \langle M_k \rangle \langle U_{k_1} \rangle \Big] \mathrm{d}\theta\mathrm{d}k + \int \Big[-\frac{4}{3}q^2 \langle M_k \rangle \langle M_q \rangle + \frac{q^2k^2}{3(4\pi)^2} \mathcal{H}_q \mathcal{H}_k \Big] \mathrm{d}k \Bigg\}.\end{aligned} \tag{B.14}$$

In a rather similar way the calculations may be carried out for the time development of the magnetic helicity, i.e. for (3.48). The only difference is that instead of $\left(\partial_t \hat{B}_{\mathbf{q},i}\right) \hat{B}^*_{\mathbf{q},i}$, terms of the form $\epsilon_{ijl} q_j \left(\partial_t \hat{B}_{\mathbf{q},l}\right) \hat{B}^*_{\mathbf{q},i}$ have to be calculated. Therefore the first steps of the

calculation will be skipped, the equation corresponding to the stage of (B.8) being the starting point:

$$\begin{aligned}
\epsilon_{ijl}q_j\left\langle\left(\partial_t\hat{B}_{\mathbf{q},l}\right)\hat{B}^*_{\mathbf{q},i}\right\rangle &= \epsilon_{ijl}q_j\Bigg(-\frac{q^2}{4\pi\sigma}\left\langle\hat{B}_{\mathbf{q},l}\hat{B}^*_{\mathbf{q},i}\right\rangle + \frac{\Delta t}{2}\Bigg\{2\frac{q^4}{(4\pi\sigma)^2}\left\langle\hat{B}_{\mathbf{q},l}\hat{B}^*_{\mathbf{q},i}\right\rangle + \frac{V}{(2\pi)^3}\iint\Big[\Big(q_aq_b\left\langle\hat{B}_{\mathbf{k},a}\hat{B}^*_{\mathbf{k}',b}\right\rangle\left\langle\hat{v}_{\mathbf{q}-\mathbf{k},l}\hat{v}^*_{\mathbf{q}-\mathbf{k}',i}\right\rangle \\
&- q_aq_b\left\langle\hat{B}_{\mathbf{k},a}\hat{B}^*_{\mathbf{k}',i}\right\rangle\left\langle\hat{v}_{\mathbf{q}-\mathbf{k},l}\hat{v}^*_{\mathbf{q}-\mathbf{k}',b}\right\rangle - q_aq_b\left\langle\hat{B}_{\mathbf{k},l}\hat{B}^*_{\mathbf{k}',b}\right\rangle\left\langle\hat{v}_{\mathbf{q}-\mathbf{k},a}\hat{v}^*_{\mathbf{q}-\mathbf{k}',i}\right\rangle + q_aq_b\left\langle\hat{B}_{\mathbf{k},l}\hat{B}^*_{\mathbf{k}',i}\right\rangle\left\langle\hat{v}_{\mathbf{q}-\mathbf{k},a}\hat{v}^*_{\mathbf{q}-\mathbf{k}',b}\right\rangle \\
&- q_ak_b\left\langle\hat{B}_{\mathbf{k}',b}\hat{B}^*_{\mathbf{q},i}\right\rangle\left\langle\hat{v}_{\mathbf{q}-\mathbf{k},l}\hat{v}^*_{-\mathbf{k}+\mathbf{k}',a}\right\rangle + q_ak_b\left\langle\hat{B}_{\mathbf{k}',b}\hat{B}^*_{\mathbf{q},i}\right\rangle\left\langle\hat{v}_{\mathbf{q}-\mathbf{k},a}\hat{v}^*_{-\mathbf{k}+\mathbf{k}',l}\right\rangle + q_ak_b\left\langle\hat{B}_{\mathbf{k}',a}\hat{B}^*_{\mathbf{q},i}\right\rangle\left\langle\hat{v}_{\mathbf{q}-\mathbf{k},l}\hat{v}^*_{-\mathbf{k}+\mathbf{k}',b}\right\rangle \\
&- q_ak_b\left\langle\hat{B}_{\mathbf{k}',l}\hat{B}^*_{\mathbf{q},i}\right\rangle\left\langle\hat{v}_{\mathbf{q}-\mathbf{k},a}\hat{v}^*_{-\mathbf{k}+\mathbf{k}',b}\right\rangle + k'_aq_b\left\langle\hat{B}_{\mathbf{k},b}\hat{B}^*_{\mathbf{q},i}\right\rangle\left\langle\hat{v}_{\mathbf{q}-\mathbf{k}-\mathbf{k}',a}\hat{v}^*_{-\mathbf{k}',l}\right\rangle - q_bk'_a\left\langle\hat{B}_{\mathbf{k},l}\hat{B}^*_{\mathbf{q},i}\right\rangle\left\langle\hat{v}_{\mathbf{q}-\mathbf{k}-\mathbf{k}',a}\hat{v}^*_{-\mathbf{k}',b}\right\rangle\Big) \\
&+ \frac{1}{4\pi\rho}\Big(-q_ak'_a\left\langle\hat{B}_{\mathbf{q}-\mathbf{k}-\mathbf{k}',b}\hat{B}^*_{-\mathbf{k}',b}\right\rangle\left\langle\hat{B}_{\mathbf{k},l}\hat{B}^*_{\mathbf{q},i}\right\rangle - q_ak'_a\left\langle\hat{B}_{\mathbf{q}-\mathbf{k}-\mathbf{k}',b}\hat{B}^*_{-\mathbf{k},l}\right\rangle\left\langle\hat{B}_{\mathbf{k}',b}\hat{B}^*_{\mathbf{q},i}\right\rangle - q_ak'_a\left\langle\hat{B}_{\mathbf{q}-\mathbf{k}-\mathbf{k}',b}\hat{B}^*_{\mathbf{q},i}\right\rangle\left\langle\hat{B}_{\mathbf{k}',b}\hat{B}^*_{-\mathbf{k},l}\right\rangle \\
&+ q_ak'_l\left\langle\hat{B}_{\mathbf{q}-\mathbf{k}-\mathbf{k}',b}\hat{B}^*_{-\mathbf{k},a}\right\rangle\left\langle\hat{B}_{\mathbf{k}',b}\hat{B}^*_{\mathbf{q},i}\right\rangle + q_ak'_l\left\langle\hat{B}_{\mathbf{k},a}\hat{B}^*_{-\mathbf{k}',b}\right\rangle\left\langle\hat{B}_{\mathbf{q}-\mathbf{k}-\mathbf{k}',b}\hat{B}^*_{\mathbf{q},i}\right\rangle + q_ak'_l\left\langle\hat{B}_{\mathbf{k},a}\hat{B}^*_{\mathbf{q},i}\right\rangle\left\langle\hat{B}_{\mathbf{q}-\mathbf{k}-\mathbf{k}',b}\hat{B}^*_{-\mathbf{k}',b}\right\rangle \\
&+ q_ak'_b\left\langle\hat{B}_{\mathbf{q}-\mathbf{k}-\mathbf{k}',b}\hat{B}^*_{-\mathbf{k}',a}\right\rangle\left\langle\hat{B}_{\mathbf{k},l}\hat{B}^*_{\mathbf{q},i}\right\rangle + q_ak'_b\left\langle\hat{B}_{\mathbf{k}',a}\hat{B}^*_{-\mathbf{k},l}\right\rangle\left\langle\hat{B}_{\mathbf{q}-\mathbf{k}-\mathbf{k}',b}\hat{B}^*_{\mathbf{q},i}\right\rangle + q_ak'_b\left\langle\hat{B}_{\mathbf{k}',a}\hat{B}^*_{\mathbf{q},i}\right\rangle\left\langle\hat{B}_{\mathbf{q}-\mathbf{k}-\mathbf{k}',b}\hat{B}_{\mathbf{k},l}\right\rangle \\
&- q_ak'_b\left\langle\hat{B}_{\mathbf{q}-\mathbf{k}-\mathbf{k}',b}\hat{B}^*_{-\mathbf{k},a}\right\rangle\left\langle\hat{B}_{\mathbf{k}',l}\hat{B}^*_{\mathbf{q},i}\right\rangle - q_ak'_b\left\langle\hat{B}_{\mathbf{k},a}\hat{B}^*_{-\mathbf{k}',l}\right\rangle\left\langle\hat{B}_{\mathbf{q}-\mathbf{k}-\mathbf{k}',b}\hat{B}^*_{\mathbf{q},i}\right\rangle - q_ak'_b\left\langle\hat{B}_{\mathbf{k},a}\hat{B}^*_{\mathbf{q},i}\right\rangle\left\langle\hat{B}_{\mathbf{q}-\mathbf{k}-\mathbf{k}',b}\hat{B}^*_{-\mathbf{k}',l}\right\rangle\Big)\Big]\mathrm{d}^3k'\mathrm{d}^3k\Bigg\}\Bigg).
\end{aligned} \tag{B.15}$$

Here again several terms are zero in the ensemble average, namely the first, the seventh, the ninth and the tenth terms inside the first parenthesis. Furthermore, it turns out that the remaining terms from that parenthesis only contribute expressions of the symbolic form $f(q,k,\theta)U\mathcal{H}$ (with some regular function f of the corresponding quantities), while the second parenthesis gives a sum of terms looking like $f(q,k,\theta)M\mathcal{H}$. Combining and simplifying all of these therefore gives

$$\begin{aligned}
\epsilon_{ijl}q_j\left\langle\left(\partial_t\hat{B}_{\mathbf{q},l}\right)\hat{B}^*_{\mathbf{q},i}\right\rangle &= \frac{i\rho q^2}{(4\pi)^2\sigma}\left\langle\mathcal{H}_q\right\rangle + \frac{\Delta t}{2}\Bigg\{-2\frac{i\rho q^4}{(4\pi)^3\sigma^2}\left\langle\mathcal{H}_q\right\rangle + \int\Bigg[-\frac{\rho}{(4\pi)^2i}\frac{q^2k^2\sin^2\theta}{k_1^4}\left\langle U_{k_1}\right\rangle\left\langle\mathcal{H}_q\right\rangle + \frac{\rho}{(4\pi)^2i}\frac{q^4\sin^2\theta}{k_1^4}\left\langle U_{k_1}\right\rangle\left\langle\mathcal{H}_k\right\rangle \\
&+ \frac{\rho}{(4\pi)^2i}\frac{1}{k^2}\left(-qk\cos\theta + k^2 + \frac{1}{2}k^2\sin^2\theta\right)\left\langle M_q\right\rangle\left\langle\mathcal{H}_k\right\rangle - \frac{\rho}{(4\pi)^2i}\frac{1}{k^2}\left(q^2 + \frac{1}{2}q^2\sin^2\theta + qk\cos\theta\right)\left\langle M_k\right\rangle\left\langle\mathcal{H}_q\right\rangle\Bigg]\mathrm{d}^3k\Bigg\}.
\end{aligned} \tag{B.16}$$

Transforming the $\int ...\,\mathrm{d}^3k$ integral into $2\pi\int ...\,k^2\sin\theta\mathrm{d}\theta\mathrm{d}k$, evaluating the θ-integral for the last two terms and, finally, according to (3.48),

multiplying everything by $8\pi i/\rho$ in order to get an expression for $\langle \partial_t \mathcal{H}_q \rangle$, results in

$$\langle \partial_t \mathcal{H}_q \rangle = \frac{8\pi i}{\rho} \epsilon_{ijl} q_j \left\langle \left(\partial_t \hat{B}_{\mathbf{q},l} \right) \hat{B}^*_{\mathbf{q},i} \right\rangle = -\frac{2q^2}{4\pi\sigma} \langle \mathcal{H}_q \rangle + \Delta t \Bigg\{ \frac{2q^4}{(4\pi\sigma)^2} \langle \mathcal{H}_q \rangle + \iint \Bigg[-\frac{q^2 k^4 \sin^3\theta}{2k_1^4} \langle U_{k_1} \rangle \langle \mathcal{H}_q \rangle + \frac{q^4 k^2 \sin^3\theta}{2k_1^4} \langle U_{k_1} \rangle \langle \mathcal{H}_k \rangle \Bigg] \mathrm{d}\theta \mathrm{d}k$$
$$+ \int \left[\frac{4}{3} k^2 \langle M_q \rangle \langle \mathcal{H}_k \rangle - \frac{4}{3} q^2 \langle M_k \rangle \langle \mathcal{H}_q \rangle \right] \mathrm{d}k \Bigg\} . \tag{B.17}$$

Finally, in order to calculate (3.47), one has to consider $(\partial_t \hat{v}_{\mathbf{q},i})\, \hat{v}^*_{\mathbf{q},i}$, therefore

$$(\partial_t \hat{v}_{\mathbf{q},i})\, \hat{v}^*_{\mathbf{q},i} = \frac{iV^{\frac{1}{2}}}{(2\pi)^{\frac{3}{2}}} \int \Big[-k_a \hat{v}_{\mathbf{q}-\mathbf{k},a} \hat{v}_{\mathbf{k},i} \hat{v}^*_{\mathbf{q},i} + \frac{1}{4\pi\rho} k_a \hat{B}_{\mathbf{q}-\mathbf{k},a} \hat{B}_{\mathbf{k},i} \hat{v}^*_{\mathbf{q},i} - \frac{1}{4\pi\rho} \hat{B}_{\mathbf{q}-\mathbf{k},a} \hat{B}_{\mathbf{k},a} k_i \hat{v}^*_{\mathbf{q},i} \Big] \mathrm{d}^3 k$$
$$+ \frac{\Delta t}{2} \Bigg(\frac{iV^{\frac{1}{2}}}{(2\pi)^{\frac{3}{2}}} \frac{1}{4\pi\sigma} \frac{1}{4\pi\rho} \iint \Big\{ \Big[k^2 + (\mathbf{q}-\mathbf{k})^2 \Big] \Big[k_i \hat{B}_{\mathbf{q}-\mathbf{k},a} \hat{B}_{\mathbf{k},a} \hat{v}^*_{\mathbf{q},i} - k_a \hat{B}_{\mathbf{q}-\mathbf{k},a} \hat{B}_{\mathbf{k}} \hat{v}^*_{\mathbf{q},i} \Big] \Big\} \mathrm{d}^3 k' \mathrm{d}^3 k + \frac{V}{(2\pi)^3} \iint \Big\{ k_a k'_b \hat{v}_{\mathbf{q}-\mathbf{k},a} \hat{v}^*_{\mathbf{q}-\mathbf{k}',b} \hat{v}_{\mathbf{k},i} \hat{v}^*_{\mathbf{k}',i}$$
$$- k_a k'_b \hat{v}_{\mathbf{q}-\mathbf{k},a} \hat{v}_{\mathbf{k}-\mathbf{k}',b} \hat{v}_{\mathbf{k}',i} \hat{v}^*_{\mathbf{q},i} - k'_a k_b \hat{v}_{\mathbf{q}-\mathbf{k}-\mathbf{k}',a} \hat{v}_{\mathbf{k}',b} \hat{v}_{\mathbf{k},i} \hat{v}^*_{\mathbf{q},i} + \frac{1}{4\pi\rho} \Big[-k_a k'_b \hat{B}^*_{\mathbf{q}-\mathbf{k}',b} \hat{B}^*_{\mathbf{k}',i} \hat{v}_{\mathbf{q}-\mathbf{k},a} \hat{v}_{\mathbf{k},i} + k_a k'_i \hat{B}^*_{\mathbf{q}-\mathbf{k}',b} \hat{B}^*_{\mathbf{k}',b} \hat{v}_{\mathbf{q}-\mathbf{k},a} \hat{v}_{\mathbf{k},i}$$
$$- k_a k'_b \hat{B}_{\mathbf{q}-\mathbf{k},a} \hat{B}_{\mathbf{k},i} \hat{v}^*_{\mathbf{q}-\mathbf{k}',b} \hat{v}^*_{\mathbf{k}',i} + k_i k'_b \hat{B}_{\mathbf{q}-\mathbf{k},a} \hat{B}_{\mathbf{k},a} \hat{v}^*_{\mathbf{q}-\mathbf{k}',b} \hat{v}^*_{\mathbf{k}',i} + k_a k'_b \hat{B}_{\mathbf{k}-\mathbf{k}',b} \hat{B}_{\mathbf{k}',i} \hat{v}_{\mathbf{q}-\mathbf{k},a} \hat{v}^*_{\mathbf{q},i} - k_a k'_i \hat{B}_{\mathbf{k}-\mathbf{k}',b} \hat{B}_{\mathbf{k}',b} \hat{v}_{\mathbf{q}-\mathbf{k},a} \hat{v}^*_{\mathbf{q},i}$$
$$- k_a k_b \hat{B}_{\mathbf{q}-\mathbf{k},a} \hat{B}_{\mathbf{k}',b} \hat{v}_{\mathbf{k}-\mathbf{k}',i} \hat{v}^*_{\mathbf{q},i} + k_a k_b \hat{B}_{\mathbf{q}-\mathbf{k},a} \hat{B}_{\mathbf{k}',i} \hat{v}_{\mathbf{k}-\mathbf{k}',b} \hat{v}^*_{\mathbf{q},i} - q_a k_b \hat{B}_{\mathbf{k}',a} \hat{B}_{\mathbf{k}} \hat{v}_{\mathbf{q}-\mathbf{k}-\mathbf{k}',b} \hat{v}^*_{\mathbf{q},i} + k_a q_b \hat{B}_{\mathbf{k},i} \hat{B}_{\mathbf{k}',a} \hat{v}_{\mathbf{q}-\mathbf{k}-\mathbf{k}',b} \hat{v}^*_{\mathbf{q},i}$$
$$+ k'_a k_b \hat{B}_{\mathbf{q}-\mathbf{k}-\mathbf{k}',a} \hat{B}_{\mathbf{k}',b} \hat{v}_{\mathbf{k},i} \hat{v}^*_{\mathbf{q},i} - k_a k'_a \hat{B}_{\mathbf{q}-\mathbf{k}-\mathbf{k}',b} \hat{B}_{\mathbf{k}',b} \hat{v}_{\mathbf{k},i} \hat{v}^*_{\mathbf{q},i} + k_a k_i \hat{B}_{\mathbf{q}-\mathbf{k},b} \hat{B}_{\mathbf{k}',a} \hat{v}_{\mathbf{k}-\mathbf{k}',b} \hat{v}^*_{\mathbf{q},i} - k_a k_i \hat{B}_{\mathbf{q}-\mathbf{k},b} \hat{B}_{\mathbf{k}',b} \hat{\mathbf{v}}_{\mathbf{k}-\mathbf{k}',a} \hat{v}^*_{\mathbf{q},i}$$
$$+ q_a k_i \hat{B}_{\mathbf{k}',a} \hat{B}_{\mathbf{k},b} \hat{v}_{\mathbf{q}-\mathbf{k}-\mathbf{k}',b} \hat{v}^*_{\mathbf{q},i} - k_a k_i \hat{B}_{\mathbf{k},b} \hat{B}_{\mathbf{k}',a} \hat{v}_{\mathbf{q}-\mathbf{k}-\mathbf{k}',b} \hat{v}^*_{\mathbf{q},i} - q_a k_i \hat{B}_{\mathbf{k},b} \hat{B}_{\mathbf{k}',b} \hat{v}_{\mathbf{q}-\mathbf{k}-\mathbf{k}',a} \hat{v}^*_{\mathbf{q},i} + k_a k_i \hat{B}_{\mathbf{k},b} \hat{B}_{\mathbf{k}',b} \hat{v}_{\mathbf{q}-\mathbf{k}-\mathbf{k}',a} \hat{v}^*_{\mathbf{q},i} \Big] + \frac{1}{(4\pi\rho)^2} \Big[$$
$$k_a k'_b \hat{B}_{\mathbf{q}-\mathbf{k},a} \hat{B}_{\mathbf{k},i} \hat{B}^*_{\mathbf{q}-\mathbf{k}',b} \hat{B}^*_{\mathbf{k}',i} - k_a k'_i \hat{B}_{\mathbf{q}-\mathbf{k},a} \hat{B}_{\mathbf{k},i} \hat{B}^*_{\mathbf{q}-\mathbf{k}',b} \hat{B}^*_{\mathbf{k}',b} - k_i k'_b \hat{B}_{\mathbf{q}-\mathbf{k},a} \hat{B}_{\mathbf{k},a} \hat{B}^*_{\mathbf{q}-\mathbf{k}',b} \hat{B}^*_{\mathbf{k}',i} + k_i k'_i \hat{B}_{\mathbf{q}-\mathbf{k},a} \hat{B}_{\mathbf{k},a} \hat{B}^*_{\mathbf{q}-\mathbf{k}',b} \hat{B}^*_{\mathbf{k}',b} \Big] \Big\} \mathrm{d}^3 k' \mathrm{d}^3 k \Bigg) . \tag{B.18}$$

In the same way as for (B.3) now the ensemble average is taken, i.e. one gets various terms of the form $\langle \hat{v}_i \hat{v}_j \rangle$, $\langle \hat{v}_i \hat{v}_j \hat{v}_k \rangle$ $\left\langle \hat{B}_i \hat{v}_j \hat{v}_k \right\rangle$, $\left\langle \hat{B}_i \hat{B}_j \hat{v}_k \hat{v}_l \right\rangle$ and $\langle \hat{v}_i \hat{v}_j \hat{v}_k \hat{v}_l \rangle$, which, with Isserlis' Theorem, (1.142), and $\left\langle \hat{v} \hat{B} \right\rangle = 0$ become

$$\left\langle \hat{B}_i \hat{B}_j \hat{v}_k \right\rangle = \langle \hat{v}_i \hat{v}_j \hat{v}_k \rangle = 0 , \tag{B.19}$$

$$\left\langle \hat{B}_i \hat{B}_j \hat{v}_k \hat{v}_l \right\rangle = \left\langle \hat{B}_i \hat{B}_j \right\rangle \langle \hat{v}_k \hat{v}_l \rangle \ , \tag{B.20}$$

$$\langle \hat{v}_i \hat{v}_j \hat{v}_k \hat{v}_l \rangle \overset{(1.143)}{=} \langle \hat{v}_i \hat{v}_j \rangle \langle \hat{v}_k \hat{v}_l \rangle + \langle \hat{v}_i \hat{v}_k \rangle \langle \hat{v}_j \hat{v}_l \rangle + \langle \hat{v}_i \hat{v}_l \rangle \langle \hat{v}_j \hat{v}_k \rangle \ . \tag{B.21}$$

Furthermore, since $\mathbf{B}(\mathbf{r})$ and $\mathbf{v}(\mathbf{r})$ are real, it means that the complex conjugate of their Fourier Transform is again given by

$$\hat{\mathbf{B}}^*_{\mathbf{q}} = \hat{\mathbf{B}}_{-\mathbf{q}} \, , \, \hat{\mathbf{v}}^*_{\mathbf{q}} = \hat{\mathbf{v}}_{-\mathbf{q}} \, , \tag{B.22}$$

and hence

$$\begin{aligned}
&\left\langle (\partial_t \hat{v}_{\mathbf{q},i}) \, \hat{v}^*_{\mathbf{q},i} \right\rangle = \frac{\Delta t}{2} \Bigg(\frac{V}{(2\pi)^3} \iint \Big\{ k_a k'_b \left\langle \hat{v}_{\mathbf{q}-\mathbf{k},a} \hat{v}^*_{\mathbf{q}-\mathbf{k}',b} \right\rangle \left\langle \hat{v}_{\mathbf{k},i} \hat{v}^*_{\mathbf{k}',i} \right\rangle + k_a k'_b \left\langle \hat{v}_{\mathbf{q}-\mathbf{k},a} \hat{v}^*_{-\mathbf{k},i} \right\rangle \left\langle \hat{v}_{-\mathbf{k}',i} \hat{v}^*_{\mathbf{q}-\mathbf{k}',b} \right\rangle + k_a k'_b \left\langle \hat{v}_{\mathbf{q}-\mathbf{k},a} \hat{v}^*_{\mathbf{k}',i} \right\rangle \left\langle \hat{v}_{\mathbf{k},i} \hat{v}^*_{\mathbf{q}-\mathbf{k}',b} \right\rangle \\
&- k_a k'_b \left\langle \hat{v}_{\mathbf{q}-\mathbf{k},a} \hat{v}^*_{-\mathbf{k}+\mathbf{k}',b} \right\rangle \left\langle \hat{v}_{\mathbf{k}',i} \hat{v}^*_{\mathbf{q},i} \right\rangle - k_a k'_b \left\langle \hat{v}_{\mathbf{q}-\mathbf{k},a} \hat{v}^*_{-\mathbf{k}',i} \right\rangle \left\langle \hat{v}_{\mathbf{k}-\mathbf{k}',b} \hat{v}^*_{\mathbf{q},i} \right\rangle - k_a k'_b \left\langle \hat{v}_{\mathbf{q}-\mathbf{k},a} \hat{v}^*_{\mathbf{q},i} \right\rangle \left\langle \hat{v}_{\mathbf{k}-\mathbf{k}',b} \hat{v}^*_{-\mathbf{k}',i} \right\rangle \\
&- k'_a k_b \left\langle \hat{v}_{\mathbf{q}-\mathbf{k}-\mathbf{k}',a} \hat{v}^*_{-\mathbf{k}',b} \right\rangle \left\langle \hat{v}_{\mathbf{k},i} \hat{v}^*_{\mathbf{q},i} \right\rangle - k'_a k_b \left\langle \hat{v}_{\mathbf{q}-\mathbf{k}-\mathbf{k}',a} \hat{v}^*_{-\mathbf{k},i} \right\rangle \left\langle \hat{v}_{\mathbf{k}',b} \hat{v}^*_{\mathbf{q},i} \right\rangle - k'_a k_b \left\langle \hat{v}_{\mathbf{q}-\mathbf{k}-\mathbf{k}',a} \hat{v}^*_{\mathbf{q},i} \right\rangle \left\langle \hat{v}_{\mathbf{k},i} \hat{v}^*_{\mathbf{k}',b} \right\rangle \\
&+ \frac{1}{4\pi\rho} \Big[- k_a k'_b \left\langle \hat{B}_{-\mathbf{q}+\mathbf{k}',b} \hat{B}^*_{\mathbf{k}',i} \right\rangle \left\langle \hat{v}_{\mathbf{q}-\mathbf{k},a} \hat{v}^*_{-\mathbf{k},i} \right\rangle + k_a k'_i \left\langle \hat{B}_{-\mathbf{q}+\mathbf{k}',b} \hat{B}^*_{\mathbf{k}',b} \right\rangle \left\langle \hat{v}_{\mathbf{q}-\mathbf{k},a} \hat{v}^*_{-\mathbf{k},i} \right\rangle - k_a k'_b \left\langle \hat{B}_{\mathbf{q}-\mathbf{k},a} \hat{B}^*_{-\mathbf{k},i} \right\rangle \left\langle \hat{v}_{-\mathbf{q}+\mathbf{k}',b} \hat{v}^*_{\mathbf{k}',i} \right\rangle \\
&+ k_i k'_b \left\langle \hat{B}_{\mathbf{q}-\mathbf{k},a} \hat{B}^*_{-\mathbf{k},a} \right\rangle \left\langle \hat{v}_{-\mathbf{q}+\mathbf{k}',b} \hat{v}^*_{\mathbf{k}',i} \right\rangle + k_a k'_b \left\langle \hat{B}_{\mathbf{k}-\mathbf{k}',b} \hat{B}^*_{-\mathbf{k}',i} \right\rangle \left\langle \hat{v}_{\mathbf{q}-\mathbf{k},a} \hat{v}^*_{\mathbf{q},i} \right\rangle - k_a k'_i \left\langle \hat{B}_{\mathbf{k}-\mathbf{k}',b} \hat{B}^*_{-\mathbf{k}',b} \right\rangle \left\langle \hat{v}_{\mathbf{q}-\mathbf{k},a} \hat{v}^*_{\mathbf{q},i} \right\rangle \\
&- k_a k_b \left\langle \hat{B}_{\mathbf{q}-\mathbf{k},a} \hat{B}^*_{-\mathbf{k}',a} \right\rangle \left\langle \hat{v}_{\mathbf{k}-\mathbf{k}',i} \hat{v}^*_{\mathbf{q},i} \right\rangle + k_a k_b \left\langle \hat{B}_{\mathbf{q}-\mathbf{k},a} \hat{B}^*_{-\mathbf{k}',i} \right\rangle \left\langle \hat{v}_{\mathbf{k}-\mathbf{k}',b} \hat{v}^*_{\mathbf{q},i} \right\rangle - q_a k_b \left\langle \hat{B}_{\mathbf{k},i} \hat{B}^*_{-\mathbf{k}',a} \right\rangle \left\langle \hat{v}_{\mathbf{q}-\mathbf{k}-\mathbf{k}',b} \hat{v}^*_{\mathbf{q},i} \right\rangle \\
&+ k_a q_b \left\langle \hat{B}_{\mathbf{k},i} \hat{B}^*_{-\mathbf{k}',a} \right\rangle \left\langle \hat{v}_{\mathbf{q}-\mathbf{k}-\mathbf{k}',b} \hat{v}^*_{\mathbf{q},i} \right\rangle + k'_a k_b \left\langle \hat{B}_{\mathbf{q}-\mathbf{k}-\mathbf{k}',a} \hat{B}^*_{-\mathbf{k}',b} \right\rangle \left\langle \hat{v}_{\mathbf{k},i} \hat{v}^*_{\mathbf{q},i} \right\rangle - k_a k'_a \left\langle \hat{B}_{\mathbf{q}-\mathbf{k}-\mathbf{k}',b} \hat{B}^*_{-\mathbf{k}',b} \right\rangle \left\langle \hat{v}_{\mathbf{k},i} \hat{v}^*_{\mathbf{q},i} \right\rangle \\
&+ k_a k_i \left\langle \hat{B}_{\mathbf{q}-\mathbf{k},b} \hat{B}^*_{-\mathbf{k}',a} \right\rangle \left\langle \hat{v}_{\mathbf{k}-\mathbf{k}',b} \hat{v}^*_{\mathbf{q},i} \right\rangle - k_a k_i \left\langle \hat{B}_{\mathbf{q}-\mathbf{k},b} \hat{B}^*_{-\mathbf{k}',b} \right\rangle \left\langle \hat{v}_{\mathbf{k}-\mathbf{k}',a} \hat{v}^*_{\mathbf{q},i} \right\rangle + q_a k_i \left\langle \hat{B}_{\mathbf{k},b} \hat{B}^*_{-\mathbf{k}',a} \right\rangle \left\langle \hat{v}_{\mathbf{q}-\mathbf{k}-\mathbf{k}',b} \hat{v}^*_{\mathbf{q},i} \right\rangle \\
&- k_a k_i \left\langle \hat{B}_{\mathbf{k},b} \hat{B}^*_{-\mathbf{k}',a} \right\rangle \left\langle \hat{v}_{\mathbf{q}-\mathbf{k}-\mathbf{k}',b} \hat{v}^*_{\mathbf{q},i} \right\rangle - q_a k_i \left\langle \hat{B}_{\mathbf{k},b} \hat{B}^*_{-\mathbf{k}',b} \right\rangle \left\langle \hat{v}_{\mathbf{q}-\mathbf{k}-\mathbf{k}',a} \hat{v}^*_{\mathbf{q},i} \right\rangle + k_a k_i \left\langle \hat{B}_{\mathbf{k},b} \hat{B}^*_{-\mathbf{k}',b} \right\rangle \left\langle \hat{v}_{\mathbf{q}-\mathbf{k}-\mathbf{k}',a} \hat{v}^*_{\mathbf{q},i} \right\rangle \Big] \\
&+ \frac{1}{(4\pi\rho)^2} \Big[k_a k'_b \left\langle \hat{B}_{\mathbf{q}-\mathbf{k},a} \hat{B}^*_{-\mathbf{k},i} \right\rangle \left\langle \hat{B}_{-\mathbf{q}+\mathbf{k}',b} \hat{B}^*_{\mathbf{k}',i} \right\rangle + k_a k'_b \left\langle \hat{B}_{\mathbf{q}-\mathbf{k},a} \hat{B}^*_{\mathbf{q}-\mathbf{k}',b} \right\rangle \left\langle \hat{B}_{\mathbf{k},i} \hat{B}^*_{\mathbf{k}',i} \right\rangle + k_a k'_b \left\langle \hat{B}_{\mathbf{q}-\mathbf{k},a} \hat{B}^*_{\mathbf{k}',i} \right\rangle \left\langle \hat{B}_{\mathbf{k},i} \hat{B}^*_{\mathbf{q}-\mathbf{k}',b} \right\rangle \\
&- k_a k'_i \left\langle \hat{B}_{\mathbf{q}-\mathbf{k},a} \hat{B}^*_{-\mathbf{k},i} \right\rangle \left\langle \hat{B}_{-\mathbf{q}+\mathbf{k}',b} \hat{B}^*_{\mathbf{k}',b} \right\rangle - k_a k'_i \left\langle \hat{B}_{\mathbf{q}-\mathbf{k},a} \hat{B}^*_{\mathbf{q}-\mathbf{k}',b} \right\rangle \left\langle \hat{B}_{\mathbf{k},i} \hat{B}^*_{\mathbf{k}',b} \right\rangle - k_a k'_i \left\langle \hat{B}_{\mathbf{q}-\mathbf{k},a} \hat{B}^*_{\mathbf{k}',b} \right\rangle \left\langle \hat{B}_{\mathbf{k},i} \hat{B}^*_{\mathbf{q}-\mathbf{k}',b} \right\rangle \\
&- k_i k'_b \left\langle \hat{B}_{\mathbf{q}-\mathbf{k},a} \hat{B}^*_{-\mathbf{k},a} \right\rangle \left\langle \hat{B}_{-\mathbf{q}+\mathbf{k}',b} \hat{B}^*_{\mathbf{k}',i} \right\rangle - k_i k'_b \left\langle \hat{B}_{\mathbf{q}-\mathbf{k},a} \hat{B}^*_{\mathbf{q}-\mathbf{k}',b} \right\rangle \left\langle \hat{B}_{\mathbf{k},a} \hat{B}^*_{\mathbf{k}',i} \right\rangle - k_i k'_b \left\langle \hat{B}_{\mathbf{q}-\mathbf{k},a} \hat{B}^*_{\mathbf{k}',i} \right\rangle \left\langle \hat{B}_{\mathbf{k},a} \hat{B}^*_{\mathbf{q}-\mathbf{k}',b} \right\rangle \\
&+ k_i k'_i \left\langle \hat{B}_{\mathbf{q}-\mathbf{k},a} \hat{B}^*_{-\mathbf{k},a} \right\rangle \left\langle \hat{B}_{-\mathbf{q}+\mathbf{k}',b} \hat{B}^*_{\mathbf{k}',b} \right\rangle + k_i k'_i \left\langle \hat{B}_{\mathbf{q}-\mathbf{k},a} \hat{B}^*_{\mathbf{q}-\mathbf{k}',b} \right\rangle \left\langle \hat{B}_{\mathbf{k},a} \hat{B}^*_{\mathbf{k}',b} \right\rangle + k_i k'_i \left\langle \hat{B}_{\mathbf{q}-\mathbf{k},a} \hat{B}^*_{\mathbf{k}',b} \right\rangle \left\langle \hat{B}_{\mathbf{k},a} \hat{B}^*_{\mathbf{q}-\mathbf{k}',b} \right\rangle \Big] \Big\} \mathrm{d}^3 k' \mathrm{d}^3 k \Bigg) \, .
\end{aligned} \tag{B.23}$$

Following the steps done for $\left\langle \left(\partial_t \hat{B}_{\mathbf{q},i}\right) \hat{B}^*_{\mathbf{q},i} \right\rangle$ above, now, equivalently, the relations (1.127) and (1.131) are used before taking the d^3k'-integral. It turns out that doing this makes the first to sixth as well as the tenth and the eleventh terms inside the square bracket belonging to the $1/(4\pi\rho)$ expression equal to zero concerning the non-helical contribution. Furthermore, one can directly say that for most of the terms there is no finite value for the (magnetic) helicity terms given, the only non-zero ones being inside the $1/(4\pi\rho)^2$ bracket. Simplifying all these expressions finally gives

$$\begin{aligned}\left\langle (\partial_t \hat{v}_{\mathbf{q},i})\, \hat{v}^*_{\mathbf{q},i} \right\rangle = \frac{\Delta t}{2} \int \Bigg[& \frac{1}{8\pi^2} \frac{1}{q^2} \sin^2\theta \left\langle M_k \right\rangle \left\langle U_q \right\rangle + \frac{1}{16\pi^2} \frac{q^2}{k k_1^4} \sin^2\theta \left(3k - q\cos\theta\right) \left\langle U_k \right\rangle \left\langle U_{k_1} \right\rangle + \frac{1}{16\pi^2} \frac{k^2}{q k_1^4} \sin^2\theta \left(-3q + k\cos\theta\right) \left\langle U_q \right\rangle \left\langle U_{k_1} \right\rangle \\ & - \frac{1}{8\pi^2} \frac{k^2}{q^2 k_1^4} \sin^2\theta \left(q^2 + k^2 - qk\cos\theta\right) \left\langle M_{k_1} \right\rangle \left\langle U_q \right\rangle + \frac{1}{16\pi^2} \frac{q}{k k_1^4} \left(qk\sin^2\theta + 2k_1^2\cos\theta\right) \left\langle M_k \right\rangle \left\langle M_{k_1} \right\rangle \\ & + \frac{4}{(8\pi)^4} \frac{q}{k_1^2} \left(-2q - q\sin^2\theta + 2k\cos\theta\right) \left\langle \mathcal{H}_k \right\rangle \left\langle \mathcal{H}_{k_1} \right\rangle \Bigg] \mathrm{d}^3k \end{aligned} \tag{B.24}$$

and therefore

$$\begin{aligned}\left\langle \partial_t U_q \right\rangle \overset{(3.47)}{=} 4\pi q^2 \left\langle (\partial_t \hat{v}_{\mathbf{q},i})\, \hat{v}^*_{\mathbf{q},i} \right\rangle = \frac{\Delta t}{2} \int \Bigg[& \frac{1}{2\pi} \sin^2\theta \left\langle M_k \right\rangle \left\langle U_q \right\rangle + \frac{1}{4\pi} \frac{q^4}{k k_1^4} \sin^2\theta \left(3k - q\cos\theta\right) \left\langle U_k \right\rangle \left\langle U_{k_1} \right\rangle + \frac{1}{4\pi} \frac{qk^2}{k_1^4} \sin^2\theta \big(- 3q \\ & + k\cos\theta\big) \left\langle U_q \right\rangle \left\langle U_{k_1} \right\rangle - \frac{1}{2\pi} \frac{k^2}{k_1^4} \sin^2\theta \left(q^2 + k^2 - qk\cos\theta\right) \left\langle M_{k_1} \right\rangle \left\langle U_q \right\rangle + \frac{1}{4\pi} \frac{q^3}{k k_1^4} \left(qk\sin^2\theta + 2k_1^2\cos\theta\right) \left\langle M_k \right\rangle \left\langle M_{k_1} \right\rangle \\ & + \frac{2}{(8\pi)^3} \frac{q^3}{k_1^2} \left(-2q - q\sin^2\theta + 2k\cos\theta\right) \left\langle \mathcal{H}_k \right\rangle \left\langle \mathcal{H}_{k_1} \right\rangle \Bigg] \mathrm{d}^3k \,. \end{aligned} \tag{B.25}$$

Here again the integral can be rewritten as $\int \ldots \mathrm{d}^3k = 2\pi \int \ldots k^2 \sin\theta \mathrm{d}\theta \mathrm{d}k$ and the θ integration evaluated for the first term, giving

$$\begin{aligned}\left\langle \partial_t U_q \right\rangle = \Delta t \Bigg\{ & \int \left[\frac{2}{3} k^2 \left\langle M_k \right\rangle \left\langle U_q \right\rangle\right] \mathrm{d}k + \iint \Bigg[\frac{1}{4} \frac{q^4 k}{k_1^4} \left(3k - q\cos\theta\right) \sin^3\theta \left\langle U_k \right\rangle \left\langle U_{k_1} \right\rangle + \frac{1}{4} \frac{qk^4}{k_1^4} \left(-3q + k\cos\theta\right) \sin^3\theta \left\langle U_q \right\rangle \left\langle U_{k_1} \right\rangle - \frac{1}{2} \frac{k^4}{k_1^4} \big(q^2 + k^2 \\ & - qk\cos\theta\big) \sin^3\theta \left\langle M_{k_1} \right\rangle \left\langle U_q \right\rangle + \frac{1}{4} \frac{q^3 k}{k_1^4} \left(qk\sin^2\theta + 2k_1^2\cos\theta\right) \sin\theta \left\langle M_k \right\rangle \left\langle M_{k_1} \right\rangle + \frac{1}{(16\pi)^2} \frac{q^3 k^2}{k_1^2} \left(-2q - q\sin^2\theta + 2k\cos\theta\right) \left\langle \mathcal{H}_k \right\rangle \left\langle \mathcal{H}_{k_1} \right\rangle \Bigg] \mathrm{d}\theta \mathrm{d}k \Bigg\} . \end{aligned} \tag{B.26}$$

B.3 Variable Transformations

For some applications it may be useful to transform the main equations, (B.14), (B.26) and (B.17), in some other coordinates. The first transformation presented here is given by the replacement $\mu \equiv \cos\theta$, which implies $\mathrm{d}\mu = -\sin\theta \mathrm{d}\theta$, such that they become

$$\begin{aligned}\langle \partial_t M_q \rangle = &-\frac{2q^2}{4\pi\sigma}\langle M_q\rangle + \Delta t\Bigg\{\frac{2q^4}{(4\pi\sigma)^2}\langle M_q\rangle + \iint_{-1}^{1}\Big[-\frac{q^2k^4}{2k_1^4}\left(1-\mu^2\right)\langle M_q\rangle\langle U_{k_1}\rangle \\ &+\frac{q^4}{2k_1^2}\left(1-\mu^2\right)\frac{q^2+k^2-qk\mu}{q^2+k^2-2qk\mu}\langle M_k\rangle\langle U_{k_1}\rangle\Big]\mathrm{d}\mu\mathrm{d}k + \int\Big[-\frac{4}{3}q^2\langle M_k\rangle\langle M_q\rangle + \frac{1}{3}\frac{1}{(4\pi)^2}q^2k^2\langle\mathcal{H}_q\rangle\langle\mathcal{H}_k\rangle\Big]\mathrm{d}k\Bigg\}\end{aligned} \tag{B.27}$$

as well as

$$\begin{aligned}\langle \partial_t U_q \rangle = \Delta t\Bigg\{&\int\left[\frac{2}{3}k^2\langle M_k\rangle\langle U_q\rangle\right]\mathrm{d}k + \iint_{-1}^{1}\Big[\frac{1}{4}\frac{q^4k}{k_1^4}(3k-q\mu)\left(1-\mu^2\right)\langle U_k\rangle\langle U_{k_1}\rangle + \frac{1}{4}\frac{qk^4}{k_1^4}(-3q+k\mu)\left(1-\mu^2\right)\langle U_q\rangle\langle U_{k_1}\rangle - \frac{1}{2}\frac{k^4}{k_1^4}\big(q^2+k^2 \\ &-qk\mu\big)\left(1-\mu^2\right)\langle M_{k_1}\rangle\langle U_q\rangle + \frac{1}{4}\frac{q^3k}{k_1^4}\left(qk\left(1-\mu^2\right)+2k_1^2\mu\right)\langle M_k\rangle\langle M_{k_1}\rangle + \frac{1}{(16\pi)^2}\frac{q^3k^2}{k_1^2}\left(-2q-q\left(1-\mu^2\right)+2k\mu\right)\langle\mathcal{H}_k\rangle\langle\mathcal{H}_{k_1}\rangle\Big]\mathrm{d}\mu\mathrm{d}k\Bigg\}\end{aligned} \tag{B.28}$$

and

$$\begin{aligned}\langle \partial_t \mathcal{H}_q \rangle = &-\frac{2q^2}{4\pi\sigma}\langle\mathcal{H}_q\rangle + \Delta t\Bigg\{\frac{2q^4}{(4\pi\sigma)^2}\langle\mathcal{H}_q\rangle + \iint_{-1}^{1}\Big[-\frac{q^2k^4\left(1-\mu\right)^2}{2k_1^4}\langle U_{k_1}\rangle\langle\mathcal{H}_q\rangle \\ &+\frac{q^4k^2\left(1-\mu^2\right)}{2k_1^4}\langle U_{k_1}\rangle\langle\mathcal{H}_k\rangle\Big]\mathrm{d}\mu\mathrm{d}k + \int\left[\frac{4}{3}k^2\langle M_q\rangle\langle\mathcal{H}_k\rangle - \frac{4}{3}q^2\langle M_k\rangle\langle\mathcal{H}_q\rangle\right]\mathrm{d}k\Bigg\}.\end{aligned} \tag{B.29}$$

These results may be used to make another transformation of variables in order to have integrals depending on k and k_1. Since it is

$$\mu = \frac{q^2+k^2-k_1^2}{2qk}\,, \tag{B.30}$$

the transformation rule involving the Jacobi determinant is given by

$$\mathrm{d}k\mathrm{d}\mu = \det J\mathrm{d}k\mathrm{d}k_1 = -\frac{k_1}{qk}\mathrm{d}k\mathrm{d}k_1\,, \tag{B.31}$$

which, for some function $f(k,\mu)$, means

$$\int_0^\infty \int_{-1}^1 f(k,\mu)\mathrm{d}\mu\mathrm{d}k = \int_0^\infty \int_{\sqrt{q^2+k^2-2qk}}^{\sqrt{q^2+k^2+2qk}} \frac{k_1}{qk} f(k, \frac{q^2+k^2-k_1^2}{2qk})\mathrm{d}k_1\mathrm{d}k = \int_0^\infty \int_{|q-k|}^{|q+k|} \frac{k_1}{qk} f(k, \frac{q^2+k^2-k_1^2}{2qk})\mathrm{d}k_1\mathrm{d}k\,. \tag{B.32}$$

Therefore (B.27)-(B.29) become

$$\begin{aligned}
\langle \partial_t M_q \rangle = &-\frac{2q^2}{4\pi\sigma}\langle M_q\rangle + \Delta t\Bigg\{ \frac{2q^4}{(4\pi\sigma)^2}\langle M_q\rangle + \int \left(-\frac{4}{3}q^2\langle M_q\rangle\langle M_k\rangle + \frac{1}{3}\frac{1}{(4\pi)^2}q^2k^2\langle \mathcal{H}_q\rangle\langle \mathcal{H}_k\rangle\right)\mathrm{d}k \\
&+ \iint_{|q-k|}^{q+k}\Bigg[\left(-\frac{q^7}{16k^3k_1^3}+\frac{q^5}{16k^3k_1}+\frac{q^5}{16kk_1^3}+\frac{q^3k}{16k_1^3}+\frac{3q^3}{8kk_1}+\frac{q^3k_1}{16k^3}-\frac{qk^3}{16k_1^3}+\frac{qk}{16k_1}+\frac{qk_1}{16k}-\frac{qk_1^3}{16k^3}\right)\langle M_k\rangle\langle U_{k_1}\rangle \\
&+ \left(\frac{k^5}{8qk_1^3}-\frac{k^3}{4qk_1}-\frac{qk^3}{4k_1^3}+\frac{kk_1}{8q}-\frac{qk}{4k_1}+\frac{q^3k}{8k_1^3}\right)\langle M_q\rangle\langle U_{k_1}\rangle\Bigg]\mathrm{d}k_1\mathrm{d}k\Bigg\}
\end{aligned} \tag{B.33}$$

and

$$\begin{aligned}
\langle \partial_t U_q \rangle = \Delta t\Bigg\{ &\int \frac{2}{3}k^2\langle M_k\rangle\langle U_q\rangle\,\mathrm{d}k + \iint_{|q-k|}^{q+k}\Bigg[\left(-\frac{q^5}{16kk_1^3}+\frac{q^3k}{8k_1^3}+\frac{3q^3}{8kk_1}-\frac{qk^3}{16k_1^3}+\frac{3qk}{8k_1}-\frac{5qk_1}{16k}\right)\langle M_k\rangle\langle M_{k_1}\rangle \\
&+ \left(\frac{q^7}{32k^3k_1^3}-\frac{7q^5}{32kk_1^3}-\frac{3q^5}{32k^3k_1}+\frac{11q^3k}{32k_1^3}+\frac{5q^3}{16kk_1}+\frac{3q^3k_1}{32k^3}-\frac{5qk^3}{32k_1^3}+\frac{9qk}{32k_1}-\frac{3qk_1}{32k}-\frac{qk_1^3}{32k^3}\right)\langle U_k\rangle\langle U_{k_1}\rangle \\
&+ \left(-\frac{k^7}{32q^3k_1^3}+\frac{7k^5}{32qk_1^3}+\frac{3k^5}{32q^3k_1}-\frac{11qk^3}{32k_1^3}-\frac{5k^3}{16qk_1}-\frac{3k^3k_1}{32q^3}+\frac{5q^3k}{32k_1^3}-\frac{9qk}{32k_1}+\frac{3kk_1}{32q}+\frac{kk_1^3}{32q^3}\right)\langle U_q\rangle\langle U_{k_1}\rangle \\
&+ \left(\frac{k^7}{16q^3k_1^3}-\frac{k^5}{16qk_1^3}-\frac{k^5}{16q^3k_1}-\frac{qk^3}{16k_1^3}-\frac{3k^3}{8qk_1}-\frac{k^3k_1}{16q^3}-\frac{qk}{16k_1}+\frac{q^3k}{16k_1^3}-\frac{kk_1}{16q}+\frac{kk_1^3}{16q^3}\right)\langle M_{k_1}\rangle\langle U_q\rangle\Bigg\} \\
&+ \frac{1}{(8\pi)^2}\left(\frac{q^5}{16kk_1}-\frac{3q^3k}{8k_1}-\frac{q^3k_1}{8k}+\frac{5qk^3}{16k_1}-\frac{3qkk_1}{8}+\frac{qk_1^3}{16k}\right)\langle \mathcal{H}_k\rangle\langle \mathcal{H}_{k_1}\rangle\Bigg]\mathrm{d}k_1\mathrm{d}k\Bigg\},
\end{aligned} \tag{B.34}$$

as well as

$$\langle \partial_t \mathcal{H}_q \rangle = -\frac{2q^2}{4\pi\sigma} \langle \mathcal{H}_q \rangle + \Delta t \Bigg\{ \frac{2q^4}{(4\pi\sigma)^2} \langle \mathcal{H}_q \rangle + \int \left(\frac{4}{3} k^2 \langle M_q \rangle \langle \mathcal{H}_k \rangle - \frac{4}{3} q^2 \langle M_k \rangle \langle \mathcal{H}_q \rangle \right) \mathrm{d}k$$
$$+ \iint_{|q-k|}^{q+k} \left[\left(\frac{q^3 k}{8k_1^3} - \frac{qk^3}{4k_1^3} - \frac{qk}{4k_1} + \frac{k^5}{8qk_1^3} - \frac{k^3}{4qk_1} + \frac{kk_1}{8q} \right) \langle U_{k_1} \rangle \langle H_q \rangle + \left(-\frac{q^5}{8kk_1^3} + \frac{q^3 k}{4k_1^3} + \frac{q^3}{4kk_1} - \frac{qk^3}{8k_1^3} + \frac{qk}{4k_1} - \frac{qk_1}{8k} \right) \langle U_{k_1} \rangle \langle \mathcal{H}_k \rangle \right] \mathrm{d}k_1 \mathrm{d}k \Bigg\} . \tag{B.35}$$

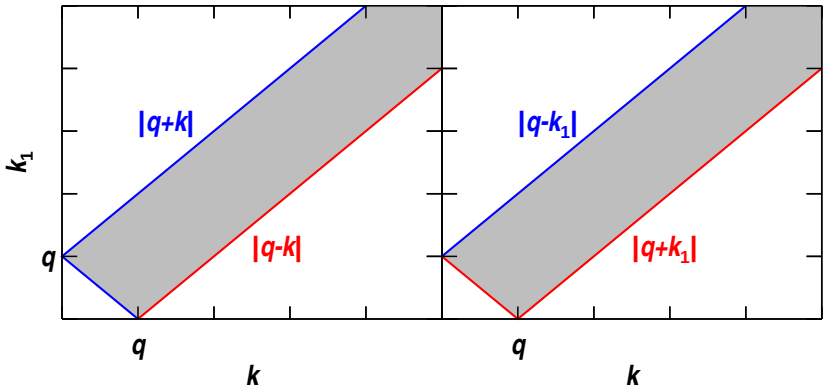

Figure B.1: A sketch of the integration domain. The change from the left to the right panel corresponds to the change of the integration limits as indicated in (B.36). As one can see it only leads to a different view of the integration domain while it does not change its shape.

Due to the symmetry of the k-k_1 integration domain for the double integral in k and k_1, as can be seen in Fig. B.1, one can change the integration order by the following rule:

$$\int_0^\infty \int_{|q-k|}^{q+k} f\left(k, k_1\right) \mathrm{d}k_1 \mathrm{d}k = \int_0^\infty \int_{|q-k_1|}^{q+k_1} f\left(k, k_1\right) \mathrm{d}k \mathrm{d}k_1 \,, \tag{B.36}$$

i.e. by appropriately adjusting the integration limits it is possible to calculate the k_1 integration first. As an example, taking the last term

from (B.33), one can perform the following transformation:

$$\begin{aligned}
&\Delta t \int_0^\infty \int_{|q-k|}^{q+k} \left(\frac{k^5}{8qk_1^3} - \frac{k^3}{4qk_1} - \frac{qk^3}{4k_1^3} + \frac{kk_1}{8q} - \frac{qk}{4k_1} + \frac{q^3k}{8k_1^3} \right) \langle M_q \rangle \langle U_{k_1} \rangle \, \mathrm{d}k_1 \mathrm{d}k \\
&= \Delta t \int_0^\infty \int_{|q-k_1|}^{q+k_1} \left(\frac{k^5}{8qk_1^3} - \frac{k^3}{4qk_1} - \frac{qk^3}{4k_1^3} + \frac{kk_1}{8q} - \frac{qk}{4k_1} + \frac{q^3k}{8k_1^3} \right) \langle M_q \rangle \langle U_{k_1} \rangle \, \mathrm{d}k_1 \mathrm{d}k \\
&= \Delta t \int_0^\infty \left(-\frac{2}{3} q^2 \langle M_q \rangle \langle U_{k_1} \rangle \right) \mathrm{d}k_1 = \Delta t \int_0^\infty \left(-\frac{2}{3} q^2 \langle M_q \rangle \langle U_k \rangle \right) \mathrm{d}k \,,
\end{aligned} \tag{B.37}$$

where in the last step the dummy integration variable has been renamed from k_1 to k. The same procedure can also be applied to the terms containing $\langle U_q \rangle \langle U_{k_1} \rangle$ and $\langle M_{k_1} \rangle \langle U_q \rangle$ in (B.34) and the term containing $\langle U_{k_1} \rangle \langle H_q \rangle$ in (B.35), giving the final result

$$\begin{aligned}
\langle \partial_t M_q \rangle = &-\frac{2q^2}{4\pi\sigma} \langle M_q \rangle + \Delta t \Bigg(\frac{2q^4}{(4\pi\sigma)^2} \langle M_q \rangle + \int_0^\infty \Bigg\{ -\frac{2}{3} q^2 \langle M_q \rangle \langle U_k \rangle - \frac{4}{3} q^2 \langle M_q \rangle \langle M_k \rangle + \frac{1}{3} \frac{1}{(4\pi)^2} q^2 k^2 \langle \mathcal{H}_q \rangle \langle \mathcal{H}_k \rangle \\
&+ \int_{|q-k|}^{q+k} \left[\left(-\frac{q^7}{16k^3k_1^3} + \frac{q^5}{16k^3k_1} + \frac{q^5}{16kk_1^3} + \frac{q^3k}{16k_1^3} + \frac{3q^3}{8kk_1} + \frac{q^3k_1}{16k^3} - \frac{qk^3}{16k_1^3} + \frac{qk}{16k_1} + \frac{qk_1}{16k} - \frac{qk_1^3}{16k^3} \right) \langle M_k \rangle \langle U_{k_1} \rangle \right] \mathrm{d}k_1 \Bigg\} \mathrm{d}k \Bigg)
\end{aligned} \tag{B.38}$$

and

$$\begin{aligned}
\langle \partial_t U_q \rangle = \Delta t \int_0^\infty \Bigg\{ &-\frac{2}{3} q^2 \langle M_k \rangle \langle U_q \rangle - \frac{2}{3} q^2 \langle U_q \rangle \langle U_k \rangle + \int_{|q-k|}^{q+k} \Bigg[\left(-\frac{q^5}{16kk_1^3} + \frac{q^3k}{8k_1^3} + \frac{3q^3}{8kk_1} - \frac{qk^3}{16k_1^3} + \frac{3qk}{8k_1} - \frac{5qk_1}{16k} \right) \langle M_k \rangle \langle M_{k_1} \rangle \\
&+ \left(\frac{q^7}{32k^3k_1^3} - \frac{7q^5}{32kk_1^3} - \frac{3q^5}{32k^3k_1} + \frac{11q^3k}{32k_1^3} + \frac{5q^3}{16kk_1} + \frac{3q^3k_1}{32k^3} - \frac{5qk^3}{32k_1^3} + \frac{9qk}{32k_1} - \frac{3qk_1}{32k} - \frac{qk_1^3}{32k^3} \right) \langle U_k \rangle \langle U_{k_1} \rangle \\
&+ \frac{1}{(8\pi)^2} \left(\frac{q^5}{16kk_1} - \frac{3q^3k}{8k_1} - \frac{q^3k_1}{8k} + \frac{5qk^3}{16k_1} - \frac{3qkk_1}{8} + \frac{qk_1^3}{16k} \right) \langle \mathcal{H}_k \rangle \langle \mathcal{H}_{k_1} \rangle \Bigg] \mathrm{d}k_1 \Bigg\} \mathrm{d}k
\end{aligned} \tag{B.39}$$

as well as

$$\begin{aligned}
\langle \partial_t \mathcal{H}_q \rangle = &-\frac{2q^2}{4\pi\sigma} \langle \mathcal{H}_q \rangle + \Delta t \Bigg(\frac{2q^4}{(4\pi\sigma)^2} \langle \mathcal{H}_q \rangle + \int_0^\infty \Bigg\{ \frac{4}{3} k^2 \langle M_q \rangle \langle \mathcal{H}_k \rangle - \frac{4}{3} q^2 \langle M_k \rangle \langle \mathcal{H}_q \rangle - \frac{2}{3} q^2 \langle U_k \rangle \langle \mathcal{H}_q \rangle \\
&+ \int_{|q-k|}^{q+k} \left[\left(-\frac{q^5}{8kk_1^3} + \frac{q^3k}{4k_1^3} + \frac{q^3}{4kk_1} - \frac{qk^3}{8k_1^3} + \frac{qk}{4k_1} - \frac{qk_1}{8k} \right) \langle U_{k_1} \rangle \langle \mathcal{H}_k \rangle \right] \mathrm{d}k_1 \Bigg\} \mathrm{d}k \Bigg) \,.
\end{aligned} \tag{B.40}$$

In (k,θ)-coordinates, i.e. rewriting (B.27)-(B.29), this fully simplified expression reads

$$\begin{aligned}\langle \partial_t M_q \rangle = -\frac{2q^2}{4\pi\sigma}\langle M_q\rangle + \Delta t\Bigg(\frac{2q^4}{(4\pi\sigma)^2}\langle M_q\rangle + \int_0^\infty \Big\{ -\frac{2}{3}q^2\langle M_q\rangle\langle U_k\rangle - \frac{4}{3}q^2\langle M_q\rangle\langle M_k\rangle + \frac{1}{3}\frac{1}{(4\pi)^2}q^2k^2\langle \mathcal{H}_q\rangle\langle \mathcal{H}_k\rangle \\ + \int_0^\pi \Big[\frac{1}{2}\frac{q^4}{k_1^4}\big(q^2+k^2-qk\cos\theta\big)\sin^3\theta\,\langle M_k\rangle\langle U_{k_1}\rangle\Big]\,\mathrm{d}\theta\Big\}\mathrm{d}k\Bigg),\end{aligned} \tag{B.41}$$

$$\begin{aligned}\langle \partial_t U_q \rangle = \Delta t\int_0^\infty \Big\{ -\frac{2}{3}q^2\langle M_k\rangle\langle U_q\rangle - \frac{2}{3}q^2\langle U_q\rangle\langle U_k\rangle + \int_0^\pi \Big[\frac{1}{4}\frac{q^3k}{k_1^4}\big(qk\sin^2\theta + 2k_1^2\cos\theta\big)\sin\theta\,\langle M_k\rangle\langle M_{k_1}\rangle \\ + \frac{1}{4}\frac{q^4k}{k_1^4}(3k-q\cos\theta)\sin^3\theta\,\langle U_k\rangle\langle U_{k_1}\rangle + \frac{1}{(16\pi)^2}\frac{q^3k^2}{k_1^2}\big(-2q-q\sin^2\theta+2k\cos\theta\big)\sin\theta\,\langle \mathcal{H}_k\rangle\langle \mathcal{H}_{k_1}\rangle\Big]\,\mathrm{d}\theta\Big\}\mathrm{d}k\end{aligned} \tag{B.42}$$

and

$$\langle \partial_t \mathcal{H}_q \rangle = -\frac{2q^2}{4\pi\sigma}\langle \mathcal{H}_q\rangle + \Delta t\Bigg(\frac{2q^4}{(4\pi\sigma)^2}\langle \mathcal{H}_q\rangle + \int_0^\infty \Big\{\frac{4}{3}k^2\langle M_q\rangle\langle \mathcal{H}_k\rangle - \frac{4}{3}q^2\langle M_k\rangle\langle \mathcal{H}_q\rangle - \frac{2}{3}q^2\langle U_k\rangle\langle \mathcal{H}_q\rangle + \int_0^\pi \Big[\frac{1}{2}\frac{q^4k^2}{k_1^4}\sin^3\theta\,\langle U_{k_1}\rangle\langle \mathcal{H}_k\rangle\Big]\,\mathrm{d}\theta\Big\}\mathrm{d}k\Bigg). \tag{B.43}$$

Bibliography

[1] R. Durrer and A. Neronov, *Cosmological Magnetic Fields: Their Generation, Evolution and Observation*, Astron. Astrophys. Rev. **21** (2013), no. 1 1–109. DOI:10.1007/s00159-013-0062-7 [arXiv:1303.7121[astro-ph.CO]].

[2] A. Neronov and I. Vovk, *Evidence for Strong Extragalactic Magnetic Fields from Fermi Observations of TeV Blazars*, Science **328** (2010), no. 5974 73–75. DOI:10.1126/science.1184192 [arXiv:1006.3504[astro-ph.HE]].

[3] K. Dolag, M. Kachelrieß, S. Ostapchenko and R. Tomàs, *Lower Limit on the Strength and Filling Factor of Extragalactic Magnetic Fields*, Astrophys. J. Lett. **727** (2011) L4. DOI:10.1088/2041-8205/727/1/L4 [arXiv:1009.1782[astro-ph.HE]].

[4] P. d'Avezac, G. Dubus and B. Giebels, *Cascading on Extragalactic Background Light*, Astron. Astrophys. **469** (2007) 857–860. DOI:10.1051/0004-6361:20066712 [arXiv:0704.3910[astro-ph]].

[5] A. E. Broderick, P. Chang and C. Pfrommer, *The Cosmological Impact of Luminous TeV Blazars. I. Implications of Plasma Instabilities for the Intergalactic Magnetic Field and Extragalactic Gamma-Ray Background*, Astrophys. J. **752** (2012), no. 1 22. DOI:10.1088/0004-637X/752/1/22 [arXiv:1106.5494[astro-ph.CO]].

[6] R. Schlickeiser, D. Ibscher and M. Supsar, *Plasma Effects on Fast Pair Beams in Cosmic Voids*, Astrophys. J. **758** (2012), no. 2 102. DOI:10.1088/0004-637X/758/2/102.

[7] J. M. Wagstaff, R. Banerjee, D. Schleicher and G. Sigl, *Unavoidable Strong Magnetic Fields in the Early Universe*, arXiv:1304.4723[astro-ph.CO]. Submitted to Phys. Rev. Lett.

[8] A. Saveliev, K. Jedamzik and G. Sigl, *Time Evolution of the Large-Scale Tail of Non-Helical Primordial Magnetic Fields with Back-Reaction of the Turbulent Medium*, Phys. Rev. D **86** (2012) 103010. DOI:10.1103/PhysRevD.86.103010 [arXiv:1208.0444[astro-ph.CO]].

[9] A. Saveliev, K. Jedamzik and G. Sigl, *Evolution of Helical Cosmic Magnetic Fields as Predicted by Magnetohydrodynamic Closure Theory*, Phys. Rev. D **87** (2013) 123001. DOI:10.1103/PhysRevD.87.123001 [arXiv:1304.3621[astro-ph.CO]].

[10] A. Saveliev, C. Evoli and G. Sigl, *The Role of Plasma Instabilities in the Propagation of Gamma-Rays from Distant Blazars*, arXiv:1311.6752[astro-ph.HE]. Submitted to Mon. Not. R. Astron. Soc.

[11] M. S. Longair, *High Energy Astrophysics*. Cambridge University Press, 2011.

[12] J. D. Jackson, *Classical Electrodynamics*. John Wiley & Sons, 1975.

[13] J. D. Jackson, *From Lorentz to Coulomb and Other Explicit Gauge Transformations*, Am. J. Phys. **70** (2002), no. 9 917–928. DOI:10.1119/1.1491265 [arXiv:physics/0204034].

[14] A. R. Choudhuri, *The Physics of Fluids and Plasmas: An Introduction for Astrophysicists*. Cambridge University Press, 1998.

[15] M. A. Berger and G. Field, *The Topological Properties of Magnetic Helicity*, J. Fluid Mech. **147** (1984) 133. DOI:10.1017/S0022112084002019.

[16] M. A. Berger, *Introduction to Magnetic Helicity*, Plasma Phys. Control. Fusion **41** (1999), no. 12B B167. DOI:10.1088/0741-3335/41/12B/312.

[17] H. K. Moffatt, *The Degree of Knottedness of Tangled Vortex Lines*, J. Fluid Mech. **35** (1969) 117. DOI:10.1017/S0022112069000991.

[18] L. Woltjer, *A Theorem on Force-Free Magnetic Fields*, Proc. Nat. Acad. Sci. USA **44** (1958) 489–491. DOI:10.1073/pnas.44.6.489.

[19] J. B. Taylor, *Relaxation of Toroidal Plasma and Generation of Reverse Magnetic Fields*, Phys. Rev. Lett. **33** (1974) 1139–1141. DOI:10.1103/PhysRevLett.33.1139.

[20] A. Brandenburg and K. Subramanian, *Astrophysical Magnetic Fields and Nonlinear Dynamo Theory*, Phys. Rep. **417** (2005), no. 1-4 1–209. DOI:10.1016/j.physrep.2005.06.005 [arXiv:astro-ph/0405052].

[21] A. S. Monin, *On the Nature of Turbulence*, Usp. Fiz. Nauk [Sov. Phys. Usp.] **21** (1978) 429–442. DOI:10.1070/PU1978v021n05ABEH005554.

[22] H. Tennekes and J. L. Lumley, *A First Course in Turbulence*. MIT Press, 1982.

[23] U. Frisch and S. A. Orszag, *Turbulence: Challenges for Theory and Experiment*, Phys. Today **43** (1990), no. 1 24. DOI:10.1063/1.881235.

[24] J. Leray, *Sur le mouvement d'un liquide visqueux emplissant l'espace*, Acta Math. **63** (1934) 193–248. DOI:10.1007/BF02547354.

[25] D. Ruelle and F. Takens, *On the Nature of Turbulence*, Commun. Math. Phys **20** (1971), no. 3 167–192. DOI:10.1007/BF01646553.

[26] A. Muriel, *Three Related Proposals for a Theoretical Definition of Turbulence*, Physica A **388** (2009), no. 4 311–317. DOI:10.1016/j.physa.2008.10.036.

[27] A. S. Monin and A. M. Yaglom, *Statistical Fluid Mechanics, Vol. 1: Mechanics of Turbulence*. MIT Press, 2007.

[28] J. Piquet, *Turbulent Flows: Models and Physics*. Springer, 2001.

[29] G. I. Taylor, *Statistical Theory of Turbulence*, Proc. R. Soc. London, Ser. A **151** (1935), no. 873 421–444. DOI:10.1098/rspa.1935.0158.

[30] W. H. Matthaeus and C. Smith, *Structure of Correlation Tensors in Homogeneous Anisotropic Turbulence*, Phys. Rev. A **24** (1981) 2135–2144. DOI:10.1103/PhysRevA.24.2135.

[31] T. von Kármán and L. Howarth, *On the Statistical Theory of Isotropic Turbulence*, Proc. R. Soc. London, Ser. A **164** (1938), no. 917 192–215. DOI:10.1098/rspa.1938.0013.

[32] H. Junklewitz and T. A. Enßlin, *Imprints of Magnetic Power and Helicity Spectra on Radio Polarimetry Statistics*, Astron. Astrophys. **530** (2011) A88. DOI:10.1051/0004-6361/201015544 [arXiv:1008.1243[astro-ph.IM]].

[33] A. N. Kolmogorov, *The Local Structure of Turbulence in Incompressible Viscous Fluid for Very Large Reynolds Numbers*, Dokl. Akad. Nauk SSSR **30** (1941) 299–303.

[34] A. N. Kolmogorov, *The Local Structure of Turbulence in Incompressible Viscous Fluid for Very Large Reynolds Numbers*, Proc. R. Soc. London, Ser. A **434** (1991) 9–13. DOI:10.1098/rspa.1991.0075.

[35] A. N. Kolmogorov, *Dissipation of Energy in the Locally Isotropic Turbulence*, Dokl. Akad. Nauk SSSR **32** (1941) 16–18.

[36] A. N. Kolmogorov, *Dissipation of Energy in the Locally Isotropic Turbulence*, Proc. R. Soc. London, Ser. A **434** (1991) 15–17. DOI:10.1098/rspa.1991.0076.

[37] P. Iroshnikov, *Turbulence of a Conducting Fluid in a Strong Magnetic Field*, Sov. Astron. **7** (1964) 566, NASA ADS:1964SvA.....7..566I.

[38] R. H. Kraichnan, *Inertial-Range Spectrum of Hydromagnetic Turbulence*, Phys. Fluids **8** (1965) 1385–1387. DOI:10.1063/1.1761412.

[39] L. Isserlis, *On Certain Probable Errors and Correlation Coefficients of Multiple Frequency Distributions with Skew Regression*, Biometrika **11** (1916), no. 3 185–190. DOI:10.1093/biomet/11.3.185.

[40] L. Isserlis, *On a Formula for the Product-Moment Coefficient of any Order of a Normal Frequency Distribution in any Number of Variables*, Biometrika **12** (1918), no. 1/2 134–139. DOI:10.1093/biomet/12.1-2.134.

[41] G. C. Wick, *The Evaluation of the Collision Matrix*, Phys. Rev. **80** (1950) 268–272. DOI:10.1103/PhysRev.80.268.

[42] S. M. Carroll, *Spacetime and Geometry: An Introduction to General Relativity*. Addison-Wesley, 2009.

[43] W. L. Freedman, B. F. Madore, V. Scowcroft, C. Burns, A. Monson, S. E. Persson, M. Seibert and J. Rigby, *Carnegie Hubble Program: A Mid-Infrared Calibration of the Hubble Constant*, Astrophys. J. **758** (2012), no. 1 24. DOI:10.1088/0004-637X/758/1/24 [arXiv:1208.3281[astro-ph.CO]].

[44] **Planck** Collaboration, P. A. R. Ade *et. al.*, *Planck 2013 Results. XVI. Cosmological Parameters*, arXiv:1303.5076[astro-ph.CO].

[45] A. Friedmann, *Über die Krümmung des Raumes*, Z. Phys. **10** (1922) 377–386. DOI:10.1007/BF01332580.

[46] A. H. Guth, *Inflationary Universe: A Possible Solution to the Horizon and Flatness Problems*, Phys. Rev. D **23** (1981) 347–356. DOI:10.1103/PhysRevD.23.347.

[47] J. A. Peacock, *Cosmological Physics*. Cambridge University Press, 2007.

[48] R. Allahverdi, R. Brandenberger, F.-Y. Cyr-Racine and A. Mazumdar, *Reheating in Inflationary Cosmology: Theory and Applications*, Ann. Rev. Nucl. Part. Sci. **60** (2010) 27–51. DOI:10.1146/annurev.nucl.012809.104511 [arXiv:1001.2600[hep-th]].

[49] K. Jedamzik, V. Katalinic and A. V. Olinto, *Damping of Cosmic Magnetic Fields*, Phys. Rev. D **57** (1998) 3264–3284. DOI:10.1103/PhysRevD.57.3264 [arXiv:astro-ph/9606080].

[50] A. D. Dolgov, *Neutrinos in Cosmology*, Phys. Rep. **370** (2002) 333–535. DOI:10.1016/S0370-1573(02)00139-4 [arXiv:hep-ph/0202122].

[51] A. D. Dolgov, *Big Bang Nucleosynthesis*, Nucl. Phys. Proc. Suppl. **110** (2002) 137–143. DOI:10.1016/S0920-5632(02)01470-6 [arXiv:hep-ph/0201107].

[52] B. Ryden, *Introduction to Cosmology*. Addison-Wesley, 2006.

[53] E. W. Kolb and M. S. Turner, *The Early Universe*. Westview Press, 1990.

[54] S. Galli, R. Bean, A. Melchiorri and J. Silk, *Delayed Recombination and Cosmic Parameters*, Phys. Rev. D **78** (2008) 063532. DOI:10.1103/PhysRevD.78.063532 [arXiv:0807.1420[astro-ph]].

[55] C. L. Bennett, A. Banday, K. M. Gorski, G. Hinshaw, P. Jackson *et. al.*, *Four Year COBE DMR Cosmic Microwave Background Observations: Maps and Basic Results*, Astrophys. J. Lett. **464** (1996) L1–L4. DOI:10.1086/310075 [arXiv:astro-ph/9601067].

[56] D. J. Fixsen, *The Temperature of the Cosmic Microwave Background*, Astrophys. J. **707** (2009) 916–920. DOI:10.1088/0004-637X/707/2/916 [arXiv:0911.1955[astro-ph.CO]].

[57] **SDSS** Collaboration, R. H. Becker *et. al.*, *Evidence for Reionization at $z \sim 6$: Detection of a Gunn-Peterson trough in a $Z = 6.28$ quasar*, Astron. J. **122** (2001) 2850. DOI:10.1086/324231 [arXiv:astro-ph/0108097].

[58] H. E. Stanley, *Introduction to Phase Transitions and Critical Phenomena*. Oxford University Press, 1971.

[59] P. Coles and F. Lucchin, *Cosmology: The Origin and Evolution of Cosmic Structure*. John Wiley & Sons, 1995.

[60] T. Prokopec, *Lecture Notes for Cosmology (ns-tp430m) - Part II: The Standard Cosmological Model*, http://www.staff.science.uu.nl/ proko101/2scm.pdf.

[61] K. Kajantie and H. Kurki-Suonio, *Bubble Growth and Droplet Decay in the Quark-Hadron Phase Transition in the Early Universe*, Phys. Rev. D **34** (1986) 1719–1738. DOI:10.1103/PhysRevD.34.1719.

[62] Z. Fodor and S. D. Katz, *Critical Point of QCD at Finite T and μ, Lattice Results for Physical Quark Masses*, J. High Energy Phys. **2004** (2004), no. 04 050. DOI:10.1088/1126-6708/2004/04/050 [arXiv:hep-lat/0402006].

[63] Y. Aoki, G. Endrődi, Z. Fodor, S. D. Katz and K. Szabó, *The Order of the Quantum Chromodynamics Transition Predicted by the Standard Model of Particle Physics*, Nature **443** (2006) 675–678. DOI:10.1038/nature05120 [arXiv:hep-lat/0611014].

[64] M. Cheng *et. al.*, *Transition Temperature in QCD*, Phys. Rev. D **74** (2006) 054507. DOI:10.1103/PhysRevD.74.054507 [arXiv:hep-lat/0608013].

[65] D. J. Schwarz and M. Stuke, *Lepton Asymmetry and the Cosmic QCD Transition*, J. Cosmol. Astropart. Phys. **2009** (2009), no. 11 025. DOI:10.1103/PhysRevD.86.103010 [arXiv:0906.3434[hep-ph]].

[66] T. Boeckel, S. Schettler and J. Schaffner-Bielich, *The Cosmological QCD Phase Transition Revisited*, Prog. Part. Nucl. Phys. **66** (2011) 266–270. DOI:10.1016/j.ppnp.2011.01.017 [arXiv:1012.3342[astro-ph.CO]].

[67] T. Boeckel and J. Schaffner-Bielich, *Little Inflation at the Cosmological QCD Phase Transition*, Phys. Rev. D **85** (2012) 103506. DOI:10.1103/PhysRevD.85.103506 [arXiv:1105.0832[astro-ph.CO]].

[68] J. M. Cline, *Baryogenesis*, in *Le Houches Summer School*, 2006. arXiv:hep-ph/0609145.

[69] G. Ódor, *Universality Classes in Nonequilibrium Lattice Systems*, Rev. Mod. Phys. **76** (2004) 663–724. DOI:10.1103/RevModPhys.76.663 [arXiv:cond-mat/0205644].

[70] C. Bonati, G. Cossu, M. D'Elia, A. Di Giacomo and C. Pica, *The Order of the QCD Transition with Two Light Flavors*, Nucl. Phys. A **820** (2009) 243C–246C. DOI:10.1016/j.nuclphysa.2009.01.060.

[71] Y. Aoki, *Four-Dimensional Simulation of the Hot Electroweak Phase Transition with the SU(2) Gauge-Higgs Model*, Phys. Rev. D **56** (1997) 3860–3865. DOI:10.1103/PhysRevD.56.3860 [arXiv:hep-lat/9612023].

[72] K. Rummukainen, M. Tsypin, K. Kajantie, M. Laine and M. Shaposhnikov, *The Universality Class of the Electroweak Theory*, Nucl. Phys. B **532** (1998), no. 1-2 283–314. DOI:10.1016/S0550-3213(98)00494-5 [arXiv:hep-lat/9805013].

[73] M. Gürtler, E.-M. Ilgenfritz and A. Schiller, *Where the Electroweak Phase Transition Ends*, Phys. Rev. D **56** (1997) 3888–3895. DOI:10.1103/PhysRevD.56.3888 [arXiv:hep-lat/9704013].

[74] **ATLAS** Collaboration, G. Aad *et. al.*, *Observation of a New Particle in the Search for the Standard Model Higgs Boson with the ATLAS Detector at the LHC*, Phys. Lett. B **716** (2012) 1–29. DOI:10.1016/j.physletb.2012.08.020 [arXiv:1207.7214[hep-ex]].

[75] **CMS** Collaboration, S. Chatrchyan *et. al.*, *Observation of a New Boson at a Mass of 125 GeV with the CMS Experiment at the LHC*, Phys. Lett. B **716** (2012) 30–61. DOI:10.1016/j.physletb.2012.08.021 [arXiv:1207.7235[hep-ex]].

[76] C. Grojean, G. Servant and J. D. Wells, *First-Order Electroweak Phase Transition in the Standard Model with a Low Cutoff*, Phys. Rev. D **71** (2005) 036001. DOI:10.1103/PhysRevD.71.036001 [arXiv:hep-ph/0407019].

[77] C. Delaunay, C. Grojean and J. D. Wells, *Dynamics of Non-Renormalizable Electroweak Symmetry Breaking*, J. High Energy Phys. **2008** (2008), no. 04 029. DOI:10.1088/1126-6708/2008/04/029 [arXiv:0711.2511[hep-ph]].

[78] S. J. Huber, T. Konstandin, T. Prokopec and M. G. Schmidt, *Baryogenesis in the MSSM, nMSSM and NMSSM*, Nucl. Phys. A **785** (2007), no. 1-2 206–209. DOI:10.1016/j.nuclphysa.2006.11.154 [arXiv:hep-ph/0608017].

[79] D. J. H. Chung and A. J. Long, *Electroweak Phase Transition in the $\mu\nu$SSM*, Phys. Rev. D **81** (2010) 123531. DOI:10.1103/PhysRevD.81.123531 [arXiv:1004.0942[hep-ph]].

[80] M. Laine, G. Nardini and K. Rummukainen, *Lattice Study of an Electroweak Phase Transition at $m_h \simeq 126$ GeV*, J. Cosmol. Astropart. Phys. **1301** (2013) 011. DOI:10.1088/1475-7516/2013/01/011 [arXiv:1211.7344[hep-ph]].

[81] D. J. H. Chung, A. J. Long and L.-T. Wang, *125 GeV Higgs Boson and Electroweak Phase Transition Model Classes*, Phys. Rev. D **87** (2013) 023509. DOI:10.1103/PhysRevD.87.023509 [arXiv:1209.1819[hep-ph]].

[82] L. M. Widrow, *Origin of Galactic and Extragalactic Magnetic Fields*, Rev. Mod. Phys. **74** (2002) 775–823. DOI:10.1103/RevModPhys.74.775 [arXiv:astro-ph/0207240].

[83] H. J. Völk and A. M. Atoyan, *Early Starbursts and Magnetic Field Generation in Galaxy Clusters*, Astrophys. J. **541** (2000) 88–94. DOI:10.1086/309395 [arXiv:astro-ph/0005185].

[84] A. M. Beck, M. Hannasz, H. Lesch, R. S. Remus and F. A. Stasyszyn, *On the Magnetic Fields in Voids*, Mon. Not. R. Astron. Soc. **429** (2013) L60–L64. DOI:10.1093/mnrasl/sls026 [arXiv:1210.8360[astro-ph.CO]].

[85] S. Bertone, C. Vogt and T. Enßlin, *Magnetic Field Seeding by Galactic Winds*, Mon. Not. R. Astron. Soc. **370** (2006) 319–330. DOI:10.1111/j.1365-2966.2006.10474.x [arXiv:astro-ph/0604462].

[86] M. J. Rees, *The Origin and Cosmogonic Implications of Seed Magnetic Fields*, Q. J. R. Astron. Soc. **28** (1987) 197–206, NASA ADS:1987QJRAS..28..197R.

[87] R. A. Daly and A. Loeb, *A Possible Origin of Galactic Magnetic Fields*, Astrophys. J. **364** (1990) 451–455. DOI:10.1086/169429.

[88] T. A. Enßlin, P. L. Biermann, P. P. Kronberg and X.-P. Wu, *Cosmic Ray Protons and Magnetic Fields in Clusters of Galaxies and their Cosmological Consequences*, Astrophys. J. **477** (1997) 560. DOI:10.1086/303722 [arXiv:astro-ph/9609190].

[89] P. P. Kronberg, Q. W. Dufton, H. Li and S. A. Colgate, *Magnetic Energy of the Intergalactic Medium from Galactic Black Holes*, Astrophys. J. **560** (2001) 178–186. DOI:10.1086/322767 [arXiv:astro-ph/0106281].

[90] R. M. Kulsrud and E. G. Zweibel, *The Origin of Cosmic Magnetic Fields*, Rep. Prog. Phys. **71** (2008) 0046091. DOI:10.1088/0034-4885/71/4/046901 [arXiv:0707.2783[astro-ph]].

[91] L. M. Widrow, D. Ryu, D. R. G. Schleicher, K. Subramanian, C. G. Tsagas and R. A. Treumann, *The First Magnetic Fields*, Space Sci. Rev. **166** (2012) 37–70. DOI:10.1007/s11214-011-9833-5 [arXiv:1109.4052[astro-ph.CO]].

[92] L. Biermann, *Über den Ursprung der Magnetfelder auf Sternen und im interstellaren Raum (mit einem Anhang von A. Schlüter)*, Zeitfschrift f. Naturforschung A **5** (1950) 65.

[93] R. M. Kulsrud, *The Origin of Galactic Magnetic Fields*, in *Cosmic Magnetic Fields* (R. Wielebinski and R. Beck, eds.), vol. 664 of *Lecture Notes in Physics*, pp. 69–88. 2005. DOI:10.1007/3540313966_4.

[94] J. Silk and M. Langer, *On the First Generation of Stars*, Mon. Not. R. Astron. Soc. **371** (2006) 444–450. DOI:10.1111/j.1365-2966.2006.10689.x [arXiv:astro-ph/0606276[astro-ph]].

[95] H. Xu, B. W. O'Shea, D. C. Collins, M. L. Norman, H. Li and S. Li, *The Biermann Battery in Cosmological MHD Simulations of Population III Star Formation*, Astrophys. J. Lett. **688** (2008) L57–L60. DOI:10.1086/595617 [arXiv:0807.2647[astro-ph]].

[96] R. M. Kulsrud, R. Cen, J. P. Ostriker and D. Ryu, *The Protogalactic Origin for Cosmic Magnetic Fields*, Astrophys. J. **480** (1997) 481. DOI:10.1086/303987 [arXiv:astro-ph/9607141].

[97] G. Davies and L. M. Widrow, *A Possible Mechanism for Generating Galactic Magnetic Fields*, Astrophys. J. **540** (2000) 755–764. DOI:10.1086/309358.

[98] E. R. Harrison, *Generation of Magnetic Fields in the Radiation Era*, Mon. Not. R. Astron. Soc. **147** (1970) 279, NASA ADS:1970MNRAS.147..279H.

[99] H. Sicotte, *Large-Scale Magnetic Fields in Texture-Seeded Cosmological Models*, Mon. Not. R. Astron. Soc. **287** (1997) 1–9. DOI:10.1093/mnras/287.1.1.

[100] P. J. E. Peebles, *The Large-Scale Structure of the Universe*. Princeton University Press, 1980.

[101] F. Hoyle, *Magnetic Fields and Highly Condensed Objects*, Nature **223** (1969) 936. DOI:10.1038/223936a0.

[102] F. Miniati and A. R. Bell, *Resistive Magnetic Field Generation at Cosmic Dawn*, Astrophys. J. **729** (2011) 73. DOI:10.1088/0004-637X/729/1/73 [arXiv:1001.2011[astro-ph.CO]].

[103] D. Grasso and H. R. Rubinstein, *Magnetic Fields in the Early Universe*, Phys. Rep. **348** (2001) 163–266. DOI:10.1016/S0370-1573(00)00110-1 [arXiv:astro-ph/0009061].

[104] A. Kandus, K. E. Kunze and C. G. Tsagas, *Primordial Magnetogenesis*, Phys. Rep. **505** (2011), no. 1 1 – 58. DOI:10.1016/j.physrep.2011.03.001 [arXiv:1007.3891[astro-ph.CO]].

[105] J. M. Quashnock, A. Loeb and D. N. Spergel, *Magnetic Field Generation during the Cosmological QCD Phase Transition*, Astrophys. J. Lett. **344** (1989) L49–L51. DOI:10.1086/185528.

[106] A. Loeb, *Electromagnetic Characteristics of the Dynamics of a Self-Gravitating Quasineutral Plasma*, Phys. Rev. D **37** (1988) 3484–3494. DOI:10.1103/PhysRevD.37.3484.

[107] B. Cheng and A. V. Olinto, *Primordial Magnetic Fields Generated in the Quark-Hadron Transition*, Phys. Rev. D **50** (1994) 2421–2424. DOI:10.1103/PhysRevD.50.2421.

[108] H. Kurki-Suonio, *Baryon-Number Inhomogeneity Generation in the Cosmic Quark-Hadron Phase Transition*, Phys. Rev. D **37** (1988) 2104–2110. DOI:10.1103/PhysRevD.37.2104.

[109] G. Sigl, A. V. Olinto and K. Jedamzik, *Primordial Magnetic Fields from Cosmological First Order Phase Transitions*, Phys. Rev. D **55** (1997) 4582–4590. DOI:10.1103/PhysRevD.55.4582 [arXiv:astro-ph/9610201].

[110] P. Huet, K. Kajantie, R. G. Leigh, B.-H. Liu and L. McLerran, *Hydrodynamic Stability Analysis of Burning Bubbles in Electroweak Theory and in QCD*, Phys. Rev. D **48** (1993) 2477–2492. DOI:10.1103/PhysRevD.48.2477.

[111] G. Baym, D. Bödeker and L. McLerran, *Magnetic Fields Produced by Phase Transition Bubbles in the Electroweak Phase Transition*, Phys. Rev. D **53** (1996) 662–667. DOI:10.1103/PhysRevD.53.662 [arXiv:hep-ph/9507429].

[112] D. Grasso and A. Riotto, *On the Nature of the Magnetic Fields Generated during the Electroweak Phase Transition*, Phys. Lett. B **418** (1998) 258–265. DOI:10.1016/S0370-2693(97)01224-0 [arXiv:hep-ph/9707265].

[113] T. Vachaspati, *Magnetic Fields from Cosmological Phase Transitions*, Phys. Lett. B **265** (1991) 258–261. DOI:10.1016/0370-2693(91)90051-Q.

[114] K. Enqvist and P. Olesen, *On Primordial Magnetic Fields of Electroweak Origin*, Phys. Lett. B **319** (1993) 178–185. DOI:10.1016/0370-2693(93)90799-N [arXiv:hep-ph/9308270].

[115] M. S. Turner and L. M. Widrow, *Inflation-Produced, Large-Scale Magnetic Fields*, Phys. Rev. D **37** (1988) 2743–2754. DOI:10.1103/PhysRevD.37.2743.

[116] S. Matarrese, S. Mollerach, A. Notari and A. Riotto, *Large-Scale Magnetic Fields from Density Perturbations*, Phys. Rev. D **71** (2005) 043502. DOI:10.1103/PhysRevD.71.043502 [arXiv:astro-ph/0410687].

[117] K. Takahashi, K. Ichiki, H. Ohno and H. Hanayama, *Magnetic Field Generation from Cosmological Perturbations*, Phys. Rev. Lett. **95** (2005) 121301. DOI:10.1103/PhysRevLett.95.121301 [arXiv:astro-ph/0502283].

[118] A. D. Dolgov and D. Grasso, *Generation of Magnetic Fields and Gravitational Waves at Neutrino Decoupling*, Phys. Rev. Lett. **88** (2001) 011301. DOI:10.1103/PhysRevLett.88.011301 [arXiv:astro-ph/0106154].

[119] A. Neronov and D. V. Semikoz, *Sensitivity of γ-ray Telescopes for Detection of Magnetic Fields in the Intergalactic Medium*, Phys. Rev. D **80** (2009) 123012. DOI:10.1103/PhysRevD.80.123012 [arXiv:0910.1920[astro-ph.CO]].

[120] S. Lee, A. Olinto and G. Sigl, *Extragalactic Magnetic Field and the Highest Energy Cosmic Rays*, Astrophys. J. **455** (1995) L21. DOI:10.1086/309812 [arXiv:astro-ph/9508088].

[121] J. J. Matese and R. F. O'Connell, *Neutron Beta Decay in a Uniform Constant Magnetic Field*, Phys. Rev. **180** (1969) 1289–1292. DOI:10.1103/PhysRev.180.1289.

[122] R. F. O'Connell and J. J. Matese, *Effect of a Constant Magnetic Field on the Neutron Beta Decay Rate and its Astrophysical Implications*, Nature **222** (1969) 649–650. DOI:10.1038/222649b0.

[123] G. Greenstein, *Primordial Helium Production in "Magnetic" Cosmologies*, Nature **223** (1969) 938–939. DOI:10.1038/223938b0.

[124] C. Heiles and T. Robishaw, *Zeeman Splitting in the Diffuse Interstellar Medium – The Milky Way and Beyond*, in *Proceedings of the IAU Symposium 259 - Cosmic Magnetic Fields: From Planets to Stars and Galaxies* (K. G. Strassmeier, A. G. Kosovichev and J. E. Beckman, eds.), pp. 579–590, International Astronomical Union, 2009. DOI:10.1017/S174392130903141X.

[125] P. Zeeman, *The Effect of Magnetisation on the Nature of Light Emitted by a Substance*, Nature **55** (1897) 347. DOI:10.1038/055347a0.

[126] A. M. Wolfe, R. A. Jorgenson, T. Robishaw, C. Heiles and J. X. Prochaska, *An 84 microGauss Magnetic Field in a Galaxy at Redshift z=0.692*, Nature **455** (2008) 638. DOI:10.1038/nature07264 [arXiv:0811.2408[astro-ph]].

[127] P. P. Kronberg and M. Simard-Normandin, *New Evidence on the Origin of Rotation Measures in Extragalactic Radio Sources*, Nature **263** (1976) 653–656. DOI:10.1038/263653a0.

[128] P. P. Kronberg and J. J. Perry, *Absorption Lines, Faraday Rotation, and Magnetic Field Estimates for QSO Absorption-Line Clouds*, Astrophys. J. **263** (1982) 518–532. DOI:10.1086/160523.

[129] P. Blasi, S. Burles and A. V. Olinto, *Cosmological Magnetic Field Limits in an Inhomogeneous Universe*, Astrophys. J. **514** (1999) L79. DOI:10.1086/311958 [arXiv:astro-ph/9812487].

[130] Y. Xu, P. P. Kronberg, S. Habib and Q. W. Dufton, *A Faraday Rotation Search for Magnetic Fields in Large Scale Structure*, Astrophys. J. **637** (2006) 19–26. DOI:10.1086/498336 [arXiv:astro-ph/0509826].

[131] Y. B. Zel'dovich and I. D. Novikov, *Relativistic Astrophysics, Vol. 2: The Structure and Evolution of the Universe*. University of Chicago Press, 1983.

[132] J. D. Barrow, P. G. Ferreira and J. Silk, *Constraints on a Primordial Magnetic Field*, Phys. Rev. Lett. **78** (1997) 3610–3613. DOI:10.1103/PhysRevLett.78.3610 [arXiv:astro-ph/9701063].

[133] R. A. Sunyaev and Y. B. Zeldovich, *Small-Scale Fluctuations of Relic Radiation*, Astrophys. Space Sci. **7** (1970) 3–19. DOI:10.1007/BF00653471.

[134] R. A. Sunyaev and I. B. Zeldovich, *Microwave Background Radiation as a Probe of the Contemporary Structure and History of the Universe*, Ann. Rev. Astron. Astrophys. **18** (1980) 537–560. DOI:10.1146/annurev.aa.18.090180.002541.

[135] K. Jedamzik, V. Katalinic and A. V. Olinto, *A Limit on Primordial Small Scale Magnetic Fields from CMB Distortions*, Phys. Rev. Lett. **85** (2000) 700–703. DOI:10.1103/PhysRevLett.85.700 [arXiv:astro-ph/9911100].

[136] D. J. Fixsen, E. S. Cheng, J. M. Gales, J. C. Mather, R. A. Shafer and E. L. Wright, *The Cosmic Microwave Background Spectrum from the Full COBE FIRAS Data Set*, Astrophys. J. **473** (1996) 576. DOI:10.1086/178173 [arXiv:astro-ph/9605054].

[137] M. G. Hauser and E. Dwek, *The Cosmic Infrared Background: Measurements and Implications*, Ann. Rev. Astron. Astrophys. **39** (2001), no. 1 249–307. DOI:10.1146/annurev.astro.39.1.249 [arXiv:astro-ph/0105539].

[138] T. M. Kneiske, T. Bretz, K. Mannheim and D. H. Hartmann, *Implications of Cosmological Gamma-Ray Absorption - II. Modification of Gamma-Ray Spectra*, Astron. Astrophys. **413** (2004), no. 3 807–815. DOI:10.1051/0004-6361:20031542 [arXiv:astro-ph/0309141].

[139] T. M. Kneiske and H. Dole, *A Lower-Limit Flux for the Extragalactic Background Light*, Astron. Astrophys. **515** (2010) A19. DOI:10.1051/0004-6361/200912000 [arXiv:1001.2132[astro-ph.CO]].

[140] A. Franceschini, G. Rodighiero and M. Vaccari, *The Extragalactic Optical-Infrared Background Radiations, their Time Evolution and the Cosmic Photon-Photon Opacity*, Astron. Astrophys. **487** (2008) 837. DOI:10.1051/0004-6361:200809691 [arXiv:0805.1841[astro-ph]].

[141] J. D. Finke, S. Razzaque and C. D. Dermer, *Modeling the Extragalactic Background Light from Stars and Dust*, Astrophys. J. **712** (2010), no. 1 238. DOI:10.1088/0004-637X/712/1/238 [arXiv:0905.1115[astro-ph.HE]].

[142] R. C. Gilmore, R. S. Somerville, J. R. Primack and A. Domìnguez, *Semi-Analytic Modeling of the EBL and Consequences for Extragalactic Gamma-Ray Spectra*, Mon. Not. R. Astron. Soc. **422** (2012) 3189. DOI:10.1111/j.1365-2966.2012.20841.x [arXiv:1104.0671[astro-ph.CO]].

[143] G. Breit and J. A. Wheeler, *Collision of Two Light Quanta*, Phys. Rev. **46** (1934) 1087–1091. DOI:10.1103/PhysRev.46.1087.

[144] A. I. Nikishov, *Absorption of High Energy Photons in the Universe*, Zh. Eksp. Teor. Fiz. [Sov. Phys. JETP] **41** (1961) 549.

[145] J. V. Jelley, *High-Energy γ-Ray Absorption in Space by a 3.5 K Microwave Field*, Phys. Rev. Lett. **16** (1966) 479–481. DOI:10.1103/PhysRevLett.16.479.

[146] R. J. Gould and G. P. Schréder, *Pair Production in Photon-Photon Collisions*, Phys. Rev. **155** (1967) 1404–1407. DOI:10.1103/PhysRev.155.1404.

[147] P. Bhattacharjee and G. Sigl, *Origin and Propagation of Extremely High-Energy Cosmic Rays*, Phys. Rep. **327** (2000) 109–247. DOI:10.1016/S0370-1573(99)00101-5 [arXiv:astro-ph/9811011].

[148] R. J. Protheroe and T. Stanev, *Electron-Photon Cascading of Very High-Energy Gamma-Rays in the Infrared Background*, Mon. Not. R. Astron. Soc. **264** (1993) 191, NASA ADS:1993MNRAS.264..191P.

[149] E. Feenberg and H. Primakoff, *Interaction of Cosmic-Ray Primaries with Sunlight and Starlight*, Phys. Rev. **73** (1948) 449–469. DOI:10.1103/PhysRev.73.449.

[150] T. M. Donahue, *The Significance of the Absence of Primary Electrons for Theories of the Origin of the Cosmic Radiation*, Phys. Rev. **84** (1951) 972–980. DOI:10.1103/PhysRev.84.972.

[151] F. Aharonian, P. S. Coppi and H. J. Völk, *Very High Energy Gamma Rays from Active Galactic Nuclei: Cascading on the Cosmic Background Radiation Fields and the Formation of Pair Halos*, Astrophys. J. Lett. **423** (1994) L5–L8. DOI:10.1086/187222 [arXiv:astro-ph/9312045].

[152] A. Neronov and D. V. Semikoz, *A Method of Measurement of Extragalactic Magnetic Fields by TeV Gamma Ray Telescopes*, JETP Lett. **85** (2007), no. 10 473–477. DOI:10.1134/S0021364007100013 [arXiv:astro-ph/0604607].

[153] K. Dolag, M. Kachelrieß, S. Ostapchenko and R. Tomàs, *Blazar Halos as Probe for Extragalactic Magnetic Fields and Maximal Acceleration Energy*, Astrophys. J. **703** (2009), no. 1 1078. DOI:10.1088/0004-637X/703/1/1078 [arXiv:0903.2842[astro-ph.HE]].

[154] A. Elyiv, A. Neronov and D. V. Semikoz, *Gamma-Ray Induced Cascades and Magnetic Fields in the Intergalactic Medium*, Phys. Rev. D **80** (2009) 023010. DOI:10.1103/PhysRevD.80.023010 [arXiv:0903.3649[astro-ph.CO]].

[155] A. Neronov, D. Semikoz, M. Kachelrieß, S. Ostapchenko and E. Elyiv, *Degree-Scale GeV "Jets" from Active and Dead TeV Blazars*, Astrophys. J. Lett. **719** (2010), no. 2 L130. DOI:10.1088/2041-8205/719/2/L130 [arXiv:1002.4981[astro-ph.HE]].

[156] **HESS** Collaboration, A. Abramowski *et. al.*, *Search for Extended γ-Ray Emission around AGN with H.E.S.S. and Fermi-LAT*, arXiv:1401.2915[astro-ph.HE].

[157] R. Plaga, *Detecting Intergalactic Magnetic Fields Using Time Delays in Pulses of γ-Rays*, Nature **374** (1994) 430–432. DOI:10.1038/374430a0.

[158] X. Wang, K. S. Cheng, Z. G. Dai and T. Lu, *Constraining the Origin of TeV Photons from Gamma-Ray Bursts with Delayed MeV-GeV Emission Formed by Interaction with Cosmic Infrared / Microwave Background Photons*, Astrophys. J. **604** (2004) 306–311. DOI:10.1086/381745 [arXiv:astro-ph/0311601].

[159] S. Razzaque, P. Meszaros and B. Zhang, *GeV and Higher Energy Photon Interactions in Gamma-Ray Burst Fireballs and Surroundings*, Astrophys. J. **613** (2004), no. 2 1072–1078. DOI:10.1086/423166 [arXiv:astro-ph/0404076].

[160] K. Ichiki, S. Inoue and K. Takahashi, *Probing the Nature of the Weakest Intergalactic Magnetic Fields with the High Energy Emission of Gamma-Ray Bursts*, Astrophys. J. **682** (2008), no. 1 127. DOI:10.1086/588275 [arXiv:0711.1589[astro-ph]].

[161] K. Takahashi, K. Murase, K. Ichiki, S. Inoue and S. Nagataki, *Detectability of Pair Echos from Gamma-Ray Bursts and Intergalactic Magnetic Fields*, Astrophys. J. Lett. **687** (2008), no. 1 L5. DOI:10.1086/593118 [arXiv:0806.2825[astro-ph]].

[162] K. Murase, K. Takahashi, S. Inoue, K. Ichiki and S. Nagataki, *Probing Intergalactic Magnetic Fields in the GLAST Era through Pair Echo Emission from TeV Blazars*, Astrophys. J. Lett. **686** (2008), no. 2 L67. DOI:10.1086/592997 [arXiv:0806.2829[astro-ph]].

[163] C. D. Dermer, M. Cavadini, S. Razzaque, J. D. Finke, J. Chiang and B. Lott, *Time Delay of Cascade Radiation for TeV Blazars and the Measurement of the Intergalactic Magnetic Field*, Astrophys. J. Lett. **733** (2011), no. 2 L21. DOI:10.1088/2041-8205/733/2/L21 [arXiv:1011.6660[astro-ph.HE]].

[164] F. Tavecchio, G. Ghisellini, L. Foschini, G. Bonnoli, G. Ghirlanda and P. Coppi, *The Intergalactic Magnetic Field Constrained by Fermi/Large Area Telescope Observations of the TeV Blazar 1ES0229+200*, Mon. Not. R. Astron. Soc. **406** (2010) L70–L74. DOI:10.1111/j.1745-3933.2010.00884.x [arXiv:1004.1329[astro-ph.CO]].

[165] Y.-Z. Fan, Z. G. Dai and D. M. Wei, *Strong GeV Emission Accompanying TeV Blazar H1426+428*, Astron. Astrophys. **415** (2004) 483–486. DOI:10.1051/0004-6361:20034472 [arXiv:astro-ph/0310893].

[166] A. M. Taylor, I. Vovk and A. Neronov, *Extragalactic Magnetic Fields Constraints from Simultaneous GeV-TeV Observations of Blazars*, Astron. Astrophys. **529** (2011) A144. DOI:10.1051/0004-6361/201116441 [arXiv:1101.0932[astro-ph.HE]].

[167] I. Vovk, A. M. Taylor, D. Semikoz and A. Neronov, *Fermi/LAT Observations of 1ES 0229+200: Implications for Extragalactic Magnetic Fields and Background Light*, Astrophys. J. Lett. **747** (2012), no. 1 L14. DOI:10.1088/2041-8205/747/1/L14 [arXiv:1112.2534[astro-ph.CO]].

[168] **Fermi LAT** Collaboration, F. Aharonian *et. al.*, *Simultaneous Observations of PKS 2155-304 with HESS, Fermi, RXTE, and Atom: Spectral Energy Distributions and Variability in a Low State*, Astrophys. J. Lett. **696** (2009), no. 2 L150. DOI:10.1088/0004-637X/696/2/L150 [arXiv:0903.2924[astro-ph.HE]].

[169] **Fermi LAT, VERITAS** Collaboration, L. C. Reyes, *Simultaneous Observations of Flaring Gamma-ray Blazar 3C 66A with Fermi-LAT and VERITAS*, in *Proc. 31st ICRC*, 2009. arXiv:0907.5175[astro-ph.HE].

[170] V. A. Acciari *et. al.*, *The Discovery of Gamma-Ray Emission From the Blazar RGB J0710+591*, Astrophys. J. Lett. **715** (2010) L49–L55. DOI:10.1088/2041-8205/715/1/L49 [arXiv:1005.0041[astro-ph.HE]].

[171] T. C. Arlen, V. V. Vassiliev, T. Weisgarber, S. P. Wakely and S. Y. Shafi, *Intergalactic Magnetic Fields and Gamma Ray Observations of Extreme TeV Blazars*, arXiv:1210.2802[astro-ph.HE].

[172] T. C. Arlen and V. V. Vassiliev, *Extreme TeV Blazars and Lower Limits on Intergalactic Magnetic Fields*, in *Proc. 4th Int. Fermi Symp.*, 2012. arXiv:1303.2121[astro-ph.HE].

[173] R. Schlickeiser, S. Krakau and M. Supsar, *Plasma Effects on Fast Pair Beams. II. Reactive versus Kinetic Instability of Parallel Electrostatic Waves*, Astrophys. J. **777** (2013), no. 1 49. DOI:10.1088/0004-637X/777/1/49 [arXiv:1308.4594[astro-ph.HE]].

[174] I. B. Bernstein and S. K. Trehan, *Plasma Oscillations (I)*, Nucl. Fusion **1** (1960), no. 1 3. DOI:10.1088/0029-5515/1/1/002.

[175] B. B. Godfrey, W. R. Shanahan and L. E. Thode, *Linear Theory of a Cold Relativistic Beam Propagating along an External Magnetic Field*, Phys. Fluids **18** (1975), no. 3 346. DOI:10.1063/1.861144.

[176] R. J.-M. Grognard, *Deficiencies of the Asymptotic Solutions Commonly Found in the Quasilinear Relaxation Theory*, Aust. J. Phys. **28** (1975), no. 6 731–754. DOI:10.1071/PH750731.

[177] A. A. Galeev, R. Z. Sagdeev, V. D. Shapiro and V. I. Shevchenko, *Relaxation of High-Current Electron Beams and the Modulational Instability*, Zh. Eksp. Teor. Fiz. [Sov. Phys. JETP] **45** (1977), no. 2 266, http://www.jetp.ac.ru/cgi-bin/e/index/e/45/2/p266?a=list.

[178] B. N. Brejzman and D. D. Ryutov, *Powerful Relativistic Electron Beams in a Plasma and in a Vacuum (Theory)*, Nucl. Fusion **14** (1974), no. 6 873. DOI:10.1088/0029-5515/14/6/012.

[179] F. Miniati and A. Elyiv, *Relaxation of Blazar Induced Pair Beams in Cosmic Voids: Measurement of Magnetic Field in Voids and Thermal History of the IGM*, Astrophys. J. **770** (2013) 54. DOI:10.1088/0004-637X/770/1/54 [arXiv:1208.1761[astro-ph.CO]].

[180] **HESS** Collaboration, F. Aharonian *et. al.*, *New Constraints on the Mid-IR EBL from the HESS Discovery of VHE γ-Rays from 1ES 0229+200*, Astron. Astrophys. **475** (2007) L9–L13. DOI:10.1051/0004-6361:20078462 [arXiv:0709.4584].

[181] M. Kachelrieß, S. Ostapchenko and R. Tomàs, *ELMAG: A Monte Carlo Simulation of Electromagnetic Cascades on the Extragalactic Background Light and in Magnetic Fields*, Comp. Phys. Commun. **183** (2012) 1036–1043. DOI:10.1016/j.cpc.2011.12.025 [arXiv:1106.5508[astro-ph.HE]].

[182] A. Pallottini, A. Ferrara and C. Evoli, *Simulating Intergalactic Quasar Scintillation*, Mon. Not. R. Astron. Soc. **434** (2013) 3293–3304. DOI:10.1093/mnras/stt1249 [arXiv:1307.2573[astro-ph.CO]].

[183] **HESS** Collaboration, Y. Becherini and M. Punch, *Performance of HESS-II in Multi-Telescope Mode with a Multi-Variate Analysis*, AIP Conf. Proc. **1505** (2012) 741–744. DOI:10.1063/1.4772366.

[184] A. Reimer and M. Böttcher, *Studies of Active Galactic Nuclei with CTA*, Astrophys. J. **43** (2013) 103–111. DOI:10.1016/j.astropartphys.2012.05.011 [arXiv:1208.5926[astro-ph.HE]].

[185] A. Brandenburg, K. Enqvist and P. Olesen, *Large Scale Magnetic Fields from Hydromagnetic Turbulence in the Very Early Universe*, Phys. Rev. D **54** (1996) 1291–1300. DOI:10.1103/PhysRevD.54.1291 [arXiv:astro-ph/9602031].

[186] K. Dimopoulos and A.-C. Davis, *Evolution of Primordial Magnetic Fields*, Phys. Lett. B **390** (1997) 87–96. DOI:10.1016/S0370-2693(96)01366-4 [arXiv:astro-ph/9610013].

[187] P. Olesen, *Inverse Cascades and Primordial Magnetic Fields*, Phys. Lett. B **398** (1997), no. 3-4 321–325. DOI:10.1016/S0370-2693(97)00235-9 [arXiv:astro-ph/9610154].

[188] K. Subramanian and J. D. Barrow, *Magnetohydrodynamics in the Early Universe and the Damping of Nonlinear Alfven Waves*, Phys. Rev. D **58** (1998) 083502. DOI:10.1103/PhysRevD.58.083502 [arXiv:astro-ph/9712083].

[189] D. T. Son, *Magnetohydrodynamics of the Early Universe and the Evolution of Primordial Magnetic Fields*, Phys. Rev. D **59** (1999) 063008. DOI:10.1103/PhysRevD.59.063008 [arXiv:hep-ph/9803412].

[190] G. B. Field and S. M. Carroll, *Cosmological Magnetic Fields from Primordial Helicity*, Phys. Rev. D **62** (2000) 103008. DOI:10.1103/PhysRevD.62.103008 [arXiv:astro-ph/9811206].

[191] M. Christensson, M. Hindmarsh and A. Brandenburg, *Inverse Cascade in Decaying 3-D Magnetohydrodynamic Turbulence*, Phys. Rev. E **64** (2001) 056405. DOI:10.1103/PhysRevE.64.056405 [arXiv:astro-ph/0011321].

[192] G. Sigl, *Cosmological Magnetic Fields from Primordial Helical Seeds*, Phys. Rev. D **66** (2002) 123002. DOI:10.1103/PhysRevD.66.123002 [arXiv:astro-ph/0202424].

[193] R. Banerjee and K. Jedamzik, *Are Cluster Magnetic Fields Primordial?*, Phys. Rev. Lett. **91** (2003) 251301. DOI:10.1103/PhysRevLett.93.179901 [arXiv:astro-ph/0306211].

[194] R. Banerjee and K. Jedamzik, *The Evolution of Cosmic Magnetic Fields: From the Very Early Universe, to Recombination, to the Present*, Phys. Rev. D **70** (2004) 123003. DOI:10.1103/PhysRevD.70.123003 [arXiv:astro-ph/0410032].

[195] L. Campanelli, *Evolution of Magnetic Fields in Freely Decaying Magnetohydrodynamic Turbulence*, Phys. Rev. Lett. **98** (2007) 251302. DOI:10.1103/PhysRevLett.98.251302 [arXiv:0705.2308[astro-ph]].

[196] T. Kahniashvili, A. Brandenburg, A. G. Tevzadze and B. Ratra, *Numerical Simulations of the Decay of Primordial Magnetic Turbulence*, Phys. Rev. D **81** (2010) 123002. DOI:10.1103/PhysRevD.81.123002 [arXiv:1004.3084[astro-ph.CO]].

[197] K. Jedamzik and G. Sigl, *Evolution of the Large-Scale Tail of Primordial Magnetic Fields*, Phys. Rev. D **83** (2011), no. 10 103005. DOI:10.1103/PhysRevD.83.103005 [arXiv:1012.4794[astro-ph.CO]].

[198] A. G. Tevzadze, L. Kisslinger, A. Brandenburg and T. Kahniashvili, *Magnetic Fields from QCD Phase Transitions*, Astrophys. J. **759** (2012) 54. DOI:10.1088/0004-637X/759/1/54 [arXiv:1207.0751[astro-ph.CO]].

[199] T. Kahniashvili, A. Brandenburg, L. Campanelli, B. Ratra and A. G. Tevzadze, *Evolution of Inflation-Generated Magnetic Fields through Phase Transitions*, Phys. Rev. D **86** (2012) 103005. DOI:10.1103/PhysRevD.86.103005 [arXiv:1206.2428[astro-ph.CO]].

[200] T. Kahniashvili, A. G. Tevzadze, A. Brandenburg and A. Neronov, *Evolution of Primordial Magnetic Fields from Phase Transitions*, Phys. Rev. D **87** (2013), no. 8 083007. DOI:10.1103/PhysRevD.87.083007 [arXiv:1212.0596[astro-ph.CO]].

[201] G. Baym and H. Heiselberg, *The Electrical Conductivity in the Early Universe*, Phys. Rev. D **56** (1997) 5254–5259. DOI:10.1103/PhysRevD.56.5254 [arXiv:astro-ph/9704214].

[202] R. Banerjee, *Evolution of Primordial Magnetic Fields in the Early Universe*. PhD thesis, Ludwig-Maximilians-Universität München, 2003.

[203] C. J. Hogan, *Magnetohydrodynamic Effects of a First-Order Cosmological Phase Transition*, Phys. Rev. Lett. **51** (1983) 1488–1491. DOI:10.1103/PhysRevLett.51.1488.

[204] M. Hindmarsh and A. Everett, *Magnetic Fields from Phase Transitions*, Phys. Rev. D **58** (1998) 103505. DOI:10.1103/PhysRevD.58.103505 [arXiv:astro-ph/9708004].

[205] R. Durrer and C. Caprini, *Primordial Magnetic Fields and Causality*, J. Cosmol. Astropart. Phys. **0311** (2003) 010. DOI:10.1088/1475-7516/2003/11/010 [arXiv:astro-ph/0305059].

[206] G. K. Batchelor and I. Proudman, *The Large-Scale Structure of Homogeneous Turbulence*, Philos. Trans. R. Soc. London, Ser. A **248** (1956), no. 949 369–405. DOI:10.1098/rsta.1956.0002.

[207] R. Grappin, U. Frisch, A. Pouquet and J. Léorat, *Alfvenic Fluctuations as Asymptotic States of MHD Turbulence*, Astron. Astrophys. **105** (1982) 6–14, NASA ADS:1982A%26A...105....6G.

[208] R. Grappin, A. Pouquet and J. Léorat, *Dependence of MHD Turbulence Spectra on the Velocity Field-Magnetic Field Correlation*, Astron. Astrophys. **126** (1983) 51–58, NASA ADS:1983A%26A...126...51G.

[209] R. M. Kulsrud and S. W. Anderson, *The Spectrum of Random Magnetic Fields in the Mean Field Dynamo Theory of the Galactic Magnetic Field*, Astrophys. J. **396** (1992) 606–630. DOI:10.1086/171743.

[210] T. Shiromizu and R. Nishi, *Back Reaction to the Spectrum of Magnetic Field in the Kinetic Dynamo Theory*, Prog. Theor. Phys. **101** (1999), no. 1 39–45. DOI:10.1143/PTP.101.39 [arXiv:astro-ph/9811215].

[211] G. Bader and P. Deuflhard, *A Semi-Implicit Mid-Point Rule for Stiff Systems of Ordinary Differential Equations*, Num. Math. **41** (1983), no. 3 373–398. DOI:10.1007/BF01418331.

[212] J. M. Cornwall, *Speculations on Primordial Magnetic Helicity*, Phys. Rev. D **56** (1997) 6146–6154. DOI:10.1103/PhysRevD.56.6146 [arXiv:hep-th/9704022].

[213] R. Jackiw and S.-Y. Pi, *Creation and Evolution of Magnetic Helicity*, Phys. Rev. D **61** (2000) 105015. DOI:10.1103/PhysRevD.61.105015 [arXiv:hep-th/9911072].

[214] T. Vachaspati, *Estimate of the Primordial Magnetic Field Helicity*, Phys. Rev. Lett. **87** (2001) 251302. DOI:10.1103/PhysRevLett.87.251302 [arXiv:astro-ph/0101261].

[215] A. J. Long, E. Sabancilar and T. Vachaspati, *Leptogenesis and Primordial Magnetic Fields*, arXiv:1309.2315[astro-ph.CO].

[216] U. Frisch, A. Pouquet, J. Léorat and A. Mazure, *Possibility of an Inverse Cascade of Magnetic Helicity in Magnetohydrodynamic Turbulence*, J. Fluid Mech. **68** (1975), no. 04 769–778. DOI:10.1017/S002211207500122X.

[217] A. Pouquet, U. Frisch and J. Léorat, *Strong MHD Helical Turbulence and the Nonlinear Dynamo Effect*, J. Fluid Mech. **77** (1976) 321–354. DOI:10.1017/S0022112076002140.

[218] I. N. Bronstein, K. A. Semendyayev, G. Musiol and H. Muehlig, *Handbook of Mathematics*. Springer, 2007.

[219] W. Rudin, *Real and Complex Analysis*. McGraw-Hill, 2005.

[220] C. Runge, *Über die numerische Auflösung von Differentialgleichungen*, Math. Ann. **46** (1895) 167–178. DOI:10.1007/BF01446807.

[221] K. Heun, *Neue Methoden zur approximativen Integration der Differentialgleichungen einer unabhängigen Veränderlichen*, Z. Math. Phys. **45** (1900) 23–38.

[222] W. Kutta, *Beitrag zur näherungsweisen Integration totaler Differentialgleichungen*, Z. Math. Phys. **46** (1901) 435–453.

[223] J. C. Butcher, *The Numerical Analysis of Ordinary Differential Equations: Runge-Kutta and General Linear Methods*. John Wiley & Sons, 1987.

[224] P. Deuflhard and F. Bornemann, *Scientific Computing with Ordinary Differential Equations*. Springer, 2002.

Acknowledgments

First of all I would like to thank my supervisor Günter Sigl. I am very grateful to him for, more than four years ago, offering me the opportunity to carry out my diploma thesis and, after that, my dissertation. Since I did not have any experience in astroparticle physics before I joined the group, it was him who awoke and maintained my interest in this fascinating topic. I am thankful for his supervision and advice which often helped me to solve problems in physics of any kind which I got stuck at.

Next I would like to thank Robi Banerjee and Wilfried Buchmüller, who agreed to be referees for my dissertation and disputation, respectively, and Georg Steinbrück, the head of my doctoral board, therefore making the submission and publication of the present thesis possible.

As its main part is based on papers I published, I would like to take the opportunity and thank my co-authors – Carmelo Evoli, Karsten Jedamzik and Günter Sigl – who helped me to understand the physics of cosmic magnetic fields and therefore their importance for our Universe.

Furthermore, this thesis would not have been submitted in the form shown here without the help of various proof readers, namely Rafael Alves Batista, Karsten Jedamzik, Natacha Leite and Martin Vollmann. Thank you for pointing out my mistakes and misconceptions and thus helping me to improve the presentation of my work of the past three years!

Of course the time of my thesis would not be the same without the members of the theory astroparticle group. Many of them over the time became close friends to me which I hope to remain true even once we are or will be not united under the flag of building 67 anymore: Laura van den Aarssen, Rafael Alves Batista, Masaki Asano, Enrico Borriello, Torsten Bringmann, Benedict Broy, Francesca Calore, Sovan Chakraborty, Carmelo Evoli, Yasar Goedecke, Michael Grefe, Daisuke Hiraoka, Mitsusru Kakizaki, Jörg Kulbartz, Natacha Leite, Martin Lommatzsch, Luca Maccione, Alessandro Mirizzi, Lars Reinholz, Ninetta Saviano, Peter Schiffer, Günter Sigl, Ricard Tomas Bayo, Arjen van Vliet, Martin Vollmann and Le Zhang.

As I spent all four years in the same office, the (in)famous room no. 109, I was glad to have great office mates of which I saw many coming (and going) over the course of time, namely Rafael Alves Batista, Yasar Goedecke, Benjamin Lang, Martin Vollmann and Jan-Christoph Weise. Although I still do not know completely what they are and were doing for their theses, I could often bother them with my problems, both in physics and outside of it, which they listened to patiently, sometimes during a coffee/tea break, and helped me with their support and comradeship.

Being situated on the DESY campus (although, as should be, once again, stressed here, belonging to the University of Hamburg), I also had the opportunity to meet many different people from various countries. This internationality on site is one of the reasons why working here is a unique experience. As there are too many names to be listed here, everybody whom I met in DESY should feel addressed when I say a big "Thank you!". Very special acknowledgments go to the members of the Movie Club which, starting off as an office event, became firmly established and valued by people from all over DESY.

However, there is also a life outside DESY (so they say). Also there over the last years I was supported by many people to whom I owe special thanks for their friendship and care. Again, I cannot list everyone, thus the following names also stand for various other ones: Nicola d'Ascenzo, Victoria Bauer, Jonas Breunlin, Lukas Buhné, Daniela Caterina, Adam Dybulla, Luciana Fernandes, Aila Gengelbach, Yasar Goedecke, Martin

Görner, Lilia Hadvig, Jonas Havel, Nadja Hüdepohl, Fabian Jaensch, Dennis Lang, Lu Lu, Cosimo Maceria, Araksik Martirosian, Christiane Niemeier, the Oertel clan, Maria Petropoulou, Almut Pingel, Juliane Reinhardt, Eike Schlieckau, Franziska Schumann, Susanne Schumann, Michelle Vis, Markus Voge, Julia Weber, Jan-Christoph Weise, Max Weiß, Florian Wittkötter, Svetlana Zolotova and Tatjana Zolotova.

Finally, I would like to thank the people who cared and care the most about my well-being – my family. I am indebted to my parents and my grandmother who always supported me throughout my studies and often relieved me from the stress of everyday life, sometimes by just being there for me and sometimes by actively helping me in various situations. But I also yield thanks to my brother who cheered me up by spending time with me and by sharing interests such that throughout the years I always had a reliable companion to wrestle down the various difficulties and problems of life.